Universidade de Aveiro Departamento de Química
Ano 2017

Rita Marisa Nogueira Ferreira

Estratégias preventivas e terapêuticas para a hipertensão arterial pulmonar

Preventive and therapeutic strategies for pulmonary arterial hypertension

Universidade de Aveiro Departamento de Química
Ano 2017

Rita Marisa Nogueira Ferreira

Estratégias preventivas e terapêuticas para a hipertensão arterial pulmonar

Preventive and therapeutic strategies for pulmonary arterial hypertension

Tese apresentada à Universidade de Aveiro para cumprimento dos requisitos necessários à obtenção do grau de Doutor em Bioquímica, realizada sob a orientação científica do Doutor Tiago Alexandre Henriques Coelho, Professor Auxiliar Convidado da Faculdade de Medicina da Universidade do Porto e da Doutora Rita Maria Pinho Ferreira, Professora Auxiliar do Departamento de Química da Universidade de Aveiro.

Este trabalho é financiado por Fundos FEDER através do Programa Operacional Factores de Competitividade – COMPETE e por Fundos Nacionais através da FCT – Fundação para a Ciência e a Tecnologia no âmbito da bolsa individual «SFRH/BD/91067/2012»; da Unidade de Investigação Cardiovascular – UnIC «UID/IC/00051/2013» e da Unidade de Investigação Química Orgânica, Produtos Naturais e Agroalimentares – QOPNA «UID/QUI/00062/2013».

Dedico este trabalho aos meus pais, irmão e avó.

o júri

presidente

Doutor Paulo Jorge dos Santos Gonçalves Ferreira
Professor Catedrático da Universidade de Aveiro

vogais

Doutora Raquel Maria Fino Seiça
Professora Catedrática da Faculdade de Medicina da Universidade de Coimbra

Doutor Adelino Leite Moreira
Professor Catedrático da Faculdade de Medicina da Universidade do Porto

Doutora Paula Alexandra Martins de Oliveira
Professora Associada com Agregação da Universidade de Trás-os-Montes e Alto Douro

Doutora Margarida Sâncio Da Cruz Fardilha
Professora Auxiliar da Universidade de Aveiro

Doutor Daniel Moreira Gonçalves
Professor Auxiliar Convidado da Faculdade de Medicina da Universidade do Porto

Doutor Tiago Henriques Coelho
Professor Auxiliar Convidado da Faculdade de Medicina da Universidade do Porto (orientador)

Doutora Rute Silva Moura
Professora Auxiliar Convidada da Escola de Ciências da Universidade do Minho

agradecimentos

Aos meus orientadores, Professor Doutor Tiago Henriques Coelho e Professora Doutora Rita Ferreira, agradeço a orientação científica que me proporcionaram, as oportunidades de aprendizagem que me possibilitaram e a confiança que depositaram em mim. Agradeço, em especial, à Professora Doutora Rita Ferreira pela ajuda, disponibilidade, incentivo e motivação constantes ao longo deste percurso.

Ao Professor Doutor Rui Vitorino, agradeço toda a ajuda, disponibilidade, ensinamentos e entusiasmo.

Aos restantes co-autores dos trabalhos apresentados nesta tese agradeço a sua colaboração para a realização dos mesmos.

Ao Doutor Marc Humbert, Doutor Christophe Guignabert e todos os membros da sua equipa de investigação do INSERM UMR_S 999 e Université Paris-Sud/Paris Saclay, agradeço a simpatia com que me receberam no seu laboratório e a disponibilidade para me acompanhar e ensinar.

Aos meus colegas do Departamento de Química da Universidade de Aveiro e do Departamento de Cirurgia e Fisiologia da Faculdade de Medicina da Universidade do Porto, obrigada pela amizade, ajuda, disponibilidade, momentos de descontração e paciência nos dias menos bons.

Aos meus pais, irmão e avó agradeço todo o apoio e compreensão ao longo destes anos.

Agradeço à Unidade de Investigação Química Orgânica, Produtos Naturais e Agroalimentares (QOPNA) da Universidade de Aveiro e à Unidade de Investigação Cardiovascular (UnIC) da Universidade do Porto.

Por fim, agradeço à Fundação para a Ciência e a Tecnologia pelo financiamento através da bolsa de doutoramento SFRH/BD/91067/2012, que possibilitou a realização deste trabalho.

palavras-chave

exercício físico, inflamação, monocrotalina, hipertensão arterial pulmonar, terameprocol, remodelação vascular.

resumo

A hipertensão arterial pulmonar (HAP) é uma doença grave, caracterizada por remodelação progressiva da vasculatura pulmonar, frequentemente culminando em insuficiência do ventrículo direito (VD) e morte prematura. Apesar do progresso que tem sido feito nos últimos anos em termos de opções de tratamento, a HAP permanece uma doença incurável, com um mau prognóstico e uma elevada taxa de mortalidade. No presente trabalho, pretendeu-se explorar o potencial de diferentes abordagens preventivas e terapêuticas na HAP experimental. Para isso, três estudos experimentais foram realizados a fim de avaliar o impacto do exercício físico (Estudos I e II) ou do fármaco terameprocol (TMP) (Estudo III) na HAP. No Estudo I mostramos que o exercício físico moderado realizado ao longo da vida induziu diferentes adaptações moleculares nos ventrículos esquerdo e direito. Especificamente, o VD de animais treinados apresentou maiores alterações mitocondriais, mostrando um aumento na expressão de MnSOD e SIRT3, sugestivo de uma melhoria da capacidade antioxidante. Para explorar o impacto do exercício físico na HAP, no Estudo II avaliou-se o seu potencial efeito preventivo na insuficiência do VD secundária a HAP, no modelo animal da monocrotalina (MCT) submetido a 4 semanas de exercício físico em tapete rolante antes do desenvolvimento da doença. Os resultados indicam que o pré-condicionamento com exercício físico preveniu a remodelação da artéria pulmonar e a disfunção, hipertrofia e fibrose do VD. A nível molecular, o exercício físico preveniu o aumento do rácio MHC-beta/alfa e modulou a via de sinalização TWEAK/NF-κB. O exercício físico também preveniu o aumento da expressão da atrogina-1 e induziu um aumento da atividade da MMP-2. Com o objetivo de desenvolver novas estratégias farmacológicas para o tratamento da HAP, no Estudo III foi utilizada uma abordagem proteómica baseada em espetrometria de massa para procurar as vias moleculares moduladas pelo TMP em culturas primárias de células musculares lisas da artéria pulmonar isoladas de ratos injetados com MCT. A análise bioinformática dos dados de proteómica destacou a "regulação do tamanho da célula" e "resposta ao *stress* do retículo endoplasmático", como processos biológicos sobre-expressos pelo TMP, enquanto os processos biológicos "resposta ao TGF-beta" e "transcrição do ADN" foram encontrados sub-expressos. Dos fatores de transcrição modulados pelo TMP, a sub-expressão do HMGB1 parece estar relacionada com o efeito anti-proliferativo deste fármaco. Estas alterações moleculares induzidas pelo tratamento com TMP podem ter contribuído para a redução da remodelação vascular e consequentemente atenuado a disfunção e hipertrofia do VD associadas à HAP induzida pela MCT. Em geral, os nossos resultados sugerem que o pré-condicionamento com exercício físico e o tratamento com TMP podem ter relevância clínica na HAP. A modulação de vias de sinalização associadas à inflamação parece estar relacionada com os efeitos benéficos destas estratégias preventivas e terapêuticas.

keywords

exercise training, inflammation, monocrotaline, pulmonary arterial hypertension, terameprocol, vascular remodeling.

abstract

Pulmonary arterial hypertension (PAH) is a severe disease, characterized by progressive remodeling of the pulmonary vasculature, usually culminating in right ventricle (RV) failure and premature death. Despite the progress that has been made in the last few years in terms of treatment options, PAH remains an incurable disease, with a poor prognosis and a high mortality rate. In the current work, we intended to explore the potential of different preventive and therapeutic approaches in experimental PAH. To accomplish that, three experimental studies were performed in order to assess the impact of exercise training (Studies I and II) or the drug terameprocol (TMP) (Study III) in PAH. In Study I, we show that lifelong moderate exercise training induced different molecular adaptations in the left and right ventricles. Specifically, the RV of trained animals presented greater mitochondrial changes, showing an increased expression of MnSOD and SIRT3, suggestive of improved antioxidant capacity. To explore the impact of exercise training on PAH, in Study II we evaluated its potential preventive effect on RV failure secondary to PAH, in the monocrotaline (MCT) animal model submitted to a 4-week treadmill exercise training before disease development. Data indicate that exercise preconditioning prevented pulmonary artery remodeling and RV dysfunction, hypertrophy and fibrosis. At a molecular level, exercise training prevented the increase in beta/alpha-MHC ratio and modulated the TWEAK/NF-κB signaling pathway. Exercise training also prevented the increase of atrogin-1 expression and induced an increase in MMP-2 activity. Envisioning the development of novel pharmacological strategies for PAH treatment, in Study III we used a mass spectrometry-based proteomic approach to search for the molecular pathways modulated by TMP in pulmonary artery smooth muscle cell primary cultures isolated from rats injected with MCT. Bioinformatic analysis of proteome data highlighted the “regulation of cell size” and “response to endoplasmic reticulum stress” as biological processes up-regulated by TMP, while the biological processes “response to TGF-beta” and “DNA-templated transcription” were found down-regulated. From the transcription factors modulated by TMP, the down-regulation of HMGB1 seems to be related with the anti-proliferative effect of this drug. These molecular alterations induced by TMP treatment may have contributed to the reduction of the vascular remodeling and consequently attenuated RV dysfunction and hypertrophy associated to MCT-induced PAH. In overall, our results suggest that exercise preconditioning and TMP treatment can be of clinical relevance in PAH. The modulation of inflammation-related signaling pathways seems to be behind the benefits of these preventive and therapeutic strategies.

TABLE OF CONTENTS

LIST OF FIGURES

Chapter I

Chapter III

<u>Appendix – Supplementary data</u>

LIST OF TABLES

Chapter I

Chapter III

Appendix – Supplementary data

LIST OF ABBREVIATIONS

5-HT	Serotonin
5-HT1B	Serotonin type 1B receptor
5-HT2A	Serotonin type 2A receptor
5-HT2B	Serotonin type 2B receptor
5-HTT	Serotonin transporter
6MWD	6-minute walk distance
6MWT	6-minute walk test
ADP	Adenosine diphosphate
Ang-1	Angiopoietin-1
ATP	Adenosine triphosphate
AVD	Apoptotic volume decrease
BMP	Bone morphogenetic protein
BMPRII	Bone morphogenetic protein receptor type II
BNP	Brain natriuretic peptide
BSA	Bovine serum albumin
cAMP	Cyclic adenosine monophosphate
cav-1	Caveolin-1
CCBs	Calcium channel blockers
cGMP	Cyclic guanosine monophosphate
CSA	Cross sectional area
CTEPH	Chronic thromboembolic pulmonary hypertension
DMSO	Dimethylsulfoxide
DNA	Deoxyribonucleic acid
ECM	Extracellular matrix
ECs	Endothelial cells
EDP	End-diastolic pressure
eNOS	Endothelial nitric oxide synthase
EPCs	Endothelial progenitor cells
ER	Endoplasmic reticulum
ET-1	Endothelin-1

ETA	Endothelin-1 type A receptor
ETB	Endothelin-1 type B receptor
FBS	Fetal bovine serum
FKN	Fractalkine
GSK-3β	Glycogen synthase kinase-3β
HA	Hyaluronic acid
HIV	Human immunodeficiency virus
HMGB1	High mobility group box 1
HSP	Heat shock protein
IL	Interleukin
iNOS	Inducible nitric oxide synthase
LV	Left ventricle
MCT	Monocrotaline
MCTP	Monocrotaline pyrrole
MHC	Myosin heavy chain
MMP	Matrix metalloproteinase
MnSOD	Manganese-dependent superoxide dismutase
mRNA	Messenger ribonucleic acid
MuRF1	Muscle ring finger protein 1
NADPH	Nicotinamide adenine dinucleotide phosphate
NF-AT	Nuclear factor of activated T-cells
NF-κB	Nuclear factor kappa B
NO	Nitric oxide
NYHA – FC	New York Health Association functional class
PAB	Pulmonary artery banding
PAECs	Pulmonary artery endothelial cells
PAH	Pulmonary arterial hypertension
PAI-1	Plasminogen activator inhibitor-1
PAP	Pulmonary artery pressure
PASMCs	Pulmonary artery smooth muscle cells
PDE	Phosphodiesterase
PDGF	Platelet-derived growth factor

PECAM-1	Platelet endothelial cell adhesion molecule-1
PGC-1α	Peroxisome proliferator-activated receptor gamma coactivator-1 alpha
PGI2	Prostacyclin
PH	Pulmonary hypertension
PVR	Pulmonary vascular resistance
QOL	Quality of life
RANTES	Regulated upon activation, normal T-cell expressed and secreted
ROCK	Rho kinase
RV	Right ventricle
SDS-PAGE	Sodium dodecyl sulfate-polyacrylamide gel electrophoresis
SERCA2a	Sarco(endo)plasmic reticulum calcium-ATPase
sGC	Soluble guanylate cyclase
SIRT3	Sirtuin 3
SMCs	Smooth muscle cells
SM-MHC	Smooth muscle-myosin heavy chain
SNAPs	Soluble ATPase N-ethylmaleimide-sensitive factor association proteins
SNAREs	SNAP receptors
TASK-1	Two pore-related acid-sensitive potassium channel-1
TGF-α	Transforming growth factor-alpha
TGF-β	Transforming growth factor-beta
TMP	Terameprocol
TNF-α	Tumor necrosis factor-alpha
t-PA	Tissue plasminogen activator
TRAF6	TNF receptor-associated factor 6
TWEAK	TNF-related weak inducer of apoptosis
TXA2	Thromboxane A2
VDCC	Voltage-dependent calcium channels
VEGFR-2	Vascular endothelial growth factor receptor-2
VIP	Vasoactive intestinal peptide
WHO	World Health Organization
α-SMA	alpha-smooth muscle actin

CHAPTER I
GENERAL INTRODUCTION

General Introduction

Pulmonary arterial hypertension (PAH) is a progressive and fatal cardiopulmonary disease, which represents Group 1 within the Pulmonary Hypertension World Health Organization (WHO) clinical classification system. PAH is defined by a resting mean pulmonary artery pressure (PAP) greater than or equal to 25 mmHg, a pulmonary capillary wedge pressure less than or equal to 15 mmHg and a pulmonary vascular resistance (PVR) above 3 Wood units (Voelkel, Gomez-Arroyo et al. 2012; Hoeper, Bogaard et al. 2013; McLaughlin, Shah et al. 2015). According to the current clinical classification, PAH can be idiopathic, heritable, drug or toxin induced or associated with other diseases (connective tissue diseases, HIV infection, portal hypertension, congenital heart diseases and Schistosomiasis) (Simonneau, Gatzoulis et al. 2013). PAH has a complex and multifactorial pathogenesis in which vasoconstriction, thrombosis *in situ*, inflammation and vascular remodeling are the main pathological features (Lourenco, Fontoura et al. 2012; Malenfant, Neyron et al. 2013; Montani, Gunther et al. 2013; McLaughlin, Shah et al. 2015). Pulmonary vascular remodeling is characterized by the thickening of all three layers of the vascular wall (intima, media and adventitia). This thickening is mainly due to hypertrophy and/or hyperplasia of the predominant cell type within each of the layers (endothelial cells, smooth muscle cells (SMCs) and fibroblasts), as well as SMC resistance to apoptosis. A complex interplay among the different vascular cells, regulated by several mediators is a key contributor to the pathological features that characterize this disease (Mandegar, Fung et al. 2004; Sakao, Tatsumi et al. 2010; Shimoda and Laurie 2013; Guignabert, Tu et al. 2015). All these changes in the pulmonary vascular bed may lead to a progressive increase in PVR, imposing a pressure overload to the right ventricle (RV), which results in RV hypertrophy and eventually in RV failure and premature death (Montani, Gunther et al. 2013; Baldi, Fuso et al. 2014; McLaughlin, Shah et al. 2015).

Approximately two-thirds of PAH patients are women and the majority are diagnosed with 40-50 years of age in an advanced stage of the disease (WHO functional class III-IV) (Baptista, Meireles et al. 2013; McGoon, Benza et al. 2013). Although a rare disease, with an estimated prevalence of 15-50 cases *per* million (Peacock, Murphy et al. 2007), PAH is a fatal condition with a survival estimated as low as 2.8 years after diagnosis if left untreated (D'Alonzo, Barst et al. 1991). Until now, only a few molecular pathways targeting the pulmonary vascular endothelial dysfunction and vasoconstriction were found

to be therapeutically relevant. For instance, treatment with prostacyclin analogs, endothelin-1 receptor antagonists or phosphodiesterase type 5 inhibitors was shown to be beneficial (Provencher and Granton 2015). During the last years, PAH therapeutic options increased patient survival, exercise capacity and quality of life. However, there is currently no cure available and further understanding into the disease pathophysiology and treatment development is needed to improve PAH clinical management (McGoon, Benza et al. 2013; Humbert, Lau et al. 2014). To assist in this demanding task, preclinical models of PAH have been crucial to the identification of the molecular pathways underlying PAH development and progression and to establish novel therapeutics or improve the existing ones. Among preclinical models of PAH, the monocrotaline (MCT) animal model is the most commonly used, offering the advantage of mimic several key aspects of human PAH, including vascular remodeling, endothelial dysfunction, up-regulation of inflammatory cytokines, and RV dysfunction (Maarman, Lecour et al. 2013; Ryan, Marsboom et al. 2013). Indeed, pharmacological therapies have been tested, using the MCT animal model, increasingly targeting pulmonary vascular proliferative and apoptotic pathways, instead vasoconstriction (Huang, Liu et al. 2010; Umar, Steendijk et al. 2010; Gurtu and Michelakis 2015).

Exercise training can be seen as an attractive non-pharmacological therapeutic approach for PAH, given its anti-inflammatory properties (Gielen, Adams et al. 2003). Recent reports support inflammation as an important process in the pathogenesis of PAH-related dysfunctional RV (Watts, Gellar et al. 2008; Campian, Hardziyenka et al. 2010; Rondelet, Dewachter et al. 2012; Belhaj, Dewachter et al. 2013; Vonk-Noordegraaf, Haddad et al. 2013) that seems to be modulated by exercise training (Moreira-Goncalves, Ferreira et al. 2015). Indeed, exercise has been reported to be a beneficial non-pharmacological approach in PAH patients' rehabilitation, being seen as an adjunct to pharmacological treatment (Mereles, Ehlken et al. 2006; de Man, Handoko et al. 2009; Grunig, Ehlken et al. 2011; Grunig, Lichtblau et al. 2012; Ehlken, Lichtblau et al. 2016). However, the potential preventive role of exercise training in individuals with RV failure secondary to PAH is still unknown. Despite the unique cardioprotective phenotype promoted by exercise training (Ferreira, Moreira-Goncalves et al. 2015), the underlying molecular mechanisms require further investigation, particularly those related with long-term exercise training effects on RV. This can be of great importance, once RV function is a critical determinant of survival

in pathological conditions such as PAH (Vonk-Noordegraaf, Haddad et al. 2013; La Gerche and Claessen 2015).

Considering the questions raised, the global purpose of this work was to investigate novel non-pharmacological (exercise training) and pharmacological (terameprocol (TMP)) approaches to the clinical management of PAH. The present thesis is divided in five chapters. In the chapter I a state of the art regarding PAH pathophysiology, available therapeutic options and animal models to study the disease is presented (Reviews I-IV). Chapter II specifies the aims of the work. In the chapter III are presented the experimental studies, including the experimental design, the methods used, results obtained and a discussion of each study. A general discussion of the results and the main conclusions are presented in the chapters IV and V, respectively.

List of studies – Theoretical background:

Review I

R. Nogueira-Ferreira, R. Ferreira, and T. Henriques-Coelho (2014). "*Cellular interplay in pulmonary arterial hypertension: Implications for new therapies*", Biochimica et Biophysica Acta – Molecular Cell Research 1843(5): 885-893.

Review II

R. Nogueira-Ferreira, D. Moreira-Gonçalves, M. Santos, R. Ferreira and T. Henriques-Coelho (2016) "*Mechanisms underlying the impact of exercise training in pulmonary arterial hypertension*", (submitted).

Review III

R. Nogueira-Ferreira, G. Faria-Costa, R. Ferreira, and T. Henriques-Coelho (2016). "*Animal models for the study of pulmonary hypertension: potential and limitations*", Cardiology and Cardiovascular Medicine 1(1): 1-22.

Review IV

R. Nogueira-Ferreira, R. Vitorino, R. Ferreira, and T. Henriques-Coelho (2015). "*Exploring the monocrotaline animal model for the study of pulmonary arterial hypertension: A network approach*", Pulmonary Pharmacology and Therapeutics 35: 8-16.

CHAPTER I

STATE OF THE ART

REVIEW I – CELLULAR INTERPLAY IN PULMONARY ARTERIAL HYPERTENSION: IMPLICATIONS FOR NEW THERAPIES

Biochimica et Biophysica Acta 1843 (2014) 885–893

Contents lists available at ScienceDirect

Biochimica et Biophysica Acta

journal homepage: www.elsevier.com/locate/bbamcr

Review

Cellular interplay in pulmonary arterial hypertension: Implications for new therapies

Rita Nogueira-Ferreira [a,b,*], Rita Ferreira [a], Tiago Henriques-Coelho [b]

[a] QOPNA, Department of Chemistry, University of Aveiro, Aveiro, Portugal
[b] Department of Physiology and Cardiothoracic Surgery, Faculty of Medicine, University of Porto, Porto, Portugal

ARTICLE INFO

Article history:
Received 12 August 2013
Received in revised form 23 January 2014
Accepted 24 January 2014
Available online 31 January 2014

Keywords:
Endothelial cell
Inflammation
Smooth muscle cell
Thrombosis
Vascular remodeling
Vasoconstriction

ABSTRACT

Pulmonary arterial hypertension (PAH) is a complex and multifactorial disease characterized by vascular remodeling, vasoconstriction, inflammation and thrombosis. Although the available therapies have resulted in improvements in morbidity and survival, PAH remains a severe and devastating disease with a poor prognosis and a high mortality, justifying the need of novel therapeutic targets. An increasing number of studies have demonstrated that endothelial cells (ECs), smooth muscle cells (SMCs) and fibroblasts of the pulmonary vessel wall, as well as platelets and inflammatory cells have a role in PAH pathogenesis. This review aims to integrate the interplay among different types of cells, during PAH development and progression, and the impact of current therapies in cellular modulation. The interplay among endothelial cells, smooth muscle cells and fibroblasts present in pulmonary vessels wall, platelets and inflammatory cells is regulated by several mediators produced by these cells, contributing to the pathophysiologic features of PAH. Current therapies are mainly focused in the pulmonary vascular tone and in the endothelial dysfunction. However, once they have not been effective, novel therapies targeting other PAH features, such as inflammation and platelet dysfunction are emerging. Further understanding of the interplay among different vascular cell types involved in PAH development and progression can contribute to find novel therapeutic targets, decreasing PAH mortality and morbidity in the future.

1. Introduction

Pulmonary arterial hypertension is a progressive and life-threatening disease, multifactorial in nature [1,2]. Although the "trigger" that leads to the disease is still unknown, a complex interplay among different types of cells occurs and multiple alterations are verified: (i) intimal hyperplasia; (ii) medial hypertrophy and hyperplasia; (iii) adventitia proliferation; (iv) neointima formation and (v) occurrence of plexiform lesions. In addition, these changes are accompanied by vasoconstriction, local inflammation and thrombosis in situ [3–6].

Endothelial cells, located in the inner layer of the pulmonary artery wall, have several O_2-sensing mechanisms, including O_2-sensitive NADPH oxidases, endothelial nitric oxide synthase, and heme oxygenases [7,8]. Vascular smooth muscle cells, located in the medial layer, have multiple stretch-sensing mechanisms, and are able to convert a mechanical stimulus into an intracellular signal that leads to modulation of gene expression and cellular function, such as contraction, proliferation, apoptosis and migration [9]. Fibroblasts, present in the adventitial compartment, may be considered the principal injury-sensing cells. They may experience functional changes due to stimuli such as vascular injury (Fig. 1) [10].

Abbreviations: 5-HT, serotonin; 5-HT_{1B}, serotonin type 1B receptor; 5-HT_{2A}, serotonin type 2A receptor; 5-HT_{2B}, serotonin type 2B receptor; 5-HTT, serotonin transporter; ADP, adenosine diphosphate; ATP, adenosine triphosphate; AVD, apoptotic volume decrease; BMP, bone morphogenetic protein; BMPRII, bone morphogenetic protein receptor type II; cAMP, cyclic adenosine monophosphate; cav-1, caveolin-1; CCBs, calcium channel blockers; cGMP, cyclic guanosine monophosphate; DNA, deoxyribonucleic acid; ECM, extracellular matrix; ECs, endothelial cells; eNOS, endothelial nitric oxide synthase; EPCs, endothelial progenitor cells; ET-1, endothelin-1; ET_A, endothelin-1 type A receptor; ET_B, endothelin-1 type B receptor; FKN, fractalkine; HA, hyaluronic acid; MCT, monocrotaline; MMPs, matrix metalloproteinases; mRNA, messenger ribonucleic acid; NADPH, nicotinamide adenine dinucleotide phosphate; NO, nitric oxide; PAECs, pulmonary artery endothelial cells; PAH, pulmonary arterial hypertension; PAI-1, plasminogen activator inhibitor-1; PASMCs, pulmonary artery smooth muscle cells; PDE-5, phosphodiesterase type 5; PDGF, platelet-derived growth factor; PGI_2, prostacyclin; RANTES, Regulated upon Activation, Normal T-cell Expressed and Secreted; ROCK, Rho kinase; SMCs, smooth muscle cells; SM-MHC, smooth muscle-myosin heavy chain; SNAPs, soluble ATPase N-ethylmaleimide-sensitive factor association proteins; SNAREs, SNAP receptors; TASK-1, two pore-related acid-sensitive potassium channel-1; TGF-β, transforming growth factor-β; TNF-α, tumor necrosis factor-α; t-PA, tissue plasminogen activator; TXA_2, thromboxane A_2; VDCC, voltage-dependent calcium channels; α-SMA, α-smooth muscle actin

* Corresponding author at: Chemistry Department, University of Aveiro, Campus de Santiago, 3810-193 Aveiro, Portugal. Tel.: +351 234370700; fax: +351 234370084.
E-mail address: rmferreira@ua.pt (R. Nogueira-Ferreira).

0167-4889/$ – see front matter © 2014 Elsevier B.V. All rights reserved.
http://dx.doi.org/10.1016/j.bbamcr.2014.01.030

Table 1
Current and novel therapies for pulmonary arterial hypertension.

Current therapies	Novel therapies
Endothelial cells	
Prostacyclin analogs	Rho kinase inhibitor
Epoprostenol	Fasudil
Treprostinil	
Iloprost	
Endothelin-1 receptor antagonists	Dual endothelin-1 receptor antagonist
Bosentan	Macitentan
Ambrisentan	Pyruvate dehydrogenase kinase inhibitor
	Dichloroacetate
	Endothelial progenitor cells
Smooth muscle cells	
Phosphodiesterase inhibitors	Soluble guanylate cyclase stimulator
Sildenafil	Riociguat
Tadalafil	
Calcium channel blockers	Prostacyclin receptor agonist
Nifedipine	Selexipag
Diltiazem	
Amlodipine	
Fibroblasts	
	Elastase inhibitors
Inflammatory cells	
	Rapamycin
	Tryptolide
	Thymulin
Platelets	
	Thromboxane synthesis inhibitors
	Ozagrel
	Furegrelate

Given the role of these cell types in the regulation of several vascular processes, the next points intend to detail various aspects of the contribution of these cell types to development and progression of PAH as well as of platelets and inflammatory cells. The mediators that regulate the interplay between these distinct cell types during PAH development and progression will also be analyzed envisioning novel therapeutic targets.

2. Endothelial cells

2.1. Role in pathophysiology of PAH

Endothelial damage is a key initial event in PAH. Although the mechanisms that mediate this damage are largely unknown, insults such as chronic hypoxia, inflammation, viral infection, mechanical stretch or shear stress, can activate the endothelial apparatus and induce cell apoptosis [11]. The death of ECs leads to the appearance of apoptotic-resistant and hyper-proliferative ECs, contributing to the vascular remodeling [12]. Endothelial cells not only contribute to the vascular remodeling linked to PAH development, but also regulate the related vasoconstriction and thrombosis processes, through the production and release of several mediators [2].

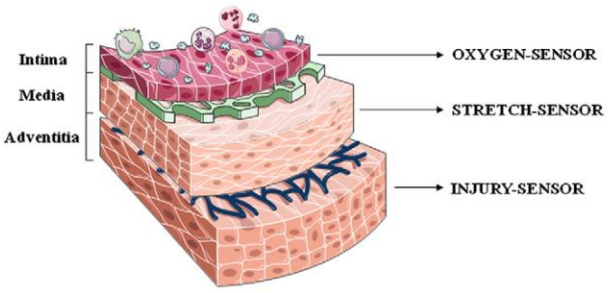

Fig. 1. "Sensing" mechanisms in the different layers of the pulmonary artery wall. Endothelial cells of the intima are equipped with mechanisms to sense differences in the oxygen supply. Medial smooth muscle cells have multiple stretch-sensing mechanisms that participate in the modulation of their functions. Fibroblasts, present in the adventitia, are considered the principal injury-sensing cells.

Endothelial cell migration and proliferation were thought to be responsible for the regeneration of injured endothelium. However, additional mechanisms were shown to replace the denuded or injured arteries. It has been reported that endothelial progenitor cells (EPCs) exert important functions in repairing and maintaining the integrity of the endothelial monolayer by replacing denuded parts of the artery [13]. After several pre-clinical studies demonstrate the beneficial effects of EPC administration, which was translated into a decrease of right ventricle systolic pressure, as well as a decrease in pulmonary and cardiac remodeling [14], clinical trials were performed. Autologous EPC administration in adult and pediatric idiopathic PAH patients showed an improvement on pulmonary hemodynamics and exercise capacity [15,16]. These results contrast with the finding that EPCs can contribute to PAH-related vascular remodeling [17]. However, given the promising results observed in clinical studies, the use of EPCs as a therapeutic option continues to be investigated. The results of the clinical trial PH (pulmonary hypertension) and Cell Therapy (PHACeT trial; ClinicalTrials.gov Identifier: NCT00469027), performed with the aim of evaluating the safety of administering autologous progenitor cells transduced with eNOS in idiopathic PAH patients are awaited. Furthermore, a combined therapy with autologous bone marrow-derived EPCs and sildenafil (a phosphodiesterase type 5 inhibitor) showed a superior efficacy than either bone marrow-derived EPCs or sildenafil alone in preventing monocrotaline (MCT)-induced PAH [18]. This combined therapy successfully abolished PAH-induced hemodynamic impacts on the right ventricle. Despite these encouraging results, it is yet unclear what is the EPC mechanism of action in PAH treatment. In this setting, a study reported that EPC infusion prevented MCT-induced PAH in athymic nude rats through a mechanism that requires the presence of natural killer cells [19].

2.2. Intracellular pathways modulated by PAH

The increase of endothelial cell permeability seems to have a huge contribution to PAH pathogenesis [20]. Stimuli that activate RhoA/ROCK, like thrombin, increase endothelial permeability. Stimuli that stimulate Rac1/p21-activated kinase, like prostacyclin (PGI_2), promote barrier integrity [20,21]. The net effect of EC permeability favors the release of mediators like endothelin-1 (ET-1), nitric oxide (NO), PGI_2 and thromboxane-A_2 (TXA_2) on SMCs and platelets. In addition, endothelial dysfunction in PAH can be reflected by a reduction in vasodilators/growth inhibitors like NO and PGI_2, and an increase in vasoconstrictors/co-mitogens like ET-1 and TXA_2 [20].

Another pathway that seems to contribute to EC permeability is the bone morphogenetic protein (BMP) signaling pathway. Recently, the loss of bone morphogenetic protein type II receptor (BMPRII) in ECs was reported to promote the extravasation of leucocytes into the pulmonary artery wall, increasing the susceptibility to inflammation [22]. Bone morphogenetic proteins are members of the transforming growth factor-β (TGF-β) family and signal via BMP type I and II receptors, which are serine/threonine kinase transmembrane receptors. This interaction with the receptors usually activates Smad1/5/8 that form complexes with Smad4 and translocate to the nucleus, regulating gene expression through the interaction with transcription factors. Besides the canonical Smad signaling, non-Smad pathways, such as the MAPK (mitogen-activated protein kinase), can also be involved [23,24]. As it is known, several gene mutations that lead to BMPRII loss of function have been associated to heritable PAH [25,26]. However, BMPRII expression is reduced in the pulmonary vasculature of patients with heritable and idiopathic PAH, independently of whether they present or not the BMPRII gene mutation [27]. In ECs, BMPRII activation seems to promote cell proliferation, migration and survival [28,29]. Loss of BMPRII function in these cells was reported to induce apoptosis, contributing to the

vascular remodeling associated to PAH [28], as described above. Recently, a study reported that BMPRII ligands, BMP2 and BMP4, stimulate eNOS (endothelial nitric oxide synthase) activity in PAECs (pulmonary artery ECs), inducing NO synthesis. Furthermore, eNOS activity stimulation was shown to be dependent on protein kinase A activation and BMP-stimulated PAEC migration needs eNOS activity. Importantly, BMP2 and BMP4 failed to stimulate eNOS phosphorylation/activation in PAECs collected from PAH patients with BMPRII gene mutations [30].

Endothelial cell mitochondrial metabolism is also affected in PAH. A shift from oxidative phosphorylation to glycolysis was reported [1]. Xu et al. [31] verified, through positron tomography scan, a significantly higher uptake of glucose in PAECs from patients with idiopathic PAH compared with ECs from controls. In addition, they demonstrated that oxygen consumption, the number of mitochondria *per* cell and the mitochondrial DNA content of idiopathic PAH endothelial cells were lower in comparison with ECs from control patients.

Alterations in the intracellular trafficking were also reported in PAH [32]. Histological and electron microscopy studies highlighted enlarged endoplasmic reticulum and Golgi stacks in pulmonary arterial lesions in human and in experimental (hypoxia and MCT) PAH [33,34]. In addition, the loss of the cell surface raft/caveolar protein caveolin-1 (cav-1) in ECs in MCT-induced PAH was shown [35]. Monocrotaline and hypoxia seem to disrupt the molecular machinery of vesicular trafficking at the level of Golgi tethers, SNAPS (soluble ATPase N-ethylmaleimide-sensitive factor association proteins) and SNARES (SNAP receptors) (Golgi blockade hypothesis) [36,37]. This disruption seems to result in the trapping of cav-1 in the Golgi of ECs, with consequent intracytoplasmic sequestration of eNOS and thus, reduction of NO production [36].

Currently, the endothelial dysfunction is a primary therapeutic target in PAH, being used drugs such as prostacyclin analogs, endothelin-1 receptor antagonists and phosphodiesterase type 5 (PDE-5) inhibitors to counteract this abnormality [38]. The first PGI_2 synthetic analog approved by the FDA was intravenous epoprostenol. Although being to date the only PAH therapy that was associated with a mortality benefit in a randomized clinical trial, epoprostenol administration might lead to catheter infections [38]. To overcome this, a more stable formulation of epoprostenol became recently available [39,40]. Treprostinil (subcutaneous, intravenous and inhaled) and iloprost (inhaled) were approved as PGI_2 analogs, also with some limitations. In the case of subcutaneous treprostinil, infusion site pain occurs in the majority of patients and inhaled iloprost needs to be administrated 6 to 9 times daily, up to 15 min each [38,41]. Currently, a phase III clinical trial is underway to evaluate the effect of an oral formulation of a PGI_2 receptor agonist named selexipag (GRIPHON trial; ClinicalTrials.gov Identifier: NCT01106014). Approved therapies targeting ET-1 pathway include the dual ET-1 receptor antagonist bosentan and the selective ET_A receptor antagonist ambrisentan, both available in oral formulations. In the case of bosentan, regular liver function tests are needed, once it is associated with an increased risk of liver dysfunction [38,41,42]. Macitentan is a new oral dual ET-1 receptor antagonist that presents an increased efficacy due to its high lipophilicity [38,43]. Sildenafil and tadalafil are oral PDE-5 inhibitors approved for the treatment of PAH. Side effects include headache, flushing, dyspepsia and myalgia [38,41]. Riociguat, a soluble guanylate cyclase stimulator, was evaluated in a phase III clinical trial and showed promising results [44]. Furthermore, fasudil [45,46] and dichloroacetate [47], a Rho kinase inhibitor and a pyruvate dehydrogenase kinase inhibitor, respectively, include drugs in development to the treatment of PAH. Dichloroacetate is in evaluation in a phase I clinical trial (ClinicalTrials.gov Identifier: NCT01083524) (see Table 1).

3. Smooth muscle cells

3.1. Role in pathophysiology of PAH

Vascular SMCs can present different phenotypes, depending on their functions. These phenotypes are characterized by differences in cell morphology, proliferation and migration rates and in the expression of protein markers [48,49]. The different phenotypes are seen in SMCs of different vessels as well as among SMCs within the same vessel [48]. A contractile SMC phenotype is typified by elongated cells, with a slow growth and migratory rates. On the contrary, synthetic SMCs have a rhomboid morphology and higher growth and migratory activities [50]. Once the protein markers used to identify SMCs are also expressed in other cell types in normal and pathologic situations, the recognition of these cells is sometimes a difficult task. Currently, the two protein markers most used to characterize a mature contractile SMC phenotype are smooth muscle-myosin heavy chain (SM-MHC) and smoothelin. SM-MHC expression has never been detected in non-SMCs in vivo. Smoothelin complements SM-MHC as a contractile SMC marker and appears to be more sensitive [10,48]. Other markers expressed in a contractile SMC include α-smooth muscle actin (α-SMA), desmin, smooth muscle-calponin and h-caldesmon. Synthetic SMCs express proteins like cellular retinol binding protein-1 and SMemb/non-muscle MHC isoform-B [48,51]. During vascular injury, SMCs "switch" from a contractile to a synthetic, proliferative phenotype to support vascular repair. Importantly, this phenotypic switch is often reversible. However, deregulation of this process can contribute to the vascular remodeling associated to PAH [52,53]. Discovering the mechanisms involved in the SMC phenotype modulation can help to control this "switch" process. Examples include pathways/mediators such as TGF-β, PDGF (platelet-derived growth factor), angiotensin II and TNF (tumor necrosis factor)-α [48]. PDGF-A and PDGF-B induce, in adult SMCs, a more synthetic phenotype [48]. Increased proliferation and migration of SMCs were observed in pig coronary arteries treated with PDGF-B [54]. In addition, PDGF-A and PDGF-B inhibition resulted in reduced SMC proliferation and migration in injured human artery [55,56]. Furthermore, TGF-β isoforms induce a contractile SMC phenotype [48]. Importantly, a recent study investigated the crosstalk between ECs and SMCs during low shear stress induced vascular remodeling and identified the factors TGF-β1 and PDGF-BB as important players in this process. The authors used an EC/SMC cocultured parallel-plate flow chamber system and each cell type was grown on the opposite sides of a porous membrane. Then shear stress was applied to ECs and the effects were observed. They reported that low shear stress induces the production of PDGF-BB and TGF-β1 by ECs and the proliferation and migration of ECs and SMCs. PDGF-BB was involved in the paracrine control of SMCs by ECs, and TGF-β1 participates in the feedback control from SMCs to ECs [57]. More recently, microRNAs (miRNAs) emerged as important modulators of SMC phenotype, and consequently as possible therapeutic targets in PAH-related vascular remodeling. These tissue and cell specific non-coding single-strand RNA molecules with approximately 19–25 nucleotides negatively regulate gene expression by base pairing to the 3′-untranslated region of mRNAs, avoiding their translation [58–60]. Several miRNAs seem to be differentially expressed during PAH development in the hypoxia and MCT-induced PAH and also in patients [61,62]. MiR-143, -145 and -204 are examples of miRNAs reported to be involved in SMC phenotype regulation. MiR-204 levels were found down-regulated in MCT and hypoxic PAH animal models [62]. In addition, in PASMCs from idiopathic PAH patients, miR-204 expression was also found to be reduced and increased levels of proliferation and lower levels of apoptosis were verified in comparison with control PASMCs. A synthetic miR-204 already showed its beneficial effects in the pulmonary arteries of MCT rats [61]. The expression of miR-143/145 was reported to be elevated in hypoxic PAH model and also in patients with heritable or idiopathic PAH. The increased expression of miR-143/145 was found to be related with PAH associated with BMPRII mutation, and so with BMP receptor function loss [63]. Importantly, BMP signaling pathway is known to induce miR-143/145 expression, and so these observations can be explained by the compensatory increase in TGF-β signaling pathway in response to the decrease in BMP signaling pathway, once TGF-β mediators also induce miR-143/145 expression [64].

3.2. Intracellular pathways modulated by PAH

Potassium (K^+) and calcium (Ca^{2+}) ions have been reported to play pivotal roles in both vasoconstriction and vascular remodeling in PAH [65]. When K^+ channels are blocked (or K^+ channels are down-regulated), PASMC membrane depolarizes and opens voltage-dependent Ca^{2+} channels (VDCC), promoting a Ca^{2+} influx, increasing $[Ca^{2+}]_{cyt}$ and causing PASMC vasoconstriction. Conversely, when K^+ channels are activated (or K^+ channel gene expression is up-regulated), the membrane hyperpolarizes and closes VDCC, inhibiting Ca^{2+} influx, decreasing $[Ca^{2+}]_{cyt}$ and causing vasodilatation [65–67]. Calcium is also an important second messenger that leads to cell proliferation and migration through the activation of transcription factors. In apoptosis, K^+ channels mediate the K^+ efflux that is necessary for apoptotic volume decrease (AVD). K^+ efflux also leads to the decrease of $[K^+]_{cyt}$, releasing the inhibition of caspases [65,67]. A defect in gene expression with attenuated function of Kv channels was reported in PASMCs from patients with pulmonary hypertension [68]. Thus, a decrease in K^+ channels gene expression and/or function stimulates PASMC proliferation by increasing $[Ca^{2+}]_{cyt}$ and inhibits PASMC apoptosis by decelerating AVD and attenuating cytoplasmic caspase activity [68]. Although numerous studies have investigated ion channels in PAH, little is known about the association between the two-pore domain K^+ channel, TASK-1, and human PASMCs. Tang et al. [69] reported the involvement of TASK-1 in the ET-1-mediated depolarization in human PASMCs. The authors concluded that ET-1 depolarizes primary human PASMCs by phosphorylating (inhibiting) TASK-1 by a mechanism in which ET-1 binds to the ET_A receptor, leading to the protein kinase C-induced phosphorylation of TASK-1 channels through phospholipase C, phosphatidylinositol 4, 5-biphosphate and diacylglycerol.

Unfortunately, only 10–15% of idiopathic PAH patients could benefit from long-term therapy with calcium channel blockers (CCBs) (nifedipine, diltiazem and amlodipine) [70,71]. During diagnosis by cardiac catheterization, patients perform an acute vasodilator test with agents such as nitric oxide, prostacyclin or adenosine. If the response to this test is positive (decrease of at least 10 mm Hg in the mean pulmonary arterial pressure, to a value of less than 40 mm Hg with an increased or unchanged cardiac output), the patient can benefit from CCB therapy [72,73].

4. Fibroblasts

4.1. Role in pathophysiology of PAH

Adventitia, the principal "injury-sensing tissue" of the vessel wall, undergoes several changes during PAH. Adventitia fibroblasts are able to proliferate with greater propensity than SMCs in response to injury, increasing extracellular matrix (ECM) component deposition, and synthesizing and releasing molecules that act on SMCs and ECs, and facilitate the recruitment of circulating leucocytes and progenitor cells. Thus, fibroblasts seem to contribute to inflammation and vascular remodeling linked to PAH [74,75].

4.2. Intracellular pathways modulated by PAH

The identification of fibroblasts is a tricky task, because of the lack of specificity and sensitivity of the markers used (vimentin and α-SMA). Vimentin does not distinguish fibroblasts from other cells of mesenchymal origin and α-SMA is only generally observed in activated fibroblasts. In addition, this last marker is observed in SMCs and in circulating smooth muscle precursors [75]. Activation of fibroblasts results in their differentiation into myofibroblasts, leading to the production of ECM proteins, such as collagen, fibronectin, tenascin and elastin. The appearance of myofibroblasts expressing α-SMA was observed in the adventitia in hypoxia-induced PAH [75]. In addition, an excessive deposition of ECM proteins in the adventitia in PAH was shown [76].

Glycosaminoglycans, like hyaluronic acid (HA), are components of the ECM that control SMC proliferation and differentiation. A study performed with idiopathic PAH human lung tissue, showed an increase in the expression of HA associated with increased hyaluronan synthase-1 (responsible for the synthesis of HA) and decreased hyaluronoglucosaminidase-1 (important in the degradation of HA) gene expression [77]. Aytekin et al. [78] verified that patients with idiopathic PAH have higher circulating levels of HA. They also showed that the expressions of HA synthase-2 and hyaluronidase-2 decrease in idiopathic PAH compared with controls. Thus, the decreased HA degradation seems to have a higher impact than the increased HA production in the elevated HA levels in PAH. It is known that HA has a variety of biological functions, which differ according to the molecular weight. HA degradation in high molecular mass (HMM) fragments (20.000–500 kDa) manifests immunosuppressant and anti-angiogenic activities. Conversely, low molecular mass (LMM) HA fragments (lower than 500 kDa) have been shown to stimulate inflammation and to promote EC and SMC proliferation and migration [79]. Once the accumulation of pro-inflammatory and pro-proliferative HA fragments resulting from matrix degradation can be associated with PAH-related inflammation and vascular remodeling, Ormiston et al. [80] studied the potential role of HA degradation at different stages of PAH progression in MCT-induced PAH. The authors found a generation of LMM HA at the early stages and an enhanced synthesis of HMM HA in advanced disease. Thus, the early generation of LMM HA fragments can lead to the inflammatory and proliferative modulation associated with PAH.

Matrix metalloproteinases (MMPs), a family of zinc enzymes produced by fibroblasts and macrophages and responsible for degradation of the ECM components, are also important to SMC and EC migration and proliferation. Excessive expression of MMPs may contribute to the pathogenesis of PAH, because MMPs may lead to fibroblast migration into the media and intima [75]. MMP activity was found to be up-regulated in adventitial fibroblasts in hypoxia and MCT-induced PAH [75,81]. Furthermore, also serine elastases can induce the release of growth factors from the ECM, promoting PASMC proliferation. Elastase activity was reported to be increased in PAH and serine elastase inhibitors already showed its beneficial effects in hypoxia and MCT-induced PAH [82–85].

5. Inflammatory cells

5.1. Role in pathophysiology of PAH

Inflammatory processes have been recognized as major pathogenic components of pulmonary vascular remodeling [86]. There are several observations demonstrating that inflammation performs a role in PAH development: i) association of inflammatory conditions such as connective tissue disorders and certain infections like human immunodeficiency virus with PAH; ii) accumulation of T cells, B cells and macrophages in plexiform lesions; iii) detection of auto-antibodies to ECs and fibroblasts, and iv) elevation in the circulating levels of certain cytokines and chemokines [1,11,87]. In addition, a study described an experimental model of antigen-induced pulmonary arterial muscularization, demonstrating that $CD4^+$ T cells, the IL-4-induced Th2 response, and endogenous IL-13 can be related with the vascular remodeling process [88].

5.2. Intracellular pathways modulated by PAH

Mast cells are implicated in inflammation and tissue remodeling. When activated, they produce several mediators including serotonin (5-HT), cytokines IL-6 and IL-13 and serine proteases chymase and tryptase that are capable to activate MMPs [89]. It was reported that mast cells are a rich source of IL-4, as well as other factors that can stimulate B-cells to secrete auto-antibodies, including anti-endothelial cell antibodies and its degranulation had been linked to the development

of pulmonary vascular remodeling in chronic hypoxic rats [90]. In addition, a study demonstrated that the accumulation and activation (degranulation) of mast cells in the lungs contribute to the development of PAH in MCT-rats and mast cell population was increased in idiopathic PAH patients compared with controls [91]. Also, Farha et al. [92] reported that mast cells may promote vascular remodeling, contributing to PAH in patients. In addition to mast cells, several other inflammatory cells like T cells, B cells and dendritic cells showed to have a role in PAH development [11,93]. Increased levels of certain cytokines, including IL-1β, IL-6 and TNF-α were observed in plasma of PAH patients [11,86,94]. Importantly, Hagen et al. [95] reported a negative feedback loop between IL-6 and the BMP pathway, mediated through p38 MAPK activity. Given the low penetrance of BMPRII mutations, alterations in other pathways may be needed to initiate PAH development and thus, the IL-6 activation can be considered an inflammatory "second hit" associated with the loss of BMP signaling that predisposes to PAH.

With the involvement of inflammation in PAH development, several anti-inflammatory and immunosuppressant therapies have emerged. Examples include rapamycin [96], tryptolide [97] and thymulin [98] that showed beneficial effects in PAH experimental models.

6. Platelets

6.1. Role in pathophysiology of PAH

Platelet dysfunction is a crucial contributor to PAH-related thrombosis [74]. In addition, also coagulation cascade abnormalities and endothelial cells seem to have a role on it. Underlying these alterations are increased levels of von Willebrand factor, plasma fibrinopeptide A, plasminogen activator inhibitor (PAI)-1, 5-HT and TXA_2, and decreased levels of tissue plasminogen activator (t-PA), thrombomodulin, NO, and PGI_2 [99,100]. Furthermore, a study recently evaluated, in PAH patients, the expression of PAR-1 (protease activator receptor-1), an important mediator of platelet activation by thrombin [101]. The authors found that the subpopulation of PAH patients that presented lower platelet counts seems to have increased platelet membrane expression of PAR-1 and PAR-mediated surface exposure of P-selectin (an adhesion molecule involved in inflammation and thrombosis), which may represent increased propensity to thrombosis.

6.2. Intracellular pathways modulated by PAH

Platelets have secretory granules which contain stored proteins and small molecules that are released in a regulated manner upon stimulation [102]. Dense granules store molecules such as ATP, ADP, 5-HT, glutamate, calcium and pyrophosphate. Alpha granules contain an extensive list of proteins, such as platelet-factor 4 (PF4/CXCL4), RANTES (CCL5), IL-1α and IL-1β, TGF-β and TNF-α [102]. Thus, platelet activation in PAH not only promotes thrombosis but also leads to the release of granule content, including mitogenic agents and vasoconstrictive substances, such as serotonin [103].

The beneficial effects of several drugs targeting the mechanisms associated with thrombosis support the important role of this process in PAH development. Examples of these drugs include thromboxane synthesis inhibitors, such as ozagrel and furegrelate. The first showed positive effects in a patient with portopulmonary hypertension and the second was tested in a hypoxia PAH experimental model [104,105].

7. Interplay between cell types involved in PAH pathogenesis

Although the mechanisms that lead to pulmonary arterial hypertension are still poorly understood, it is known that the interaction between vascular cells, inflammatory cells and platelets is involved in the structural changes that culminate in an increased pulmonary arterial pressure. This interplay is regulated by several mediators, which are highlighted in Fig. 2.

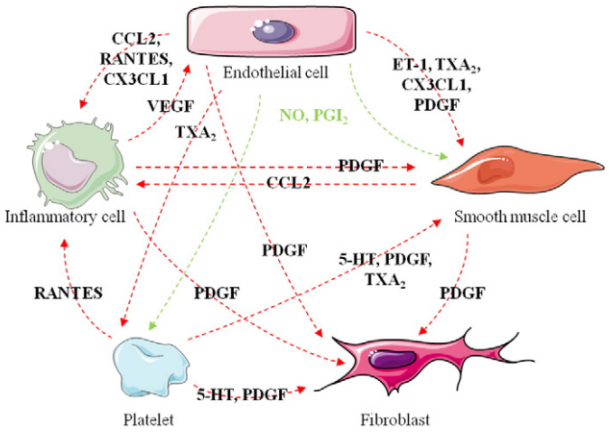

Fig. 2. Interplay between endothelial, smooth muscle and inflammatory cells, platelets and fibroblasts in pulmonary arterial hypertension. Green arrows denote the interaction between endothelial cells, platelets and smooth muscle cells, mediated by NO and PGI_2, which leads to vasodilator, anti-proliferative and anti-platelet aggregation effects. Red arrows show the interactions mediated by several mediators associated with vasoconstriction, proliferation, migration and platelet aggregation. Figure made with Servier Medical Art.

The vascular remodeling, mainly characterized by an excessive cell proliferation and a reduced apoptosis, is one of the most important features of PAH. For this structural change, ECs contribute with a pivotal role, producing and releasing mediators such as NO, PGI_2, ET-1 and TXA_2 that control platelet and SMC behavior. In addition to changes in the production levels of these mediators, also the increased endothelial barrier permeability counts to the PAH vascular alterations, by exposing the neighboring cells to these mediators [20,106].

Nitric oxide is synthesized in the endothelial cells from L-arginine by eNOS. Upon its release by endothelium, NO diffuses into vascular SMCs where it stimulates soluble guanylate cyclase (sGC) to produce the second messenger cyclic guanosine monophosphate (cGMP) from guanosine triphosphate (GTP), which has vasodilatory, anti-proliferative and anti-platelet aggregation properties [2]. The NO pathway is impaired in several ways in PAH. eNOS expression is depressed [107] and phosphodiesterase type 5 is increased in PASMCs, which leads to inactivation of cGMP [108]. The production of endogenous NOS inhibitors, asymmetrical and symmetrical dimethylarginines (ADMA and SDMA, respectively), is enhanced in PAH [109]. In addition, sGC expression is up-regulated in human PAH, as a compensatory mechanism [110]. In addition to eNOS, also iNOS (inducible NOS) seems to have a role in PAH, once a recent study reported that iNOS inhibition protected against PAH [111].

Prostaglandin, generated from arachidonic acid by fatty acid cyclooxygenase, is a substrate for both prostacyclin synthase and thromboxane synthase. Prostacyclin synthase generates PGI_2 in PAECs, which relaxes and inhibits the proliferation of vascular SMCs, and also inhibits platelet aggregation, via the stimulation of cAMP production [2]. Analysis of urinary metabolites of PGI_2 showed a decrease in the amount of excreted 6-ketoprostaglandin F1α, a prostacyclin inactive metabolite, in patients with idiopathic PAH [112]. Moreover, PAECs of PAH patients are characterized by reduced expression of prostacyclin synthase [113]. Prostacyclin receptor expression is also reduced in PASMCs [114]. Thromboxane synthase generates TXA_2, which stimulates SMC vasoconstriction and proliferation and platelet aggregation via thromboxane receptors [2]. An increase in the urinary excretion of 11-dehydrothromboxane B_2 (a stable metabolite of thromboxane A_2) [112] and in total body synthesis of TXA_2 in patients with idiopathic PAH was verified [115].

Endothelin-1 is mainly produced by ECs and acts via two receptors: ET_A and ET_B. Both receptors are found in PASMCs and mediate vasoconstriction and proliferation, whereas only the ET_B receptor is present in

ECs and mediates NO and PGI_2 release, leading to vasodilatation [116,117]. Lung and circulating ET-1 levels are increased in PAH patients [118]. Another mediator responsible for cell proliferation is PDGF, synthesized and released by several cell types (SMCs, ECs, macrophages and platelets). The expression of PDGF and its receptors was reported to be increased in the pulmonary arteries of PAH patients [119], contributing to a higher proliferation rate of SMCs and fibroblasts. Platelets also contribute to vascular remodeling through the release of factors such as PDGF, TXA_2 and 5-HT that act on fibroblasts and SMCs leading to vasoconstriction, proliferation and migration. Cellular migration is also reported in PAH and is associated with vascular wall thickness. Myofibroblasts are able to migrate from the adventitia to the media and to the intima, thus contributing to the thickening of these components. For this cell migration MMPs secreted by fibroblasts and macrophages might also contribute by degrading ECM components [75,120].

Thrombosis in small peripheral pulmonary arteries also contributes to PAH. In addition to platelets, ECs are directly involved in this process. Endothelial cells participate in the coagulation process by activating the factor X and the extrinsic pathway of coagulation via release of tissue factor. ECs also produce and release von Willebrand factor that attracts and activates platelets [121]. On the other hand, ECs can also inhibit thrombosis and promote fibrinolysis. They produce and release NO and PGI_2, two important inhibitors of platelet aggregation, preventing thrombosis. Endothelial cells participate in the fibrinolytic process through the synthesis and release of the profibrinolytic t-PA that activates plasminogen in the fibrinolytic cascade. In addition, ECs also produce the antifibrinolytic/prothrombotic PAI-1 [121]. Thus, ECs are important regulators of the balance between prothrombotic and antithrombotic processes.

PAH-related vasoconstriction also results from the interplay between several cells, including ECs, SMCs and platelets. Endothelial cells produce and release vasoconstriction mediators such as ET-1 and TXA_2 that act in SMCs and platelets [2]. On the other hand, platelets release 5-HT and TXA_2 that can act on SMCs and fibroblasts [121]. Serotonin is produced by the gastrointestinal tract enterochromaffin cells and pulmonary neuroepithelial bodies and stored in platelets [122]. It is taken up by the serotonin transporter (5-HTT or SERT) and the serotonin receptors ($5\text{-}HT_{1B}$, $5\text{-}HT_{2A}$ and $5\text{-}HT_{2B}$) in the pulmonary artery smooth muscle, endothelial cells and fibroblasts [123]. Serotonin is a vasoconstrictor that stimulates the proliferation of SMCs and fibroblasts [123,124]. A significant rise of 5-HT in plasma is observed in pulmonary hypertensive patients and the level in platelets is low [125].

In response to inflammatory/injury events, vascular cells (ECs and SMCs) can produce mediators such as cytokines and chemokines (soluble cytokines with chemoattractant function) that will be responsible for the recruitment of inflammatory cells (T cells, B cells, macrophages, dendritic cells, mast cells). These inflammatory cells can thereby continue the release of chemokines, cytokines and also growth factors, such as VEGF (vascular endothelial growth factor), which will promote EC proliferation and migration and resistance to apoptosis, contributing to the vascular remodeling [11]. Endothelial cells and SMCs are reported to release the chemokine CCL2/MCP-1 (monocyte chemotactic protein-1). The same study showed an increase in CCL2 levels in plasma and lung tissue of idiopathic PAH patients. In addition, it also showed that monocyte migration was higher in the presence of ECs from PAH patients in comparison with controls. Furthermore, ECs from PAH patients also seem to be responsible for the production and release of RANTES (Regulated upon Activation, Normal T cell Expressed and Secreted)/CCL5 in PAH patients. An increased expression of RANTES mRNA was observed in lung tissue from PAH patients [126]. Pulmonary artery ECs from PAH patients also expressed the chemokine FKN (fractalkine/CX3CL1). Elevated FKN plasma levels and an increase in FKN mRNA expression in lung tissue were observed in PAH patients, in comparison with controls. In addition, the FKN receptor (CX3CR1) expression was found to be increased in vascular SMCs and in circulating T-cells from PAH patients. Fractalkine was found to induce proliferation but not migration of cultured rat PASMCs [127,128].

8. Conclusions

Despite the success of PAH stabilization with the current medical therapy targeting pulmonary vascular tone, this disease remains associated to a poor prognosis. Furthermore, most of the alternative/novel therapeutic approaches have been studied in experimental models, and once there is no ideal animal model, the translation of data to humans is challenging. Therefore, we are still tracking the best treatment for PAH. Considering that disease progression is driven by a cellular interplay at the pulmonary artery wall that leads to vasoconstriction, thrombosis, inflammation and vascular remodeling, we believe that an effective treatment must target PAH-related cellular features.

Acknowledgements

This work was supported by Fundação para a Ciência e a Tecnologia (FCT, Portugal), European Union, QREN, FEDER and COMPETE for funding the Organic Chemistry Research Unit (QOPNA) (project PEst-C/QUI/UI0062/2013; FCOMP-01-0124-FEDER-037296), the Cardiovascular R&D Unit (project PEst-C/SAU/UI0051/2011) and the post-graduation student (grant number SFRH/BD/91067/2012).

References

[1] S.L. Archer, E.K. Weir, M.R. Wilkins, Basic science of pulmonary arterial hypertension for clinicians: new concepts and experimental therapies, Circulation 121 (2010) 2045–2066.
[2] M.R. Wilkins, Pulmonary hypertension: the science behind the disease spectrum, Eur. Respir. Rev. 21 (2012) 19–26.
[3] P. Yildiz, Molecular mechanisms of pulmonary hypertension, Clin. Chim. Acta 403 (2009) 9–16.
[4] G. Simonneau, I.M. Robbins, M. Beghetti, R.N. Channick, M. Delcroix, C.P. Denton, C.G. Elliott, S.P. Gaine, M.T. Gladwin, Z.C. Jing, M.J. Krowka, D. Langleben, N. Nakanishi, R. Souza, Updated clinical classification of pulmonary hypertension, J. Am. Coll. Cardiol. 54 (2009) S43–S54.
[5] R.T. Schermuly, H.A. Ghofrani, M.R. Wilkins, F. Grimminger, Mechanisms of disease: pulmonary arterial hypertension, Nat. Rev. Cardiol. 8 (2011) 443–455.
[6] N. Galiè, A. Torbicki, R. Barst, P. Dartevelle, S. Haworth, T. Higenbottam, H. Olschewski, A. Peacock, G. Pietra, L.J. Rubin, G. Simonneau, Guidelines on diagnosis and treatment of pulmonary arterial hypertension, Eur. Heart J. 25 (2004) 2243–2278.
[7] J.P. Ward, Oxygen sensors in context, Biochim. Biophys. Acta 1777 (2008) 1–14.
[8] P. Fraisl, M. Mazzone, T. Schmidt, P. Carmeliet, Regulation of angiogenesis by oxygen and metabolism, Dev. Cell 16 (2009) 167–179.
[9] J.H. Haga, Y.S. Li, S. Chien, Molecular basis of the effects of mechanical stretch on vascular smooth muscle cells, J. Biomech. 40 (2007) 947–960.
[10] T. Stevens, S. Phan, M.G. Frid, D. Alvarez, E. Herzog, K.R. Stenmark, Lung vascular cell heterogeneity: endothelium, smooth muscle, and fibroblasts, Proc. Am. Thorac. Soc. 5 (2008) 783–791.
[11] S.S. Pullamsetti, R. Savai, W. Janssen, B.K. Dahal, W. Seeger, F. Grimminger, H.A. Ghofrani, N. Weissmann, R.T. Schermuly, Inflammation, immunological reaction and role of infection in pulmonary hypertension, Clin. Microbiol. Infect. 17 (2011) 7–14.
[12] S. Sakao, K. Tatsumi, N.F. Voelkel, Endothelial cells and pulmonary arterial hypertension: apoptosis, proliferation, interaction and transdifferentiation, Respir. Res. 10 (2009) 95.
[13] C. Urbich, S. Dimmeler, Endothelial progenitor cells, Circ. Res. 95 (2004) 343–353.
[14] G.-P. Diller, T. Thum, M.R. Wilkins, J. Wharton, Endothelial progenitor cells in pulmonary arterial hypertension, Trends Cardiovasc. Med. 20 (2010) 22–29.
[15] X.-X. Wang, F.-R. Zhang, Y.-P. Shang, J.-H. Zhu, X.-D. Xie, Q.-M. Tao, J.-H. Zhu, J.-Z. Chen, Transplantation of autologous endothelial progenitor cells may be beneficial in patients with idiopathic pulmonary arterial hypertension: a pilot randomized controlled trial, J. Am. Coll. Cardiol. 49 (2007) 1566–1571.
[16] J.H. Zhu, X.X. Wang, F.R. Zhang, Y.P. Shang, Q.M. Tao, J.Z. Chen, Safety and efficacy of autologous endothelial progenitor cells transplantation in children with idiopathic pulmonary arterial hypertension: open-label pilot study, Pediatr. Transplant. 12 (2008) 650–655.
[17] M. Toshner, R. Voswinckel, M. Southwood, R. Al-Lamki, L.S. Howard, D. Marchesan, J. Yang, J. Suntharalingam, E. Soon, A. Exley, S. Stewart, M. Hecker, Z. Zhu, U. Gehling, W. Seeger, J. Pepke-Zaba, N.W. Morrell, Evidence of dysfunction of endothelial progenitors in pulmonary arterial hypertension, Am. J. Respir. Crit. Care Med. 180 (2009) 780–787.
[18] C.K. Sun, Y.C. Lin, C.M. Yuen, S. Chua, L.T. Chang, J.J. Sheu, F.Y. Lee, M. Fu, S. Leu, H.K. Yip, Enhanced protection against pulmonary hypertension with sildenafil and endothelial progenitor cell in rats, Int. J. Cardiol. 162 (2011) 45–58.
[19] M.L. Ormiston, Y. Deng, D.J. Stewart, D.W. Courtman, Innate immunity in the therapeutic actions of endothelial progenitor cells in pulmonary hypertension, Am. J. Respir. Cell Mol. Biol. 43 (2010) 546–554.

[20] N.W. Morrell, S. Adnot, S.L. Archer, J. Dupuis, P. Lloyd Jones, M.R. MacLean, I.F. McMurtry, K.R. Stenmark, P.A. Thistlethwaite, N. Weissmann, J.X.J. Yuan, E.K. Weir, Cellular and molecular basis of pulmonary arterial hypertension, J. Am. Coll. Cardiol. 54 (2009) S20–S31.

[21] C. Csortos, I. Kolosova, A.D. Verin, Regulation of vascular endothelial cell barrier function and cytoskeleton structure by protein phosphatases of the PPP family, Am. J. Physiol. Lung Cell. Mol. Physiol. 293 (2007) L843–L854.

[22] V.J. Burton, L.I. Ciuclan, A.M. Holmes, D.M. Rodman, C. Walker, D.C. Budd, Bone morphogenetic protein receptor II regulates pulmonary artery endothelial cell barrier function, Blood 117 (2011) 333–341.

[23] J.W. Lowery, M.P. de Caestecker, BMP signaling in vascular development and disease, Cytokine Growth Factor Rev. 21 (2010) 287–298.

[24] J. Cai, E. Pardali, G. Sanchez-Duffhues, P. ten Dijke, BMP signaling in vascular diseases, FEBS Lett. 586 (2012) 1993–2002.

[25] R.J. Davies, N.W. Morrell, Molecular mechanisms of pulmonary arterial hypertension: role of mutations in the bone morphogenetic protein type II receptor, Chest 134 (2008) 1271–1277.

[26] R.D. Machado, M.A. Aldred, V. James, R.E. Harrison, B. Patel, E.C. Schwalbe, E. Gruenig, B. Janssen, R. Koehler, W. Seeger, O. Eickelberg, H. Olschewski, C. Gregory Elliott, E. Glissmeyer, J. Carlquist, M. Kim, A. Torbicki, A. Fijalkowska, G. Szewczyk, J. Parma, M.J. Abramowicz, N. Galie, H. Morisaki, S. Kyotani, N. Nakanishi, T. Morisaki, M. Humbert, G. Simonneau, O. Sitbon, F. Soubrier, F. Coulet, N.W. Morrell, R.C. Trembath, Mutations of the TGF-β type II receptor BMPR2 in pulmonary arterial hypertension, Hum. Mutat. 27 (2006) 121–132.

[27] C. Atkinson, S. Stewart, P.D. Upton, R. Machado, J.R. Thomson, R.C. Trembath, N.W. Morrell, Primary pulmonary hypertension is associated with reduced pulmonary vascular expression of type II bone morphogenetic protein receptor, Circulation 105 (2002) 1672–1678.

[28] K. Teichert-Kuliszewska, M.J.B. Kutryk, M.A. Kuliszewski, G. Karoubi, D.W. Courtman, L. Zucco, J. Granton, D.J. Stewart, Bone morphogenetic protein receptor-2 signaling promotes pulmonary arterial endothelial cell survival, Circ. Res. 98 (2006) 209–217.

[29] G. Valdimarsdottir, M.-J. Goumans, A. Rosendahl, M. Brugman, S. Itoh, F. Lebrin, P. Sideras, P. ten Dijke, Stimulation of Id1 expression by bone morphogenetic protein is sufficient and necessary for bone morphogenetic protein-induced activation of endothelial cells, Circulation 106 (2002) 2263–2270.

[30] A. Gangopahyay, M. Oran, E.M. Bauer, J.W. Wertz, S.A. Comhair, S.C. Erzurum, P.M. Bauer, Bone morphogenetic protein receptor II is a novel mediator of endothelial nitric-oxide synthase activation, J. Biol. Chem. 286 (2011) 33134–33140.

[31] W. Xu, T. Koeck, A.R. Lara, D. Neumann, F.P. DiFilippo, M. Koo, A.J. Janocha, F.A. Masri, A.C. Arroliga, C. Jennings, R.A. Dweik, R.M. Tuder, D.J. Stuehr, S.C. Erzurum, Alterations of cellular bioenergetics in pulmonary artery endothelial cells, Proc. Natl. Acad. Sci. U. S. A. 104 (2007) 1342–1347.

[32] P.B. Sehgal, J.E. Lee, Protein trafficking dysfunctions: role in the pathogenesis of pulmonary arterial hypertension, Pulm. Circ. 1 (2011) 17–32.

[33] P.B. Sehgal, S. Mukhopadhyay, Pulmonary arterial hypertension: a disease of tethers, SNAREs and SNAPs? Am. J. Physiol. Heart Circ. Physiol. 293 (2007) H77–H85.

[34] J.S. Bonifacino, B.S. Glick, The mechanisms of vesicle budding and fusion, Cell 116 (2004) 153–166.

[35] R. Mathew, J. Huang, M. Shah, K. Patel, M. Gewitz, P.B. Sehgal, Disruption of endothelial-cell caveolin-1α/raft scaffolding during development of monocrotaline-induced pulmonary hypertension, Circulation 110 (2004) 1499–1506.

[36] S. Mukhopadhyay, F. Xu, P.B. Sehgal, Aberrant cytoplasmic sequestration of eNOS in endothelial cells after monocrotaline, hypoxia, and senescence: live-cell caveolar and cytoplasmic NO imaging, Am. J. Physiol. Heart Circ. Physiol. 292 (2007) H1373–H1389.

[37] P.B. Sehgal, S. Mukhopadhyay, F. Xu, K. Patel, M. Shah, Dysfunction of Golgi tethers, SNAREs, and SNAPs in monocrotaline-induced pulmonary hypertension, Am. J. Physiol. Lung Cell. Mol. Physiol. 292 (2007) L1526–L1542.

[38] D. Montani, M.C. Chaumais, C. Guignabert, S. Gunther, B. Girerd, X. Jais, V. Algalarrondo, L.C. Price, L. Savale, O. Sitbon, G. Simonneau, M. Humbert, Targeted therapies in pulmonary arterial hypertension, Pharmacol. Ther. 141 (2014) 172–191.

[39] A. Fuentes, A. Coralic, K.L. Dawson, A new epoprostenol formulation for the treatment of pulmonary arterial hypertension, Am. J. Health Syst. Pharm. 69 (2012) 1389–1393.

[40] O. Lambert, D. Bandilla, Stability and preservation of a new formulation of epoprostenol sodium for treatment of pulmonary arterial hypertension, Drug Des. Devel. Ther. 6 (2012) 235–244.

[41] A. Seferian, G. Simonneau, Therapies for pulmonary arterial hypertension: where are we today, where do we go tomorrow? Eur. Respir. Rev. 22 (2013) 217–226.

[42] Y. Wu, D.S. O'Callaghan, M. Humbert, An update on medical therapy for pulmonary arterial hypertension, Curr. Hypertens. Rep. 15 (2013) 614–622.

[43] T. Pulido, I. Adzerikho, R.N. Channick, M. Delcroix, N. Galiè, H.-A. Ghofrani, P. Jansa, Z.-C. Jing, F.-O. Le Brun, S. Mehta, C.M. Mittelholzer, L. Perchenet, B.K.S. Sastry, O. Sitbon, R. Souza, A. Torbicki, X. Zeng, L.J. Rubin, G. Simonneau, Macitentan and morbidity and mortality in pulmonary arterial hypertension, N. Engl. J. Med. 369 (2013) 809–818.

[44] H.-A. Ghofrani, N. Galiè, F. Grimminger, E. Grünig, M. Humbert, Z.-C. Jing, A.M. Keogh, D. Langleben, M.O. Kilama, A. Fritsch, D. Neuser, L.J. Rubin, Riociguat for the treatment of pulmonary arterial hypertension, N. Engl. J. Med. 369 (2013) 330–340.

[45] H. Fujita, Y. Fukumoto, K. Saji, K. Sugimura, J. Demachi, J. Nawata, H. Shimokawa, Acute vasodilator effects of inhaled fasudil, a specific Rho-kinase inhibitor, in patients with pulmonary arterial hypertension, Heart Vessels 25 (2010) 144–149.

[46] V. Gupta, N. Gupta, I.H. Shaik, R. Mehvar, I.F. McMurtry, M. Oka, E. Nozik-Grayck, M. Komatsu, F. Ahsan, Liposomal fasudil, a rho-kinase inhibitor, for prolonged pulmonary preferential vasodilation in pulmonary arterial hypertension, J. Control. Release 167 (2013) 189–199.

[47] V.V. McLaughlin, Looking to the future: a new decade of pulmonary arterial hypertension therapy, Eur. Respir. Rev. 20 (2011) 262–269.

[48] S.S. Rensen, P.A. Doevendans, G.J. van Eys, Regulation and characteristics of vascular smooth muscle cell phenotypic diversity, Neth. Heart J. 15 (2007) 100–108.

[49] K. Kawai-Kowase, G.K. Owens, Multiple repressor pathways contribute to phenotypic switching of vascular smooth muscle cells, Am. J. Physiol. Cell Physiol. 292 (2007) C59–C69.

[50] H. Hao, G. Gabbiani, M.-L. Bochaton-Piallat, Arterial smooth muscle cell heterogeneity, Arterioscler. Thromb. Vasc. 23 (2003) 1510–1520.

[51] A.J. Halayko, J. Solway, Invited review: molecular mechanisms of phenotypic plasticity in smooth muscle cells, J. Appl. Physiol. 90 (2001) 358–368.

[52] E.M. Rzucidlo, K.A. Martin, R.J. Powell, Regulation of vascular smooth muscle cell differentiation, J. Vasc. Surg. 45 (2007) A25–A32.

[53] S.J. House, M. Potier, J. Bisaillon, H.A. Singer, M. Trebak, The non-excitable smooth muscle: calcium signaling and phenotypic switching during vascular disease, Pflugers Arch. 456 (2008) 769–785.

[54] H. Hao, P. Ropraz, V. Verin, E. Camenzind, A. Geinoz, M.S. Pepper, G. Gabbiani, M.-L. Bochaton-Piallat, Heterogeneity of smooth muscle cell populations cultured from pig coronary artery, Arterioscler. Thromb. Vasc. 22 (2002) 1093–1099.

[55] M. Kotani, N. Fukuda, H. Ando, W.-Y. Hu, S. Kunimoto, S. Saito, K. Kanmatsuse, Chimeric DNA–RNA hammerhead ribozyme targeting PDGF A-chain mRNA specifically inhibits neointima formation in rat carotid artery after balloon injury, Cardiovasc. Res. 57 (2003) 265–276.

[56] J. Deguchi, T. Namba, H. Hamada, T. Nakaoka, J. Abe, O. Sato, T. Miyata, M. Makuuchi, K. Kurokawa, Y. Takuwa, Targeting endogenous platelet-derived growth factor B-chain by adenovirus-mediated gene transfer potently inhibits in vivo smooth muscle proliferation after arterial injury, Gene Ther. 6 (1999) 956–965.

[57] Y.X. Qi, J. Jiang, X.H. Jiang, X.D. Wang, S.Y. Ji, Y. Han, D.K. Long, B.R. Shen, Z.Q. Yan, S. Chien, Z.L. Jiang, PDGF-BB and TGF-{beta}1 on cross-talk between endothelial and smooth muscle cells in vascular remodeling induced by low shear stress, Proc. Natl. Acad. Sci. U. S. A. 108 (2011) 1908–1913.

[58] K. Yuan, M. Orcholski, X. Tian, X. Liao, V.A. de Jesus Perez, MicroRNAs: promising therapeutic targets for the treatment of pulmonary arterial hypertension, Expert Opin. Ther. Targets 17 (2013) 557–564.

[59] Y. Wang, X.Y. Xue, Y.X. Liu, K.F. Wang, X.F. Zang, J. Wang, P.L. Wang, J. Zhang, L. Pan, S.Y. Zhang, J.X. Wang, Pulmonary arterial hypertension and microRNAs—an ever-growing partnership, Arch. Med. Res. 44 (2013) 483–487.

[60] J.S. Grant, K. White, M.R. Maclean, A.H. Baker, MicroRNAs in pulmonary arterial remodeling, Cell. Mol. Life Sci. 70 (2013) 4479–4494.

[61] A. Courboulin, R. Paulin, N.J. Giguere, N. Saksouk, T. Perreault, J. Meloche, E.R. Paquet, S. Biardel, S. Provencher, J. Cote, M.J. Simard, S. Bonnet, Role for miR-204 in human pulmonary arterial hypertension, J. Exp. Med. 208 (2011) 535–548.

[62] P. Caruso, M.R. MacLean, R. Khanin, J. McClure, E. Soon, M. Southgate, R.A. MacDonald, J.A. Greig, K.E. Robertson, R. Masson, L. Denby, Y. Dempsie, L. Long, N.W. Morrell, A.H. Baker, Dynamic changes in lung microRNA profiles during the development of pulmonary hypertension due to chronic hypoxia and monocrotaline, Arterioscler. Thromb. Vasc. 30 (2010) 716–723.

[63] P. Caruso, Y. Dempsie, H.C. Stevens, R.A. McDonald, L. Long, R. Lu, K. White, K.M. Mair, J.D. McClure, M. Southwood, P. Upton, M. Xin, E. van Rooij, E.N. Olson, N.W. Morrell, M.R. MacLean, A.H. Baker, A role for miR-145 in pulmonary arterial hypertension: evidence from mouse models and patient samples, Circ. Res. 111 (2012) 290–300.

[64] B.N. Davis-Dusenbery, M.C. Chan, K.E. Reno, A.S. Weisman, M.D. Layne, G. Lagna, A. Hata, Down-regulation of Kruppel-like factor-4 (KLF4) by microRNA-143/145 is critical for modulation of vascular smooth muscle cell phenotype by transforming growth factor-beta and bone morphogenetic protein 4, J. Biol. Chem. 286 (2011) 28097–28110.

[65] E.D. Burg, C.V. Remillard, J.X. Yuan, Potassium channels in the regulation of pulmonary artery smooth muscle cell proliferation and apoptosis: pharmacotherapeutic implications, Br. J. Pharmacol. 153 (Suppl. 1) (2008) S99–S111.

[66] R.A. Fernandez, P. Sundivakkam, K.A. Smith, A.S. Zeifman, A.R. Drennan, J.X. Yuan, Pathogenic role of store-operated and receptor-operated Ca(2+) channels in pulmonary arterial hypertension, J. Signal Transduct. 2012 (2012) 951497.

[67] F.K. Kuhr, K.A. Smith, M.Y. Song, I. Levitan, J.X. Yuan, New mechanisms of pulmonary arterial hypertension: role of Ca(2)(+) signaling, Am. J. Physiol. Heart Circ. Physiol. 302 (2012) H1546–H1562.

[68] M. Mandegar, J.X.J. Yuan, Role of K+ channels in pulmonary hypertension, Vasc. Pharmacol. 38 (2002) 25–33.

[69] B. Tang, Y. Li, C. Nagaraj, R.E. Morty, S. Gabor, E. Stacher, R. Voswinckel, N. Weissmann, K. Leithner, H. Olschewski, A. Olschewski, Endothelin-1 inhibits background two-pore domain channel TASK-1 in primary human pulmonary artery smooth muscle cells, Am. J. Respir. Cell Mol. Biol. 41 (2009) 476–483.

[70] R.S. Baliga, R.J. MacAllister, A.J. Hobbs, New perspectives for the treatment of pulmonary hypertension, Br. J. Pharmacol. 163 (2011) 125–140.

[71] H. Gupta, G. Ghimire, R. Naeije, The value of tools to assess pulmonary arterial hypertension, Eur. Respir. Rev. 20 (2011) 222–235.

[72] O. Sitbon, M. Humbert, X. Jais, V. Ioos, A.M. Hamid, S. Provencher, G. Garcia, F. Parent, P. Herve, G. Simonneau, Long-term response to calcium channel blockers in idiopathic pulmonary arterial hypertension, Circulation 111 (2005) 3105–3111.

[73] N. Galie, M.M. Hoeper, M. Humbert, A. Torbicki, J.L. Vachiery, J.A. Barbera, M. Beghetti, P. Corris, S. Gaine, J.S. Gibbs, M.A. Gomez-Sanchez, G. Jondeau, W.

Klepetko, C. Opitz, A. Peacock, L. Rubin, M. Zellweger, G. Simonneau, Guidelines for the diagnosis and treatment of pulmonary hypertension: the Task Force for the Diagnosis and Treatment of Pulmonary Hypertension of the European Society of Cardiology (ESC) and the European Respiratory Society (ERS), endorsed by the International Society of Heart and Lung Transplantation (ISHLT), Eur. Heart J. 30 (2009) 2493–2537.
[74] M. Prabha, H.F. Jin, Y. Tian, C.S. Tang, J.B. Du, Mechanisms responsible for pulmonary hypertension, Chin. Med. J. (Engl.) 121 (2008) 2604–2609.
[75] K.R. Stenmark, N. Davie, M. Frid, E. Gerasimovskaya, M. Das, Role of the adventitia in pulmonary vascular remodeling, Physiology (Bethesda) 21 (2006) 134–145.
[76] A.G. Durmowicz, W.C. Parks, D.M. Hyde, R.P. Mecham, K.R. Stenmark, Persistence, re-expression, and induction of pulmonary arterial fibronectin, tropoelastin, and type I procollagen mRNA expression in neonatal hypoxic pulmonary hypertension, Am. J. Pathol. 145 (1994) 1411–1420.
[77] E. Papakonstantinou, F.M. Kouri, G. Karakiulakis, I. Klagas, O. Eickelberg, Increased hyaluronic acid content in idiopathic pulmonary arterial hypertension, Eur. Respir. J. 32 (2008) 1504–1512.
[78] M. Aytekin, S.A.A. Comhair, C. de la Motte, S.K. Bandyopadhyay, C.F. Farver, V.C. Hascall, S.C. Erzurum, R.A. Dweik, High levels of hyaluronan in idiopathic pulmonary arterial hypertension, Am. J. Physiol. Lung Cell. Mol. Physiol. 295 (2008) L789–L799.
[79] K.A. Scheibner, M.A. Lutz, S. Boodoo, M.J. Fenton, J.D. Powell, M.R. Horton, Hyaluronan fragments act as an endogenous danger signal by engaging TLR2, J. Immunol. 177 (2006) 1272–1281.
[80] M.L. Ormiston, G.R. Slaughter, Y. Deng, D.J. Stewart, D.W. Courtman, The enzymatic degradation of hyaluronan is associated with disease progression in experimental pulmonary hypertension, Am. J. Physiol. Lung Cell. Mol. Physiol. 298 (2010) L148–L157.
[81] E. Frisdal, V. Gest, A. Vieillard-Baron, M. Levame, H. Lepetit, S. Eddahibi, C. Lafuma, A. Harf, S. Adnot, M.P. Dortho, Gelatinase expression in pulmonary arteries during experimental pulmonary hypertension, Eur. Respir. J. 18 (2001) 838–845.
[82] L.J. Fu, A.Q. Zhou, J. Shen, W. Zhao, F. Li, Effect of elastase inhibitor on pulmonary hypertension induced by monocrotaline, Zhonghua Er Ke Za Zhi 42 (2004) 375–378.
[83] M. Rabinovitch, Elastase and the pathobiology of unexplained pulmonary hypertension, Chest 114 (1998) 213S–224S.
[84] K. Thompson, M. Rabinovitch, Exogenous leukocyte and endogenous elastases can mediate mitogenic activity in pulmonary artery smooth muscle cells by release of extracellular-matrix bound basic fibroblast growth factor, J. Cell. Physiol. 166 (1996) 495–505.
[85] S.H. Zaidi, X.M. You, S. Ciura, M. Husain, M. Rabinovitch, Overexpression of the serine elastase inhibitor elafin protects transgenic mice from hypoxic pulmonary hypertension, Circulation 105 (2002) 516–521.
[86] P.M. Hassoun, L. Mouthon, J.A. Barberà, S. Eddahibi, S.C. Flores, F. Grimminger, P.L. Jones, M.L. Maitland, E.D. Michelakis, N.W. Morrell, J.H. Newman, M. Rabinovitch, R. Schermuly, K.R. Stenmark, N.F. Voelkel, J.X.J. Yuan, M. Humbert, Inflammation, growth factors, and pulmonary vascular remodeling, J. Am. Coll. Cardiol. 54 (2009) S10–S19.
[87] N.W. Morrell, S.L. Archer, A. Defelice, S. Evans, M. Fiszman, T. Martin, M. Saulnier, M. Rabinovitch, R. Schermuly, D. Stewart, H. Truebel, G. Walker, K.R. Stenmark, Anticipated classes of new medications and molecular targets for pulmonary arterial hypertension, Pulm. Circ. 3 (2013) 226–244.
[88] E. Daley, C. Emson, C. Guignabert, R. de Waal Malefyt, J. Louten, V.P. Kurup, C. Hogaboam, L. Taraseviciene-Stewart, N.F. Voelkel, M. Rabinovitch, E. Grunig, G. Grunig, Pulmonary arterial remodeling induced by a Th2 immune response, J. Exp. Med. 205 (2008) 361–372.
[89] A.M. Gilfillan, J. Rivera, The tyrosine kinase network regulating mast cell activation, Immunol. Rev. 228 (2009) 149–169.
[90] A. Banasova, H. Maxova, V. Hampl, M. Vizek, V. Povysilova, J. Novotna, O. Vajnerova, O. Hnilickova, J. Herget, Prevention of mast cell degranulation by disodium cromoglycate attenuates the development of hypoxic pulmonary hypertension in rats exposed to chronic hypoxia, Respiration 76 (2008) 102–107.
[91] B.K. Dahal, D. Kosanovic, C. Kaulen, T. Cornitescu, R. Savai, J. Hoffmann, I. Reiss, H.A. Ghofrani, N. Weissmann, W.M. Kuebler, W. Seeger, F. Grimminger, R.T. Schermuly, Involvement of mast cells in monocrotaline-induced pulmonary hypertension in rats, Respir. Res. 12 (2011) 60.
[92] S. Farha, J. Sharp, K. Asosingh, M. Park, S.A. Comhair, W.H. Tang, J. Thomas, C. Farver, F. Hsieh, J.E. Loyd, S.C. Erzurum, Mast cell number, phenotype, and function in human pulmonary arterial hypertension, Pulm. Circ. 2 (2012) 220–228.
[93] L.C. Price, S.J. Wort, F. Perros, P. Dorfmuller, A. Huertas, D. Montani, S. Cohen-Kaminsky, M. Humbert, Inflammation in pulmonary arterial hypertension, Chest 141 (2012) 210–221.
[94] N. Selimovic, C.H. Bergh, B. Andersson, E. Sakiniene, H. Carlsten, B. Rundqvist, Growth factors and interleukin-6 across the lung circulation in pulmonary hypertension, Eur. Respir. J. 34 (2009) 662–668.
[95] M. Hagen, K. Fagan, W. Steudel, M. Carr, K. Lane, D.M. Rodman, J. West, Interaction of interleukin-6 and the BMP pathway in pulmonary smooth muscle, Am. J. Physiol. Lung Cell. Mol. Physiol. 292 (2007) L1473–L1479.
[96] T. Nishimura, J.L. Faul, G.J. Berry, I. Veve, R.G. Pearl, P.N. Kao, 40-O-(2-hydroxyethyl)-rapamycin attenuates pulmonary arterial hypertension and neointimal formation in rats, Am. J. Respir. Crit. Care Med. 163 (2001) 498–502.
[97] J.L. Faul, T. Nishimura, G.J. Berry, G.V. Benson, R.G. Pearl, P.N. Kao, Triptolide attenuates pulmonary arterial hypertension and neointimal formation in rats, Am. J. Respir. Crit. Care Med. 162 (2000) 2252–2258.
[98] T. Henriques-Coelho, S.M. Oliveira, R.S. Moura, R. Roncon-Albuquerque Jr., A.L. Neves, M. Santos, C. Nogueira-Silva, F. La Fuente Carvalho, A. Brandao-Nogueira, J. Correia-Pinto, A.F. Leite-Moreira, Thymulin inhibits monocrotaline-induced pulmonary hypertension modulating interleukin-6 expression and suppressing p38 pathway, Endocrinology 149 (2008) 4367–4373.
[99] V.V. McLaughlin, M.D. McGoon, Pulmonary arterial hypertension, Circulation 114 (2006) 1417–1431.
[100] K.S. Zanjani, Platelets in pulmonary hypertension: a causative role or a simple association? Iran. J. Pediatr. 22 (2012) 145–157.
[101] N.Y. Maeda, J.H. Carvalho, A.H. Otake, S.M.F. Mesquita, S.P. Bydlowski, A.A. Lopes, Platelet protease-activated receptor 1 and membrane expression of P-selectin in pulmonary arterial hypertension, Thromb. Res. 125 (2010) 38–43.
[102] G. Shi, C.N. Morrell, Platelets as initiators and mediators of inflammation at the vessel wall, Thromb. Res. 127 (2011) 387–390.
[103] H.W. Farber, J. Loscalzo, Prothrombotic mechanisms in primary pulmonary hypertension, J. Lab. Clin. Med. 134 (1999) 561–566.
[104] S.D. Hirenallur, N.D. Detweiler, S.T. Haworth, J.T. Leming, J.B. Gordon, N.J. Rusch, Furegrelate, a thromboxane synthase inhibitor, blunts the development of pulmonary arterial hypertension in neonatal piglets, Pulm. Circ. 2 (2012) 193–200.
[105] T. Maruyama, K. Ohsaki, S. Shimoda, Y. Kaji, M. Harada, Thromboxane-dependent portopulmonary hypertension, Am. J. Med. 118 (2005) 93–94.
[106] M. Humbert, D. Montani, F. Perros, P. Dorfmuller, S. Adnot, S. Eddahibi, Endothelial cell dysfunction and cross talk between endothelium and smooth muscle cells in pulmonary arterial hypertension, Vasc. Pharmacol. 49 (2008) 113–118.
[107] A. Giaid, D. Saleh, Reduced expression of endothelial nitric oxide synthase in the lungs of patients with pulmonary hypertension, N. Engl. J. Med. 333 (1995) 214–221.
[108] F. Murray, M.R. MacLean, N.J. Pyne, Increased expression of the cGMP-inhibited cAMP-specific (PDE3) and cGMP binding cGMP-specific (PDE5) phosphodiesterases in models of pulmonary hypertension, Br. J. Pharmacol. 137 (2002) 1187–1194.
[109] S. Pullamsetti, L. Kiss, H.A. Ghofrani, R. Voswinckel, P. Haredza, W. Klepetko, C. Aigner, L. Fink, J.P. Muyal, N. Weissmann, F. Grimminger, W. Seeger, R.T. Schermuly, Increased levels and reduced catabolism of asymmetric and symmetric dimethylarginines in pulmonary hypertension, FASEB J. 19 (2005) 1175–1177.
[110] R.T. Schermuly, J.-P. Stasch, S.S. Pullamsetti, R. Middendorff, D. Müller, K.-D. Schlüter, A. Dingendorf, S. Hackemack, E. Kolosionek, C. Kaulen, R. Dumitrascu, N. Weissmann, J. Mittendorf, W. Klepetko, W. Seeger, H.A. Ghofrani, F. Grimminger, Expression and function of soluble guanylate cyclase in pulmonary arterial hypertension, Eur. Respir. J. 32 (2008) 881–891.
[111] M. Seimetz, N. Parajuli, A. Pichl, F. Veit, G. Kwapiszewska, F.C. Weisel, K. Milger, B. Egemnazarov, A. Turowska, B. Fuchs, S. Nikam, M. Roth, A. Sydykov, T. Medebach, W. Klepetko, P. Jaksch, R. Dumitrascu, H. Garn, R. Voswinckel, S. Kostin, W. Seeger, R.T. Schermuly, F. Grimminger, H.A. Ghofrani, N. Weissmann, Inducible NOS inhibition reverses tobacco-smoke-induced emphysema and pulmonary hypertension in mice, Cell 147 (2011) 293–305.
[112] B.W. Christman, C.D. McPherson, J.H. Newman, G.A. King, G.R. Bernard, B.M. Groves, J.E. Loyd, An imbalance between the excretion of thromboxane and prostacyclin metabolites in pulmonary hypertension, N. Engl. J. Med. 327 (1992) 70–75.
[113] R.M. Tuder, C.D. Cool, M.W. Geraci, J. Wang, S.H. Abman, L. Wright, D. Badesch, N.F. Voelkel, Prostacyclin synthase expression is decreased in lungs from patients with severe pulmonary hypertension, Am. J. Respir. Crit. Care Med. 159 (1999) 1925–1932.
[114] Y. Hoshikawa, N.F. Voelkel, T.L. Gesell, M.D. Moore, K.G. Morris, L.A. Alger, S. Narumiya, M.W. Geraci, Prostacyclin receptor-dependent modulation of pulmonary vascular remodeling, Am. J. Respir. Crit. Care Med. 164 (2001) 314–318.
[115] I.M. Robbins, R.J. Barst, L.J. Rubin, S.P. Gaine, P.V. Price, J.D. Morrow, B.W. Christman, Increased levels of prostaglandin D2 suggest macrophage activation in patients with primary pulmonary hypertension, Chest 120 (2001) 1639–1644.
[116] Y. Kawanabe, S.M. Nauli, Endothelin, Cell. Mol. Life Sci. 68 (2011) 195–203.
[117] C.J. Rhodes, A. Davidson, J.S. Gibbs, J. Wharton, M.R. Wilkins, Therapeutic targets in pulmonary arterial hypertension, Pharmacol. Ther. 121 (2009) 69–88.
[118] A. Giaid, M. Yanagisawa, D. Langleben, R.P. Michel, R. Levy, H. Shennib, S. Kimura, T. Masaki, W.P. Duguid, D.J. Stewart, Expression of endothelin-1 in the lungs of patients with pulmonary hypertension, N. Engl. J. Med. 328 (1993) 1732–1739.
[119] F. Perros, D. Montani, P. Dorfmuller, I. Durand-Gasselin, C. Tcherakian, J. Le Pavec, M. Mazmanian, E. Fadel, S. Mussot, O. Mercier, P. Herve, D. Emilie, S. Eddahibi, G. Simonneau, R. Souza, M. Humbert, Platelet-derived growth factor expression and function in idiopathic pulmonary arterial hypertension, Am. J. Respir. Crit. Care Med. 178 (2008) 81–88.
[120] E.S. Yi, H. Kim, H. Ahn, J. Strother, T. Morris, E. Masliah, L.A. Hansen, K. Park, P.J. Friedman, Distribution of obstructive intimal lesions and their cellular phenotypes in chronic pulmonary hypertension. A morphometric and immunohistochemical study, Am. J. Respir. Crit. Care Med. 162 (2000) 1577–1586.
[121] G. Berger, Z.S. Azzam, R. Hoffman, M. Yigla, Coagulation and anticoagulation in pulmonary arterial hypertension, Isr. Med. Assoc. J. 11 (2009) 376–379.
[122] M. Humbert, N.W. Morrell, S.L. Archer, K.R. Stenmark, M.R. MacLean, I.M. Lang, B.W. Christman, E.K. Weir, O. Eickelberg, N.F. Voelkel, M. Rabinovitch, Cellular and molecular pathobiology of pulmonary arterial hypertension, J. Am. Coll. Cardiol. 43 (2004) 13S–24S.
[123] E.K. Weir, Z. Hong, A. Varghese, The serotonin transporter: a vehicle to elucidate pulmonary hypertension? Circ. Res. 94 (2004) 1152–1154.
[124] D.J. Welsh, M. Harnett, M. MacLean, A.J. Peacock, Proliferation and signaling in fibroblasts: role of 5-hydroxytryptamine2A receptor and transporter, Am. J. Respir. Crit. Care Med. 170 (2004) 252–259.
[125] P. Hervé, J.-M. Launay, M.-L. Scrobohaci, F. Brenot, G. Simonneau, P. Petitpretz, P. Poubeau, J. Cerrina, P. Duroux, L. Drouet, Increased plasma serotonin in primary pulmonary hypertension, Am. J. Med. 99 (1995) 249–254.

[126] P. Dorfmuller, V. Zarka, I. Durand-Gasselin, G. Monti, K. Balabanian, G. Garcia, F. Capron, A. Coulomb-Lhermine, A. Marfaing-Koka, G. Simonneau, D. Emilie, M. Humbert, Chemokine RANTES in severe pulmonary arterial hypertension, Am. J. Respir. Crit. Care Med. 165 (2002) 534–539.
[127] K. Balabanian, A. Foussat, P. Dorfmuller, I. Durand-Gasselin, F. Capel, L. Bouchet-Delbos, A. Portier, A. Marfaing-Koka, R. Krzysiek, A.-C. Rimaniol, G. Simonneau, D. Emilie, M. Humbert, CX3C chemokine fractalkine in pulmonary arterial hypertension, Am. J. Respir. Crit. Care Med. 165 (2002) 1419–1425.
[128] F. Perros, P. Dorfmüller, R. Souza, I. Durand-Gasselin, V. Godot, F. Capel, S. Adnot, S. Eddahibi, M. Mazmanian, E. Fadel, P. Hervé, G. Simonneau, D. Emilie, M. Humbert, Fractalkine-induced smooth muscle cell proliferation in pulmonary hypertension, Eur. Respir. J. 29 (2007) 937–943.

REVIEW II – MECHANISMS UNDERLYING THE IMPACT OF EXERCISE TRAINING IN PULMONARY ARTERIAL HYPERTENSION

Mechanisms underlying the impact of exercise training in pulmonary arterial hypertension

Rita Nogueira-Ferreira[1,2], Daniel Moreira-Gonçalves[2,3], Mário Santos[2,4], Rita Ferreira[1], Tiago Henriques-Coelho[2]

[1]QOPNA, Departamento de Química, Universidade de Aveiro, Campus Universitário de Santiago, 3810-193 Aveiro, Portugal
[2]Departamento de Cirurgia e Fisiologia, Faculdade de Medicina, Universidade do Porto, Alameda Professor Hernâni Monteiro, 4200-319 Porto, Portugal
[3]CIAFEL, Faculdade de Desporto, Universidade do Porto, R. Dr. Plácido da Costa 91, 4200-450 Porto, Portugal
[4]Unidade de Doença Vascular Pulmonar, Centro Hospitalar do Porto, Largo Prof. Abel Salazar, 4099-001 Porto, Portugal

Corresponding author (✉):
Rita Nogueira-Ferreira
Departamento de Química
Universidade de Aveiro
Campus Universitário de Santiago
3810-193 Aveiro
Portugal
e-mail: rmferreira@ua.pt

Abstract

Pulmonary arterial hypertension (PAH) is a devastating disease characterized by progressive increases in pulmonary vascular resistance that can ultimately lead to right ventricle failure and death. Patients with PAH present symptoms such as shortness of breath, fatigue, dizziness and chest pain, which impact negatively the functional capacity and quality of life. Despite the advances in recent years in disease-targeted therapies, PAH remains a disease without a cure and with a high mortality rate and an urgent need of effective therapeutic strategies. Exercise training is an established treatment in left heart failure and chronic obstructive pulmonary disease. Although exercise training was discouraged in PAH because of safety concerns, recent studies support that supervised exercise training can also provide benefits in patients with stable PAH. However, the molecular mechanisms underlying these improvements are still poorly understood. This review summarizes the emerging clinical and experimental studies describing the molecular alterations related with exercise training in PAH.

Keywords: animal models, clinical trials, exercise training, pulmonary arterial hypertension

1. Introduction

Pulmonary arterial hypertension (PAH) is a devastating disease characterized by a progressive increase in pulmonary vascular resistance, which can lead to right heart failure and premature death. By the time of diagnosis, most individuals are in the New York Heart Association (NYHA)/World Health Organization (WHO) functional class III or IV. The most commonly reported symptoms are dyspnea and fatigue, which limit physical function and quality of life (QOL) [1, 2]. Its pathophysiology remains poorly understood but includes vascular changes, namely vasoconstriction, vascular remodelling, thrombosis and inflammation (reviewed by [3, 4]). Current available therapies comprise supportive therapy (anticoagulants, diuretics and supplementary oxygen) and disease-targeted therapies (vasodilators and anti-proliferative agents) but with limited success. Unfortunately, PAH remains a progressive disease without a definite cure [5]. Thus, search for efficient approaches to treat this disease or, at least, to improve the patients' quality of life is imperative.

Exercise training is widely recognized by its preventive and therapeutic effects in several chronic diseases [6]. For instance, in chronic obstructive pulmonary disease or left heart failure, exercise training has been reported as an efficient and safe therapeutic approach, improving exercise capacity, symptoms, QOL and survival [7, 8]. In the setting of PAH, only now exercise training started to be recognized as safe and beneficial. Until recently, guidelines for PAH treatment recommended that any physical activity should be limited as it could aggravate the disease progression and increase the risk of sudden cardiac death [9, 10]. In 2009 the guidelines were revised and a short recommendation was included stating that patients should be encouraged to be active within symptom limits and, when deconditioned but controlled under medical therapy, may undertake supervised exercise training [11]. This change of position was based on data from a limited number of clinical trials showing that supervised and structured exercise training programs (moderate-intensity exercise) could improve cardiopulmonary function, exercise capacity and QOL, without major adverse events or clinical worsening, in stable PAH patients [12-14]. More recently, three important meta-analysis have been published and further strengthened the concept that exercise is safe and beneficial for well medicated PAH patients [10, 15, 16].

Despite consensus in the literature regarding the favorable effect of exercise training programs in PAH specific clinical outcomes such as exercise tolerance and QOL, the

mechanisms underlying these clinical improvements are not yet well established. Considering what we know from other chronic diseases, particularly left heart failure, it could be possible that both cardiopulmonary and skeletal muscle changes induced by exercise training could play a role in PAH. In this review we will summarize the molecular evidences retrieved from experimental and clinical studies supporting the therapeutic and preventive effect of exercise training in the set of PAH.

2. Mechanisms underlying the beneficial effects of exercise training in PAH

Understanding the mechanisms that explain the benefits of exercise training will help to clarify the impact of different exercise programs (considering the type and intensity of exercise training programs) on PAH progression. Table 1 summarizes what has been described until now in terms of molecular changes induced by exercise training in both clinical and pre-clinical studies. Information was selected from papers collected by searches done in PubMed using the terms “exercise training”, “rehabilitation”, “pulmonary hypertension” and “pulmonary arterial hypertension” in the title or abstract. Additionally, the references listed in all selected papers were also hand searched. At the end, 16 studies were considered for the molecular analysis of the impact of exercise training on PAH.

2.1.1. Clinical studies

Comment on available studies

Amongst the 17 studies exploring the effects of exercise training in PAH patients (Supplementary Table S1), only 7 included biochemical measures of some molecular mediators in training patients, though not directly related to PAH disease (Table 1). The majority of participants in the clinical studies were women, which is consistent with the predominance of PAH in female subjects. Furthermore, the age of the participants was also in accordance with the age at which the majority of patients are diagnosed (40-50 years of age) [17]. Patients were mostly in II-IV WHO/NYHA functional class with the majority belonging to functional class III. It is important to highlight that exercise training was reported to provide functional improvements even in patients in the class IV, which represents the worst stage in terms of functional impairment [18]. Regarding PAH etiology, most of the patients presented idiopathic PAH, associated with connective tissue diseases or congenital heart diseases, which are the most prevalent forms of PAH [19]. In

all these studies the exercise protocol was performed under supervised conditions and included a combination of aerobic (treadmill or cycle ergometer) and resistance training. Study duration ranged between 3 and 15 weeks. The frequency of exercise training varied between 2 and 7 sessions/week with a duration of 30-60 minutes/session. Patients were trained in hospitals or rehabilitation centers and the majority continued with a prescribed exercise-training program at home but in contact with the specialists to guarantee patient's safety and compliance. Despite the general agreement that exercise training is beneficial and safe, there are several questions that need to be addressed before any recommendation for the PAH population. There is a need for multicentric randomized clinical trials (the majority of the clinical trials were performed by the same research group); to test the safety and efficacy of home-based interventions; to determine the best exercise program for maximal benefits (frequency, intensity, duration, mode); and to clarify the time point of the disease when exercise training should be recommended and/or limited.

Cardiac adaptations

Analysis of N-terminal-pro brain natriuretic peptide (NT-proBNP) has been used as biomarker of right ventricle (RV) function, prognosis and monitoring of therapeutic intervention in PAH. It reflects cardiomyocyte injury, inflammation and ventricular remodelling, once it is secreted in response to an increase in ventricular wall stress [20, 21]. NT-proBNP levels remained unchanged in almost all studies, suggesting that the exercise training programs in use did not impact cardiac function. In one study with PAH associated with congenital heart diseases, NT-proBNP serum-levels slightly decreased after 3 weeks of exercise training but significantly increased after 15 weeks in comparison with baseline data [22]. However, no measures of cardiac function were available and several limitations (e.g. changes in the exercise program or missing values at the last follow-up visit) have been pointed that could explain these results. There is one randomized clinical trial that assessed RV function after 15 weeks of exercise training and showed increased cardiac index at rest and during exercise [23], thus suggesting improvement of RV function. Unfortunately, no molecular analysis was performed in this study. The effects of exercise training on right ventricular function and remodelling have not yet been established, neither the underlying molecular mechanisms.

Table 1 – Molecular changes induced by exercise training in clinical and experimental pulmonary arterial hypertension.

Characterization of subjects	Exercise intervention	Effect of exercise	Reference
Human studies			
• Idiopathic PAH (19) • NYHA – FC II-III (84% III) • 42 ± 13 years • 79% female	*12 weeks institution based* *3 days/week:* • bicycle training • quadriceps strength and endurance training	↑ skeletal muscle (*vastus lateralis*) type I fiber succinate dehydrogenase activity = NT-proBNP levels in the blood	[24]
• Associated PAH (8) • NYHA – FC II-III (63% III) • 28 ± 6 years • 63% male	*3 months institution based* *2 days/week:* • 10 min warm-up, with stretching of long muscle groups • resisted exercises (1–2 kg) • aerobic interval training in a bicycle ergometer during 24 min with bases at 10–25W and 30-second peaks of 20–50W (80% of HR reached in the 6MWT) *From 3rd to 12th month:* • daily flat-ground walking • similar rehabilitation exercises as done in the rehabilitation sessions	= NT-proBNP, hemoglobin and ferritin levels in the blood	[25]
• Idiopathic PAH (5) • WHO – FC II-III (60% II) • 40 ± 15 years • 80% female	*12 weeks institution based* *3 days/week:* • 10 to 15 min of cycling exercise with initial workload set at 60% of the maximal workload achieved during incremental exercise test • 2 sets of 10 to 12 repetitions for 6 to 8 different exercises involving single muscle groups (arms and quadriceps) • 15 min of brisk walking on a treadmill (85% of the mean speed of 6MWT)	= skeletal muscle (*vastus lateralis*) citrate synthase, 3-hydroxyacyl CoA dehydrogenase and phosphofructokinase activities	[26]
• Idiopathic PAH (10), Associated PAH (10) and CTEPH (2) • NYHA – FC II-III (59% II) • 52 ± 4 years • 68% female	*12 weeks institution based* *2 days/week* 1-hour sessions of exercise training, two 6-week blocks (60-80% of CPET HRmax): • *first block:* interval training with treadmill walking, cycling, and step	= NT-proBNP levels in the blood	[27]

	climbing *second block:* longer periods of continuous aerobic exercise, with resistance training by step climbing, unsupported arm/leg exercises with and without dumbbells (500-1000 g), and supporting body weight over a chair • daily home-based exercise with stair-climbing and brisk walking		
• Associated PAH (21) • WHO – FC II-IV (43% II) • 52 ± 18 years • 95% female	*3 weeks institution based:* • 7 days/week at low workloads (10 to 60 W) of interval bicycle ergometer training with a lower workload for 1⁄2 min and a higher workload for 1 min, 10 to 25 min/day. 60 min of walking, 5 days/week (flat-ground and uphill walking) • 30 min of dumbbell training of single muscle groups (500 to 1000 g) and 30 min of respiratory training, 5 days/week *12 weeks home based:* • bicycle exercise training, once daily, 15-30 min, 5 days/week • respiratory exercise and dumbbell training every other day, 15-30 min • walking twice a week	= plasma NT-proBNP and C-reactive protein levels	[28]
• Associated PAH (20) • WHO – FC II-III (70% III) • 48 ± 11 years • 80% female	Same as [28].	↑ serum NT-proBNP levels	[22]
• PAH (61) and CTEPH (26) • WHO – FC II-IV (79% III) • 56 ± 15 years • 54% female	Same as [28].	= NT-proBNP levels in the blood	[23]
Animal studies			
Male Sprague-Dawley rats with PAH induced by chronic hypoxia	• Treadmill running • 10 weeks • 5 days/week • 60 min/session • 6 weeks: progressed to 30 m/min	↑ RV and LV α1-adrenoceptor and β-adrenoceptor densities ↓ RV and LV muscarinic receptor density (assessed by radioactive	[29]

	• 4 weeks: 30 m/min • 10º incline	ligand binding assay)	
Male Wistar rats with PAH induced by monocrotaline (60 mg/kg)	• Treadmill running • 3-5 weeks • 5 days/week • First week: 60 min/session • Second to fifth weeks: 50 min/session • 10-30 m/min • 0º incline	↑ erythrocyte superoxide dismutase and glutathione S-transferase activities ↓ erythrocyte lipid peroxidation and catalase activity = erythrocyte glutathione peroxidase activity	[30]
Male Wistar rats with PAH induced by monocrotaline (60 mg/kg)	• Treadmill running • 3 weeks • 5 days/week • First and second weeks: 60 min/session • Third week: 50 min/session • 60% VO_2 max	↓ RV *p*-GSK-3β/GSK-3β protein expression	[31]
Male C57BL/6J mice with PAH induced by chronic hypoxia	• Treadmill running • 3 weeks • 5 days/week • 30 min/session • 60% VO_2 max	↑ lung PDE1c mRNA expression ↓ lung eNOS and PDE5 mRNA expression = lung PDE1a, sGCb1, PDE1b, PDE4a, PDE4b, sGCa3 and iNOS mRNA expression	[32]
Male Wistar rats with PAH induced by monocrotaline (60 mg/kg)	• Treadmill running • 3 weeks • 5 days/week • First and second weeks: 60 min/session • Third week: 50 min/session • 60% VO_2 max	↑ RV *p*-Akt protein expression ↓ RV hydrogen peroxide concentration and caspase-3 protein expression = RV PI3K, Akt and Bax/Bcl-2 protein expression	[33]
Male Sprague-Dawley rats with PAH induced by monocrotaline (50 mg/kg)	• Treadmill running • 1 bout of 45 min • 75% VO_2 max	↑ lung *p*-eNOS^{Ser1122}/eNOS protein expression ↓ lung *p*-eNOS^{Thr495}/eNOS protein expression = RV caspase-3 activity	[34]
Male Wistar rats with PAH induced by monocrotaline (60 mg/kg)	• Treadmill running • 4 weeks • 5 days/week • First week: progressed to 60 min/session at 25 m/min • Second to fourth weeks: 60 min/session at 25 m/min • 0º incline • Training occurred prior to randomizing to control vs. PAH groups	↑ RV NF-κB p105/p50, NF-κB p65 protein expression and MMP-2 activity ↓ RV beta/alpha MHC, TWEAK and atrogin-1 protein expression = RV myostatin, *p*-Smad3, p38 MAPK, TNF-α, Erk1/2, NF-κB p100/p52, Rel-B, TRAF6, MuRF1, *p*-Akt, *p*-FoxO3A protein expression and MMP-9 activity	[35]
Male Wistar rats with PAH induced by monocrotaline (60 mg/kg)	• Treadmill running • 4 weeks (early intervention)	Early and late interventions: ↑ RV SERCA2a protein	[36]

	• 2 weeks (late intervention) • 5 days/week • 60 min/session • 30 m/min • Last week: 25 m/min • 0º incline	expression, VEGF mRNA expression and mitochondria complex V activity ↓ RV ET-1 mRNA expression, serum levels of lactate and mitochondria complex V nitration = RV ATP synthase subunit β protein expression Early intervention: ↓ RV beta/alpha MHC protein expression, TNF-α/IL-10 and BNP mRNA expression	
Male Wistar rats with PAH induced by monocrotaline (60 mg/kg)	• Treadmill running • 8 weeks prior to MCT administration + 3 weeks after MCT injection • 5 days/week • 60 min/session • 15-18 m/min	= RV ryanodine receptor, phospholamban and SERCA2a mRNA expression	[37]

Legend: ↑, increase; ↓, decrease; =, no change; 6MWT, 6-minute walk test; CPET, cardiopulmonary exercise testing; CTEPH, chronic thromboembolic pulmonary hypertension; eNOS, endothelial nitric oxide synthase; ET-1, endothelin-1; GSK-3β, glycogen synthase kinase-3β; HR, heart rate; IL-10, interleukin-10; iNOS, inducible nitric oxide synthase; LV, left ventricle; MHC, myosin heavy chain; MMP, matrix metalloproteinase; MuRF1, muscle ring finger protein 1; NT-proBNP, N-terminal-pro brain natriuretic peptide; NYHA – FC, New York Heart Association functional class; PAH, pulmonary arterial hypertension; PDE, phosphodiesterase; *p*-GSK-3β, phosphorylated GSK-3β; PI3K, phosphoinositide 3-kinase; RV, right ventricle; SERCA2a, sarco(endo)plasmic reticulum calcium-ATPase; sGC, soluble guanylate cyclase; TNF-α, tumor necrosis factor-α; TRAF6, TNF receptor-associated factor 6; TWEAK, TNF-related weak inducer of apoptosis; VEGF, vascular endothelial growth factor; VO_2, oxygen uptake; WHO – FC, World Health Organization functional class.

Skeletal muscle adaptations

Several skeletal muscle abnormalities have been reported in PAH such as muscle atrophy, fiber type switching and impaired contractility. Muscle abnormalities appear to be very common and seem to contribute to dyspnea, fatigue, and exercise limitation in patients with PAH [38-40]. Skeletal muscle biopsies (*vastus lateralis*) were collected to evaluate the effects of exercise training on muscle function in two clinical studies (Table 1). Exercise training increased quadriceps strength by 13% and quadriceps endurance by 34%. This was accompanied by increased capillarisation and oxidative enzyme activity, especially of the type-I (slow) muscle fibers [24]. In another study, exercise training was

shown to decrease type-IIx fiber proportion [26]. No other molecular adaptations were reported.

2.1.2. Experimental studies

Comment on available studies

There are several studies assessing the impact of exercise training in cardiac or pulmonary vessels remodelling in experimental PAH but only 9 studies have described the molecular changes promoted by exercise training (Table 1). The pre-clinical models of PAH used to characterize the effect of exercise training were chronic hypoxia (two studies) and monocrotaline (MCT; 60 mg/kg) (seven studies) models. In general, the exercise training protocols were conducted for 2-8 weeks, 5 sessions/week, 30-60 minutes/session, at a running speed ranging from 15 to 30 meters/minute. The acute effect of exercise training was analyzed in one study, consisting in a single session of treadmill running during 45 minutes at 75% VO_2 max [34]. Treadmill is the mode of exercise used in all the studies designed to assess the effect of exercise training in experimental PAH. Treadmill training allows controlling exercise intensity and duration, and the calculation of the total amount of external work done by the animal; however, it is a form of forced exercise and requires constant observation to prevent animal injuries [41]. To the best of our knowledge, only one study evaluated the effect of voluntary access to a running wheel, a protocol that took an average of 4 weeks (depending on rats' health status), showing that exercise training improved animals' survival and delayed the progression to right heart failure, but no molecular mechanisms were studied [42]. The majority of the experimental studies evaluated exercise training as a therapeutic approach once the exercise program was performed after disease implementation. However, in one study the preventive effect of exercise training was tested using a protocol consisting in 4 weeks of treadmill running before MCT injection followed by 4 weeks with animal movements confined to the cage´s space [35]. Recently, another study evaluated the preventive effect of exercise training using a protocol consisting in 8 weeks of treadmill running before MCT injection followed by 3 weeks of treadmill running [37]. Right ventricle and lung tissues were the samples more analyzed. Additionally, analysis of protein expression by western blotting, mRNA expression by PCR and also assessment of enzymatic activity are the most common methodologies used to evaluate the molecular changes associated with exercise training.

Cardiac adaptations

In the majority of the studies, exercise training showed beneficial effects on cardiac remodelling [30-37, 42, 43]. Still, other reported no improvement [44] or aggravation [45]. From those that studied the molecular changes associated with exercise training, mediators related with proliferation, apoptosis, oxidative stress, inflammation and proteolysis were evaluated, given the relevance of these processes in RV adaptation to PAH [46, 47].

An exercise-training program consisting in 3 weeks of treadmill running post-MCT injection revealed an improvement in RV function by invasive hemodynamic analysis. RV remodelling was related with the glycogen synthase kinase (GSK) signalling, with a decreased ratio between the phosphorylated (inactive protein with pro-hypertrophic function) and dephosphorylated (active protein with anti-hypertrophic function) form of the protein GSK-3β in the exercised MCT rats [31]. GSK-3β is implicated in cardiac growth and regulates the calcineurin/NFAT (nuclear factor of activated T-cells) signalling, phosphorylating NFAT that is dephosphorylated by calcineurin. NFAT phosphorylation prevents its nuclear translocation, thereby limiting access to target genes. However, in its phosphorylated form, this protein exerts a pro-hypertrophic role, through the decrease in NFAT phosphorylation and the consequent increase of its translocation to the nucleus, activating the transcription of hypertrophic response genes [48-50]. Using the same exercise training protocol, hydrogen peroxide concentration and apoptotic signalling was shown to be reduced in RV of exercised animals, paralleled by a decrease in RV caspase-3 protein expression and an increase in phosphorylated (activated) Akt levels [33]. This serine/threonine kinase is involved in physiologic cardiac growth and cardiomyocyte survival [49, 51, 52]. Additionally, the systemic lipid peroxidation and activity of antioxidant enzymes was assessed in MCT rats submitted to treadmill running during 3, 4 or 5 weeks post-MCT injection. Exercise training reduced oxidative stress given by decreased lipid peroxidation and increased superoxide dismutase and glutathione S-transferase activities, which was related to prevention of RV hypertrophy and increased animals' survival [30]. Oxidative stress is an important contributor to RV remodelling and dysfunction in PAH. High cellular levels of reactive oxygen species seem to be involved in the activation of pro-apoptotic pathways in the failing RV in PAH, cardiomyocyte hypertrophy, matrix remodelling and contractile dysfunction [53].

The impact of exercise training performed in different stages of the disease was also evaluated. After 1 week of habituation, a group of animals ran during 4 weeks post-MCT injection (early exercise training) and other group ran during 2 weeks after 2 weeks of MCT injection (late exercise training). Both exercise interventions (early and late) improved cardiac function. These benefits of exercise training were associated with improvements in markers of cardiac remodelling (SERCA2a, beta/alfa MHC), neurohumoral activation (endothelin-1, BNP, vascular endothelial growth factor), metabolism and mitochondrial oxidative stress (complex V activity and nitration) and inflammation (TNF-α/IL-10). Alterations on cardiomyocyte and extracellular matrix, neurohumoral activation, inflammation, mitochondrial and metabolic disturbances and oxidative stress have been pointed out as key contributors to RV remodelling and dysfunction in PAH [46, 54]. Importantly, greater positive effects were observed when exercise training was initiated in an earlier time point of the disease [36].

Four weeks of treadmill running before MCT injection followed by 4 weeks of sedentary behavior revealed that prior exercise training prevented cardiac dysfunction and maladaptative remodelling, by modulating inflammation and proteolysis. In fact, exercise training decreased the expression of the pro-inflammatory cytokine TWEAK and modulated the downstream regulators from the NF-κB pathway, prevented the increase of the ubiquitin ligase atrogin-1 expression and induced a shift of metalloproteinases (MMP) activity from MMP-9 to MMP-2 activity [35]. In another study, prior exercise training was also shown to exert cardioprotective effects by decreasing hypertrophy and improving heart function but without modifying calcium transport genes (ryanodine receptor, phospholamban and SERCA2a) in the RV [37].

Acute exercise (45 minutes of treadmill run at 75% of VO_2 max) was also shown to provide some benefit as it transitorily normalized the RV systolic pressure of MCT-induced stable PAH (evaluation was performed 17 days after administration of 50 mg/kg of MCT), without evidence of acute right ventricular inflammation or myocyte apoptosis [34]. The effect of an acute exercise bout in advanced stage of the disease remains to be determined.

Pulmonary adaptations

The impact of exercise training on pulmonary vasculature remodelling remains inconclusive, with experimental studies showing improvement [31, 32, 34, 35], no improvement [30, 33, 36, 43, 44] or aggravation [45]. However, only two studies explored the molecular mechanisms associated with exercise training effects, giving emphasis to pathways involved in the vasodilatation process. The mRNA expression of lung mediators involved in the nitric oxide synthase/soluble guanylate cyclase/phosphodiesterase (NOS/sGC/PDE) pathway was evaluated in mice with PAH induced by chronic exposure to hypoxia submitted to 3 weeks of treadmill running. No vasodilatory shift of the NOS/sGC/PDE enzyme expression was observed after exercise training, despite the improvement in pulmonary vascular remodelling (decrease in small pulmonary vessel muscularization) [32]. Curiously, an acute running bout was shown to induce a transitory acute reduction in pulmonary artery pressure that was associated with lung endothelial NOS (eNOS) activation, supporting a mechanism of acute NO-mediated pulmonary vasodilatation [34]. The NO pathway is impaired in several ways in PAH and is an important therapeutic target. Nitric oxide activates sGC, catalyzing cyclic guanosine monophosphate (cGMP) synthesis. cGMP causes vasodilation and inhibits smooth muscle cell proliferation and platelet aggregation. An induction of eNOS activity can increase NO production, contributing to promote vasodilatation [55, 56].

Skeletal muscle adaptations

The effect of exercise training on skeletal muscle in the pre-clinical settings of PAH remains poorly studied. The preventive effects of exercise training in PAH-related muscle wasting was evaluated in Wistar rats injected with MCT [57]. Four weeks of treadmill running before MCT injection followed by 4 weeks of sedentary behavior prevented the PAH-related decrease in cross-sectional area and MHC-I expression in *gastrocnemius* muscle. Additionally, the phosphorylated forms of Akt and mTOR protein levels increased in exercised groups. Akt is involved in protein synthesis stimulation by activating mTOR and its downstream effectors, being also associated with muscle atrophy prevention by inhibiting the activity of FoxOs, thereby supressing the expression of the E3 ubiquitin ligases atrogin-1 and MuRF1 [58-60]. Exercise training also prevented the increase in atrogin-1 expression in *gastrocnemius* muscle and the increase of C-reactive protein and

IL-1β serum levels. Thus, the preventive effect of exercise training in muscle wasting seems to be related with the modulation of proteolysis and inflammation. Exercise training performed during 4 weeks post-MCT injection also increased *gastrocnemius* muscle weight and fiber cross-sectional area. However, no molecular alterations related with the therapeutic effect of exercise training on PAH-induced muscle wasting were evaluated [36].

3. Conclusions

Experimental and clinical evidences support exercise training as a beneficial and safe non-pharmacological approach to be included in multimodal strategies for the clinical management of PAH. Indeed, exercise training seems to modulate diverse molecular mechanisms in varied target organs (overviewed in figure 1), associated with proliferation, apoptosis, oxidative stress, inflammation, proteolysis and vasodilatation.

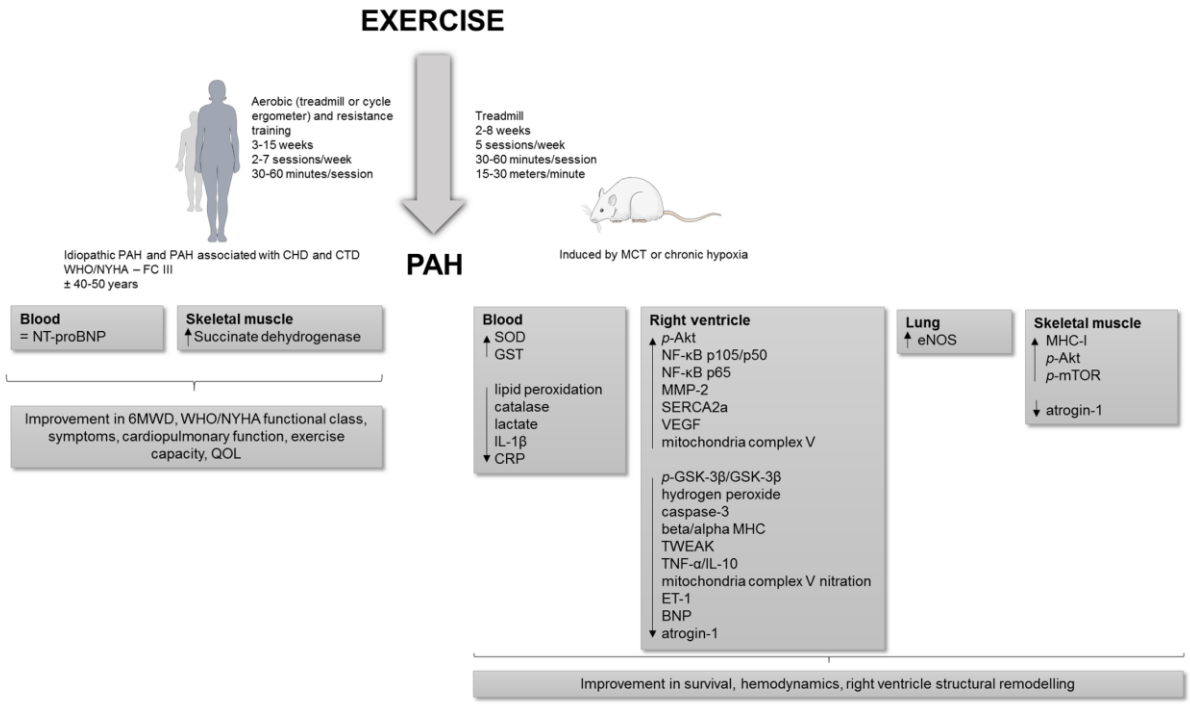

Figure 1 – Molecular changes underlying exercise training effects in clinical and experimental pulmonary arterial hypertension. Figure made with Servier Medical Art. Legend: ↑, increase; ↓, decrease; =, no change; 6MWD, 6-minute walk distance; CHD, congenital heart disease; CRP; C-reactive protein; CTD, connective tissue disease; eNOS, endothelial nitric oxide synthase; ET-1, endothelin-1; GSK-3β, glycogen synthase kinase-3β; GST, glutathione S-transferase; IL, interleukin; MCT, monocrotaline; MHC, myosin heavy chain; MMP-2, matrix metalloproteinase-2; mTOR, mammalian target of rapamycin; NT-proBNP, N-terminal-pro

brain natriuretic peptide; NYHA – FC, New York Heart Association functional class; PAH, pulmonary arterial hypertension; *p*-GSK-3β, phosphorylated GSK-3β; QOL, quality of life; SERCA2a, sarco(endo)plasmic reticulum calcium-ATPase; SOD, superoxide dismutase; TNF-α, tumor necrosis factor-α; TWEAK, TNF-related weak inducer of apoptosis; VEGF, vascular endothelial growth factor; WHO – FC, World Health Organization functional class.

However, more studies are needed with different training programs and a better phenotyping of patients, envisioning the recommendation of exercise training for the clinical management of PAH and the identification of molecular therapeutic targets that mimic or potentiate the effect of exercise.

Conflict of interests

The authors declare no competing interests.

Acknowledgements

This work was supported by Portuguese Foundation for Science and Technology (FCT), European Union, QREN, FEDER and COMPETE for funding the QOPNA research unit (UID/QUI/00062/2013), CIAFEL (UID/DTP/00617/2013), Unidade de Investigação Cardiovascular (UID/IC/00051/2013) and the post-graduation students (grant numbers SFRH/BD/91067/2012 to R.N.F and SFRH/BPD/90010/2012 to D.M.G.).

References

1. Delcroix, M. and L. Howard, *Pulmonary arterial hypertension: the burden of disease and impact on quality of life.* Eur Respir Rev, 2015. **24**(138): p. 621-9.
2. Matura, L.A., A. Mcdonough, and D.L. Carroll, *Cluster analysis of symptoms in pulmonary arterial hypertension: a pilot study.* Eur J Cardiovasc Nurs, 2012. **11**(1): p. 51-61.
3. Montani, D., S. Gunther, P. Dorfmuller, F. Perros, B. Girerd, G. Garcia, X. Jais, L. Savale, E. Artaud-Macari, L.C. Price, M. Humbert, G. Simonneau, and O. Sitbon, *Pulmonary arterial hypertension.* Orphanet J Rare Dis, 2013. **8**: p. 97.
4. Malenfant, S., A.S. Neyron, R. Paulin, F. Potus, J. Meloche, S. Provencher, and S. Bonnet, *Signal transduction in the development of pulmonary arterial hypertension.* Pulm Circ, 2013. **3**(2): p. 278-93.

5. Humbert, M., E.M. Lau, D. Montani, X. Jais, O. Sitbon, and G. Simonneau, *Advances in therapeutic interventions for patients with pulmonary arterial hypertension.* Circulation, 2014. **130**(24): p. 2189-208.
6. Pedersen, B.K. and B. Saltin, *Exercise as medicine – evidence for prescribing exercise as therapy in 26 different chronic diseases.* Scand J Med Sci Sports, 2015. **25**: p. 1-72.
7. Gloeckl, R., B. Marinov, and F. Pitta, *Practical recommendations for exercise training in patients with COPD.* Eur Respir Rev, 2013. **22**(128): p. 178-186.
8. Tabet, J.Y., P. Meurin, A.B. Driss, H. Weber, N. Renaud, A. Grosdemouge, F. Beauvais, and A. Cohen-Solal, *Benefits of exercise training in chronic heart failure.* Arch Cardiovasc Dis, 2009. **102**(10): p. 721-30.
9. Gaine, S.P. and L.J. Rubin, *Primary pulmonary hypertension.* Lancet, 1998. **352**(9129): p. 719-25.
10. Buys, R., A. Avila, and V.A. Cornelissen, *Exercise training improves physical fitness in patients with pulmonary arterial hypertension: a systematic review and meta-analysis of controlled trials.* BMC Pulm Med, 2015. **15**: p. 40.
11. Galie, N., M.M. Hoeper, M. Humbert, A. Torbicki, J.L. Vachiery, J.A. Barbera, M. Beghetti, P. Corris, S. Gaine, J.S. Gibbs, M.A. Gomez-Sanchez, G. Jondeau, W. Klepetko, C. Opitz, A. Peacock, L. Rubin, M. Zellweger, and G. Simonneau, *Guidelines for the diagnosis and treatment of pulmonary hypertension: the Task Force for the Diagnosis and Treatment of Pulmonary Hypertension of the European Society of Cardiology (ESC) and the European Respiratory Society (ERS), endorsed by the International Society of Heart and Lung Transplantation (ISHLT).* Eur Heart J, 2009. **30**(20): p. 2493-537.
12. Marra, A.M., B. Egenlauf, E. Bossone, C. Eichstaedt, E. Grunig, and N. Ehlken, *Principles of rehabilitation and reactivation: pulmonary hypertension.* Respiration, 2015. **89**(4): p. 265-73.
13. Fowler, R.M., K.R. Gain, and E. Gabbay, *Exercise intolerance in pulmonary arterial hypertension.* Pulm Med, 2012. **2012**: p. 359204.
14. Mereles, D., N. Ehlken, S. Kreuscher, S. Ghofrani, M.M. Hoeper, M. Halank, F.J. Meyer, G. Karger, J. Buss, J. Juenger, N. Holzapfel, C. Opitz, J. Winkler, F.F. Herth, H. Wilkens, H.A. Katus, H. Olschewski, and E. Grunig, *Exercise and*

respiratory training improve exercise capacity and quality of life in patients with severe chronic pulmonary hypertension. Circulation, 2006. **114**(14): p. 1482-9.

15. Pandey, A., S. Garg, M. Khunger, D.J. Kumbhani, K.M. Chin, and J.D. Berry, *Efficacy and safety of exercise training in chronic pulmonary hypertension: systematic review and meta-analysis.* Circ Heart Fail, 2015. **8**(6): p. 1032-43.
16. Yuan, P., X.T. Yuan, X.Y. Sun, B. Pudasaini, J.M. Liu, and Q.H. Hu, *Exercise training for pulmonary hypertension: a systematic review and meta-analysis.* Int J Cardiol, 2015. **178**: p. 142-6.
17. Mcgoon, M.D., R.L. Benza, P. Escribano-Subias, X. Jiang, D.P. Miller, A.J. Peacock, J. Pepke-Zaba, T. Pulido, S. Rich, S. Rosenkranz, S. Suissa, and M. Humbert, *Pulmonary arterial hypertension: epidemiology and registries.* J Am Coll Cardiol, 2013. **62**(25 Suppl): p. D51-9.
18. Grunig, E., M. Lichtblau, N. Ehlken, H.A. Ghofrani, F. Reichenberger, G. Staehler, M. Halank, C. Fischer, H.J. Seyfarth, H. Klose, A. Meyer, S. Sorichter, H. Wilkens, S. Rosenkranz, C. Opitz, H. Leuchte, G. Karger, R. Speich, and C. Nagel, *Safety and efficacy of exercise training in various forms of pulmonary hypertension.* Eur Respir J, 2012. **40**(1): p. 84-92.
19. Peacock, A.J., N.F. Murphy, J.J. Mcmurray, L. Caballero, and S. Stewart, *An epidemiological study of pulmonary arterial hypertension.* Eur Respir J, 2007. **30**(1): p. 104-9.
20. Rosenthal, J.L. and M.S. Jacob, *Biomarkers in pulmonary arterial hypertension.* Curr Heart Fail Rep, 2014. **11**(4): p. 477-84.
21. Pezzuto, B., R. Badagliacca, R. Poscia, S. Ghio, M. D'alto, P. Vitulo, M. Mule, C. Albera, M. Volterrani, F. Fedele, and C.D. Vizza, *Circulating biomarkers in pulmonary arterial hypertension: update and future direction.* J Heart Lung Transplant, 2015. **34**(3): p. 282-305.
22. Becker-Grunig, T., H. Klose, N. Ehlken, M. Lichtblau, C. Nagel, C. Fischer, M. Gorenflo, H. Tiede, D. Schranz, A. Hager, H. Kaemmerer, O. Miera, S. Ulrich, R. Speich, S. Uiker, and E. Grunig, *Efficacy of exercise training in pulmonary arterial hypertension associated with congenital heart disease.* Int J Cardiol, 2013. **168**(1): p. 375-81.

23. Ehlken, N., M. Lichtblau, H. Klose, J. Weidenhammer, C. Fischer, R. Nechwatal, S. Uiker, M. Halank, K. Olsson, W. Seeger, H. Gall, S. Rosenkranz, H. Wilkens, D. Mertens, H.J. Seyfarth, C. Opitz, S. Ulrich, B. Egenlauf, and E. Grunig, *Exercise training improves peak oxygen consumption and haemodynamics in patients with severe pulmonary arterial hypertension and inoperable chronic thrombo-embolic pulmonary hypertension: a prospective, randomized, controlled trial.* Eur Heart J, 2016. **37**(1): p. 35-44.
24. De Man, F.S., M.L. Handoko, H. Groepenhoff, A.J. Van 'T Hul, J. Abbink, R.J. Koppers, H.P. Grotjohan, J.W. Twisk, H.J. Bogaard, A. Boonstra, P.E. Postmus, N. Westerhof, W.J. Van Der Laarse, and A. Vonk-Noordegraaf, *Effects of exercise training in patients with idiopathic pulmonary arterial hypertension.* Eur Respir J, 2009. **34**(3): p. 669-75.
25. Martinez-Quintana, E., G. Miranda-Calderin, A. Ugarte-Lopetegui, and F. Rodriguez-Gonzalez, *Rehabilitation program in adult congenital heart disease patients with pulmonary hypertension.* Congenit Heart Dis, 2010. **5**(1): p. 44-50.
26. Mainguy, V., F. Maltais, D. Saey, P. Gagnon, S. Martel, M. Simon, and S. Provencher, *Effects of a rehabilitation program on skeletal muscle function in idiopathic pulmonary arterial hypertension.* J Cardiopulm Rehabil Prev, 2010. **30**(5): p. 319-23.
27. Fox, B.D., M. Kassirer, I. Weiss, Y. Raviv, N. Peled, D. Shitrit, and M.R. Kramer, *Ambulatory rehabilitation improves exercise capacity in patients with pulmonary hypertension.* J Card Fail, 2011. **17**(3): p. 196-200.
28. Grunig, E., F. Maier, N. Ehlken, C. Fischer, M. Lichtblau, N. Blank, C. Fiehn, F. Stockl, F. Prange, G. Staehler, F. Reichenberger, H. Tiede, M. Halank, H.J. Seyfarth, S. Wagner, and C. Nagel, *Exercise training in pulmonary arterial hypertension associated with connective tissue diseases.* Arthritis Res Ther, 2012. **14**(3): p. R148.
29. Favret, F., K.K. Henderson, R.L. Clancy, J.P. Richalet, and N.C. Gonzalez, *Exercise training alters the effect of chronic hypoxia on myocardial adrenergic and muscarinic receptor number.* J Appl Physiol (1985), 2001. **91**(3): p. 1283-8.
30. Souza-Rabbo, M.P., L.F. Silva, J.A. Auzani, M. Picoral, N. Khaper, and A. Bello-Klein, *Effects of a chronic exercise training protocol on oxidative stress and right*

ventricular hypertrophy in monocrotaline-treated rats. Clin Exp Pharmacol Physiol, 2008. **35**(8): p. 944-8.

31. Colombo, R., R. Siqueira, C.U. Becker, T.G. Fernandes, K.M. Pires, S.S. Valenca, M.P. Souza-Rabbo, A.S. Araujo, and A. Bello-Klein, *Effects of exercise on monocrotaline-induced changes in right heart function and pulmonary artery remodeling in rats.* Can J Physiol Pharmacol, 2013. **91**(1): p. 38-44.
32. Weissmann, N., D.M. Peters, C. Klopping, K. Kruger, C. Pilat, S. Katta, M. Seimetz, H.A. Ghofrani, R.T. Schermuly, M. Witzenrath, W. Seeger, F. Grimminger, and F.C. Mooren, *Structural and functional prevention of hypoxia-induced pulmonary hypertension by individualized exercise training in mice.* Am J Physiol Lung Cell Mol Physiol, 2014. **306**(11): p. L986-95.
33. Colombo, R., R. Siqueira, A. Conzatti, T.R. Fernandes, A.M. Tavares, A.S. Araujo, and A. Bello-Klein, *Aerobic exercise promotes a decrease in right ventricle apoptotic proteins in experimental cor pulmonale.* J Cardiovasc Pharmacol, 2015. **66**(3): p. 246-53.
34. Brown, M.B., T.J. Chingombe, A.B. Zinn, J.G. Reddy, R.A. Novack, S.A. Cooney, A.J. Fisher, R.G. Presson, T. Lahm, and I. Petrache, *Novel assessment of haemodynamic kinetics with acute exercise in a rat model of pulmonary arterial hypertension.* Exp Physiol, 2015. **100**(6): p. 742-54.
35. Nogueira-Ferreira, R., D. Moreira-Goncalves, A.F. Silva, J.A. Duarte, A. Leite-Moreira, R. Ferreira, and T. Henriques-Coelho, *Exercise preconditioning prevents MCT-induced right ventricle remodeling through the regulation of TNF superfamily cytokines.* Int J Cardiol, 2016. **203**: p. 858-866.
36. Moreira-Goncalves, D., R. Ferreira, H. Fonseca, A.I. Padrao, N. Moreno, A.F. Silva, F. Vasques-Novoa, N. Goncalves, S. Vieira, M. Santos, F. Amado, J.A. Duarte, A.F. Leite-Moreira, and T. Henriques-Coelho, *Cardioprotective effects of early and late aerobic exercise training in experimental pulmonary arterial hypertension.* Basic Res Cardiol, 2015. **110**(6): p. 57.
37. Pacagnelli, F.L., A.K. De Almeida Sabela, K. Okoshi, T.B. Mariano, D.H. Campos, R.F. Carvalho, A.C. Cicogna, and L.C. Vanderlei, *Preventive aerobic training exerts a cardioprotective effect on rats treated with monocrotaline.* Int J Exp Pathol, 2016. **97**(3): p. 238-247.

38. Batt, J., S.S. Ahmed, J. Correa, A. Bain, and J. Granton, *Skeletal muscle dysfunction in idiopathic pulmonary arterial hypertension.* Am J Respir Cell Mol Biol, 2014. **50**(1): p. 74-86.
39. Bauer, R., C. Dehnert, P. Schoene, A. Filusch, P. Bartsch, M.M. Borst, H.A. Katus, and F.J. Meyer, *Skeletal muscle dysfunction in patients with idiopathic pulmonary arterial hypertension.* Respir Med, 2007. **101**(11): p. 2366-9.
40. Mainguy, V., F. Maltais, D. Saey, P. Gagnon, S. Martel, M. Simon, and S. Provencher, *Peripheral muscle dysfunction in idiopathic pulmonary arterial hypertension.* Thorax, 2010. **65**(2): p. 113-7.
41. Ferreira, R., D. Moreira-Goncalves, A.L. Azevedo, J.A. Duarte, F. Amado, and R. Vitorino, *Unraveling the exercise-related proteome signature in heart.* Basic Res Cardiol, 2015. **110**(1): p. 454.
42. Natali, A.J., E.D. Fowler, S.C. Calaghan, and E. White, *Voluntary exercise delays heart failure onset in rats with pulmonary artery hypertension.* Am J Physiol Heart Circ Physiol, 2015. **309**(3): p. H421-4.
43. Favret, F., K.K. Henderson, J. Allen, J.P. Richalet, and N.C. Gonzalez, *Exercise training improves lung gas exchange and attenuates acute hypoxic pulmonary hypertension but does not prevent pulmonary hypertension of prolonged hypoxia.* J Appl Physiol (1985), 2006. **100**(1): p. 20-5.
44. Hargett, L.A., L.J. Hartman, A.K. Scruggs, J.M. Mclendon, A.K. Haven, and N.N. Bauer, *Severe pulmonary arterial hypertensive rats are tolerant to mild exercise.* Pulm Circ, 2015. **5**(2): p. 349-55.
45. Handoko, M.L., F.S. De Man, C.M. Happe, I. Schalij, R.J. Musters, N. Westerhof, P.E. Postmus, W.J. Paulus, W.J. Van Der Laarse, and A. Vonk-Noordegraaf, *Opposite effects of training in rats with stable and progressive pulmonary hypertension.* Circulation, 2009. **120**(1): p. 42-9.
46. Voelkel, N.F., J. Gomez-Arroyo, A. Abbate, and H.J. Bogaard, *Mechanisms of right heart failure-A work in progress and a plea for failure prevention.* Pulm Circ, 2013. **3**(1): p. 137-43.
47. Vonk-Noordegraaf, A., F. Haddad, K.M. Chin, P.R. Forfia, S.M. Kawut, J. Lumens, R. Naeije, J. Newman, R.J. Oudiz, S. Provencher, A. Torbicki, N.F. Voelkel, and P.M. Hassoun, *Right heart adaptation to pulmonary arterial*

hypertension: physiology and pathobiology. J Am Coll Cardiol, 2013. **62**(25 Suppl): p. D22-33.

48. Dorn, G.W. and T. Force, *Protein kinase cascades in the regulation of cardiac hypertrophy.* J Clin Invest, 2005. **115**(3): p. 527-37.
49. Weeks, K.L. and J.R. Mcmullen, *The athlete's heart vs. the failing heart: can signaling explain the two distinct outcomes?* Physiology (Bethesda), 2011. **26**(2): p. 97-105.
50. Antos, C.L., T.A. Mckinsey, N. Frey, W. Kutschke, J. Mcanally, J.M. Shelton, J.A. Richardson, J.A. Hill, and E.N. Olson, *Activated glycogen synthase-3 beta suppresses cardiac hypertrophy in vivo.* Proc Natl Acad Sci U S A, 2002. **99**(2): p. 907-12.
51. Su, C.C., J.Y. Yang, H.B. Leu, Y. Chen, and P.H. Wang, *Mitochondrial Akt-regulated mitochondrial apoptosis signaling in cardiac muscle cells.* Am J Physiol Heart Circ Physiol, 2012. **302**(3): p. H716-23.
52. Mcmullen, J.R. and G.L. Jennings, *Differences between pathological and physiological cardiac hypertrophy: novel therapeutic strategies to treat heart failure.* Clin Exp Pharmacol Physiol, 2007. **34**(4): p. 255-62.
53. Redout, E.M., A. Van Der Toorn, M.J. Zuidwijk, C.W. Van De Kolk, C.J. Van Echteld, R.J. Musters, C. Van Hardeveld, W.J. Paulus, and W.S. Simonides, *Antioxidant treatment attenuates pulmonary arterial hypertension-induced heart failure.* Am J Physiol Heart Circ Physiol, 2010. **298**(3): p. H1038-47.
54. Bogaard, H.J., K. Abe, A. Vonk Noordegraaf, and N.F. Voelkel, *The right ventricle under pressure: cellular and molecular mechanisms of right-heart failure in pulmonary hypertension.* Chest, 2009. **135**(3): p. 794-804.
55. Dasgupta, A., L. Bowman, C.L. D'arsigny, and S.L. Archer, *Soluble guanylate cyclase: a new therapeutic target for pulmonary arterial hypertension and chronic thromboembolic pulmonary hypertension.* Clin Pharmacol Ther, 2015. **97**(1): p. 88-102.
56. Nogueira-Ferreira, R., R. Ferreira, and T. Henriques-Coelho, *Cellular interplay in pulmonary arterial hypertension: implications for new therapies.* Biochim Biophys Acta, 2014. **1843**(5): p. 885-93.

57. Gonçalves, D., T. Henriques-Coelho, R. Ferreira, H. Fonseca, M.J. Neuparth, J. Justino, D. Duarte, S. Vieira, F. Amado, J.A. Duarte, and A. Leite-Moreira, *Exercise preconditioning prevents skeletal muscle wasting in monocrotaline-induced cardiac cachexia.* FASEB J, 2012. **26**(1 Supplement): p. 1078.31.

58. Bonaldo, P. and M. Sandri, *Cellular and molecular mechanisms of muscle atrophy.* Dis Model Mech, 2013. **6**(1): p. 25-39.

59. Saini, A., A.-S. Nasser, and C.E.H. Stewart, *Waste management—Cytokines, growth factors and cachexia.* Cytokine Growth Factor Rev, 2006. **17**(6): p. 475-486.

60. Schiaffino, S., K.A. Dyar, S. Ciciliot, B. Blaauw, and M. Sandri, *Mechanisms regulating skeletal muscle growth and atrophy.* FEBS J, 2013. **280**(17): p. 4294-314.

REVIEW III – ANIMAL MODELS FOR THE STUDY OF PULMONARY HYPERTENSION: POTENTIAL AND LIMITATIONS

Cardiology and Cardiovascular Medicine

Volume 1, Issue 1 Review Article

Animal Models for the Study of Pulmonary Hypertension: Potential and Limitations

Rita Nogueira-Ferreira[1,2], Gabriel Faria-Costa[2], Rita Ferreira[1], Tiago Henriques-Coelho[2]

[1]QOPNA, Department of Chemistry, University of Aveiro, Portugal

[2]Department of Physiology and Cardiothoracic Surgery, Faculty of Medicine, University of Porto, Portugal

[*]Corresponding Author(s):

Tiago Henriques-Coelho, Department of Physiology and Cardiothoracic Surgery, Faculty of Medicine, University of Porto, Portugal, E-mail: henriques.coelho@gmail.com

Rita Nogueira-Ferreira, QOPNA, Department of Chemistry, University of Aveiro, Portugal, E-mail: rmferreira@ua.pt

Received: 12 September 2016; **Accepted:** 25 September 2016; **Published:** 28 September 2016

Abstract

Pulmonary hypertension (PH) is a multifactorial disease, commonly associated with heart failure. Different experimental models have emerged to help in the understanding of the molecular and cellular mechanisms associated with human PH, providing also a useful approach to test experimental therapies for PH treatment. Although there is no ideal animal model that mimics human PH, animal models have clearly provided valuable insights into the characterization of the cellular and molecular pathways underlying PH onset and progression, and have been successfully applied in the discovery of novel therapeutic approaches. In here we summarize the features of the animal models described within the field of PH research, either the physical, chemical and genetic models, emphasizing its advantages and limitations.

Keywords: **A**nimal models; Chronic hypoxia; Monocrotaline; Pulmonary hypertension

Abbreviations:

5-HTT	Serotonin transporter
Ang-1	Angiopoietin-1
BMPRII	Bone morphogenetic protein receptor type II
IL-6	Interleukin-6
MCT	Monocrotaline
PAB	Pulmonary artery banding
PAECs	Pulmonary artery endothelial cells
PAH	Pulmonary arterial hypertension
PAP	Pulmonary artery pressure
PASMCs	Pulmonary artery smooth muscle cells
PH	Pulmonary hypertension
RV	Right ventricle
TGF-α	Transforming growth factor-α
TNF-α	Tumor necrosis factor-α
VEGFR-2	Vascular endothelial growth factor receptor-2
VIP	Vasoactive intestinal peptide

1. Introduction

The World Health Organization classified pulmonary hypertension (PH) into five groups which share a mean, resting, pulmonary artery pressure (PAP) ≥ 25 mmHg. The Group 1 is pulmonary arterial hypertension (PAH), Group 2 is PH associated with left heart disease, Group 3 is PH associated with lung disease and/or hypoxia, Group 4 is PH associated with chronic thromboembolic disease (CTEPH), and Group 5 is PH associated with unclear multifactorial mechanisms (5th World Symposium on PH, Nice, 2013) [1, 2]. Each group reflects specific etiology, pathological and hemodynamic characteristics and therapeutic approaches. However, there are common processes to the pathology of all PH groups. Vasoconstriction, remodeling, thrombosis, and inflammation are the basic mechanisms of pulmonary vascular pathology in PH. Nevertheless, their relevance, origin, and order of appearance may differ depending on the etiology [2-5]. Over the last years, major advances in the understanding of

PH pathogenesis allowed a delay in disease progression, reducing the symptoms and increasing the quality of life of PH patients. Unfortunately, PH remains a disease without cure [6]. The fact that the disease is usually diagnosed in advanced stages difficult its study in humans. Animal model studies have allowed the investigation of the various phases of disease progression, being crucial to understand the pathophysiology of PH, and to test experimental therapies. Furthermore, they provide us advantages in terms of economy, control of the experimental conditions, replicability and drug testing envisioning its safety translation to humans [7, 8].

An ideal PH model should manifest the key clinical, hemodynamic and histopathological features of human PH [7]. Pulmonary hypertension is a complex disease of diverse etiology and so there is no single animal model that accurately reproduces the human disease, even focusing on just one of PH groups [9]. Consequently, a vast list of PH experimental models is currently available (Table 1). Each model has its own characteristics and allows the investigation of specific hypothesis. Some of them are used in the study of different groups of human PH, once they present molecular and pathological features common to those groups [4]. We grouped these models according to the stimuli that result in PH development (physical, chemical, genetic and multiple) and we critically highlight the general advantages and limitations of their use in PH research.

2. Physical Animal Models

The chronic hypoxia model is one of the most used to study PH pathogenesis and treatment. Its pathological features of pulmonary vasoconstriction and vascular medial hypertrophy mimic the ones observed in human PH [10]. Although being a model of Group 3 PH, it is often used to make conclusions regarding Group 1 PH (PAH) [11]. Chronic hypoxia can be induced by exposing animals to normal air at hypobaric pressure or to oxygen-poor air at normal pressure [12]. This decrease in oxygen pressure causes a strong pulmonary vasoconstrictor response that is characteristic of this model [13]. However, there is little evidence of right ventricle (RV) failure, that is usually the main cause of death in PAH patients [10]. Furthermore, the response to hypoxia varies among animal species, making difficult the translation of findings to human [11, 13].

Another described animal model of PH resulting from a physical stimulus involves repeated microembolizations with the injection of synthetic microspheres, such as Sephadex® microspheres to induce chronic emboli. Thus, this model is useful to study chronic thromboembolism PH (Group 4 PH). The possibility of target different-sized

vessels depending on the diameter size of the microspheres used is an advantage of this approach. However, although this model allows moderate PH development, attention should be taken regarding the microspheres material, since no cellular reaction related with the material type is desired [13, 14].

The surgical models, on the other hand, are designed to mimic the increased blood flow and pressures imposed on the RV in Group 1 PH. There are two main surgical methods used until today: pulmonary artery banding (PAB) and aorto-caval shunt. The PAB consists in a constriction imposed in the pulmonary artery, which leads to an increased afterload in the RV that drives the hypertrophic response. Thus, it allows separate the cardiac disease from the pulmonary disease, which is not present in this model. Given this, PAB does not replicate the human pathology entirely, but is useful to understand the mechanisms of RV dysfunction, already pointed out as the main determinant of prognosis [11, 15]. The aorto-caval shunt is a volume overload method which displays similar RV hypertrophy when compared with PAB. This model can be combined with the monocrotaline (MCT) model, leading to more severe disease development [4, 11, 16]. The main disadvantages of these surgical methods are related with the fact that they require highly technical skills and are usually associated with a high percentage of animal death [11]. Although not being as used as the chronic hypoxia model, these models are still common. Recently, a novel model of pulmonary artery banding emerged related with an easier method of constricting the pulmonary artery. This new method resulted in a significantly lower surgical mortality and revealed significantly more signs of RV dysfunction [17].

3. Chemically-Induced Animal Models

Chemically-induced PH models can offer advantage in terms of application simplicity and costs. Amongst these, the MCT animal model is the most broadly used to study PH, in particular the pathophysiology and therapeutic application in the Group 1 PH [8, 11, 18]. Indeed, for more than one decade, most studies on therapy of PAH have employed the MCT model [19]. As recently reviewed [20], the administration of the alkaloid MCT affects both the lungs and the heart, modulating primarily biological processes associated with the vascular remodeling and inflammation, two key pathological features of human PH. However, an important drawback is that the response to MCT is variable among species, strains and even animals [13]. The most common specie used in the MCT model is the rat because it is the one that best develops PAH features after the drug injection [21, 22].

MCT effects require conversion to an active form (MCT pyrrole) in the liver by cytochrome P450, which makes the model dependent on the animals-based metabolic differences [4]. For instance, mice must be injected with the MCT pyrrole active form and not MCT itself. However, the disease development is far less extensive, stagnating in an acute lung injury [22]. Other animals less used are dogs [23] or pigs [24], which can replicate human PAH more successfully than rodent models. Still, these kinds of animals are more expensive and the disease takes longer to develop [11]. In spite of the limitations of the MCT model, it is largely used once, in comparison with the other models, it is reproducible, less expensive and does not need particular technical skills [25]. Furthermore, it mimics human PH in terms of hemodynamic and histopathological severity, and high mortality [26].

Experimental models	Animal species	Pathological findings	Advantages	Limitations	PH group	References
Physical stimuli						
Chronic hypoxia	Guinea pig, mouse, pig, rat, sheep	Chronic hypoxia exposure results in pulmonary vasoconstriction, muscularization of non-muscular arterioles, increased media thickness and matrix deposition	• Widely used • Simple implementation	• Hypoxia response is variable among animal species	1/3	[27-30]
Vascular obstruction	Dog, pig, rat, sheep	Pulmonary arteries embolization caused by intravenous administration of synthetic microspheres	• Useful to study chronic pulmonary thromboembolism • Possibility of target different-sized vessels depending on the diameter size of the microspheres	• Possibility of cellular reaction with the microsphere material	4	[14, 30-34]

Increased blood flow	Dog, pig, rat, sheep	Surgical formation of a left-to-right shunt causes an increase in pulmonary blood flow, leading to PH with vascular remodeling	• Useful to mimic some congenital heart diseases and study the RV response to increased pressure and flow	• Requires highly technical skills • Generally associated with a high percentage of animal death	1	[30, 35-37]
Pulmonary artery banding	Mouse, rat, goat	Pulmonary artery banding leads to progressive pulmonary artery stenosis and RV hypertrophy			1	[8, 38, 39]
Chemical stimuli						
Monocrotaline	Dog, pig, rat, sheep	A single MCT injection induces PH characterized by vascular remodeling, increased muscularization, vascular inflammation, RV hypertrophy	• The most broadly used PH animal model • Simple implementation(one single injection) • Relatively inexpensive	• MCT response is variable among species, strains and animals	1	[24, 25, 30, 40-43]
α-Naphthylthiourea	Rat	Repeated injections induce pulmonary vascular remodeling associated with PH development and RV hypertrophy. ANTU-related PH could mimic chemotherapy associated pulmonary vascular changes	• Simple implementation • Relatively inexpensive	• Mimic only a few features of human PH, not being commonly used models	No defined group	[44, 45]
Bleomycin	Mouse, rabbit, rat	Bleomycin administration leads to pulmonary fibrosis development with increased lung inflammation and muscularization. Useful to study PH in interstitial lung diseases			3	[46-49]

Group B Streptococcus	Pig, sheep	Group B Streptococcus exposure induces vasoconstriction in persistent PH of the newborn	• Simple implementation • Relatively inexpensive	• Mimic only a few features of human PH, not being commonly used models	1'' (Persistent pulmonary hypertension of the newborn)	[50-52]
Genetic stimuli						
Ang-1 overexpression	Rat	Transgenic rats overexpressing Ang-1 develop increased pulmonary arterial muscularization and vascular occlusion	• Useful to study the role of specific pathways in PH development and progression	• May not sum up all the complex features of PH • Expensive models	1	[53]
IL-6 overexpression	Mouse	Mice overexpressing IL-6 develop PH with increased pulmonary arterial muscularization and RV hypertrophy. IL-6 effects are augmented by hypoxia			1	[54]
S100A4/Mts1 overexpression	Mouse	Approximately 5% of transgenic mice overexpressing the calcium binding protein S100A4/Mts1 develop pulmonary arterial changes resembling human plexogenic arteriopathy			1	[55]
5-HTT overexpression	Mouse	5-HTT overexpression leads to PH development with pulmonary arterial remodeling and RV hypertrophy. Increased hypoxia-induced remodeling			1	[56]

TGF-α overexpression	Mouse	TGF-α overexpression leads to disruption of pulmonary vascular development and induction of severe PH and vascular remodeling characterized by abnormally extensive muscularization of small pulmonary arteries	• Useful to study the role of specific pathways in PH development and progression	• May not sum up all the complex features of PH • Expensive models	1	[57]
TNF-α overexpression	Mouse	Mice overexpressing TNF-α develop chronic lung inflammation, pulmonary emphysema, severe PH, RV hypertrophy			1	[58]
Apolipoprotein-E knockout	Mouse	Apolipoprotein-E knockout mice develop PH with increased pulmonary arterial muscularization and RV hypertrophy. Useful to study insulin resistance and obesity as risk factors for PH development			1	[59]
BMPRII knockout	Mouse	Loss of BMPRII signaling leads to an increase in media smooth muscle thickness and muscularization of small pulmonary arteries			1	[60]
Neprilysin knockout	Mouse	Neprilysin knockout mice present severe PH characterized by muscularization of the distal pulmonary arteries, thickening of the proximal media and adventitia and RV hypertrophy in response to hypoxia			1	[61]

VIP knockout	Mouse	VIP knockout mice develop moderately severe PH with pulmonary vascular remodeling, increased muscularization of the pulmonary arteries and RV hypertrophy. The condition is associated with increased mortality	• Useful to study the role of specific pathways in PH development and progression	• May not sum up all the complex features of PH • Expensive models	1	[62]
Fawn-hooded rat	Rat	Rat strain with a disorder characterized by a deficient serotonin uptake into platelets and with immature developed lungs and a reduced number of alveoli, PH development			1/3	[8, 63]
Broiler chicken	Chicken	Broiler chicken strain is characterized by PH development, possibly by a mitochondrial dysfunction			1/3	[64-67]
Multiple stimuli						
SU5416 + chronic hypoxia	Mouse, rat	VEGFR-2 blockade coupled with chronic hypoxia leads to PH development with complex plexiform-like lesions formation	• Mimic more accurately human PH than single stimuli models, once they exhibit more severe PH and/or vascular lesions (neointimal and plexiform lesions)	• Can be expensive and/or require technical skills	1/3	[68-70]
Athymic + SU5416	Rat	Athymic rats treated with VEGFR-2 blocker develop severe PH with vascular remodeling			1	[71]
Athymic + MCT	Rat	Athymic rats treated with MCT develop severe PH with a greater number of mast cells and severer histopathological changes, such as thickening of the alveolar wall			1	[72]

MCT + pneumonectomy	Rat	Monocrotaline administration coupled with pneumonectomy leads to PH development with additional neointimal lesions formation	• Mimic more accurately human PH than single stimuli models, once they exhibit more severe PH and/or vascular lesions (neointimal and plexiform lesions)	• Can be expensive and/or require technical skills	1	[73]
Young age + MCT + pneumonectomy	Rat	Monocrotaline administration with pneumonectomy in young rats leads to PH development with plexiform-like lesions formation			1	[74]
Endothelin receptor-B deficiency + MCT	Rat	Monocrotaline administration in endothelin receptor-B deficiency rats leads to acceleration of PH progression, enhances the appearance of cellular and molecular markers related with PH pathobiology and develops neointimal lesions			1	[75]

Table 1: Animal models of pulmonary hypertension.

5-HTT : Serotonin Transporter; Ang-1 : Angiopoietin-1; BMPRII : Bone Morphogenetic Protein Receptor Type II; IL-6 : Interleukin-6; TGF-α : Transforming Growth Factor-α; TNF-α : Tumor Necrosis Factor-α; VEGFR-2 : Vascular Endothelial Growth Factor Receptor-2; VIP : Vasoactive Intestinal Peptide.

4. Genetic Animal Models

In the past few years, numerous genetic animal models have emerged in the field of PH research [11, 13, 30]. The transgenic and knockout models allow the evaluation of the effect of overexpressing or downregulating a specific gene in the susceptibility to the development of PH. The high diversity of these models reflects the different molecular pathways underlying PH development [4, 9]. Even though there is not a clear separation, we can group the genetic models by the main processes that they interfere with: vascular tone and inflammation/vascular remodeling. Independently of the group, the most common specie used is the mouse, which is harder to handling in the experimental procedures, such as hemodynamic evaluation [11].

Endothelin (ET)-1 is a potent vasoconstrictor that drives PH development and progression, by acting in its receptors (ET_A and ET_B). ET_A is expressed mainly in pulmonary artery smooth muscle cells (PASMCs) and is related to PASMC proliferation and vasoconstriction. On the other hand, ET_B is expressed in pulmonary artery endothelial cells (PAECs) and PASMCs. Activation of ET_B in the PAECs causes vasodilatation *via* the release of nitric oxide and prostaglandin, while stimulation of ET_B in the PASMCs causes vasoconstriction [76]. Nevertheless, both heterozygote ET-1 knockouts and ET-1 overexpressers transgenic models fail to alter pulmonary vascular pressures *per se* [4]. Yet, ET_B receptor knockout mice have the vasodilatory effect of this receptor blunted and is linked with enhanced appearance of cellular and molecular markers related with PH pathobiology and development of neointimal lesions when in combination with MCT [75]. Serotonin (5-HT) is also an important regulator of vascular tone associated with PH pathogenesis [3]. Genetic models with 5-HT related alterations greatly contributed to the current knowledge of this mediators' role. Consistently, tryptophan hydroxylase 1 (involved in 5-HT synthesis) knockout mice [77], 5-HTT (5-HT transporter) knockout [78] and 5-HT1B (5-HT receptor) knockout [79] attenuate hypoxia-induced PH, while 5-HTT gene overexpressing mice present a more severe form of the disease [56].

Inflammation is a key feature of PH pathogenesis, being already a therapeutic target [80, 81]. Genetic models are particularly useful for studying the effect of specific cytokines in PH pathophysiology. Among others, TNF-α [58] and TGF-α [57] overexpression is linked to PH. But, by far, the best studied models are the ones that target IL-6 related pathways. In fact, it is documented an increase in serum expression of IL-6 in patients with PAH, which positively correlates with the mortality rate [82, 83]. The mouse model of IL-6 overexpression was first implemented by Steiner *et al.* [54]. They found RV hypertrophy, an increased muscularization throughout the entire pulmonary vascular bed and the formation of occlusive neointimal angioproliferative lesions composed of endothelial cells and T-lymphocytes. Consistently, Savale *et al.* [84] found, in an IL-6 knockout model, diminished susceptibility to hypoxia-induced PH. They reported a decrease in media thickening of pulmonary vessels in IL-6 deficient mice and also a role of IL-6 in PASMC migration. Altogether, the IL-6 overexpressing mouse seems to be a model that resembles many of the pathologic features of PH. As a matter of fact, IL-6 has been proposed to regulate several pathways that are implicated in PH. It is believed that IL-6 drives the hyperproliferative state of PASMCs, modulates several pro- and anti-apoptotic factors [54] and the BMP signaling cascade [85]. Since a mutation of the *BMPRII* gene that encodes for the bone morphogenetic protein receptor II was discovered to be a

principal mutation in hereditary PAH [86], there have been attempts to create BMPRII-deficient mice. However, the complete deletion of the gene is incompatible with life and heterozygotes do not develop adequate disease severity [11]. This problem was overcome by the appearance of smooth muscle-specific transgenic mice expressing a dominant-negative BMPRII under control of a tetracycline gene switch system [60]. There is consistent evidence of the disease development in this model, namely an increase in RV systolic pressure, RV hypertrophy, an increase in muscularization of small pulmonary arteries and some blood flow changes [60, 87]. The BMPRII ligands are also targets of research in the field of PAH. BMP-2 and BMP-4 are the most important factors of this class and act in opposite ways in response to hypoxia: BMP-2 knockout mice have increase severity while the opposite happens with BMP-4 knockout mice [88].

The protein S100A4/Mst1 is part of a family of calcium-binding proteins whose functions are related with cell proliferation, differentiation, cytoskeletal dynamics and apoptosis [4, 8]. Interestingly, the transgenic mice overexpressing S100A4/Mst1 model was initially developed aiming the study of S100A4/Mst1 role in metastatic cancer [89]. However, it was observed that approximately 5% of the S100A4/Mst1 overexpressing mice develop pulmonary vascular remodeling similar to that observed in PH [55]. Thus, the importance of this model in PH study is related with the presence of pulmonary vascular changes resembling human plexiform lesions, which is a feature absent in the majority of the PH models. Noteworthy, although the majority of the PH models show increased male susceptibility, contrary of what is observed in human PH; two genetic animal models (mice overexpressing the protein S100A4/Mts1 and mice overexpressing the serotonin transporter) showed a PH development female gender specific [90]. The fact that genetic models may not sum up all the complex features of PH, once they focus in the study of particular pathways is a limitation [11]. Furthermore, genetically modified mice are expensive, which may cause a limitation in the number of samples [91].

5. Animal Models Involving Multiple Stimuli

Animal models that involve chronic hypoxia and MCT models have been developed aiming more severe PH and/or vascular lesions such as neointimal and plexiform lesions [92]. These occlusive lesions, which result from smooth muscle and endothelial cell proliferation, are hallmarks of Group 1 PH, being major contributors for the high pulmonary vascular resistance in PAH [93, 94]. However, they are absent in the most common single stimuli animal

models. Those models that combine multiple insults result in more severe PH than single stimuli, suggesting that the pathogenesis of PH requires several insults [11]. SU5416 is a small molecule inhibitor of the vascular endothelial growth factor receptor-2 (VEGFR-2). Given that VEGF is important for normal endothelial cell function, its blockade was expected to induce endothelial cell dysfunction, stimulate apoptosis-resistant endothelial cell proliferation and consequently cause PH [93]. Indeed, the SU5416/chronic hypoxia model is the most used multiple stimuli model to study both PH pathogenesis and treatment. Interestingly, this model demonstrated resistance to some drugs commonly used in PAH patients, being thus refractory to treatment as it is verified in most PAH patients [8, 93, 95]. However, a limitation of SU5416/chronic hypoxia model is the absence of perivascular inflammation, a key feature of human PAH [10, 11]. Another relevant multiple model consists in MCT administration coupled with pneumonectomy, which add to the MCT model vascular characteristics the presence of neointimal lesions [73]. Nevertheless, it requires technical skills associated with the experimental procedure.

6. Conclusion and Future Perspectives

The complexity of the molecular mechanisms underlying PH pathogenesis and the diverse etiology that characterizes this disease makes the implementation of animal models a truly demanding task. Although a “gold” animal model in PH research does not exist, there are several animal models available nowadays, each one presenting specific features of the disease, allowing the investigation of key aspects of the disease. These models are important not only for the discovery and exploration of the molecular pathways underlying disease pathogenesis but also for the assessment of therapeutic suitability to treat PH patients.

However, caution should be taken when translating data from animal models to the human context considering the different aspects of the disease in animal models. So, efforts should continue to be done in the development of animal models that more exactly mimic the features of each group of human PH. The current trend is the use of two animal models, such as MCT and chronic hypoxia, to demonstrate that data obtained are model independent and to facilitate data translation to the human clinical set. The simultaneous use of distinct PH animal models to test an experimental therapy is expected to continue and even increase once raises the hypothesis of its suitability for PH patients.

Acknowledgements

This work was supported by Fundação para a Ciência e a Tecnologia (FCT, Portugal), European Union, QREN, FEDER and COMPETE for funding the Organic Chemistry Research Unit (QOPNA) (UID/QUI/00062/2013), the Cardiovascular R&D Unit (UID/IC/00051/2013) and the post-graduation student (grant number SFRH/BD/91067/2012).

Conflicts of Interest

The authors report no conflicts of interest.

References

1. Simonneau G, Robbins IM, Beghetti M, Channick RN, Delcroix M, et al. Updated clinical classification of pulmonary hypertension. J Am Coll Cardiol 6 (2013): 34-41.
2. McLaughlin VV, Shah SJ, Souza R, Humbert M. Management of pulmonary arterial hypertension. J Am Coll Cardiol 65 (2015): 1976-1997.
3. Wilkins MR. Pulmonary hypertension: the science behind the disease spectrum. Eur Respir Rev 21 (2012): 19-26.
4. West J, Hemnes A. Experimental and transgenic models of pulmonary hypertension. Compr Physiol 1 (2011): 769-782.
5. Zanjani KS. Platelets in pulmonary hypertension: a causative role or a simple association? Iran J Pediatr 22 (2012): 145-157.
6. Colvin KL and Yeager ME. Animal models of pulmonary hypertension: matching disease mechanisms to etiology of the human disease. J Pulm Respir Med 4 (2014): 198.
7. Ryan JK, Bloch K and Archer SL. Rodent models of pulmonary hypertension: harmonisation with the world health organisation's categorisation of human PH. Int J Clin Pract Suppl 172 (2011): 15-34.
8. Maarman GS, Lecour G, Butrous F, Thienemann and Sliwa K. A comprehensive review: the evolution of animal models in pulmonary hypertension research; are we there yet? Pulm Circ. 3 (2013): 739-56.
9. Das M, Fessel J, Tang H, West J. A process-based review of mouse models of pulmonary hypertension. Pulm Circ 2 (2012): 415-433.

10. Zhao L. Chronic hypoxia-induced pulmonary hypertension in rat: the best animal model for studying pulmonary vasoconstriction and vascular medial hypertrophy. Drug Discov Today Dis Models 7 (2010): 83-88.
11. Ryan JJ, Marsboom G, Archer SL. Rodent models of group 1 pulmonary hypertension. Handb Exp Pharmacol 218 (2013): 105-149.
12. Voelkel NF, Tuder RM. Hypoxia-induced pulmonary vascular remodeling: a model for what human disease? J Clin Invest 106 (2000): 733-738.
13. Barman SA, Zhu S, White RE. RhoA/Rho-kinase signaling: a therapeutic target in pulmonary hypertension. Vasc Health Risk Manag 5 (2009): 663-671.
14. Shelub I, van Grondelle A, McCullough R, Hofmeister S, Reeves JT. A model of embolic chronic pulmonary hypertension in the dog. J Appl Physiol Respir Environ Exerc Physiol 56 (1984): 810-815.
15. Vonk Noordegraaf A, Galiè N. The role of the right ventricle in pulmonary arterial hypertension. Eur Respir Rev 20 (2011): 243-253.
16. Van Albada ME, Schoemaker RG, Kemna MS, Cromme-Dijkhuis AH, R. Van Veghel, et al. The role of increased pulmonary blood flow in pulmonary arterial hypertension. Eur Respir J 26 (2005): 487-93.
17. Hirata M, Ousaka D, Arai S, Okuyama M. Tarui S, et al. Novel model of pulmonary artery banding leading to right heart failure in rats. Biomed Res Int 2015 (2015): 1-10.
18. Dias-Neto M, Luísa-Neves A, Pinho S, Gonçalves N, Mendes M, et al. Pathophysiology of infantile pulmonary arterial hypertension induced by monocrotaline. Pediatr Cardiol 2015. 36 (2015): 1000-1013.
19. Umar S, Steendijk P, Ypey DL, Atsma DE, van der Wall EE, et al. Novel approaches to treat experimental pulmonary arterial hypertension: a review. J Biomed Biotechnol 2010 (2010): 702836.
20. Nogueira-Ferreira RR, Vitorino R. Ferreira and T. Henriques-Coelho. Exploring the monocrotaline animal model for the study of pulmonary arterial hypertension: A network approach. Pulm Pharmacol Ther 35 (2015): 8-16.
21. Schoental R, Head MA. Pathological changes in rats as a result of treatment with monocrotaline. Br J Cancer 9 (1955): 229-237.
22. Dumitrascu R, Koebrich S, Dony E, Weissmann N, Savai R, et al. Characterization of a murine model of monocrotaline pyrrole-induced acute lung injury. BMC Pulm Med 8 (2008): 25.

23. Okada M, Yamashita C and Okada K. Establishment of canine pulmonary hypertension with dehydromonocrotaline. Importance of larger animal model for lung transplantation. Transplantation 60 (1995): 9-13.
24. Zeng GQ, Liu R, Liao HX, Zhang XF, Qian YX, et al. Single intraperitoneal injection of monocrotaline as a novel large animal model of chronic pulmonary hypertension in Tibet minipigs. PLoS One 8(2013): e78965.
25. Gomez-Arroyo JG, Farkas L, Alhussaini AA, Farkas D, Kraskauskas D, et al. The monocrotaline model of pulmonary hypertension in perspective. Am J Physiol Lung Cell Mol Physiol 302 (2012): L363-L369.
26. Naeije R, Dewachter L. [Animal models of pulmonary arterial hypertension]. Rev Mal Respir 24 (2007): 481-496.
27. Meyrick B and Reid L. Hypoxia-induced structural changes in the media and adventitia of the rat hilar pulmonary artery and their regression. Am J Pathol 100 (1980): 151-178.
28. Steudel W, Scherrer-Crosbie M, Bloch KD, Weimann J, Huang PL, et al. Sustained pulmonary hypertension and right ventricular hypertrophy after chronic hypoxia in mice with congenital deficiency of nitric oxide synthase 3. J Clin Invest 101 (1998): 2468-2477.
29. Janssens SP, Thompson BT, Spence CR, Hales CA. Polycythemia and vascular remodeling in chronic hypoxic pulmonary hypertension in guinea pigs. J Appl Physiol 71 (1991): 2218-2223.
30. Marsboom GR and Janssens SP. Models for pulmonary hypertension. Drug Discov Today Dis Models 1 (2004): 289-296.
31. Weimann J, Zink W, Gebhard MM, Gries A, Martin E, et al. Effects of oxygen and nitric oxide inhalation in a porcine model of recurrent microembolism. Acta Anaesthesiol Scand 44(2000): 1109-1115.
32. Zagorski J, Debelak J, Gellar M, Watts JA and Kline JA. Chemokines accumulate in the lungs of rats with severe pulmonary embolism induced by polystyrene microspheres. J Immunol 171 (2003): 5529-5536.
33. Jones AE, Watts JA, Debelak JP, Thornton LR, Younger JG, et al. Inhibition of prostaglandin synthesis during polystyrene microsphere-induced pulmonary embolism in the rat. Am J Physiol Lung Cell Mol Physiol. 284 (2003): L1072-L1081.
34. Weimann J, Zink W, Schnabel PA, Jakob H, Gebhard MM, et al. Selective vasodilation by nitric oxide inhalation during sustained pulmonary hypertension following recurrent microembolism in pigs. J Crit Care 14 (1999): 133-140.

35. Rondelet B, Kerbaul F, Motte S, Van Beneden R, Remmelink M, et al. Bosentan for the prevention of overcirculation-induced experimental pulmonary arterial hypertension. Circulation 107 (2003): 1329-1335.
36. Corno AF, Tozzi P, Genton CY and Von Segesser LK. Surgically induced unilateral pulmonary hypertension: time-related analysis of a new experimental model. Eur J Cardiothorac Surg 23(2003): 513-517.
37. Reddy VM, Meyrick B, Wong J, Khoor A, Liddicoat JR, et al. In utero placement of aortopulmonary shunts: a model of postnatal pulmonary hypertension with increased pulmonary blood flow in lambs. Circulation 92 (1995): 606-613.
38. Dias CA, Assad RS, Caneo LF, Abduch MCD, Aiello VD, et al. Reversible pulmonary trunk banding. II. An experimental model for rapid pulmonary ventricular hypertrophy. J Thorac Cardiovasc Surg 124 (2002): 999-1006.
39. Bogaard HJ, Mizuno S, Hussaini AA, Toldo S, Abbate A, et al. Suppression of histone deacetylases worsens right ventricular dysfunction after pulmonary artery banding in rats. Am J Respir Crit Care Med 183 (2011): 1402-1410.
40. Hilliker KS, Bell TG, Roth RA. Pneumotoxicity and thrombocytopenia after single injection of monocrotaline. Am J Physiol 242 (1982): H573-H579.
41. Sugita T, Hyers TM, Dauber IM, Wagner WW, Mcmurtry IF, et al. Reeves Lung vessel leak precedes right ventricular hypertrophy in monocrotaline-treated rats. J Appl Physiol Respir Environ Exerc Physiol 54 (1983): 371-374.
42. Rosenberg HC and Rabinovitch M. Endothelial injury and vascular reactivity in monocrotaline pulmonary hypertension. Am J Physiol 255(1988): H1484-H1491.
43. Ito KM, Sato M, Ushijima K, Nakai M and Ito K. Alterations of endothelium and smooth muscle function in monocrotaline-induced pulmonary hypertensive arteries. Am J Physiol Heart Circ Physiol 279 (2000): H1786-H1795.
44. Azoulay E, Eddahibi S, Marcos E, Levame M, Harf A, et al. Granulocyte colony-stimulating factor enhances alpha-naphthylthiourea-induced pulmonary hypertension. J Appl Physiol 94 (1985): 2027-2033.
45. Hill NS, O'brien RF and Rounds S. Repeated lung injury due to alpha-naphthylthiourea causes right ventricular hypertrophy in rats. J Appl Physiol Respir Environ Exerc Physiol 56 (1984): 388-396.

46. Ortiz LA, Champion HC, Lasky JA, Gambelli F, Gozal E, et al. Enalapril protects mice from pulmonary hypertension by inhibiting TNF-mediated activation of NF-kappaB and AP-1. Am J Physiol Lung Cell Mol Physiol 282 (2002): L1209-L1221.
47. Bowden DH. Unraveling pulmonary fibrosis: the bleomycin model. Lab Invest 50 (1984): 487-488.
48. Harrison JH Jr, Lazo JS. High dose continuous infusion of bleomycin in mice: a new model for drug-induced pulmonary fibrosis. J Pharmacol Exp Ther 243 (1987): 1185-1194.
49. Lynch DA, Hirose N, Cherniack RM and Doherty DE. Bleomycin-induced lung disease in an animal model: correlation between computed tomography-determined abnormalities and lung function. Acad Radiol 4 (1997): 102-107.
50. Curtis J, Kim G, Wehr NB, Levine RL. Group B streptococcal phospholipid causes pulmonary hypertension. Proc Natl Acad Sci U S A 100 (2003): 5087-5090.
51. Navarrete CT, Devia C, Lessa AC, Hehre D, Young K, et al. The role of endothelin converting enzyme inhibition during group B streptococcus-induced pulmonary hypertension in newborn piglets. Pediatr Res 54 (2003): 387-392.
52. Carpenter DT, Larkin HR, Chang AS, Morris E, O'neill JT, et al. Superoxide dismutase and catalase do not affect the pulmonary hypertensive response to group B Streptococcus in the lamb. Pediatr Res 49 (2001): 181-188.
53. Chu D, Sullivan CC, Du L, Cho AJ, Kido M, et al. A new animal model for pulmonary hypertension based on the overexpression of a single gene angiopoietin-1. Ann Thorac Surg 77 (2004): 449-456.
54. Steiner MK, Syrkina OL, Kolliputi N, Mark EJ, Hales CA, et al. Interleukin-6 overexpression induces pulmonary hypertension. Circ Res 104 (2009): 236-244.
55. Greenway S, Van Suylen RJ, Du Marchie Sarvaas G, Kwan E, Ambartsumian N, et al. S100A4/Mts1 produces murine pulmonary artery changes resembling plexogenic arteriopathy and is increased in human plexogenic arteriopathy. Am J Pathol 164 (2004): 253-262.
56. Maclean MR, Deuchar GA, Hicks MN, Morecroft I, Shen S, et al. Overexpression of the 5-hydroxytryptamine transporter gene: effect on pulmonary hemodynamics and hypoxia-induced pulmonary hypertension. Circulation 109 (2004): 2150-2155.

57. Le Cras TD, Hardie WD, Fagan K, Whitsett JA, Korfhagen TR. Disrupted pulmonary vascular development and pulmonary hypertension in transgenic mice overexpressing transforming growth factor-alpha. Am J Physiol Lung Cell Mol Physiol 285 (2003): L1046-L1054.
58. Fujita M, Shannon JM, Irvin CG, Fagan KA, Cool C, et al. Overexpression of tumor necrosis factor-alpha produces an increase in lung volumes and pulmonary hypertension. Am J Physiol Lung Cell Mol Physiol 280 (2001): L39-L49.
59. Hansmann G, Wagner RA, Schellong S, De Jesus Perez VA, Urashima T, et al. Pulmonary arterial hypertension is linked to insulin resistance and reversed by peroxisome proliferator–activated receptor-? activation. Circulation 115 (2007): 1275-1284.
60. West J, Fagan K, Steudel W, Fouty B, Lane K, et al. Pulmonary hypertension in transgenic mice expressing a dominant-negative BMPRII gene in smooth muscle. Circ Res 94 (2004): 1109-1114.
61. Dempsey EC, Wick MJ, Karoor V, Barr EJ, Tallman DW, et al. Neprilysin null mice develop exaggerated pulmonary vascular remodeling in response to chronic hypoxia. Am J Pathol 174 (2009): 782-796.
62. Said SI, Hamidi SA, Dickman KG, Szema AM, Lyubsky S, et al. Moderate pulmonary arterial hypertension in male mice lacking the vasoactive intestinal peptide gene. Circulation 115 (2007): 1260-1268.
63. Le Cras TD, Kim DH, Gebb S, Markham NE, Shannon JM, et al. Abnormal lung growth and the development of pulmonary hypertension in the Fawn-Hooded rat. Am J Physiol 277 (1999): L709-L718.
64. Martinez-Lemus LA, Hester RK, Becker EJ, Jeffrey JS, and Odom TW. Pulmonary artery endothelium-dependent vasodilation is impaired in a chicken model of pulmonary hypertension. Am J Physiol 277 (1999): R190-R197.
65. Xiang RP, Sun WD, Zhang KC, Li JC, Wang JY, et al. Sodium chloride-induced acute and chronic pulmonary hypertension syndrome in broiler chickens. Poult Sci 83 (2004): 732-736.
66. Cawthon D, Iqbal M, Brand J, Mcnew R and Bottje WG. Investigation of proton conductance in liver mitochondria of broilers with pulmonary hypertension syndrome. Poult Sci 83 (2004): 259-265.
67. Iqbal M, Cawthon D, Wideman Jr RF, and Bottje WG. Lung mitochondrial dysfunction in pulmonary hypertension syndrome. I. Site-specific defects in the electron transport chain. Poult Sci 80 (2001): 485-495.

68. Abe K, Toba M, Alzoubi A, Ito M, Fagan KA, et al. Formation of plexiform lesions in experimental severe pulmonary arterial hypertension. Circulation 121 (2010): 2747-2754.
69. Taraseviciene-Stewart L, Kasahara Y, Alger L, Hirth P, Mc Mahon G, et al. Inhibition of the VEGF receptor 2 combined with chronic hypoxia causes cell death-dependent pulmonary endothelial cell proliferation and severe pulmonary hypertension. Faseb J 15 (2001): 427-438.
70. Ciuclan L, Bonneau O, Hussey M, Duggan N, Holmes AM, et al. A novel murine model of severe pulmonary arterial hypertension. Am J Respir Crit Care Med 184 (2011): 1171-82.
71. Taraseviciene-Stewart L, Nicolls MR, Kraskauskas D, Scerbavicius R, Burns N, et al. Absence of T cells confers increased pulmonary arterial hypertension and vascular remodeling. Am J Respir Crit Care Med 175 (2007): 1280-1289.
72. Miyata M, Sakuma F, Ito M, Ohira H, Sato Y, et al. Athymic nude rats develop severe pulmonary hypertension following monocrotaline administration. Int Arch Allergy Immunol 121 (2000): 246-52.
73. Okada K, Tanaka Y, Bernstein M, Zhang W, Patterson GA, et al. Pulmonary hemodynamics modify the rat pulmonary artery response to injury. A neointimal model of pulmonary hypertension. Am J Pathol 151 (1997): 1019-1025.
74. White RJ, Meoli DF, Swarthout RF, Kallop DY, Galaria II, et al. Plexiform-like lesions and increased tissue factor expression in a rat model of severe pulmonary arterial hypertension. Am J Physiol Lung Cell Mol Physiol 293 (2007): L583-L590.
75. Ivy DD, Mcmurtry IF, Colvin K, Imamura M, Oka M, et al. Development of occlusive neointimal lesions in distal pulmonary arteries of endothelin B receptor-deficient rats: a new model of severe pulmonary arterial hypertension. Circulation 111 (2005): 2988-2996.
76. Galié N, Manes A, Branzi A. The endothelin system in pulmonary arterial hypertension. Cardiovasc Res 61 (2004): 227-237.
77. Izikki M, Hanoun N, Marcos E, Savale L, Barlier-Mur AM, et al. Tryptophan hydroxylase 1 knockout and tryptophan hydroxylase 2 polymorphism: effects on hypoxic pulmonary hypertension in mice. Am J Physiol Lung Cell Mol Physiol 293 (2007): L1045-L1052.
78. Eddahibi S, Hanoun N, Lanfumey L, Lesch KP, Raffestin B, et al. Attenuated hypoxic pulmonary hypertension in mice lacking the 5-hydroxytryptamine transporter gene. J Clin Invest 105 (2000): 1555-1562.

79. Keegan A, Morecroft I, Smillie D, Hicks MN, Maclean MR. Contribution of the 5-HT(1B) receptor to hypoxia-induced pulmonary hypertension: converging evidence using 5-HT(1B)-receptor knockout mice and the 5-HT(1B/1D)-receptor antagonist GR127935. Circ Res 89 (2001): 1231-1239.
80. Mathew R. Inflammation and pulmonary hypertension. Cardiol Rev 18 (2010): 67-72.
81. Henriques-Coelho T, Oliveira SM, Moura RS, Roncon-Albuquerque Jr R, Neves AL, Thymulin inhibits monocrotaline-induced pulmonary hypertension modulating interleukin-6 expression and suppressing p38 pathway. Endocrinology 149 (2008): 4367-4373.
82. Selimovic N, Bergh CH, Andersson B, Sakiniene E, Carlsten H, et al. Growth factors and interleukin-6 across the lung circulation in pulmonary hypertension. Eur Respir J 34 (2009): 662-668.
83. Heresi GA, Aytekin M, Hammel JP, Wang S, Chatterjee S, et al. Plasma interleukin-6 adds prognostic information in pulmonary arterial hypertension. Eur Respir J 43 (2014): 912-914.
84. Savale L, Tu L, Rideau D, Izziki M, Maitre B, et al. Impact of interleukin-6 on hypoxia-induced pulmonary hypertension and lung inflammation in mice. Respir Res 10 (2009): 6.
85. Hagen M, Fagan K, Steudel W, Carr M, Lane K, et al. Interaction of interleukin-6 and the BMP pathway in pulmonary smooth muscle. Am J Physiol Lung Cell Mol Physiol 292 (2007): L1473-L1479.
86. Thomson JR, Machado RD, Pauciulo MW, Morgan NV, Humbert M. Sporadic primary pulmonary hypertension is associated with germline mutations of the gene encoding BMPR-II a receptor member of the TGF-beta family. J Med Genet 37 (2000): 741-745.
87. Yasuda T, Tada Y, Tanabe N, Tatsumi K, West J. Rho-kinase inhibition alleviates pulmonary hypertension in transgenic mice expressing a dominant-negative type II bone morphogenetic protein receptor gene. Am J Physiol Lung Cell Mol Physiol 301 (2011): L667-L674.
88. Anderson L, Lowery JW, Frank DB, Novitskaya T, Jones M, et al. Bmp2 and Bmp4 exert opposing effects in hypoxic pulmonary hypertension. Am J Physiol Regul Integr Comp Physiol 298 (2000): R833-R842.
89. Ambartsumian N, Grigorian M, Lukanidin E. Genetically modified mouse models to study the role of metastasis-promoting S100A4(mts1) protein in metastatic mammary cancer. J Dairy Res 72 (2005): 27-33.
90. Dempsie Y, MacLean MR. The influence of gender on the development of pulmonary arterial hypertension. Exp Physiol 98 (2013): 1257-1261.
91. Leong XF, Ng CY, Jaarin K. Animal Models in Cardiovascular Research: Hypertension and Atherosclerosis. Biomed Res Int 2015 (2015): 528757.

92. Stenmark KR, Meyrick B, Galie N, Mooi WJ, McMurtry IF. Animal models of pulmonary arterial hypertension: the hope for etiological discovery and pharmacological cure. Am J Physiol Lung Cell Mol Physiol 297 (2009): L1013-L1032.
93. Nicolls MR, Mizuno S, Taraseviciene-Stewart L, Farkas L, Drake JI, et al. New models of pulmonary hypertension based on VEGF receptor blockade-induced endothelial cell apoptosis. Pulm Circ 2 (2012): 434-442.
94. Firth AL, Mandel J, Yuan JX. Idiopathic pulmonary arterial hypertension. Dis Model Mech 3 (2010): 268-273.
95. Taraseviciene-Stewart L, Scerbavicius R, Choe KH, Cool C, Wood K, et al. Simvastatin causes endothelial cell apoptosis and attenuates severe pulmonary hypertension. Am J Physiol Lung Cell Mol Physiol 291 (2006): L668-L676.

REVIEW IV – EXPLORING THE MONOCROTALINE ANIMAL MODEL FOR THE STUDY OF PULMONARY ARTERIAL HYPERTENSION: A NETWORK APPROACH

Pulmonary Pharmacology & Therapeutics 35 (2015) 8–16

Contents lists available at ScienceDirect

Pulmonary Pharmacology & Therapeutics

journal homepage: www.elsevier.com/locate/ypupt

Exploring the monocrotaline animal model for the study of pulmonary arterial hypertension: A network approach

Rita Nogueira-Ferreira [a, b], Rui Vitorino [a, c], Rita Ferreira [a, *], Tiago Henriques-Coelho [b, **]

[a] QOPNA, Department of Chemistry, University of Aveiro, Aveiro, Portugal
[b] Department of Physiology and Cardiothoracic Surgery, Faculty of Medicine, University of Porto, Porto, Portugal
[c] iBiMED, Institute for Biomedical Research, University of Aveiro, Aveiro, Portugal

ARTICLE INFO

Article history:
Received 11 May 2015
Received in revised form
16 September 2015
Accepted 18 September 2015
Available online 21 September 2015

Keywords:
Inflammation
Preclinical models
Pulmonary arterial hypertension
Vascular remodeling

ABSTRACT

Pulmonary arterial hypertension (PAH) is responsible for the premature death mainly because of progressive and severe heart failure. This disease is characterized by increased pulmonary vascular tone, inflammatory cell infiltration, vascular remodeling and occlusion of vessels with thrombi, frequently leading to right heart failure. Aiming to better comprehend the complexity of PAH and find novel therapeutic strategies or improve the existing ones, a variety of preclinical models have emerged. Although there is no ideal preclinical model of PAH currently available, animal models have been used to assist in the identification of the molecular pathways underlying PAH development and progression, and in the identification of novel therapeutics. Among preclinical models of PAH, monocrotaline (MCT) animal model offers the advantage of mimic several key aspects of human PAH, including vascular remodeling, proliferation of smooth muscle cells, endothelial dysfunction, upregulation of inflammatory cytokines, and right ventricle failure, requiring a single drug injection. This review summarizes the advantages and limitations of MCT animal model to the study of the molecular mechanisms underlying PAH pathogenesis, envisioning to improve the diagnosis and management of this complex disease.

1. Introduction

Pulmonary hypertension (PH) is defined by a mean pulmonary artery pressure (PAP) at or above 25 mmHg. Once PH is associated with a variety of clinical conditions, a classification system has been developed based on PH etiology: Group 1 – pulmonary arterial hypertension (PAH), Group 2 – PH due to left heart diseases, Group 3 – PH due to lung diseases and/or hypoxia, Group 4 – chronic thromboembolic PH (CTEPH) and Group 5 – PH with unclear multifactorial mechanisms; according to the 5th World Symposium on PH held in Nice in 2013 [1,2]. PAH is a progressive and fatal cardiopulmonary disease that includes a heterogeneous group of patients counting individuals with idiopathic PAH, heritable PAH and with several conditions associated with PAH (connective tissue disorders, congenital diseases, portal hypertension, HIV, drugs and toxins) [1,3–5]. The pathogenic mechanisms underlying PAH include vascular remodeling, inflammation, vasoconstriction and *in situ* thrombosis. All these changes in the pulmonary vascular bed may lead to increased pulmonary vascular resistance and consequent elevated PAP, increasing the right ventricle (RV) afterload, which results in RV hypertrophy and eventually in RV failure [3,6]. Although PAH current treatments have showed a beneficial impact on patient survival and quality of life, this disease remains without cure and PAH-related mortality is still extremely high [7]. The limited success of PAH treatment is mainly due to the poorly understanding of its pathophysiology and to the lack of effective empiric therapeutic regimens. Thus, preclinical models emerge as a tool to aid in the comprehension of the pathophysiological mechanisms of such a multifactorial and complex disease and they are also helpful in the investigation of novel therapeutic strategies [8]. The advantages of using preclinical models are connected to the following issues: i) control of the experimental procedure; ii) animal availability in large numbers, offering replicability and statistical power and iii) evaluation of the risk-benefit ratio of a drug usage, ensuring drug safety in human [9–12].

* Corresponding author. Department of Chemistry, University of Aveiro, 3810-193 Aveiro, Portugal.
** Corresponding author. Department of Physiology and Cardiothoracic Surgery, Faculty of Medicine, University of Porto, Alameda Professor Hernâni Monteiro, 4200-319 Porto, Portugal.
E-mail addresses: ritaferreira@ua.pt (R. Ferreira), henriques.coelho@gmail.com (T. Henriques-Coelho).

http://dx.doi.org/10.1016/j.pupt.2015.09.007
1094-5539/

Abbreviations

BMPRII	Bone morphogenetic protein receptor type II
cav-1	Caveolin-1
cGMP	Cyclic guanosine monophosphate
DNA	Deoxyribonucleic acid
eNOS	Endothelial nitric oxide synthase
ET_B	Endothelin-1 type B receptor
iNOS	Inducible nitric oxide synthase
LV	Left ventricle
MCT	Monocrotaline
MCTP	Monocrotaline pyrrole
mRNA	Messenger ribonucleic acid
PAH	Pulmonary arterial hypertension
PAP	Pulmonary artery pressure
PCR	Polymerase chain reaction
PECAM-1	Platelet endothelial cell adhesion molecule-1
PH	Pulmonary hypertension
RV	Right ventricle
TGF-β	Transforming growth factor-β

Animal models have been used to study PAH pathogenesis, as well as the effects of drug interventions [9,11]. The choice of the animal model is mainly dictated by the scientific question to be answered [13]. An animal model should mimic the human disease and allow the determination of relevant clinical, biochemical, hemodynamic and histopathological features. Nevertheless, no model mimics exactly all the features of human disease [9,11,14] and so, several PAH experimental models are currently available [8,12]. Amongst the several existing PAH experimental models, the monocrotaline (MCT) model is perhaps the one that has most contributed to the understanding of PAH pathophysiology and to the development of therapeutics; thus it follows a more detailed description of the features of this animal model.

2. The monocrotaline model of pulmonary arterial hypertension

Although the MCT animal model was introduced more than 40 years ago [15,16] and despite its frequent use, the mechanism underlying PAH development by MCT administration remains poorly understood [17]. MCT is a pyrrolizidine alkaloid present in the stems, leaves, and seeds of the plant *Crotalaria spectabilis* and in all the other plants of the *Crotalaria* genus, but in a lower concentration. The toxicity of MCT is essentially hepatic and cardiopulmonary, affecting both animals and humans. Importantly, if applied topically or injected it does not cause localized toxicity. MCT causes lesions in several organs after absorption and hepatic bioactivation [18]. Within the liver, MCT may undergo several chemical reactions, leading to toxic and non-toxic products. Monocrotaline pyrrole (MCTP), also called dehydromonocrotaline, is a toxic metabolite of MCT formed by the enzyme cytochrome P-450 3A in the liver [17,19,20]. Typically, the MCT model is based upon a single MCT injection (usually 60 mg/kg) applied intraperitoneally or subcutaneously, resulting in the development of PAH after 3–4 weeks [17,20]. However, other doses have been used and a dose-dependent response to MCT has been observed [20,21]. Once MCT-induced PAH progression to death might be too quick, a lower dose of MCT (30 mg/kg) that results in milder PAH was reported in works focused on the study of the mechanisms underlying PAH-related compensated RV hypertrophy [21,22]. Although the MCT active compound, MCTP, is degraded rapidly in aqueous solutions such as plasma (half-life of 3–4 s), its accumulation in erythrocytes, where it conserves the capability to interact with lung tissue, partially explains MCT exposure effects over weeks [20,23]. Regarding the time-course of MCT effects, within hours after injection, signs of pulmonary vascular endothelial damage were reported. After 1 week, an increase in endothelial damage, inflammatory infiltration and edema were observed, but without an increase in PAP. Two weeks after MCT injection, PAP was increased, leading to RV hypertrophy by the third week after drug administration. By 5–6 weeks, half of the injected rats die [24,25].

2.1. Advantages and limitations of monocrotaline model

The MCT model is commonly used by researchers because it is reproducible, inexpensive and does not require particular technical skills [20]. MCT-induced PAH is similar to human PAH in terms of hemodynamic and histopathological severity, and high mortality [26]. However, MCT-induced PAH differs from human PAH by the presentation of an initial permeability lung edema, with early loss of the endothelial barrier and prominent inflammatory adventitial proliferation [26]. Nevertheless, MCT administration combined with pneumonectomy results in the development of histopathological features similar to human PAH, namely neointimal and plexiform lesions [27,28].

The response to MCT is variable among species, strains and animals because the differences in the pharmacokinetics of MCT involving degradation and hepatic formation of the MCT pyrrole or conjugation and excretion [19]. The preferred specie for the study of MCT-induced PAH is currently the rat. Clinical signs of illness are usually not evident immediately after a single exposure of rats to doses of MCT that result in PAH. Within 3–7 days, rats show anorexia, listlessness, failure to gain weight and tachypnea. As lung injury and vascular remodeling progress, animals develop variable degrees of dyspnea, weakness, diarrhea, and peripheral cyanosis [29]. Smaller species, such as mouse, in addition to be harder to image and catheterize, rarely develop significant PAH, have less RV hypertrophy and pulmonary arterial remodeling [21]. One possible explanation is that mice metabolize MCT in a different way comparing with other species [20]. Thus, to overcome the problem of MCT metabolism, the active MCT compound was administrated in mice. However, it was insufficient to reproduce PAH and mice developed acute lung injury in an early phase and lung fibrosis in a late phase [30]. The use of larger animals, such as dogs, usually replicate human PAH more successfully than do rodent models; however, their utility is limited by their size, high cost of the model, the slower disease progression and the ethical limitations related with large animal studies [21,31,32].

2.2. Pathological alterations in monocrotaline-induced pulmonary arterial hypertension

Monocrotaline induces several molecular and cellular alterations at all layers of pulmonary vessels, which consequently lead to modifications at cardiac level. Although MCT can cause injury in other organs (such as liver and kidney), lung and right ventricle are undoubtedly the most studied tissues aiming to better understand the molecular mechanisms underlying PAH in humans and looking for therapeutic strategies. Table 1 summarizes studies that have been conducted to evaluate the expression of various mediators in different tissues (lung, RV and LV) and biological fluids (plasma and serum) in the MCT rat model.

2.2.1. Pulmonary vascular and cardiac lesions

The pulmonary vascular endothelium is thought to be the early target of MCTP toxicity based on circulatory proximity to the liver

Table 1
Protein and mRNA expression of several mediators in monocrotaline-induced pulmonary arterial hypertension in rat.

		Mediator	Gene name	Protein/mRNA expression	Technique	Dose/mg.Kg^{-1}	References
Lung		Hsp27	Hspb1	+	2-DE coupled with nano-LC-MS/MS	60	[49]
		Tropomyosin β chain	Tpm2	+			
		F-actin capping protein β subunit	Capzb	+			
		Septin 2	Sept2	+			
		Peroxiredoxin 2	Prdx2	–			
		14-3-3 ε	Ywhah	+			
		ERp57	Pdia3	+			
		CLIC 1	Clic1	+			
		Hsc70	Hspa8	+	Western blot		
		14-3-3 α/β	Ywhab	+	2-DE coupled with nano-LC-MS/MS Western blot		
		ET-1	Edn1	+	Radioimmunoassay	60	[36]
		eNOS	Nos3	+	Northern blot	60	[37]
				–	Western blot		
		Caveolin-1	Cav1	–	Immunofluorescence Western blot	60	[39]
				–	Western blot	60	[68]
		Tie2	Not available	–	Western blot	60	[68]
		Bcl-xL	Bcl2l1	+			
		sGC alpha1	Gucy1a3	–			
		sGC beta1	Gucy1b3	–			
		IκB alpha	Nfkbia	–			
		Hsp90	Hsp90aa1 Hsp90ab1	–			
		PECAM-1	Pecam1	–	Immunofluorescence	60	[39]
		PCNA	Pcna	+			
		5-HTT	Slc6a4	+	Western blot Real time PCR	60	[41]
		Survivin	Birc5	+	Western blot Real time PCR	60	[42]
		Kv1.5	Kcna5	–	Immunohistochemistry	60	[43]
		Kv2.1	Kcnb1	–	Western blot Real time PCR		
		TGF-β receptor 2	Tgfbr2	–	Immunohistochemistry Western blot Real time PCR	60	[44]
		Activin-A receptor-like kinase-1	Acvrl1	–	Western blot Real time PCR		
		Smad-3	Smad3	–	Immunohistochemistry		
		Smad-4	Smad4	–	Western blot Real time PCR		
		BMPRII	Bmpr2	–	Western blot	60	[45]
		Tenascin-C	Tnc	+	Immunohistochemistry Northern blot	60	[46]
		ET_B receptor	Ednrb	–	Northern blot	60	[69]
		VEGF	Vegfa	–	Northern blot	60	[70]
		IL-6	Il6	+	Immunohistochemistry Real time PCR	60	[71]
		IL-1α	Il1a	+	Northern blot Radioimmunoassay	60	[72]
		IL-1β	Il1b	+	Northern blot		
		CLIC 4	Clic4	+	Immunohistochemistry Western blot	60	[73]
		Lipocalin-2	Lcn2	+	Immunohistochemistry Western blot Real time PCR	60	[74]
		IGF-1	Igf1	+	Real time PCR	60	[75]
		MMP-2	Mmp2	+	Zymography (activity) Immunohistochemistry Real time PCR	60	[76]
		CTGF	Ctgf	+	Reverse transcription PCR	60	[77]
		Fhl-1	Fhl1	+	Western blot Real time PCR	60	[78]
		HMGB1	Hmgb1	+	Immunohistochemistry	60	[79]
Heart	Right ventricle	ANP	Nppa	+	Northern blot	60	[70]
				+	Real time PCR	60	[66]
				+	Ribonuclease protection assay	60	[80]
		VEGF	Vegfa	–	Northern blot	60	[70]
		Fractalkine	Cx3cl1	+	Real time PCR	60	[71]
		IL-1β	Il1b	+	Real time PCR	60	[66,71]
		IL-6	Il6	+			
		Ghrelin	Ghrl	+	Real time PCR	60	[75]
		IGF-1	Igf1	+			
		Oxytocin receptor	Oxtr	–	Western blot Real time PCR	60	[66]

Table 1 (*continued*)

	Mediator	Gene name	Protein/mRNA expression	Technique	Dose/mg.Kg^{-1}	References
	iNOS	Nos2	+	Western blot		
	Hexokinase-1	Hk1	+	Immunohistochemistry Western blot	50	[81]
				Real time PCR		
	LDHA	Ldha	+	Real time PCR		
	Kv4.2	Kcnd2	–	Reverse transcription PCR	60	[82]
			–	Ribonuclease protection assay	60	[83]
	Kv4.3	Kcnd3	–	Reverse transcription PCR	60	[82]
			–	Ribonuclease protection assay	60	[83]
	Kv1.2	Kcna2	–	Ribonuclease protection assay	60	[83]
	Kv1.5	Kcna5	–			
	Kv2.1	Kcnb1	–			
	BNP	Nppb	+	Real time PCR	60	[66,84,85]
			+	Ribonuclease protection assay	60	[80]
	TNF-α	Tnf	+	Real time PCR	60	[84]
	Apelin	Apln	–	Real time PCR	60	[85]
	APJ	Aplnr	–			
	Angiotensin II	Not available	+			
	ACE	Ace	+	Real time PCR	60	[84,86]
				Reverse transcription PCR		
	Renin	Ren1	+	Reverse transcription	60	[86]
	Angiotensinogen	Agt	+	PCR		
	TGF-β1	Tgfb1	+			
	eNOS	Nos3	+			
	ET-1	Edn1	+	Real time PCR	60	[84–86]
				Reverse transcription PCR		
			? *	Radioimmunoassay	50	[87]
	big-ET1	Not available	? *	Radioimmunoassay	50	[87]
	ClC-3 chloride channel	Clcn3	+	Western blot	60	[88]
Left ventricle	eNOS	Nos3	+	Western blot	60	[66]
				Real time PCR		
	iNOS	Nos2	–	Western blot		
	GLUT4	Slc2a4	–			
	BNP	Nppb	+	Real time PCR	60	[66]
			+	Ribonuclease protection assay	60	[80]
	ANP	Nppa	+	Real time PCR	60	[66]
			+	Ribonuclease protection assay	60	[80]
	Angiotensinogen	Agt	+	Reverse transcription PCR	60	[86]
	ET-1	Edn1	+	Real time PCR	60	[85,86,89]
				Reverse transcription PCR		
	ACE	Ace	+	Real time PCR	60	[89]
	Tenascin-C	Tnc	+			
	MHC-β	A<beta> MHC	+	SDS-PAGE		
Plasma	ET-1	Edn1	+	Enzyme immunoassay	60	[69,84]
			+	Radioimmunoassay	50	[87]
	BNP	Nppb	+	Radioimmunoassay	60	[80]
	TNF-α	Tnf	+	Enzyme immunoassay	60	[84]
	IL-6	Il6	+			
	Apelin	Apln	+	ELISA	60	[85]
	Ang-(1-7)	Not available	+			
	big ET-1	Not available	+	Radioimmunoassay	50	[87]
	ANP	Nppa	+	Radioimmunoassay	50	[87]
	Angiotensin II	Not available	+	Radioimmunoassay	60	[80]
			+	Radioimmunoassay	50	[87]
	Fibronectin	Fn1	+	ELISA	3.5 (MCTP)	[90]
Serum	HMGB1	Hmgb1	+	ELISA	60	[79]
	MCP-1	Ccl2	+	ELISA	60	[91]

Legend: 5-HTT, serotonin transporter; ACE, angiotensin-converting enzyme; ANG-(1-7), angiotensin 1-7 chain; ANP, atrial natriuretic peptide; APJ, apelin receptor; BMPRII, bone morphogenetic protein receptor type II; BNP, brain natriuretic peptide; CLIC, chloride intracellular channel; CTGF, connective tissue growth factor; eNOS, endothelial nitric oxide synthase; ERp57, endoreticuloplasmin 57; ET-1, endothelin-1; Fhl-1, four-and-a-half LIM domain-1; GC, guanylate cyclase; HMGB1, high mobility group box-1; Hsp27, heat shock protein 27; IGF-1, insulin growth factor-1; IL, interleukin; JNK1/2, c-Jun N-terminal kinase 1/2; LDHA, lactate dehydrogenase A; LV, left ventricle; MCP-1, monocyte chemoattractant protein-1; MCTP, monocrotaline pyrrole; MHC, myosin heavy chain; MMP-2, matrix metalloproteinase-2; PCNA, proliferating cell nuclear antigen; PECAM-1, platelet endothelial cell adhesion molecule-1; RV, right ventricle; STAT3, signal transducer and activator of transcription 3; Tie2, angiopoietin receptor; TGF-β1, transforming growth factor-β1; TNF-α, tumor necrosis factor-α; VEGF, vascular endothelial growth factor. * normalized to tissue weight.

[33]. Endothelial cells hypertrophy and increased DNA synthesis were observed within 7–14 days after MCT(P) treatment [34,35]. Moreover, MCT intoxication is associated with increased intima expression of endothelin-1 (ET-1) [36] and decreased expressions of ET_B and eNOS (Table 1) [26,37]. In addition, the loss of the cell surface raft/caveolae protein caveolin-1 (cav-1) was observed in endothelial cells in MCT-induced PAH. A reduction in the expression of other endothelial cell membrane proteins known to colocalize with cav-1 was reported, such as platelet endothelial cell adhesion molecule-1 (Table 1) [38,39]. Changes in the medial pulmonary artery layer seem to occur after intima alterations and are characterized by increased DNA synthesis, hypertrophy and hyperplasia of smooth muscle, and extension of smooth muscle to normally non muscular pulmonary arteries [18,40]. The expression of the serotonin transporter and survivin are increased in the media [41,42], while there is a decreased expression of voltage-gated potassium channels, including Kv1.5 and Kv2.1 (Table 1) [43]. The use of the MCT model showed a decrease in the expression of TGF-β

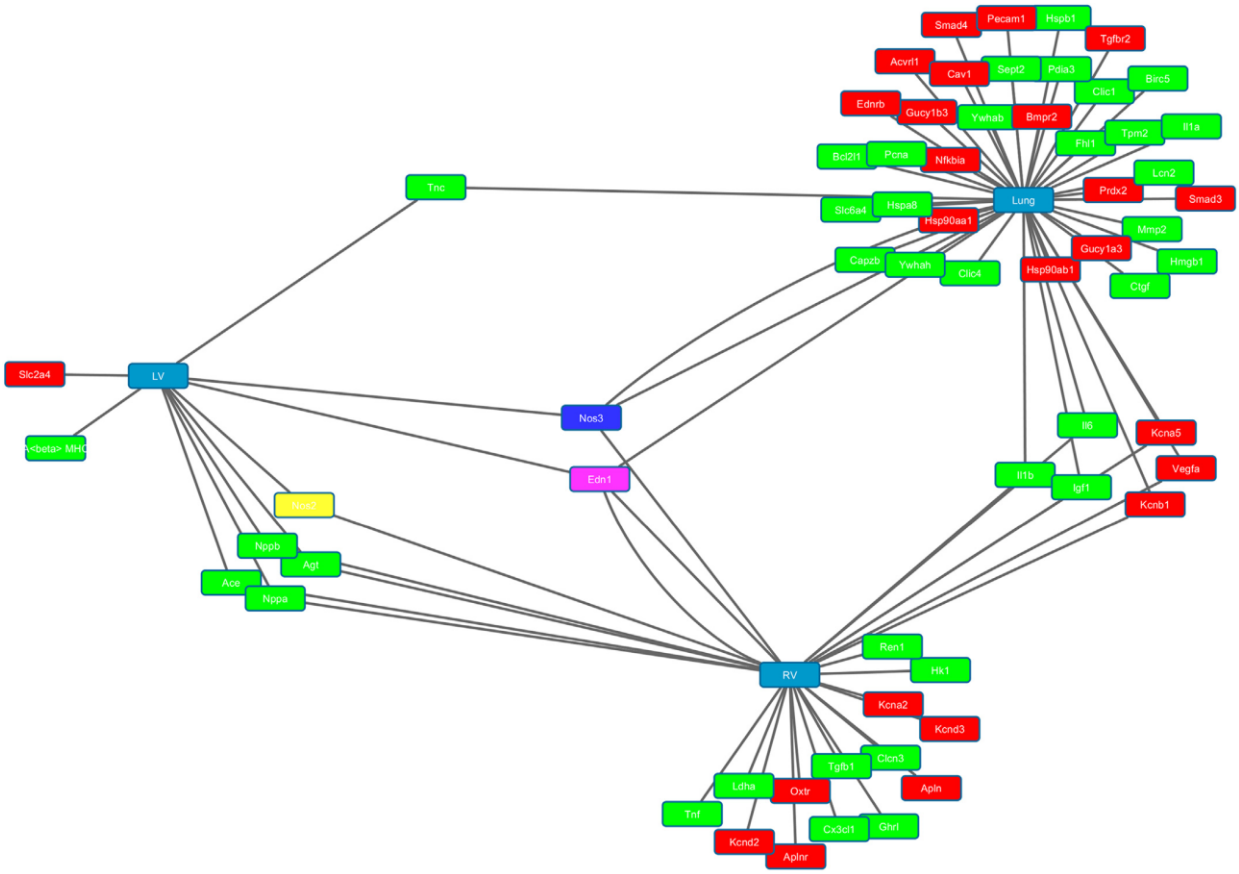

Fig. 1. Cytoscape network [50] of the mediators up- and down-regulated in MCT-induced PAH in lung, RV and LV rat tissues (listed in Table 1). Mediators up-regulated are presented in green and the down-regulated in red. Node colored dark blue represents the protein eNOS that is common to the three organs, described as being up-regulated in the heart (LV and RV) and up- or down-regulated in the lung depending on the technique used for its expression evaluation (Table 1). Node colored yellow represents the protein iNOS, common to both ventricles, but whose expression was described to be increased in RV and decreased in LV (Table 1). Node colored violet represents the protein endothelin-1, common to the three organs, being up-regulated in the lung and LV and up- or down-regulated in the RV (Table 1). Gene names above each node correspond to the mediators listed in Table 1. (For interpretation of the references to colour in this figure legend, the reader is referred to the web version of this article.)

receptor, activin-A receptor-like kinase-1, Smad-3, -4 and BMPRII protein in the lungs of MCT rats, suggesting the impairment of TGF-β and BMPRII signaling in MCT-induced PAH, a feature also observed in human PAH (Table 1) [44,45]. On the other hand, MCT administration increased apoptosis of endothelial cells leading to proliferation of pulmonary arterial smooth muscle cells and its resistance to apoptosis [8]. Lesions of the adventitia caused by MCT(P) in rats are initially characterized by the infiltration of inflammatory cells (macrophages, dendritic cells, and mast cells) [8,18]. Lungs from MCT-intoxicated rats present increased expression of several pro-inflammatory cytokines such as IL-1β, IL-6 and MCP-1. Furthermore, an adventitial increased production of extracellular matrix proteins, like elastin, fibronectin, collagen and tenascin-C was reported (Table 1) [26,46].

Rats chronically exposed to MCT develop RV hypertrophy [16,47,48]. The macroscopic evidence of right heart enlargement is accompanied by an increased rate of ventricular protein synthesis [47]. Marked increases in both cross-sectional area and cell length were observed in myocytes from the RV of rats treated with MCT. There is a general agreement that the cardiac lesions occur as a physiologic response to an increased workload that results from a sustained elevation in PAP. Hypertrophy has not been observed in the left ventricle (LV), although neurohumoral activation has been reported (Table 1) [18,48].

2.3. Integrative perspective of the molecular pathways modulated by monocrotaline-induced pulmonary arterial hypertension

In order to get a deep insight into the molecular and cellular processes associated with MCT preclinical model, an integrative analysis of the biological processes modulated in MCT-induced PAH in the lungs, RV and LV was performed using bioinformatic tools. This analysis was accomplished considering the information from Table 1 that was collected from relevant scientific papers identified by searches done in PubMed using the terms “monocrotaline”, “pulmonary arterial hypertension”, “experimental pulmonary hypertension”, “lung” and “heart” in the title or abstract. The references listed in the included papers were also hand searched. As can be depicted from Table 1, the methodological approaches most used to study MCT-related molecular alterations relied on the analysis of mRNA expression by real-time PCR and of protein expression through western blot. Most of the works that analyzed mRNA in the lung, the most studied organ in PAH, also assessed the levels of the corresponding protein and concordant data was verified, with few exceptions (Table 1). To the best of our knowledge, only one study was performed using mass spectrometry-based protein profiling of lung, which resulted in the identification of nine proteins modulated by the disease [49]. In the study of RV, mRNA expression analysis was preferred (Table 1). The majority of

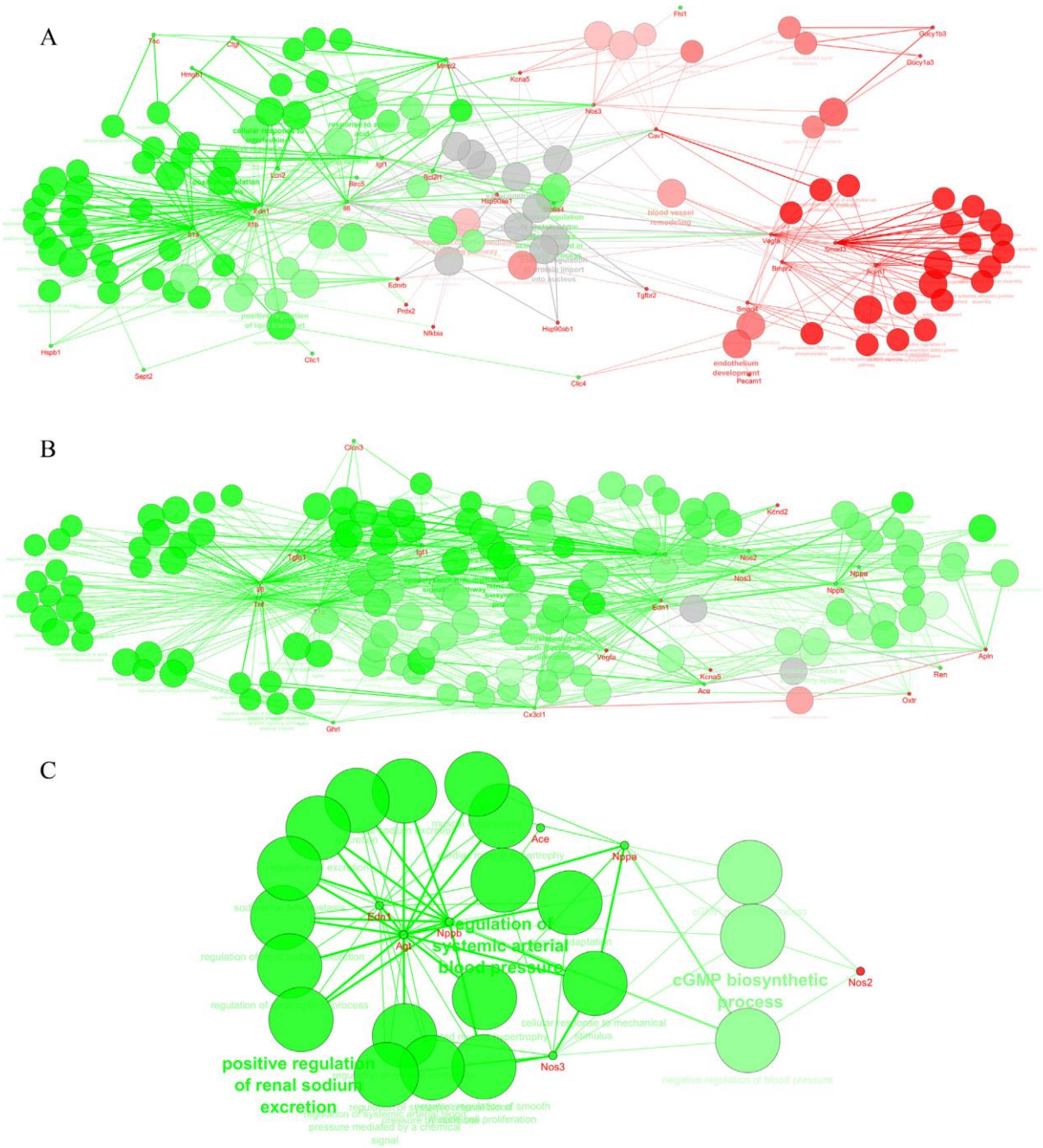

Fig. 2. ClueGo + CluePedia analysis [51,52] of protein–protein interactions considering the proteins described as up- and down-regulated in MCT-induced PAH in lung (A), RV (B) and LV (C) rat tissues (listed in Table 1). Green nodes represent the prevalent biological processes in the MCT animal model, whereas red nodes refer to the ones down-regulated. (For interpretation of the references to colour in this figure legend, the reader is referred to the web version of this article.)

the studies evaluated protein levels and mRNA expression in the third and fourth week after MCT administration. The application of Cytoscape platform [50] for the visualization and integration of the proteins reported to be modulated by MCT-induced PAH in lung, RV and LV, and ClueGO + CluePedia analysis for the investigation of the interrelations within each cluster [51,52], highlighted the molecular networks underlying PAH pathogenesis (Figs. 1 and 2). Fig. 1 emphasizes the specificity of tissue adaptation to the disease, with only the up-regulation of TnC being common to lung and LV, and the up-regulation of interleukin (IL)-6, IL-1β and IGF, and the down-regulation of VEGF and of the voltage-gated potassium channels Kv1.5 and Kv2.1 being observed both in lung and RV. According to ClueGO + CluePedia analysis, inflammation is up-regulated by MCT in lung and heart, for which contributed the

biological processes cellular response to IL-1, regulation of IL-6 production, prostaglandin secretion, chemokine and cytokine biosynthetic and metabolic processes (Fig. 2A and B). It is not yet completely understood how inflammation contributes to the pathogenesis of human PAH; despite being undoubtedly a prominent feature in human PAH. Inflammation can initiate the vascular remodeling, be an integral part of its spread or a response to the ongoing remodeling [53]. This is supported by histological findings of infiltration of various inflammatory cells (macrophages, T and B lymphocytes, dendritic cells) around the plexiform lesions and increased presence of circulating chemokines and cytokines in patients with severe PAH [54–56].

In the lung, the down-regulation of endothelium development was also highlighted by network analysis (Fig. 2A), being mostly associated with the down-regulation of proteins from the BMPRII signaling pathway. A decrease in BMPRII was also described in human disease [57]. The inhibition of the BMPRII protein in endothelial cells is reported to be associated with the induction of apoptosis, leading to smooth muscle cell proliferation, contributing to the remodeling of pulmonary arteries in PAH patients [58]. The observation that MCT modulates the biological processes of negative regulation of potassium ion transport, positive regulation of mitosis and negative regulation of apoptosis supports the described vascular remodeling associated with the MCT animal model. Although the vascular remodeling in PAH patients is also characterized by an increase in cell proliferation and a decrease in apoptosis, in part due to the deregulation of the potassium channels [59], there are important differences regarding this feature. In PAH patients, early vascular abnormalities include intima and medial hypertrophy, adventitial thickening, and extension of muscle, with vaso-occlusive lesions developing at later stages [60]. Occlusive neointimal and plexiform lesions are not observed when MCT model is used alone, but are induced by the combination of MCT with pneumonectomy [27,28]. A decrease in blood vessel remodeling was noted in the lungs (Fig. 2A), mostly related with the decreased expression of the proangiogenic factor VEGF, being this observation associated with the vessel loss described in MCT model [61]. On the contrary, markers of angiogenesis (including VEGF) were already reported in plexiform lesions of patients with severe PAH, suggesting that its overexpression can be related with the development of obliterative lesions [62–64].

Processes such as nitric oxide (NO) mediated signal transduction, cGMP biosynthetic and metabolic processes are down-regulated in the lungs (Fig. 2A), being associated with a decrease in vasodilatation, an increase in smooth muscle cell proliferation and platelet aggregation related with the NO role in PAH pathogenesis [65]. Of note, the protein eNOS (Nos3), an enzyme responsible for NO synthesis, was found to be up- or down-regulated in the lung depending on the technique used for its evaluation (Northern and Western blot, respectively) (Table 1). This discrepancy suggests a stimulation of eNOS transcription in MCT model, but for example, post-translational modifications can interfere with eNOS protein expression in the lung. In addition, the iNOS protein (Nos2), also responsible for NO production, was found to be up-regulated in RV and down-regulated in LV (Table 1). This protein is described to be associated with the inflammatory cytokine effects in the heart, suggesting that these effects may or may not be mediated by iNOS in the different ventricles [66]. Nitric oxide pathway is already well known as being affected in PAH patients and is recognized as a PAH therapeutic target [67].

3. Conclusions

Regardless of intense investigation, PAH pathogenesis is very complex and intricate. Although no single preclinical model can completely recapitulate the diverse forms of PAH, the MCT model has been successfully applied in the elucidation of the molecular and cellular pathways related with PAH development and progression, looking hopefully for novel therapeutic approaches. The integrative analysis of data from literature highlighted the biological processes associated with the vascular remodeling and inflammation as the most affected by MCT-induced PAH. Moreover, this animal model was successfully used to assess the therapeutic effect of three main classes of drugs currently used in the clinical set, specifically endothelin receptor antagonists, phosphodiesterase inhibitors, prostacyclin analogues, which emphasize its usefulness in the study of PAH.

Conflict of interests

The authors declare no competing interests.

Acknowledgments

This work was supported by Fundação para a Ciência e a Tecnologia (FCT, Portugal), European Union, QREN, FEDER and COMPETE for funding the Organic Chemistry Research Unit (QOPNA) (project PEst-C/QUI/UI0062/2013), the Cardiovascular R&D Unit (project PEst-C/SAU/UI0051/2011) and the post-graduation student (grant number SFRH/BD/91067/2012).

References

[1] G. Simonneau, M.A. Gatzoulis, I. Adatia, D. Celermajer, C. Denton, A. Ghofrani, et al., Updated clinical classification of pulmonary hypertension, J. Am. Coll. Cardiol. 62 (2013) D34–D41.
[2] K.R. Stenmark, B. Meyrick, N. Galie, W.J. Mooi, I.F. McMurtry, Animal models of pulmonary arterial hypertension: the hope for etiological discovery and pharmacological cure, Am. J. Physiol. Lung Cell Mol. Physiol. 297 (2009) L1013–L1032.
[3] F. Baldi, L. Fuso, E. Arrighi, S. Valente, Optimal management of pulmonary arterial hypertension: prognostic indicators to determine treatment course, Ther. Clin. Risk Manag. 10 (2014) 825–839.
[4] J.L. Rosenthal, M.S. Jacob, Biomarkers in pulmonary arterial hypertension, Curr. Heart Fail Rep. 11 (2014) 477–484.
[5] D. Montani, S. Gunther, P. Dorfmuller, F. Perros, B. Girerd, G. Garcia, et al., Pulmonary arterial hypertension, Orphanet J. Rare Dis. 8 (2013) 97.
[6] A.P. Lourenco, D. Fontoura, T. Henriques-Coelho, A.F. Leite-Moreira, Current pathophysiological concepts and management of pulmonary hypertension, Int. J. Cardiol. 155 (2012) 350–361.
[7] M.D. McGoon, R.L. Benza, P. Escribano-Subias, X. Jiang, D.P. Miller, A.J. Peacock, et al., Pulmonary arterial hypertension: epidemiology and registries, J. Am. Coll. Cardiol. 62 (2013) D51–D59.
[8] G. Maarman, S. Lecour, G. Butrous, F. Thienemann, K. Sliwa, A comprehensive review: the evolution of animal models in pulmonary hypertension research; are we there yet? Pulm. Circ. 3 (2013) 739–756.
[9] S.A. Doggrell, L. Brown, Rat models of hypertension, cardiac hypertrophy and failure, Cardiovasc Res. 39 (1998) 89–105.
[10] R.D. Patten, M.R. Hall-Porter, Small animal models of heart failure: development of novel therapies, past and present, Circ. Heart Fail. 2 (2009) 138–144.
[11] I.M. Robbins, Advancing therapy for pulmonary arterial hypertension: can animal models help? Am. J. Respir. Crit. Care Med. 169 (2004) 5–6.
[12] J. Ryan, K. Bloch, S.L. Archer, Rodent models of pulmonary hypertension: harmonisation with the world health organisation's categorisation of human PH, Int. J. Clin. Pract. Suppl. (2011) 15–34.
[13] G. Ruiter, F.S. de Man, I. Schalij, S. Sairras, K. Grunberg, N. Westerhof, et al., Reversibility of the monocrotaline pulmonary hypertension rat model, Eur. Respir. J. 42 (2013) 553–556.
[14] K.L. Colvin, M.E. Yeager, Animal models of pulmonary hypertension: matching disease mechanisms to etiology of the human disease, J. Pulm. Respir. Med. 4 (2014).
[15] J.J. Lalich, L. Merkow, Pulmonary arteritis produced in rat by feeding Crotalaria spectabilis, Lab. Investig. 10 (1961) 744–750.
[16] J.M. Kay, P. Harris, D. Heath, Pulmonary hypertension produced in rats by ingestion of Crotalaria spectabilis seeds, Thorax 22 (1967) 176–179.
[17] M.E. Campian, M. Hardziyenka, M.C. Michel, H.L. Tan, How valid are animal models to evaluate treatments for pulmonary hypertension? Naunyn Schmiedeb. Arch. Pharmacol. 373 (2006) 391–400.
[18] A.E. Schultze, R.A. Roth, Chronic pulmonary hypertension–the monocrotaline model and involvement of the hemostatic system, J. Toxicol. Environ. Health B Crit. Rev. 1 (1998) 271–346.

[19] S.A. Barman, S. Zhu, R.E. White, RhoA/Rho-kinase signaling: a therapeutic target in pulmonary hypertension, Vasc. Health Risk Manag. 5 (2009) 663–671.

[20] J.G. Gomez-Arroyo, L. Farkas, A.A. Alhussaini, D. Farkas, D. Kraskauskas, N.F. Voelkel, et al., The monocrotaline model of pulmonary hypertension in perspective, Am. J. Physiol. Lung Cell Mol. Physiol. 302 (2012) L363–L369.

[21] J.J. Ryan, G. Marsboom, S.L. Archer, Rodent models of group 1 pulmonary hypertension, Handb. Exp. Pharmacol. 218 (2013) 105–149.

[22] H.P. Buermans, E.M. Redout, A.E. Schiel, R.J. Musters, M. Zuidwijk, P.P. Eijk, et al., Microarray analysis reveals pivotal divergent mRNA expression profiles early in the development of either compensated ventricular hypertrophy or heart failure, Physiol. Genom. 21 (2005) 314–323.

[23] R.J. Huxtable, C.C. Yan, S. Wild, S. Maxwell, R. Cooper, Physicochemical and metabolic basis for the differing neurotoxicity of the pyrrolizidine alkaloids, trichodesmine and monocrotaline, Neurochem. Res. 21 (1996) 141–146.

[24] J. West, A. Hemnes, Experimental and transgenic models of pulmonary hypertension, Compr. Physiol. 1 (2011) 769–782.

[25] B. Meyrick, W. Gamble, L. Reid, Development of Crotalaria pulmonary hypertension: hemodynamic and structural study, Am. J. Physiol. 239 (1980) H692–H702.

[26] R. Naeije, L. Dewachter, Animal models of pulmonary arterial hypertension, Rev. Mal. Respir. 24 (2007) 481–496.

[27] K. Okada, Y. Tanaka, M. Bernstein, W. Zhang, G.A. Patterson, M.D. Botney, Pulmonary hemodynamics modify the rat pulmonary artery response to injury. A neointimal model of pulmonary hypertension, Am. J. Pathol. 151 (1997) 1019–1025.

[28] R.J. White, D.F. Meoli, R.F. Swarthout, D.Y. Kallop, I.I. Galaria, J.L. Harvey, et al., Plexiform-like lesions and increased tissue factor expression in a rat model of severe pulmonary arterial hypertension, Am. J. Physiol. Lung Cell Mol. Physiol. 293 (2007) L583–L590.

[29] R. Schoental, M.A. Head, Pathological changes in rats as a result of treatment with monocrotaline, Br. J. Cancer 9 (1955) 229–237.

[30] R. Dumitrascu, S. Koebrich, E. Dony, N. Weissmann, R. Savai, S.S. Pullamsetti, et al., Characterization of a murine model of monocrotaline pyrrole-induced acute lung injury, BMC Pulm. Med. 8 (2008) 25.

[31] M. Okada, C. Yamashita, K. Okada, Establishment of canine pulmonary hypertension with dehydromonocrotaline. Importance of larger animal model for lung transplantation, Transplantation 60 (1995) 9–13.

[32] R. Gust, D.P. Schuster, Vascular remodeling in experimentally induced subacute canine pulmonary hypertension, Exp. Lung Res. 27 (2001) 1–12.

[33] H.C. Thomas, M.W. Lame, S.K. Dunston, H.J. Segall, D.W. Wilson, Monocrotaline pyrrole induces apoptosis in pulmonary artery endothelial cells, Toxicol. Appl. Pharmacol. 151 (1998) 236–244.

[34] P.B. Lappin, K.L. Ross, L.E. King, P.J. Fraker, R.A. Roth, The response of pulmonary vascular endothelial cells to monocrotaline pyrrole: cell proliferation and DNA synthesis in vitro and in vivo, Toxicol. Appl. Pharmacol. 150 (1998) 37–48.

[35] B.O. Meyrick, L.M. Reid, Crotalaria-induced pulmonary hypertension. Uptake of 3H-thymidine by the cells of the pulmonary circulation and alveolar walls, Am. J. Pathol. 106 (1982) 84–94.

[36] H.F. Frasch, C. Marshall, B.E. Marshall, Endothelin-1 is elevated in monocrotaline pulmonary hypertension, Am. J. Physiol. Lung Cell Mol. Physiol. 276 (1999) L304–L310.

[37] R.C. Tyler, M. Muramatsu, S.H. Abman, T.J. Stelzner, D.M. Rodman, K.D. Bloch, et al., Variable expression of endothelial NO synthase in three forms of rat pulmonary hypertension, Am. J. Physiol. Lung Cell Mol. Physiol. 276 (1999) L297–L303.

[38] R. Mathew, Cell-specific dual role of caveolin-1 in pulmonary hypertension, Pulm. Med. 2011 (2011) 573432.

[39] R. Mathew, J. Huang, M. Shah, K. Patel, M. Gewitz, P.B. Sehgal, Disruption of endothelial-cell caveolin-1α/raft scaffolding during development of monocrotaline-induced pulmonary hypertension, Circulation 110 (2004) 1499–1506.

[40] P.B. Lappin, R.A. Roth, Hypertrophy and prolonged DNA synthesis in smooth muscle cells characterize pulmonary arterial wall thickening after monocrotaline pyrrole administration to rats, Toxicol. Pathol. 25 (1997) 372–380.

[41] C. Guignabert, B. Raffestin, R. Benferhat, W. Raoul, P. Zadigue, D. Rideau, et al., Serotonin transporter inhibition prevents and reverses monocrotaline-induced pulmonary hypertension in rats, Circulation 111 (2005) 2812–2819.

[42] M.S. McMurtry, S.L. Archer, D.C. Altieri, S. Bonnet, A. Haromy, G. Harry, et al., Gene therapy targeting survivin selectively induces pulmonary vascular apoptosis and reverses pulmonary arterial hypertension, J. Clin. Investig. 115 (2005) 1479–1491.

[43] M.S. McMurtry, S. Bonnet, X. Wu, J.R.B. Dyck, A. Haromy, K. Hashimoto, et al., Dichloroacetate prevents and reverses pulmonary hypertension by inducing pulmonary artery smooth muscle cell apoptosis, Circ. Res. 95 (2004) 830–840.

[44] A. Zakrzewicz, F.M. Kouri, B. Nejman, G. Kwapiszewska, M. Hecker, R. Sandu, et al., The transforming growth factor-beta/Smad2,3 signalling axis is impaired in experimental pulmonary hypertension, Eur. Respir. J. 29 (2007) 1094–1104.

[45] M.F. Ramos, M.W. Lame, H.J. Segall, D.W. Wilson, Smad signaling in the rat model of monocrotaline pulmonary hypertension, Toxicol. Pathol. 36 (2008) 311–320.

[46] P.L. Jones, M. Rabinovitch, Tenascin-C is induced with progressive pulmonary vascular disease in rats and is functionally related to increased smooth muscle cell proliferation, Circ. Res. 79 (1996) 1131–1142.

[47] R. Huxtable, S. Paplanus, J. Laugharn, The prevention of monocrotaline-induced right ventricular hypertrophy, Chest 71 (1977) 308–310.

[48] A.P. Lourenço, R. Roncon-Albuquerque, C. Brás-Silva, B. Faria, J. Wieland, T. Henriques-Coelho, et al., Myocardial dysfunction and neurohumoral activation without remodeling in left ventricle of monocrotaline-induced pulmonary hypertensive rats, Am. J. Physiol. Heart Circ. Physiol. 291 (2006) H1587–H1594.

[49] S. Laudi, W. Steudel, K. Jonscher, W. Schoning, B. Schniedewind, U. Kaisers, et al., Comparison of lung proteome profiles in two rodent models of pulmonary arterial hypertension, Proteomics 7 (2007) 2469–2478.

[50] R. Saito, M.E. Smoot, K. Ono, J. Ruscheinski, P.L. Wang, S. Lotia, et al., A travel guide to Cytoscape plugins, Nat. Methods 9 (2012) 1069–1076.

[51] G. Bindea, B. Mlecnik, H. Hackl, P. Charoentong, M. Tosolini, A. Kirilovsky, et al., ClueGO: a Cytoscape plug-in to decipher functionally grouped gene ontology and pathway annotation networks, Bioinformatics 25 (2009) 1091–1093.

[52] G. Bindea, J. Galon, B. Mlecnik, CluePedia Cytoscape plugin: pathway insights using integrated experimental and in silico data, Bioinformatics 29 (2013) 661–663.

[53] L.C. Price, S.J. Wort, F. Perros, P. Dorfmuller, A. Huertas, D. Montani, et al., Inflammation in pulmonary arterial hypertension, Chest 141 (2012) 210–221.

[54] M. Rabinovitch, C. Guignabert, M. Humbert, M.R. Nicolls, Inflammation and immunity in the pathogenesis of pulmonary arterial hypertension, Circ. Res. 115 (2014) 165–175.

[55] H. El Chami, P.M. Hassoun, Immune and inflammatory mechanisms in pulmonary arterial hypertension, Prog. Cardiovasc Dis. 55 (2012) 218–228.

[56] A. Groth, B. Vrugt, M. Brock, R. Speich, S. Ulrich, L.C. Huber, Inflammatory cytokines in pulmonary hypertension, Respir. Res. 15 (2014) 47.

[57] C. Atkinson, S. Stewart, P.D. Upton, R. Machado, J.R. Thomson, R.C. Trembath, et al., Primary pulmonary hypertension is associated with reduced pulmonary vascular expression of type II bone morphogenetic protein receptor, Circulation 105 (2002) 1672–1678.

[58] X. Yang, L. Long, P.N. Reynolds, N.W. Morrell, Expression of mutant BMPR-II in pulmonary endothelial cells promotes apoptosis and a release of factors that stimulate proliferation of pulmonary arterial smooth muscle cells, Pulm. Circ. 1 (2011) 103–110.

[59] J.X.-J. Yuan, A.M. Aldinger, M. Juhaszova, J. Wang, J.V. Conte, S.P. Gaine, et al., Dysfunctional voltage-gated K+ channels in pulmonary artery smooth muscle cells of patients with primary pulmonary hypertension, Circulation 98 (1998) 1400–1406.

[60] L.A. Shimoda, S.S. Laurie, Vascular remodeling in pulmonary hypertension, J. Mol. Med. (Berl) 91 (2013) 297–309.

[61] A. Campbell, Y. Zhao, R. Sandhu, D. Stewart, Cell-based gene transfer of vascular endothelial growth factor attenuates monocrotaline-induced pulmonary hypertension, Circulation 104 (2001) 2242–2248.

[62] R.M. Tuder, M. Chacon, L. Alger, J. Wang, L. Taraseviciene-Stewart, Y. Kasahara, et al., Expression of angiogenesis-related molecules in plexiform lesions in severe pulmonary hypertension: evidence for a process of disordered angiogenesis, J. Pathol. 195 (2001) 367–374.

[63] L. Farkas, M. Kolb, Vascular repair and regeneration as a therapeutic target for pulmonary arterial hypertension, Respiration 85 (2013) 355–364.

[64] S. Hirose, Y. Hosoda, S. Furuya, T. Otsuki, E. Ikeda, Expression of vascular endothelial growth factor and its receptors correlates closely with formation of the plexiform lesion in human pulmonary hypertension, Pathol. Int. 50 (2000) 472–479.

[65] M.R. Wilkins, Pulmonary hypertension: the science behind the disease spectrum, Eur. Respir. Rev. 21 (2012) 19–26.

[66] T.L. Broderick, Y. Wang, J. Gutkowska, D. Wang, M. Jankowski, Down-regulation of oxytocin receptors in right ventricle of rats with monocrotaline-induced pulmonary hypertension, Acta Physiol. (Oxf.) 200 (2010) 147–158.

[67] P. Crosswhite, Z. Sun, Nitric oxide, oxidative stress and inflammation in pulmonary arterial hypertension, J. Hypertens. 28 (2010) 201–212.

[68] J. Huang, J.H. Wolk, M.H. Gewitz, R. Mathew, Progressive endothelial cell damage in an inflammatory model of pulmonary hypertension, Exp. Lung Res. 36 (2010) 57–66.

[69] R. Yorikane, T. Miyauchi, S. Sakai, T. Sakurai, I. Yamaguchi, Y. Sugishita, et al., Altered expression of ETB-receptor mRNA in the lung of rats with pulmonary hypertension, J. Cardiovasc Pharmacol. 22 (Suppl. 8) (1993) S336–S338.

[70] C. Partovian, S. Adnot, S. Eddahibi, E. Teiger, M. Levame, P. Dreyfus, et al., Heart and lung VEGF mRNA expression in rats with monocrotaline- or hypoxia-induced pulmonary hypertension, Am. J. Physiol. 275 (1998) H1948–H1956.

[71] T. Henriques-Coelho, S.M. Oliveira, R.S. Moura, R. Roncon-Albuquerque Jr., A.L. Neves, M. Santos, et al., Thymulin inhibits monocrotaline-induced pulmonary hypertension modulating interleukin-6 expression and suppressing p38 pathway, Endocrinology 149 (2008) 4367–4373.

[72] N.F. Voelkel, R.M. Tuder, J. Bridges, W.P. Arend, Interleukin-1 receptor antagonist treatment reduces pulmonary hypertension generated in rats by monocrotaline, Am. J. Respir. Cell Mol. Biol. 11 (1994) 664–675.

[73] B. Wojciak-Stothard, V.B. Abdul-Salam, K.H. Lao, H. Tsang, D.C. Irwin, C. Lisk, et al., Aberrant chloride intracellular channel 4 expression contributes to endothelial dysfunction in pulmonary arterial hypertension, Circulation 129 (2014) 1770–1780.

[74] G. Wang, X. Liu, L. Meng, S. Liu, L. Wang, J. Li, et al., Up-regulated lipocalin-2 in pulmonary hypertension involving in pulmonary artery SMC resistance to

apoptosis, Int. J. Biol. Sci. 10 (2014) 798–806.
[75] T. Henriques-Coelho, J. Correia-Pinto, R. Roncon-Albuquerque Jr., M.J. Baptista, A.P. Lourenco, S.M. Oliveira, et al., Endogenous production of ghrelin and beneficial effects of its exogenous administration in monocrotaline-induced pulmonary hypertension, Am. J. Physiol. Heart Circ. Physiol. 287 (2004) H2885–H2890.
[76] E. Frisdal, V. Gest, A. Vieillard-Baron, M. Levame, H. Lepetit, S. Eddahibi, et al., Gelatinase expression in pulmonary arteries during experimental pulmonary hypertension, Eur. Respir. J. 18 (2001) 838–845.
[77] Y.S. Lee, J. Byun, J.A. Kim, J.S. Lee, K.L. Kim, Y.L. Suh, et al., Monocrotaline-induced pulmonary hypertension correlates with upregulation of connective tissue growth factor expression in the lung, Exp. Mol. Med. 37 (2005) 27–35.
[78] G. Kwapiszewska, M. Wygrecka, L.M. Marsh, S. Schmitt, R. Trosser, J. Wilhelm, et al., Fhl-1, a new key protein in pulmonary hypertension, Circulation 118 (2008) 1183–1194.
[79] P.S. Yang, D.H. Kim, Y. Lee, S.E. Lee, W. Kang, H.J. Chang, et al., Glycyrrhizin, inhibitor of high mobility group box-1, attenuates monocrotaline-induced pulmonary hypertension and vascular remodeling in rats, Respir. Res. 15 (2014) 148.
[80] S. Usui, A. Yao, M. Hatano, O. Kohmoto, T. Takahashi, R. Nagai, et al., Upregulated neurohumoral factors are associated with left ventricular remodeling and poor prognosis in rats with monocrotaline-induced pulmonary arterial hypertension, Circ. J. 70 (2006) 1208–1215.
[81] W.H. Zhang, M.H. Qiu, X.J. Wang, K. Sun, Y. Zheng, Z.C. Jing, Up-regulation of hexokinase1 in the right ventricle of monocrotaline induced pulmonary hypertension, Respir. Res. 15 (2014) 119.
[82] T.T. Zhang, B. Cui, D.Z. Dai, Downregulation of Kv4.2 and Kv4.3 channel gene expression in right ventricular hypertrophy induced by monocrotaline in rat, Acta Pharmacol. Sin. 25 (2004) 226–230.
[83] J.K. Lee, A. Nishiyama, F. Kambe, H. Seo, S. Takeuchi, K. Kamiya, et al., Downregulation of voltage-gated K(+) channels in rat heart with right ventricular hypertrophy, Am. J. Physiol. 277 (1999) H1725–H1731.
[84] D. Fontoura, J. Oliveira-Pinto, M. Tavares-Silva, S. Leite, F. Vasques-Novoa, P. Mendes-Ferreira, et al., Myocardial and anti-inflammatory effects of chronic bosentan therapy in monocrotaline-induced pulmonary hypertension, Rev. Port. Cardiol. 33 (2014) 213–222.
[85] I. Falcao-Pires, N. Goncalves, T. Henriques-Coelho, D. Moreira-Goncalves, R. Roncon-Albuquerque Jr., A.F. Leite-Moreira, Apelin decreases myocardial injury and improves right ventricular function in monocrotaline-induced pulmonary hypertension, Am. J. Physiol. Heart Circ. Physiol. 296 (2009) H2007–H2014.
[86] H.K. Park, S.J. Park, C.S. Kim, Y.W. Paek, J.U. Lee, W.J. Lee, Enhanced gene expression of renin-angiotensin system, TGF-beta1, endothelin-1 and nitric oxide synthase in right-ventricular hypertrophy, Pharmacol. Res. 43 (2001) 265–273.
[87] F. Brunner, Cardiac endothelin and big endothelin in right-heart hypertrophy due to monocrotaline-induced pulmonary hypertension in rat, Cardiovasc Res. 44 (1999) 197–206.
[88] Y.-P. Dai, S. Bongalon, W.J. Hatton, J.R. Hume, I.A. Yamboliev, ClC-3 chloride channel is upregulated by hypertrophy and inflammation in rat and canine pulmonary artery, Br. J. Pharmacol. 145 (2005) 5–14.
[89] J. Correia-Pinto, T. Henriques-Coelho, R. Roncon-Albuquerque Jr., A.P. Lourenco, G. Melo-Rocha, F. Vasques-Novoa, et al., Time course and mechanisms of left ventricular systolic and diastolic dysfunction in monocrotaline-induced pulmonary hypertension, Basic Res. Cardiol. 104 (2009) 535–545.
[90] A.E. Schultze, J.J. Emeis, R.A. Roth, Cellular fibronectin and von Willebrand factor concentrations in plasma of rats treated with monocrotaline pyrrole, Biochem. Pharmacol. 51 (1996) 187–191.
[91] Y. Kasahara, H. Kimura, K. Kurosu, K. Sugito, N. Mukaida, K. Matsushima, et al., MCAF/MCP-1 protein expression in a rat model for pulmonary hypertension induced by monocrotaline, Chest 114 (1998) 67S.

CHAPTER II

AIMS

Aims

Pulmonary arterial hypertension remains a devastating disease without a cure, with most of the patients being diagnosed at a very advanced stage. So, the general goal of the present thesis was to explore novel preventive and therapeutic approaches for the clinical management of PAH. To accomplish this, specific purposes were outlined in the original research articles (experimental studies I, II and III) that comprise chapter III:

i) to better characterize the functional, structural and molecular adaptations induced by lifelong aerobic exercise training in the right ventricle (Study I).

ii) to evaluate the preventive effects of exercise training on right ventricle dysfunction and remodeling secondary to MCT-induced PAH (Study II).

iii) to explore the *in vivo* effects of terameprocol in the MCT model of PAH and the biological processes modulated by this drug in primary cultures of pulmonary artery smooth muscle cells (PASMCs) (Study III).

List of studies – Original research papers:

Paper I

R. Nogueira-Ferreira, R. Ferreira, A. I. Padrão, P. Oliveira, M. Santos, A. N. Kavazis, R. Vitorino, D. Moreira-Gonçalves (2016). "*Different susceptibility to metabolic adaptations in the right and left ventricle of rats following one year of moderate exercise training*", (submitted).

Paper II

R. Nogueira-Ferreira, D. Moreira-Gonçalves, A.F. Silva, J.A. Duarte, A. Leite-Moreira, R. Ferreira, T. Henriques-Coelho (2016). "*Exercise preconditioning prevents MCT-induced right ventricle remodeling through the regulation of TNF superfamily cytokines*", International Journal of Cardiology 203: 858-866.

Paper III

R. Nogueira-Ferreira, M. J. Ferreira-Pinto, A. F. Silva, R. Vitorino, J. Justino, R. Costa, D. Moreira-Gonçalves, J. F. Quignard, T. Ducret, J. P. Savineau, A. F. Leite-Moreira, R. Ferreira, T. Henriques-Coelho (2016). "*HMGB1 down-regulation mediates terameprocol*

vascular anti-proliferative effect in experimental pulmonary hypertension", Journal of Cellular Physiology (Epub ahead of print).

CHAPTER III

EXPERIMENTAL WORK

STUDY I – DIFFERENT SUSCEPTIBILITY TO METABOLIC ADAPTATIONS IN THE RIGHT AND LEFT VENTRICLE OF RATS FOLLOWING ONE YEAR OF MODERATE EXERCISE TRAINING

Different susceptibility to metabolic adaptations in the right and left ventricle of rats following one year of moderate exercise training

Rita Nogueira-Ferreira[1,2], Rita Ferreira[1], Ana Isabel Padrão[1,3], Paula Oliveira[4], Manuel Santos[2], Andreas N. Kavazis[5], Rui Vitorino[2,6], Daniel Moreira-Gonçalves[2,3*]

[1]QOPNA, Departamento de Química, Universidade de Aveiro, Campus Universitário de Santiago, 3810-193 Aveiro, Portugal

[2]Departamento de Cirurgia e Fisiologia, Faculdade de Medicina, Universidade do Porto, Alameda Professor Hernâni Monteiro, 4200-319 Porto, Portugal

[3]CIAFEL, Faculdade de Desporto, Universidade do Porto, R. Dr. Plácido da Costa 91, 4200-450 Porto, Portugal

[4]CITAB, Departamento de Ciências Veterinárias, Universidade de Trás-os-Montes e Alto Douro, Quinta de Prados, 5001-911 Vila Real, Portugal

[5]School of Kinesiology, Auburn University, Auburn, Alabama, USA

[6]iBiMED, Departamento de Ciências Médicas, Universidade de Aveiro, Campus Universitário de Santiago, 3810-193 Aveiro, Portugal

Running head: Lifelong exercise induces RV remodeling

***Corresponding author (✉):**
Daniel Moreira Gonçalves
Departamento de Cirurgia e Fisiologia
Faculdade de Medicina, Universidade do Porto
Alameda Professor Hernâni Monteiro, 4200-319 Porto, Portugal
E-mail: danielmgon@gmail.com

Abstract

Aim: Aerobic exercise training induces a unique cardioprotective phenotype, but it does not promote the same structural and functional adaptations to the right ventricle and left ventricle. In the present study we aimed to better characterize the molecular pathways involved in right ventricle remodeling induced by aerobic exercise training.

Methods: Sprague-Dawley rats were randomly assigned to control and exercise groups. Animals in exercise group were submitted to moderate treadmill exercise for 54 weeks. After the experimental period, hemodynamic analysis were performed and right and left ventricles were harvested for morphological and biochemical analysis.

Results: Data showed that long-term moderate exercise training improves cardiac function, especially diastolic function. In right ventricle, long-term exercise training induced an increase of manganese superoxide dismutase and sirtuin 3, suggestive of improved antioxidant capacity. The content of connexin-43 and c-kit was not modulated by exercise training in right and left ventricles.

Conclusion: Our results show that lifelong moderate aerobic exercise training enhances the right ventricle mitochondrial ability to produce ATP and so meet the energetic demands imposed by exercise, resulting in improved cardiac function.

Keywords: cardiac adaptation, hemodynamics, metabolism, mitochondria, oxidative stress, treadmill exercise

Introduction

Endurance exercise training is widely recognized to induce a unique cardioprotective phenotype, making it an useful intervention for the prevention and treatment of cardiovascular diseases [1]. Cardiac hypertrophy is one of the major adaptations promoted by aerobic exercise, which confers mechanical advantages as it normalizes wall stress, decreases oxygen consumption and increases work capacity [1]. Cross-sectional cardiac magnetic resonance imaging (cMRI) studies have consistently reported an increase in cardiac mass and volumes of both ventricles in endurance trained athletes compared to age and sex-matched sedentary subjects [2, 3]. Increase in cardiomyocyte length and width are considered the greater contributors to this physiologic cardiac growth but recent findings also support a role for the generation of new cardiomyocytes [4].

Exercise-induced intrinsic changes in the LV have been well characterized, but data depicting the changes that occur in the RV following aerobic exercise training is scarcer. This is very important as there is growing body of evidence showing that adaptations of the RV do not always match those observed in the LV [5]. Indeed, for the same cardiac output, the RV has to deal with higher load and stroke work during endurance exercise as the pulmonary vascular bed can only reduce its resistance by 30–50% during exercise as compared with greater reductions in systemic vascular resistance (>75%). Moreover, RV wall stress at peak exercise intensities rises by 170% compared to rest, with only a 23% increase in the LV wall stress (reviewed by [5]). The greater hemodynamic overload imposed to the RV may justify distinct ventricular adaptations to exercise in the long term. In this sense, one year of endurance exercise training in previously untrained individuals was shown to result in a more pronounced increase in RV mass and volume than in the LV, paralleled with improved function [2]. Strenuous exercise was also associated with RV structural, electrical and functional changes that were related with pro-arrhythmogenic remodeling in some athletes [5, 6]. Evidence from animal studies further strengthens the notion that exercise differently impacts RV and LV by showing that long-term endurance exercise resulted in the development of myocardial fibrosis, myocardial stiffness and diastolic dysfunction in the RV, but not in LV [7, 8].

Thus, while it is becoming clear that the structural and functional adaptations that occur in the RV following endurance exercise training may not parallel those observed in the LV, it is important to clarify exercise-related RV remodeling. So, the purpose of the present work

was to add new insights on the functional, structural and biochemical changes induced by lifelong aerobic exercise training of moderate intensity on RV using an animal model.

Material and Methods

Animals and experimental design

Housing and experimental treatment were in accordance with the *Guide for the Care and Use of Laboratory Animals* from the Institute for Laboratory Animal Research (ILAR, 2011). The experiments were approved by the local Ethics Committee for Animal Experimentation (licence number 008961) and performed in accordance to European Parliament Directive 2010/63/EU. Twenty female Sprague-Dawley rats (age: 5 weeks; weight: 130 ± 2.4 g at the beginning of the experiment, provided by Harlan Laboratories Models (Barcelona, Spain) were randomly assigned into the following two groups: sedentary (SED; n=10; with restricted movement to the cage space) and exercised (EX; n=10; submitted to treadmill exercise training). All animals were maintained in a controlled environment at a room temperature of 22 ºC, on a 12:12 h light-dark reverse cycle, and with food (standard diet 4RF21®, Mucedola, Italy) and water *ad libitum*.

Exercise training program

Animals in the exercise-training group were habituated to treadmill running for 2 weeks. During this period the running time and intensity were gradually increased until the animals were running 60 min/day at 20 m/min. After the habituation period, EX animals ran 5 days/week for 60 min/day at 20 m/min (~50% of VO_2 max) [9] for 54 weeks. All EX animals completed the training program.

Experimental preparations for hemodynamic evaluation

Twenty-four hours after the end of the exercise training protocol, all animals were anesthetized by inhalation with a mixture of 4% sevoflurane with oxygen and placed over a heating pad, to maintain the body temperature at 37 ºC. Animals were tracheostomized for mechanical ventilation with oxygen-enriched air (60 cpm, tidal volume set at 1 ml/100 g, model 683: TOPO, Kent Scientific, Torrington, USA). The right jugular vein was cannulated under binocular surgical microscopy (Wild M651.MS-D; Leica, Herbugg, Switzerland) for administration of prewarmed 0.9% NaCl solution in order to balance the

perioperative fluid losses. The heart was exposed by a median sternotomy and the pericardium was extensively opened. Lastly, two-conductance catheters (SPR-324; Millar Instruments, Houston, USA) were positioned on the LV and RV to assess cardiac performance in baseline conditions. The animals were allowed to stabilize for 15 min before the collection of the hemodynamic data.

Hemodynamic measurements

Hemodynamic data collection was performed as previously described in detail [10]. Parameters were recorded and on-line converted to a digital data with a sample frequency of 1,000 Hz. Hemodynamic parameters included: Peak systolic pressure (Pmax), end-diastolic (EDP) and end-systolic (ESP) pressure, peak rate of pressure rise (dP/dtmax) and peak rate of pressure decay (dP/dtmin). The tau (time constant of relaxation rate) was estimated by fitting the isovolumetric pressure fall to a monoexponential function. All animals completed the experimental protocol. Data were stored and analyzed with Millar conductance data acquisition and analysis software (PVAN3.5).

Tissue collection

After completing the acquisition of the hemodynamic data, all animals were sacrificed through exsanguination. The heart and lungs were excised and weighted. Under binocular magnification (×3.5) the LV free wall and RV free wall were dissected and weighted independently. Heart weight, LV and RV were normalized to tibia length. The left *gastrocnemius* was also removed and weighted. Samples from lungs, LV and RV from all animals were collected and fixed in a solution of 4% (v/v) buffered paraformaldehyde for latter histological analysis. Also, samples of LV and RV from all animals were collected for biochemical analysis.

Histologic and immunohistochemical analysis

Cubic pieces from cardiac muscle (RV and LV) and right lung were fixed [4% (v/v) buffered paraformaldehyde] by diffusion for 24 h and subsequently dehydrated with graded ethanol and included in paraffin blocks. Serial sections (5 μm of thickness) of paraffin blocks were cut by using a microtome and mounted on silane-coated slides. The slides were dewaxed in xylene and hydrated through graded alcohols finishing in

phosphate buffered saline solution. Deparaffinized sections of heart were stained for hematoxylin-eosin or Sirius Red for the analysis of cross sectional area and fibrosis, and sections of the lungs were stained with hematoxylin-eosin for the analysis of medial hypertrophy of pulmonary artery, as previously described by us [11]. Additional deparaffinized sections of cardiac tissue were prepared for immunohistochemical staining of connexin-43 (ab11370; Abcam, Cambridge, UK) and c-kit (sc-168; Santa Cruz, Heidelberg, Germany), as previously described by us [12].

Analysis of myosin heavy chain (MHC) isoform content

Right and left ventricle sections were weighted and homogenized (in the proportion of 1:19) in 100 mM phosphate buffer, pH 7.4, containing 0.02% bovine serum albumin (BSA), with a tightly fitted Potter-Elvehjem homogenizer and Teflon pestle at 0-4 °C. Total protein concentration was spectrophotometrically assayed with the DC method (Bio-Rad, California, USA). MHC isoforms content was evaluated as previously described [13].

Right and left ventricle muscle preparation for biochemical analysis

A portion (~10 mg) of right and left ventricle muscle was homogenized in 100 mM phosphate buffer, pH 7.4, supplemented with protease inhibitor, using a Teflon pestle on a motor-driven Potter-Elvehjem glass homogenizer at 0-4 ºC (3-5 times for 5 s at low speed, with a final burst at a higher speed). The protein content of the cardiac muscle homogenates was assayed with the Bio-Rad DC method, following the instructions of the manufacturer, using BSA as a standard.

Citrate synthase activity

Citrate synthase activity was measured in RV and LV homogenates using the method described by Coore *et al*. [14]. In brief, the CoASH released from the reaction of acetyl-CoA with oxaloacetate was measured by its reaction with 5, 5'-dithiobis-(2-nitrobenzoic acid) (DTNB) at 412 nm (molar extinction coefficient of 13.6 $mM^{-1}cm^{-1}$).

Isolation of mitochondria from cardiac muscle

Mitochondria isolation was performed as previously described [15]. In brief, samples from both ventricles were minced in an ice-cold isolation medium containing 250 mM sucrose,

0.5 mM EGTA, 10 mM HEPES-KOH (pH 7.4) and 0.1% defatted BSA. The minced blood-free tissue was resuspended in isolation medium containing subtilopeptidase A type VIII (1 mg/g tissue) and homogenized. The homogenate was centrifuged at 14,500g for 10 min, and the pellet was gently resuspended in isolation medium. The suspension was centrifuged (750g, 10 min) and the resulting supernatant was centrifuged again (12,000g, 10 min). The new pellet was resuspended and re-pelleted (12,000g, 10 min) in isolation medium minus the BSA. Finally, the pellet, containing the mitochondrial fraction, was resuspended in a medium containing 250 mM sucrose, 10 mM HEPES-KOH, pH 7.4. Phosphatase and protease inhibitors were added and all the procedures were performed at 4 ºC. The protein content was assayed with the Bio-Rad DC assay using BSA as a standard. ATP synthase activity was evaluated in mitochondrial extracts as previously described [16].

Immunoblotting analysis

Equivalent amounts of right and left ventricles protein or mitochondrial protein were electrophoresed on a 12.5% SDS-PAGE as described by Laemmli [17]. Gels were blotted onto nitrocellulose membranes (Whatman®, Protan®, Merck, Darmstadt, Germany) in transfer buffer (25 mM Tris, 192 mM glycine, pH 8.3 and 20% methanol) for 2 h (200 mA). Then, nonspecific binding was blocked with 5% (w/v) nonfat dry milk in TBS-T (100 mM Tris, 1.5 mM NaCl, pH 8.0 and 0.5% Tween 20). Membranes were incubated with primary antibody solution diluted 1:1000 in 5% (w/v) nonfat dry milk in TBS-T (mouse anti-ATP synthase subunit beta, ab14730, Abcam; rabbit anti-GAPDH, ab9485, Abcam; rabbit anti-ETFDH, ab91508, Abcam; mouse anti-MnSOD, ALX-804-265-C100, Alexis, Farmingdale, New York.; rabbit anti-PGC1 alpha, ab54481, Abcam; rabbit anti-mtTFA, sc-28200, Santa Cruz; mouse anti-total OXPHOS, ab110413, Abcam; rabbit anti-c-kit, sc-168, Santa Cruz; rabbit anti-connexin-43, ab63851, Abcam; rabbit anti-SIRT3, #2627, Cell Signalling, Massachusetts, USA; rabbit anti-RAF1, ab32025, Abcam). After a 2 h incubation at room temperature with agitation, membranes were washed with TBS-T and incubated, with agitation, with anti-mouse or anti-rabbit IgG peroxidase secondary antibody (Merck) diluted 1:1000 in 5% (w/v) nonfat dry milk in TBS-T.

For the protein carbonyl derivative assay, a given volume (V) of the sample containing 20 μg of protein was derivatized with 2,4-dinitrophenylhydrazine (DNPH). Briefly, the

sample was mixed with 1 V of 12% SDS, 2 V of 2 mM DNPH/10% trifluoroacetic acid, followed by 30 min of incubation in the dark, after which 1.5 V of 2 M Tris-base/18.3% of β-mercaptoethanol was added for neutralization. After diluting the derivatized proteins in TBS to obtain a final concentration of 0.001 μg/μL, a 100 μL volume was slot-blotted into a nitrocellulose membrane. For 3-nitrotyrosine expression, 30 μg of protein from RV and LV samples were diluted in TBS to obtain a final protein concentration of 0.001 μg/μL and a volume of 100 μL was slot-blotted into a nitrocellulose membrane. The slot-blot membranes were processed as above using anti-3-nitrotyrosine (MAB 5404, EMD Millipore, Merck, Darmstadt, Germany) or anti-DNP (MAB 2223, EMD Millipore) primary antibodies diluted 1:1000 in 5% w/v nonfat dry milk in TBS-T.

Immunoreactive bands were detected with enhanced chemiluminescence reagents (ECL, Amersham Pharmacia Biotech, Uppsala, Sweden) according to the manufacturer's procedure and images were recorded using X-ray films (Amersham Hyperfilm ECL, GE Healthcare). The films were scanned in Molecular Imager Gel Doc XR+System (Bio-Rad) and analyzed with Image Lab software (v4.1, Bio-Rad). Protein loading was controlled by Ponceau S staining once the expression of structural proteins as actin or tubulin was previously noticed to change with exercise training.

Statistical analysis

Values are given as mean ± standard deviation for all variables. Kolmogorov-Smirnov test was performed to check the normality of the data. When variables were normally distributed, significant differences between the groups were evaluated using an unpaired t-test (data sets with 2 variables) or a two-way analysis of variance (data sets with 4 variables) followed by the Bonferroni post hoc test. Kruskal-Wallis test followed by Dunn's Multiple Comparison Test was used for non-parametric variables (histological data). Results were considered significantly different when $P<0.05$. Statistical analysis was performed with Graph Pad Prism software, version 5.0.

Results

Impact of lifelong exercise training on morphometric parameters and cardiac hemodynamics

Fifty-four weeks of endurance exercise training resulted in a significant increase of body weight ($P<0.05$), *gastrocnemius* mass ($P<0.001$) and a decrease in RV weight and RV/tibia ratio ($P<0.01$; Table 1). No significant alterations were observed for lungs mass, lungs/tibia, heart weight, LV weight, heart/tibia or LV/tibia length.

Table 1 – Morphometric characterization.

	Sedentary	**Exercise**
Body weight (Kg)	0.291 ± 0.031	0.323 ± 0.036*
Gastrocnemius mass (g)	1.988 ± 0.120	2.230 ± 0.170***
Lungs mass (g)	1.946 ± 0.287	1.931 ± 0.356
Lungs/tibia	0.501 ± 0.076	0.472 ± 0.101
Heart mass (g)	1.051 ± 0.121	1.041 ± 0.120
Heart/tibia	0.271 ± 0.030	0.264 ± 0.035
Left ventricle (g)	0.572 ± 0.084	0.600 ± 0.109
Left ventricle/tibia	0.147 ± 0.020	0.145 ± 0.030
Right ventricle (g)	0.225 ± 0.068	0.170 ± 0.017**
Right ventricle/tibia	0.058 ± 0.016	0.043 ± 0.004**

Values are presented as mean ± standard deviation (n=10 *per* group). * P<0.05 vs. SED; ** P<0.01 vs. SED; *** P<0.001 vs. SED.

Hemodynamic RV and LV profile at baseline conditions is presented in Table 2. Long-term exercise training resulted in a significant decrease in resting heart rate ($P<0.05$). In comparison to the SED group, EX group had higher LV Pmax ($P<0.01$), ESP ($P<0.01$) and lower EDP ($P<0.05$). No significant alterations were detected in the remaining LV hemodynamic parameters between SED and EX.

Table 2 – Hemodynamic evaluation at basal conditions.

	Sedentary		**Exercise**	
HR (bpm)	313.10 ± 28.42		292.20 ± 17.83*	
	RV	**LV**	**RV**	**LV**
Pmax (mmHg)	32.48 ± 3.79	146.50 ± 16.92###	26.93 ± 1.43	160.40 ± 12.48**+++
Pmin (mmHg)	0.22 ± 0.04	1.83 ± 1.72#	0.25 ± 0.14	1.76 ± 1.59+
ESP (mmHg)	31.61 ± 4.56	143.00 ± 15.87###	25.75 ± 2.11	157.90 ± 12.06**+++
EDP (mmHg)	5.18 ± 0.73	8.74 ± 4.36#	4.13 ± 1.56	5.80 ± 1.97*
dP/dtmax (mmHg/s)	1999.00 ± 118.70	9658.00 ± 1706.00###	1928.00 ± 224.00	9768.00 ± 764.80+++
dP/dtmin (mmHg/s)	-1654.00 ± 391.30	-10550.00 ± 1950.00###	-1211.00 ± 265.80	-11070.00 ± 376.70+++
Tau (ms)	11.62 ± 4.66	11.59 ± 1.39	11.53 ± 3.10	11.55 ± 0.95

LV: left ventricle, RV: right ventricle, HR: heart rate, Pmax: maximum pressure, Pmin: minimum pressure, ESP: end systolic pressure, EDP: end diastolic pressure, dP/dtmax: maximum rate of pressure elevation, dP/dtmin: maximum rate of pressure decay, Tau: isovolumic relaxation constant. Values are presented as mean ± standard deviation (n=10 *per* group). * P<0.05 vs. respective SED group; ** P<0.01 vs. respective SED group; # P<0.05 vs. SEDRV; ### P<0.001 vs. SEDRV; + P<0.05 vs. EXRV; +++ P<0.001 vs. EXRV.

Regarding the RV, no significant alterations were detected in the hemodynamic parameters between SED and EX. Comparing RV and LV hemodynamics within each condition (i.e., SED and EX), Pmax is significantly higher in LV (P<0.001) as well as Pmin (P<0.05), ESP (P<0.001), dP/dtmax (P<0.001) and dP/dtmin (P<0.001).

Effect of lifelong exercise training on histological parameters

Lifelong exercise training resulted in a significant increase of LV cardiomyocyte cross sectional area (CSA) when compared to SED animals (P<0.001; Figure 1).

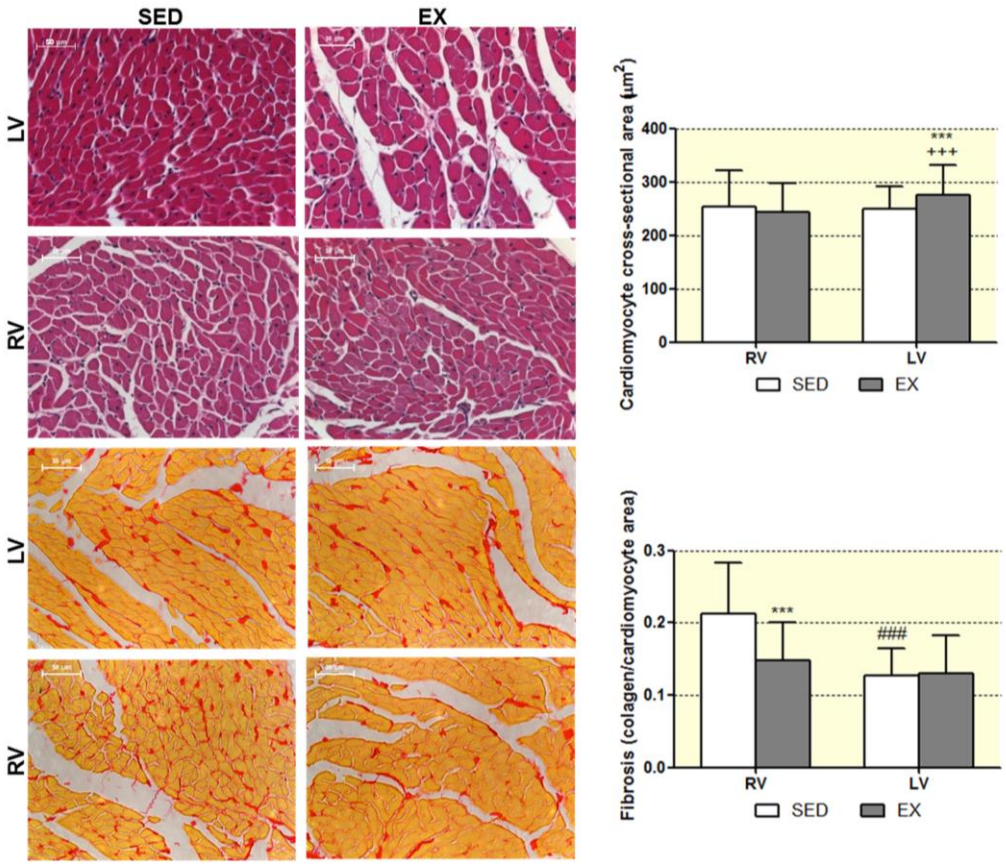

Figure 1 – Effect of exercise training on LV and RV cardiomyocyte CSA and fibrosis. LV: left ventricle, RV: right ventricle. Values are presented as mean ± standard deviation (n=10 *per* group). *** P<0.001 vs. respective SED group; ### P<0.001 vs. SEDRV; +++ P<0.001 vs. EXRV.

In exercised animals, higher cardiomyocyte CSA were observed in LV compared to RV (P<0.001). Exercise training prevented the accumulation of fibrosis in the RV (P<0.001). Accumulation of fibrosis was higher in the RV of SED animals (P<0.001 vs. LV). Medial hypertrophy of pulmonary artery was also significantly reduced in EX animals in comparison to SED (P<0.01; Figure 2).

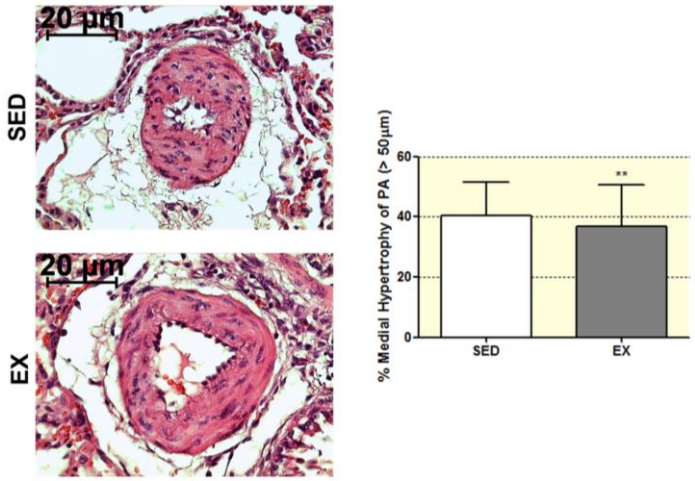

Figure 2 – Effect of exercise training on pulmonary artery hypertrophy. Values are presented as mean ± standard deviation (n= 6 *per* group). ** P<0.01 vs. SED.

To explore if lifelong exercise training has an impact in the cardiac conduction system, we determined the levels of connexin-43 (Cx43) and we also performed immunohistological analysis to assess its cellular location. No significant alterations of Cx43 content and cellular location were observed in both ventricles of trained animals (Figure 3a-b). However, the content of Cx43 was significantly higher in LV than in RV of EX animals (P<0.05; Figure 3a).

Moreover, after 54 weeks of endurance training there were no signs of cardiac progenitor cells activation in both ventricles given by the expression levels of c-kit (Figure 3c), a marker of a major type of cardiac progenitor cells [18]. No differences in the pattern of immunostaining were observed among trained and sedentary animals (data not shown). No expression differences of c-kit were noticed among ventricles within each group.

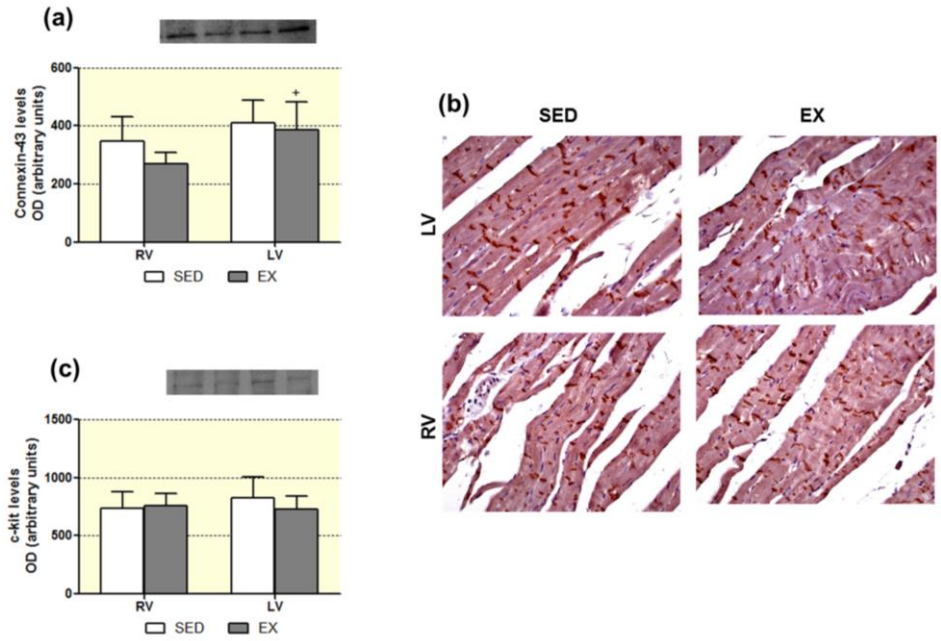

Figure 3 – Effect of exercise training on connexin-43 content (a) and cell location in LV and RV (b), and on c-kit content (c). LV: left ventricle, RV: right ventricle. Values are presented as mean ± standard deviation (n=6 *per* group). + P<0.05 vs. EXRV.

MHC isoform profiling of right and left ventricles

Figure 4 shows MHC isoforms' profile of RV and LV muscles from sedentary and exercised animals. Two isoforms were observed in the gel, with predominance of alpha-MHC. Lifelong exercise training had no effect on beta/alpha MHC ratio in both ventricles, despite the significant lower levels of this ratio in LV (P<0.05).

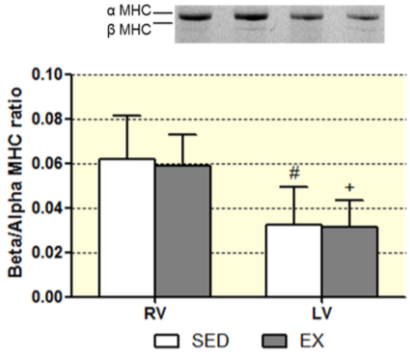

Figure 4 – Effect of exercise training on MHC isoform ratio in LV and RV. LV: left ventricle, RV: right ventricle. Values are presented as mean ± standard deviation (n=6 *per* group). # P<0.05 vs. SEDRV; + P<0.05 vs. EXRV.

Effects of exercise training protocol in cardiac metabolic remodeling

In order to evaluate the impact of 54 weeks of exercise training on heart metabolism, the levels of metabolic enzymes were evaluated by western blotting in RV and LV extracts. No changes were noted on the levels of ATP synthase while levels of the glycolytic enzyme glyceraldehyde-3-phosphate dehydrogenase (GAPDH) were significantly lower in the RV of exercised animals in comparison to sedentary rats ($P<0.01$ vs. SED; Figure 5a and b). The ratio ATP synthase to GAPDH, a rough marker of oxidative metabolism, was also increased in RV of exercised animals though without statistical significance (Figure 5c). As shown in Figure 5d, exercise training did not promote significant alterations in the cardiac levels of the subunits NDUFB8 from complex I, SDHB from complex II, UQCRC2 from complex III, MTCO1 from complex IV and ATP5A and ATP5B from complex V of oxidative phosphorylation (OXPHOS), respectively, in none of the ventricles. However, when the content of ATP5B was analyzed in mitochondria isolated from cardiac muscle (pool of both ventricles) it was noticed a significant increase of its content and of complex V activity in trained animals ($P<0.01$ vs SED; Figure 5f and 5g). These data suggest that despite no alterations in OXPHOS subunits levels in RV and LV, exercise increased mitochondrial ability to produce ATP. Moreover, the content of the electron transfer flavoprotein:ubiquinone oxidoreductase (ETFDH), which conducts electrons from nine different mitochondrial FAD-containing acyl-CoA dehydrogenases of fatty acid β-oxidation to the ubiquinone pool of the main respiratory chain [19], was not modulated by lifelong exercise training in none of the ventricles (Figure 5e), suggesting no alterations in fatty acid oxidation.

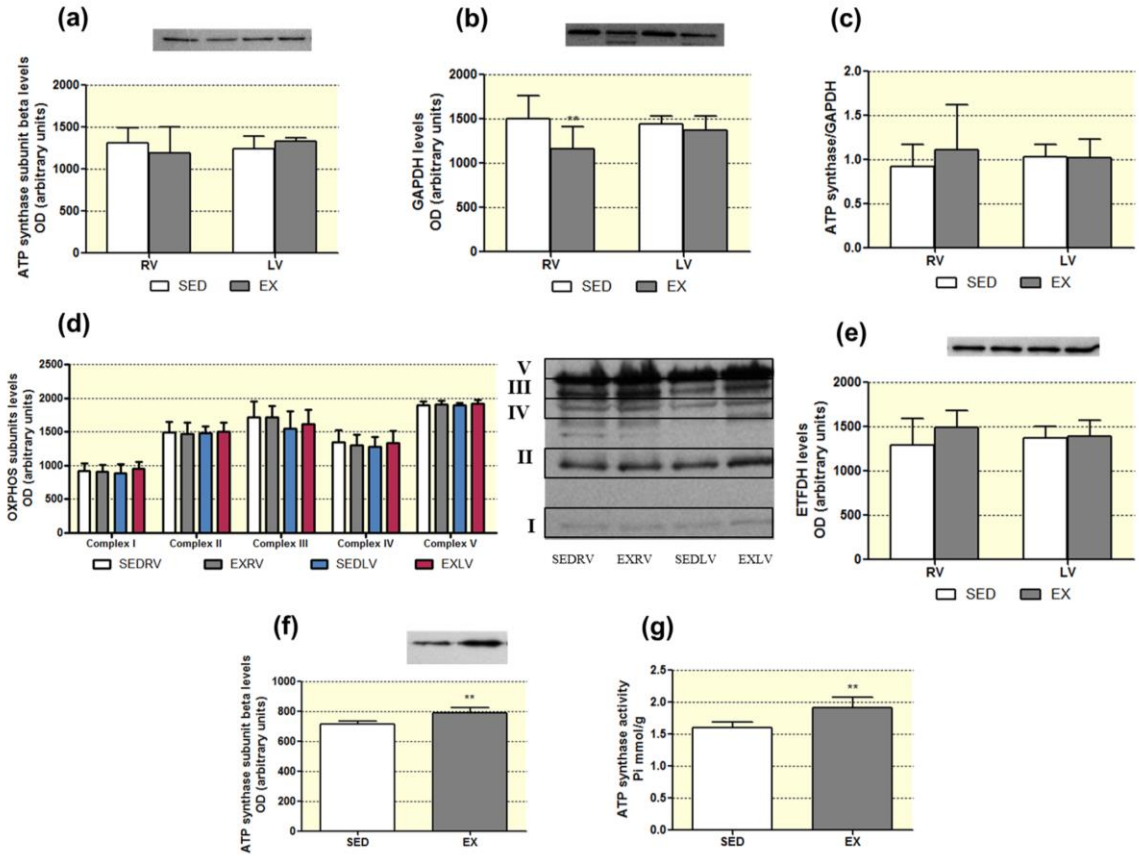

Figure 5 – Effect of exercise training on the levels of ATP synthase subunit β (a), GAPDH (b), ratio ATP synthase to GAPDH (c), OXPHOS subunits (d), ETFDH (e) in RV and LV and on the content of mitochondrial ATP synthase subunit β (f) and ATP synthase activity (g). LV: left ventricle, RV: right ventricle, OXPHOS: oxidative phosphorylation, GAPDH: glyceraldehyde 3-phosphate dehydrogenase, ETFDH: electron transfer flavoprotein:ubiquinone oxidoreductase. Values are presented as mean ± standard deviation (n=6 *per* group). ** P<0.01 vs. respective SED group.

After 54 weeks of endurance training there were no significant differences of citrate synthase (CS) activity between RV or LV in SED and EX groups (Figure 6a). CS activity has been suggested as a marker of mitochondrial content [20], so data point to no alterations in the pool of mitochondria from each ventricle due to lifelong exercise training. However, LV presented a significantly higher density of mitochondria than RV (P<0.001 vs. SEDRV and P<0.01 vs. EXRV). The levels of PGC-1α, a key player in the regulation of mitochondria biogenesis [21], were significantly lower in the LV of exercised animals in comparison to its RV (P<0.05) and in comparison to the LV of sedentary animals (P<0.01; Figure 6b). Differences between RV and LV of exercised animals were more expressive when the levels of PGC-1α were normalized to the number of mitochondria given by CS

activity (P<0.001; Figure 6c). So, data suggest that mitochondrial biogenesis is decreased in exercised LV. A similar trend of PGC-1α levels was noticed for the content of the mitochondrial transcription factor mtTFA, which was lower in exercised LV (P<0.05; Figure 6d).

The levels of RAF-1 were measured since this kinase has been implicated in the control of mitochondrial ROS and Ca^{2+} [1]. However, no expression differences were noticed among trained and sedentary animals in both ventricles (Figure 6f), in opposition to the observed in isolated mitochondria (Supplementary Figure S1).

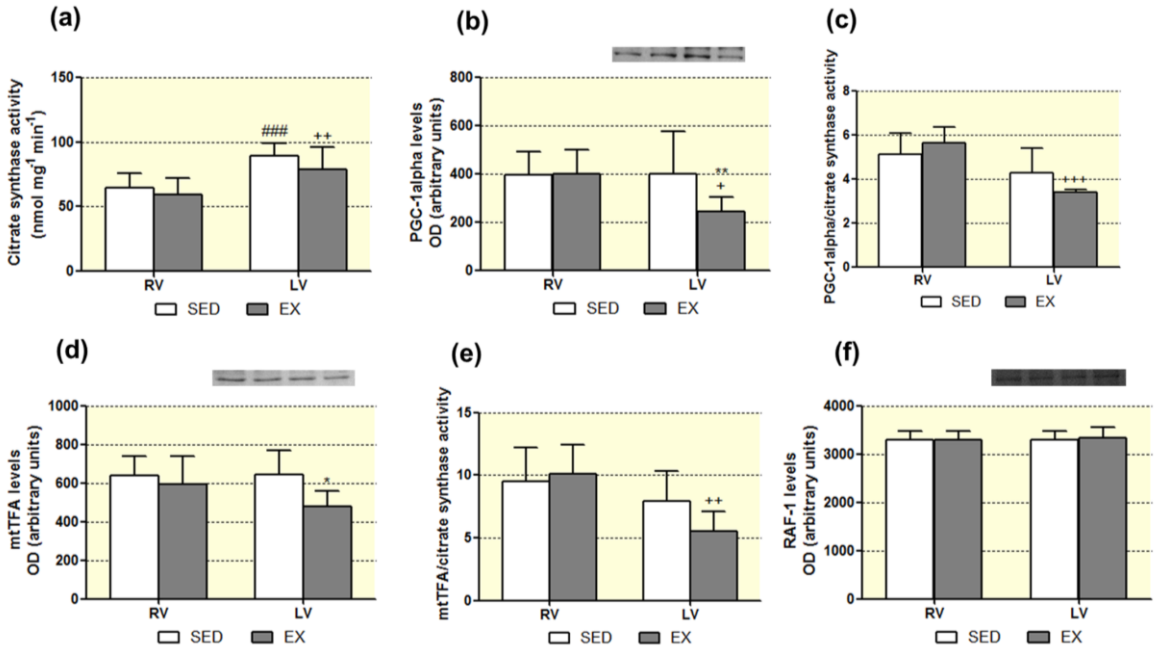

Figure 6 – Effect of exercise training on CS activity (a), PGC-1α content (b), ratio PGC-1α to CS activity (c), mtTFA content (d), ratio mtTFA to CS activity (e), RAF-1 content (f) in RV and LV. LV: left ventricle, RV: right ventricle, CS: citrate synthase, PGC-1α: peroxisome proliferator-activated receptor-gamma coactivator-1 alpha, mtTFA: mitochondrial transcription factor A, RAF-1: RAF proto-oncogene serine/threonine-protein kinase. Values are presented as mean ± standard deviation (n=6 *per* group). * P<0.05 vs. respective SED group; ** P<0.01 vs. respective SED group; ### P<0.001 vs. SEDRV; + P<0.05 vs. EXRV; ++ P<0.01 vs. EXRV; +++ P<0.001 vs. EXRV.

The levels of the deacetylase SIRT3 were determined in LV and RV extracts (Figure 7a-b), considering its role in the regulation of mitochondrial metabolic pathways [22]. No expression differences were noticed in both ventricles due to lifelong exercise training. However, when data was normalized to CS activity, significant differences among ventricles were observed. Specifically, higher values were observed for RV compared to

LV (P<0.001), and exercise training promoted an increased content of SIRT3 *per* mitochondria in RV (P<0.05; Figure 7b). Data from the analysis of isolated mitochondria confirmed this exercise-related increase of SIRT3 levels (Supplementary Figure S1).

Being a target of SIRT3 [22], it was expected that MnSOD showed an expression profile similar to SIRT3. Indeed, in RV from exercised animals there was a significant increase of MnSOD content (P<0.05; Figure 7c). Even more pronounced differences were detected when data was normalized to CS activity (P<0.001; Figure 7d). Moreover, the amount of this antioxidant enzyme *per* mitochondria was significantly higher in RV than in LV of exercised animals (P<0.001; Figure 7d).

In order to evaluate the impact of 54-weeks of endurance training on oxidative stress, we analyzed the content of oxidized proteins. In the RV of trained animals it was observed a significant increase of nitrated proteins (P<0.01; Figure 7f). The content of carbonylated proteins was also higher in the RV of exercised animals, though not statistically significant (Figure 7e). In LV, no alterations in the content of nitrated or carbonylated proteins were observed among experimental groups (Figure 7e and 7f).

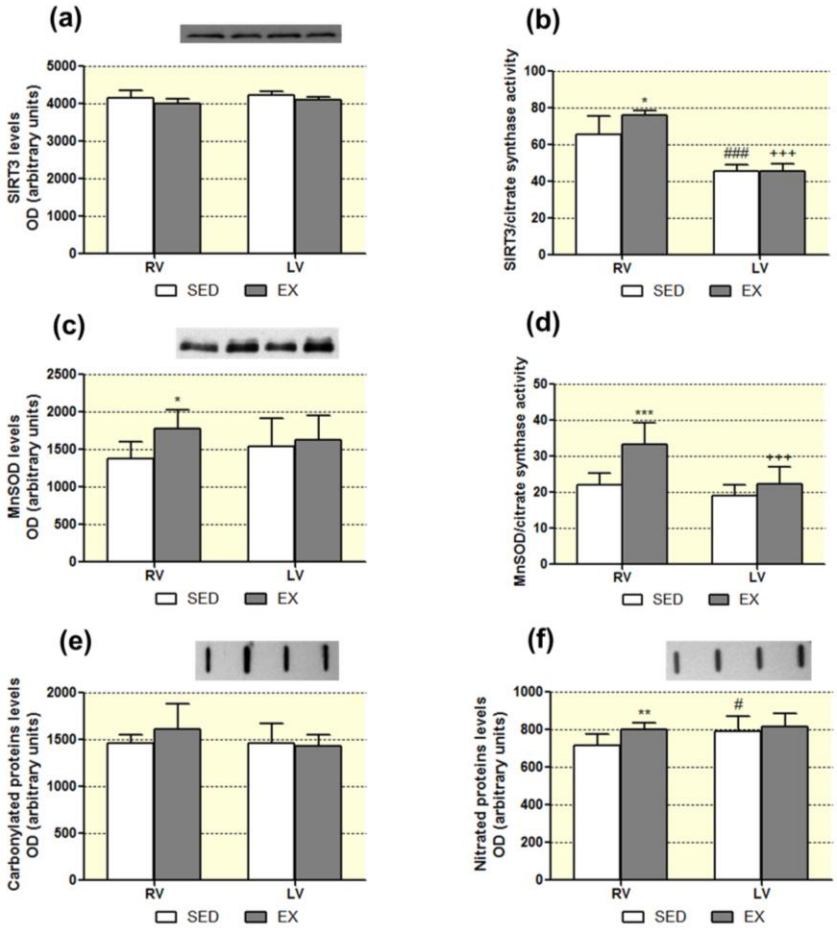

Figure 7 – Effect of exercise training on SIRT3 content (a) and on the ratio SIRT3 to CS activity (b), on MnSOD content (c), on the ratio MnSOD to CS activity (d), on carbonylated (e) and nitrated (f) proteins in RV and LV. LV: left ventricle, RV: right ventricle, CS: citrate synthase, MnSOD: manganese dependent superoxide dismutase, SIRT3: NAD-dependent deacetylase sirtuin-3. Values are presented as mean ± standard deviation (n=6 *per* group). * P<0.05 vs. respective SED group; ** P<0.01 vs. respective SED group; *** P<0.001 vs. respective SED group; # P<0.05 vs. SEDRV; ### P<0.001 vs. SEDRV; +++ P<0.001 vs. EXRV.

Discussion

Despite the well-documented benefits of endurance exercise training in promoting health, we are still searching for identifying novel molecular mechanisms underlying the long-term functional and structural changes that occur in the heart. Studies on the effects of exercise training have traditionally focused on the LV, despite the fact that overall cardiac performance is determined by two pumps in series. Even in healthy individuals, exercise imposes a disproportionate load on the RV, which may promote RV dysfunction if exercise is sufficiently intense and prolonged [23]. This observation supports the notion that the

adaptations of the RV to exercise training are not necessarily similar to those reported for LV. To add new insights on this topic, we analyzed RV and LV functional, structural and molecular adaptations promoted by one year of endurance exercise training. Rats from EX group performed endurance training for 54-weeks, which in humans corresponds to approximately 35 years of training [24], one of the longest exercise training programs performed in animal models.

In response to endurance exercise, the heart changes in size, shape, structure and physiology. Indeed, exercise training was reported to induce up to a 60% increase in LV mass, and up to 17–32% in cardiomyocyte size [4]. In the present study, no variation in the LV mass was observed in exercised animals, despite the 10% increase in cardiomyocyte size (Table 1 and Figure 1). This can be attributed in part to the maintenance of a low running intensity throughout the entire duration of the study as cardiac hypertrophy is known to be intensity-dependent [25]. Exercise-induced cardiomyocyte hypertrophy was related to significantly augmented systolic pressures, either maximum or at end-systole, which indicates a rescue from systolic function decline [26]. Regarding the diastolic proprieties, EX animals presented a lower EDP suggesting a less stiff myocardium. Because our histological data did not show any difference regarding collagen deposition, we believe that these differences could be explained in part by intrinsic changes to the cardiomyocytes [27]. In RV, we observed significantly less mass increase in exercised animals, which we attribute mainly to the prevention of fibrosis. The similar results of RV cardiomyocyte size between SED and EX were intriguing as exercise training was expected to cause hypertrophy. Thus, we believe that the RV of SED animals suffered some degree of hypertrophy secondary to RV afterload as suggested by a non-significant increase of 20% in RV Pmax and a significant increase of 10% in pulmonary artery hypertrophy, and exercise was able to prevent it. This interpretation is corroborated by clinical data from the general population showing that pulmonary artery pressures also increases with age [28]. As in the systemic circulation, the pulmonary vasculature may be affected by age-associated arterial remodeling, though in a lower magnitude, leading to pulmonary vascular stiffening and increases in pulmonary artery pressures [28-30]. Pulmonary artery pressure is also directly affected by downstream left heart filling pressures [28] and we observed that sedentary animals had a greater increase in LV EDP.

Besides hypertrophy of the pre-existing myocytes, it has been reported that exercise training induces the formation of new cardiomyocytes from progenitor/stem cells [18, 31, 32]. These studies suggest that c-kit positive cardiac stem cells are necessary and sufficient for functional cardiac regeneration and repair [18, 32]. Data from the present study do not support the activation of c-kit positive cardiac stem cells in response to 54-weeks of moderate exercise training (Figure 3), in opposition to the reported for 4 weeks of treadmill exercise [32] or 21 days of swimming [18]. These apparent contradictory findings might be justified, at least in part, by the aging process. Indeed, the percentage of cardiomyocytes emerging from the c-kit positive lineage was reported to astonishingly decrease with aging, and so unlikely to impact cardiac function [31]. Another factor could be related to the moderate intensity of our exercise training protocol as it was shown that c-kit positive cardiac stem cells activation is exercise-intensity dependent [32].

Long-term endurance training has been associated with arrhythmogenic cardiac remodeling of the RV [6, 33]. In the current study, we observed a significant reduction of Cx43 expression in RV of exercised animals in comparison to their LV values. Cx43 is the main gap junctional cardiac protein responsible for the rapid conduction of the action potential across the heart and its disturbance was implicated in the induction of arrhythmia [34, 35]. Moreover, down-regulation of Cx43 expression was previously shown with the use of the nonspecific beta-blocker propranolol, indicating that sympathetic tone is involved in Cx43 regulation [36]. While we are not able to relate the susceptibility of the RV to arrhythmia with Cx43 expression, it could be possible that the lower expression of Cx43 is an adaptive response to the increased vagal tone observed in the trained animals.

The main molecular adaptations of heart to long-term exercise training were seen at the metabolic level, mainly in the RV. The oxidative metabolism was increased in the RV of trained animals, mainly due to a significant reduction of glycolysis without a significant compensation by fatty acid oxidation (Figure 5). So, data from our study do not support the metabolic shift towards a reliance on glycolysis, as reported during cardiac hypertrophic growth [37, 38]. As a consequence of the metabolic adaptation of RV towards an oxidative phenotype, there was an increase of nitrated proteins, possibly due to augmented NO levels, and of MnSOD content. Increased generation of NO leads to the formation of peroxynitrite, which then reacts with proteins' tyrosine residues [39]. The up-regulation of MnSOD and the increased production of NO associated with eNOS activity have been

pointed out as a cardioprotective mechanism induced by exercise training [1, 40]. Even when exercise was performed during aging, MnSOD activity was reported to significantly increase in heart [41].

Despite the described effect of exercise training in endorsing mitochondrial biogenesis [1], our data do not support this cardiac adaptation. PGC-1α, which plays a key role in regulating genes involved in myocardial fuel metabolism and mitochondrial biogenesis [42], and the content of mitochondria, roughly assessed by CS activity [43], were not significantly modulated by 54-weeks of exercise (Figure 6). However, there is no consensus in the literature regarding the impact of exercise training on mitochondrial biogenesis in the heart. For instance, 6 weeks of swimming was shown to promote an up-regulation of mitochondrial biogenesis in heart [38], whereas 3 months of running did not impact mitochondrial density in LV [42]. In the regulation of PGC-1α expression, the deacetylase activity of SIRT3 has a key role [42]. This deacetylase also regulates the activity of several metabolic pathways harbored in mitochondria, namely antioxidant enzymes [22], protecting the heart against oxidative stress [44]. Lifelong exercise training induced an up-regulation of SIRT3 *per* mitochondria in RV (Figure 7). Once the expression profile of SIRT3 was similar to its target MnSOD, we might speculate that this mitochondrial deacetylase has mainly an antioxidant role in trained RV. Altogether, data suggest that heart adaptation to lifelong exercise training occurs mainly at the mitochondria level, resulting in an increased ability of this organelle to produce ATP (Figure 5) to support the cardiomyocytes' contractile apparatus. The lower mitochondrial density of RV compared to LV might explain, at least in part, the greater molecular alterations noticed in trained RV that could be considered a beneficial adaptation to meet the greater work requirements imposed by exercise [5].

We believe that a more marked effect of exercise training would be detected if we progressively increased the training intensity throughout the entire duration of the training period. However, our emphasis was on duration and we clearly show that one year of low intensity protocol is able to induce changes at the functional, structural and molecular level. Future studies should address the impact of exercise intensity in the aging heart.

In conclusion, findings from the present study show that lifelong moderate exercise training: i) improved the cardiac function, especially diastolic, with no apparent involvement of cardiac stem cells; ii) did not modulate the levels of Cx43; iii) increased

the antioxidant capacity of RV; iv) had no impact on mitochondrial biogenesis, but improved the mitochondrial ability to produce ATP and so meet the energetic demands imposed by exercise during the aging process.

Acknowledgments

This work was supported by Portuguese Foundation for Science and Technology (FCT), European Union, QREN, FEDER and COMPETE for funding the QOPNA research unit (project PEst-C/QUI/UI0062/2013), CIAFEL (UID/DTP/00617/2013), Unidade de Investigação Cardiovascular (UID/IC/00051/2013), iBiMED (UID/BIM/04501/2013), the research project (EXPL/DTP-DES/1010/2013, FCOMP-01-0124-FEDER-041115) and post-graduation students (grant numbers SFRH/BD/91067/2012 to R.N.F and SFRH/BPD/90010/2012 to D.M.G.). The authors would like to thank Celeste Resende for their assistance in sample preparation for morphological analysis.

Conflict of interest

The authors declare no conflicts of interests, financial or otherwise.

References

1. Ferreira, R., D. Moreira-Goncalves, A.L. Azevedo, J.A. Duarte, F. Amado, and R. Vitorino, *Unraveling the exercise-related proteome signature in heart.* Basic Res Cardiol, 2015. **110**(1): p. 454.
2. Arbab-Zadeh, A., M. Perhonen, E. Howden, R.M. Peshock, R. Zhang, B. Adams-Huet, M.J. Haykowsky, and B.D. Levine, *Cardiac remodeling in response to 1 year of intensive endurance training.* Circulation, 2014. **130**(24): p. 2152-61.
3. Scharhag, J., G. Schneider, A. Urhausen, V. Rochette, B. Kramann, and W. Kindermann, *Athlete's heart: right and left ventricular mass and function in male endurance athletes and untrained individuals determined by magnetic resonance imaging.* J Am Coll Cardiol, 2002. **40**(10): p. 1856-63.
4. Lerchenmuller, C. and A. Rosenzweig, *Mechanisms of exercise-induced cardiac growth.* Drug Discov Today, 2014. **19**(7): p. 1003-9.
5. La Gerche, A., T. Roberts, and G. Claessen, *The response of the pulmonary circulation and right ventricle to exercise: exercise-induced right ventricular*

dysfunction and structural remodeling in endurance athletes (2013 Grover Conference series). Pulm Circ, 2014. **4**(3): p. 407-16.

6. Heidbuchel, H., J. Hoogsteen, R. Fagard, L. Vanhees, H. Ector, R. Willems, and J. Van Lierde, *High prevalence of right ventricular involvement in endurance athletes with ventricular arrhythmias. Role of an electrophysiologic study in risk stratification.* Eur Heart J, 2003. **24**(16): p. 1473-80.
7. Gay-Jordi, G., E. Guash, B. Benito, J. Brugada, S. Nattel, L. Mont, and A. Serrano-Mollar, *Losartan prevents heart fibrosis induced by long-term intensive exercise in an animal model.* PLoS One, 2013. **8**(2): p. e55427.
8. Benito, B., G. Gay-Jordi, A. Serrano-Mollar, E. Guasch, Y. Shi, J.C. Tardif, J. Brugada, S. Nattel, and L. Mont, *Cardiac arrhythmogenic remodeling in a rat model of long-term intensive exercise training.* Circulation, 2011. **123**(1): p. 13-22.
9. Lawler, J.M., S.K. Powers, J. Hammeren, and A.D. Martin, *Oxygen cost of treadmill running in 24-month-old Fischer-344 rats.* Med Sci Sports Exerc, 1993. **25**(11): p. 1259-64.
10. Moreira-Goncalves, D., T. Henriques-Coelho, H. Fonseca, R. Ferreira, A.I. Padrao, C. Santa, S. Vieira, A.F. Silva, F. Amado, A. Leite-Moreira, and J.A. Duarte, *Intermittent cardiac overload results in adaptive hypertrophy and provides protection against left ventricular acute pressure overload insult.* J Physiol, 2015. **593**(17): p. 3885-97.
11. Moreira-Goncalves, D., R. Ferreira, H. Fonseca, A.I. Padrao, N. Moreno, A.F. Silva, F. Vasques-Novoa, N. Goncalves, S. Vieira, M. Santos, F. Amado, J.A. Duarte, A.F. Leite-Moreira, and T. Henriques-Coelho, *Cardioprotective effects of early and late aerobic exercise training in experimental pulmonary arterial hypertension.* Basic Res Cardiol, 2015. **110**(6): p. 57.
12. Moreira-Goncalves, D., T. Henriques-Coelho, H. Fonseca, R.M. Ferreira, F. Amado, A. Leite-Moreira, and J.A. Duarte, *Moderate exercise training provides left ventricular tolerance to acute pressure overload.* Am J Physiol Heart Circ Physiol, 2011. **300**(3): p. H1044-52.
13. Nogueira-Ferreira, R., D. Moreira-Goncalves, A.F. Silva, J.A. Duarte, A. Leite-Moreira, R. Ferreira, and T. Henriques-Coelho, *Exercise preconditioning prevents*

MCT-induced right ventricle remodeling through the regulation of TNF superfamily cytokines. Int J Cardiol, 2016. **203**: p. 858-866.

14. Coore, H.G., R.M. Denton, B.R. Martin, and P.J. Randle, *Regulation of adipose tissue pyruvate dehydrogenase by insulin and other hormones.* Biochem J, 1971. **125**(1): p. 115-27.
15. Ferreira, R., R. Vitorino, A.I. Padrao, G. Espadas, F.M. Mancuso, D. Moreira-Goncalves, G. Castro-Sousa, T. Henriques-Coelho, P.A. Oliveira, A.S. Barros, J.A. Duarte, E. Sabido, and F. Amado, *Lifelong exercise training modulates cardiac mitochondrial phosphoproteome in rats.* J Proteome Res, 2014. **13**(4): p. 2045-55.
16. Padrão, A.I., R.M.P. Ferreira, R. Vitorino, R.M.P. Alves, M.J. Neuparth, J.A. Duarte, and F. Amado, *OXPHOS susceptibility to oxidative modifications: The role of heart mitochondrial subcellular location.* Biochim Biophys Acta, 2011. **1807**(9): p. 1106-1113.
17. Laemmli, U.K., *Cleavage of structural proteins during the assembly of the head of bacteriophage T4.* Nature, 1970. **227**(5259): p. 680-5.
18. Xiao, J., T. Xu, J. Li, D. Lv, P. Chen, Q. Zhou, and J. Xu, *Exercise-induced physiological hypertrophy initiates activation of cardiac progenitor cells.* Int J Clin Exp Pathol, 2014. **7**(2): p. 663-9.
19. Antunes, D., A.I. Padrao, E. Maciel, D. Santinha, P. Oliveira, R. Vitorino, D. Moreira-Goncalves, B. Colaco, M.J. Pires, C. Nunes, L.L. Santos, F. Amado, J.A. Duarte, M.R. Domingues, and R. Ferreira, *Molecular insights into mitochondrial dysfunction in cancer-related muscle wasting.* Biochim Biophys Acta, 2014. **1841**(6): p. 896-905.
20. Figueiredo, P.A., S.K. Powers, R.M. Ferreira, H.J. Appell, and J.A. Duarte, *Aging impairs skeletal muscle mitochondrial bioenergetic function.* J Gerontol A Biol Sci Med Sci, 2009. **64**(1): p. 21-33.
21. Vitorino, R., D. Moreira-Goncalves, and R. Ferreira, *Mitochondrial plasticity in cancer-related muscle wasting: potential approaches for its management.* Curr Opin Clin Nutr Metab Care, 2015. **18**(3): p. 226-33.
22. Amado, F.M., A. Barros, A.L. Azevedo, R. Vitorino, and R. Ferreira, *An integrated perspective and functional impact of the mitochondrial acetylome.* Expert Rev Proteomics, 2014. **11**(3): p. 383-94.

23. La Gerche, A. and G. Claessen, *Is exercise good for the right ventricle? Concepts for health and disease.* Can J Cardiol, 2015. **31**(4): p. 502-508.
24. Sengupta, P., *The laboratory rat: relating its age with human's.* Int J Prev Med, 2013. **4**(6): p. 624-630.
25. Wisloff, U., O. Ellingsen, and O.J. Kemi, *High-intensity interval training to maximize cardiac benefits of exercise training?* Exerc Sport Sci Rev, 2009. **37**(3): p. 139-46.
26. Bal, M.P., W.B. De Vries, F.R. Van Der Leij, M.F. Van Oosterhout, J. Baan, E.E. Van Der Wall, F. Van Bel, and P. Steendijk, *Left ventricular pressure-volume relationships during normal growth and development in the adult rat--studies in 8- and 50-week-old male Wistar rats.* Acta Physiol Scand, 2005. **185**(3): p. 181-91.
27. Loffredo, F.S., A.P. Nikolova, J.R. Pancoast, and R.T. Lee, *Heart failure with preserved ejection fraction: molecular pathways of the aging myocardium.* Circ Res, 2014. **115**(1): p. 97-107.
28. Lam, C.S., B.A. Borlaug, G.C. Kane, F.T. Enders, R.J. Rodeheffer, and M.M. Redfield, *Age-associated increases in pulmonary artery systolic pressure in the general population.* Circulation, 2009. **119**(20): p. 2663-70.
29. Lansing, A.I., T.B. Rosenthal, and M. Alex, *Significance of medial age changes in the human pulmonary artery.* J Gerontol, 1950. **5**(3): p. 211-5.
30. Mackay, E.H., J. Banks, B. Sykes, and G. Lee, *Structural basis for the changing physical properties of human pulmonary vessels with age.* Thorax, 1978. **33**(3): p. 335-44.
31. Van Berlo, J.H., O. Kanisicak, M. Maillet, R.J. Vagnozzi, J. Karch, S.C. Lin, R.C. Middleton, E. Marban, and J.D. Molkentin, *c-kit+ cells minimally contribute cardiomyocytes to the heart.* Nature, 2014. **509**(7500): p. 337-41.
32. Waring, C.D., C. Vicinanza, A. Papalamprou, A.J. Smith, S. Purushothaman, D.F. Goldspink, B. Nadal-Ginard, D. Torella, and G.M. Ellison, *The adult heart responds to increased workload with physiologic hypertrophy, cardiac stem cell activation, and new myocyte formation.* Eur Heart J, 2014. **35**(39): p. 2722-31.
33. La Gerche, A., A.T. Burns, D.J. Mooney, W.J. Inder, A.J. Taylor, J. Bogaert, A.I. Macisaac, H. Heidbuchel, and D.L. Prior, *Exercise-induced right ventricular*

dysfunction and structural remodelling in endurance athletes. Eur Heart J, 2012. **33**(8): p. 998-1006.

34. Jones, S.A., *Ageing to arrhythmias: conundrums of connections in the ageing heart.* J Pharm Pharmacol, 2006. **58**(12): p. 1571-6.
35. Chang, Y., T. Yu, H. Yang, and Z. Peng, *Exhaustive exercise-induced cardiac conduction system injury and changes of cTnT and Cx43.* Int J Sports Med, 2015. **36**(1): p. 1-8.
36. Tiscornia, G.C., R. Moretta, M.A. Argenziano, C.E. Amorena, and E.A. Garcia Gras, *Inhibition of connexin 43 in cardiac muscle during intense physical exercise.* Scand J Med Sci Sports, 2014. **24**(2): p. 336-44.
37. Lehman, J.J. and D.P. Kelly, *Transcriptional activation of energy metabolic switches in the developing and hypertrophied heart.* Clin Exp Pharmacol Physiol, 2002. **29**(4): p. 339-45.
38. Vettor, R., A. Valerio, M. Ragni, E. Trevellin, M. Granzotto, M. Olivieri, L. Tedesco, C. Ruocco, A. Fossati, R. Fabris, R. Serra, M.O. Carruba, and E. Nisoli, *Exercise training boosts eNOS-dependent mitochondrial biogenesis in mouse heart: role in adaptation of glucose metabolism.* Am J Physiol Endocrinol Metab, 2014. **306**(5): p. E519-28.
39. Van Der Loo, B., R. Labugger, J.N. Skepper, M. Bachschmid, J. Kilo, J.M. Powell, M. Palacios-Callender, J.D. Erusalimsky, T. Quaschning, T. Malinski, D. Gygi, V. Ullrich, and T.F. Luscher, *Enhanced peroxynitrite formation is associated with vascular aging.* J Exp Med, 2000. **192**(12): p. 1731-44.
40. Powers, S.K., A.J. Smuder, A.N. Kavazis, and J.C. Quindry, *Mechanisms of exercise-induced cardioprotection.* Physiology (Bethesda), 2014. **29**(1): p. 27-38.
41. Gunduz, F., U.K. Senturk, O. Kuru, B. Aktekin, and M.R. Aktekin, *The effect of one year's swimming exercise on oxidant stress and antioxidant capacity in aged rats.* Physiol Res, 2004. **53**(2): p. 171-6.
42. Li, L., C. Muhlfeld, B. Niemann, R. Pan, R. Li, D. Hilfiker-Kleiner, Y. Chen, and S. Rohrbach, *Mitochondrial biogenesis and PGC-1alpha deacetylation by chronic treadmill exercise: differential response in cardiac and skeletal muscle.* Basic Res Cardiol, 2011. **106**(6): p. 1221-34.

43. Figueiredo, P.A., R.M. Ferreira, H.J. Appell, and J.A. Duarte, *Age-induced morphological, biochemical, and functional alterations in isolated mitochondria from murine skeletal muscle.* J Gerontol A Biol Sci Med Sci, 2008. **63**(4): p. 350-9.
44. Mann, N. and A. Rosenzweig, *Can exercise teach us how to treat heart disease?* Circulation, 2012. **126**(22): p. 2625-2635.

STUDY II – EXERCISE PRECONDITIONING PREVENTS MCT-INDUCED RIGHT VENTRICLE REMODELING THROUGH THE REGULATION OF TNF SUPERFAMILY CYTOKINES

International Journal of Cardiology 203 (2016) 858–866

Contents lists available at ScienceDirect

International Journal of Cardiology

journal homepage: www.elsevier.com/locate/ijcard

Exercise preconditioning prevents MCT-induced right ventricle remodeling through the regulation of TNF superfamily cytokines

Rita Nogueira-Ferreira [a,b], Daniel Moreira-Gonçalves [b,c,*], Ana Filipa Silva [b], José Alberto Duarte [c], Adelino Leite-Moreira [b,d,e], Rita Ferreira [a], Tiago Henriques-Coelho [b,**]

[a] QOPNA, Department of Chemistry, University of Aveiro, Aveiro, Portugal
[b] Department of Physiology and Cardiothoracic Surgery, Faculty of Medicine, University of Porto, Porto, Portugal
[c] CIAFEL, Faculty of Sport, University of Porto, Porto, Portugal
[d] Cardiovascular Research Centre, Faculty of Medicine, University of Porto, Portugal
[e] Department of Cardiothoracic Surgery, Hospital of São João, Porto, Portugal

ARTICLE INFO

Article history:
Received 3 October 2015
Received in revised form 6 November 2015
Accepted 7 November 2015
Available online 10 November 2015

Keywords:
Exercise training
Heart failure
Pro-inflammatory cytokines
Pulmonary arterial hypertension
Right ventricle muscle

ABSTRACT

Background: Exercise training has been recognized as a non-pharmacological therapeutic approach in several chronic diseases; however it remains to be tested if exercise preconditioning can positively interfere with the natural history of pulmonary arterial hypertension (PAH). This is important since the majority of these patients are diagnosed at advanced stages of the disease, when right ventricle (RV) impairment is already present.
Objectives: In the current study, we evaluated the preventive effect of exercise preconditioning on RV failure secondary to PAH, with a focus on the signaling pathways modulated by pro-inflammatory cytokines from TNF superfamily.
Methods: We analyzed the RV muscle from adult male Wistar rats exposed to a 4-week treadmill exercise training or sedentary regime, prior to the administration of monocrotaline (MCT) to induce PAH or with saline solution (controls).
Results: Data indicate that exercise preconditioning prevented cardiac hypertrophy and RV diastolic dysfunction. At a molecular level, exercise modulated the TWEAK/NF-κB signaling axis and prevented the shift in MHC isoforms towards an increased expression of beta-MHC. Exercise preconditioning also prevented the increase of atrogin-1 expression, and induced a shift of MMP activity from MMP-9 to MMP-2 activity.
Conclusions: Altogether, data support exercise as a preventive strategy for the management of PAH, which is of particular relevance for the familial form of PAH that is manifested by greater severity or earlier onset.

1. Introduction

Pulmonary arterial hypertension (PAH) is a progressive disorder that affects both the pulmonary vasculature and the heart. The initial insult involves the pulmonary vasculature but survival of patients is determined by the right ventricle (RV) adaptation. Despite its importance for the patient outcome, little is known about the mechanisms responsible for the development of RV dysfunction on PAH. Several molecular disturbances have been suggested to contribute for RV dysfunction [1–4]. Recent reports support inflammation as a major contributor in the initiation and progression of RV dysfunction in PAH. Increased chemokine expression, and infiltration of both neutrophils and monocyte/macrophages were detected in the RV myocardium early after an acute increase in afterload [5–8]. Progressive activation of neutrophils was also noted as the RV progressed from hypertrophy to failure in the MCT-PAH model [9]. Released pro-inflammatory cytokines as TNF-α may depress cardiac contractility by promoting hypertrophy, apoptosis and fibrosis [7]. Additional evidence of the importance of inflammation in PAH is provided by data suggesting that anti-inflammatory therapies have beneficial effects on both pulmonary vasculature and RV function [10–12].

In opposition to the therapeutic proprieties of exercise training on PAH [13], it remains to be tested if exercise preconditioning can provide a protective background that could positively interfere with the natural history of the disease. Exercise preconditioning has the unique ability to provide a cardioprotective phenotype, which confers tolerance to several cardiac acute insults like ischemia–reperfusion, myocardial infarction, doxorubicin toxicity and acute pressure overload [14,15]. This cardioprotective effect seems to be related, in part, with intrinsic modifications at the level of the cardiomyocyte [15,16], making them more prepared to deal and tolerate increased functional demands. The

* Corresponding to: D. Moreira-Gonçalves, CIAFEL, Faculty of Sport, University of Porto, Rua Dr. Plácido Costa, 91, 4200-450 Porto, Portugal.
** Corresponding to: T. Henriques-Coelho, Department of Physiology and Cardiothoracic Surgery, Faculty of Medicine, University of Porto, Alameda Professor Hernâni Monteiro, 4200-319 Porto, Portugal.
E-mail addresses: danielmgon@gmail.com (D. Moreira-Gonçalves), henriques.coelho@gmail.com (T. Henriques-Coelho).

http://dx.doi.org/10.1016/j.ijcard.2015.11.066
0167-5273/

potential benefit of exercise preconditioning is of great relevance if we consider that the majority of PAH patients are diagnosed at advanced stages of the disease, when RV impairment is already present. Moreover, in the familial form of PAH exercise preconditioning might be seen as a measure to prevent the severity or early onset of the disease.

In this study, we aimed to evaluate the long-term cardioprotective effects of exercise preconditioning on RV dysfunction and remodeling secondary to MCT-induced PAH. Focus was given to the signaling pathways modulated by the pro-inflammatory cytokines of the tumor necrosis factor (TNF) superfamily considering their involvement in PAH pathogenesis [17].

2. Materials and methods

2.1. Animal and experimental design

Housing and experimental treatment were in accordance with the *Guide for the Care and Use of Laboratory Animals* from the Institute for Laboratory Animal Research (ILAR, 1996). The experiments were complied with the current national laws (DL 129/92, DL 197/96, P1131/97). Fifty male Wistar rats (age: 5 weeks; weight: 150 g; Charles River Laboratories, Barcelona, Spain) were housed in groups of 5 rats/cage and were maintained in a room at normal environment (21–24 °C; ~50–60% humidity) receiving food and water ad libitum in 12 h light/dark cycles. After one week of quarantine, 25 rats were randomly divided and submitted to treadmill exercise training (Ex) and the other 25 remained with their movement confined to the cages' area for 4 weeks. Animals from the Ex group were submitted to a treadmill exercise training program for 4 weeks during 5 days/week [14]. Exercise duration and treadmill speed were gradually increased over the course of the first week of training until animals achieved 60 min/day at 25 m/min. All animals from the Ex group completed the training protocol. Sedentary animals were placed on a non-moving treadmill three times *per* week (5 min/session) for acclimatization. After ending their respective protocols, rats were again randomly divided as follows: i) Ex + Cont (n = 10) and SED + Cont (n = 10) injected with saline solution or ii) Ex + MCT (n = 15) and SED + MCT (n = 15), injected subcutaneously with monocrotaline (MCT) (60 mg/Kg, s.c., Sigma). After that, all the animals remained with movement confined to their cage's space for an additional 4 week-period. During the protocol 6 rats from SED + MCT and 4 from Ex + MCT groups died. After 4 weeks of MCT or vehicle administration, hemodynamic evaluation was performed.

2.2. Hemodynamic evaluation

Animals were anesthetized by inhalation of a mixture of sevoflurane (8% for induction and 2.5–3% for maintenance) and oxygen, endotracheally intubated for mechanical ventilation (150 min^{-1}, 100% O_2, 14–16 cm H_2O inspiratory pressure, with tidal volume adjusted to animal weight, and 5 cm H_2O end-expiratory pressure; TOPO Small Animal Ventilator - Kent Scientific, Dual Mode) and placed over a heating pad. Under binocular surgical microscopy (Leica, Wild 384,000), the right jugular vein was cannulated for fluid administration (prewarmed 0.9% NaCl solution, 32 mL/Kg/h) to compensate for perioperative losses. The heart was exposed through a median sternotomy. A catheter was then placed in the RV in order to obtain hemodynamic data (PVR-1045, Millar Instruments, Houston, TX). After complete instrumentation, the animal preparation was allowed to stabilize for 15 min. Hemodynamic recordings were made with respiration suspended at end-expiration under basal conditions and during preload reductions (inferior vena cava occlusion). Data was continuously acquired (MPVS 300, Millar Instruments), digitally recorded at 1000 Hz (ML880 PowerLab 16/30, Millar TM Instruments), and analyzed (LabChart, ADInstruments). After complete hemodynamic assessment, animals were euthanized by exsanguination under anesthesia. The *gastrocnemius* muscle, heart and lungs were excised and weighted. Lung samples were used for histological analysis. The right ventricle was separated, weighted and then used for histological analysis (cardiomyocyte hypertrophy and fibrosis), MHC isoforms quantification, western blotting analysis and zymography.

2.3. Histological analysis

Cubic pieces from RV were fixed [4% (*v*/*v*) buffered paraformaldehyde] by diffusion during 24 h and subsequently dehydrated with graded ethanol and included in paraffin blocks. Xilene was used in the transition between dehydration and impregnation. Serial sections (5 μm of thickness) of paraffin blocks were cut by a microtome and mounted on silane-coated slides. The slides were dewaxed in xylene and hydrated through graded alcohols finishing in phosphate buffered saline solution (pH 7.2). Deparaffinized sections were stained for hematoxylin–eosin. Cardiomyocyte surface area (CSA) was measured, and only round to ovoid nucleated myocytes were considered for analysis. In order to determine the amount of cardiac fibrosis, RV sections were stained with Picrosirius red and quantified as described before [18]. For quantitative comparisons, 4 random microscopic fields (magnification of ×400) from 5 animals were considered. All analysis were made in a blinded manner.

2.4. Right ventricle muscle preparation for biochemical analysis

A portion (~20–25 mg) of RV muscle was homogenized in homogenization buffer (0.25 M sucrose, 1 mM EDTA, 20 mM HEPES, pH 7.6; 100 mg of tissue/mL of buffer) using a Teflon pestle on a motor-driven Potter-Elvehjem glass homogenizer at 0–4 °C (3–5 times for 5 s at low speed, with a final burst at a higher speed). The protein content of the cardiac muscle homogenate was assayed with the Bio-Rad DC method, following the instructions of the manufacturer, using bovine serum albumin (BSA) as a standard.

2.5. Analysis of myosin heavy chain (MHC) isoform content

Right ventricle sections were weighed and homogenized (in the proportion of 1:19) in 100 mM phosphate buffer, pH 7.4, containing 0.02% bovine serum albumin, with a tightly fitted Potter-Elvehjem homogenizer and Teflon pestle at 0–4 °C. Total protein concentration was spectrophotometrically assayed with the Bio-Rad DC method. MHC isoforms were separated by gel electrophoresis following the procedure described by Talmadge and Roy [19]. One μg of protein sample from each group studied was applied in the same gel. The stacking gel consisted of 30% glycerol and 4% acrylamide: *N*,*N*′-methylene-bis-acrylamide in the ratio of 50:1, 70 mM Tris (pH 6.7), 4 mM EDTA, and 0.4% sodium dodecyl sulfate (SDS). The separating gels were composed of 30% glycerol, 8% acrylamide-bis (50:1), 0.2 M Tris (pH 8.8), 0.1 M glycine, and 0.4% SDS. Polymerization was initiated with 0.05% *N*,*N*,*N*′,*N*′-tetramethylethylenediamine and 0.1% ammonium persulfate. The gels were run in a Mini-Protean system (Bio-Rad) at 4 °C. The running conditions were 70 V (constant voltage) for 24 h. The gels were stained with Coomassie Colloidal, scanned in Molecular Imager Gel Doc XR + System (Bio-Rad) and optical density analysis of MHC bands was performed using Image Lab software (v4.1, Bio-Rad).

2.6. Western blotting analysis

Equivalent amounts of RV protein of each experimental group (40 μg) were electrophoresed on a 12.5% SDS-PAGE as described by Laemmli [20]. Gels were blotted onto a nitrocellulose membrane (Whatman®, Protan®) in transfer buffer (25 mM Tris, 192 mM glycine, pH 8.3 and 20% methanol) during 2 h (200 mA). Then, nonspecific binding was blocked with 5% (*w*/*v*) nonfat dry milk in TBS-T (100 mM Tris, 1.5 mM NaCl, pH 8.0 and 0.5% Tween 20). The membrane was incubated with primary antibody solution diluted 1:1000 in 5% (*w*/*v*) nonfat dry milk

in TBS-T (rabbit anti-GDF8 (myostatin), ab996, abcam; rabbit anti-Smad3, ab51451, abcam; rabbit anti-p38 MAPK, #9212, Cell Signaling; mouse anti-TNF-alpha, ab1793, abcam; rabbit anti-TWEAK, ab37170, abcam; rabbit anti-NF-κB p105/p50, ab32360, abcam; rabbit anti-NF-κB p65, ab16502, abcam; rabbit anti-phospho-p44/42 MAPK (Erk1/2), #4370, Cell Signaling; mouse anti-NF-κB p100/p52, ab71108, abcam; rabbit anti-Rel B, ab150305, abcam; rabbit anti-TRAF6, ab33915, abcam; rabbit anti-MuRF1, ab77577, abcam; rabbit anti-atrogin-1, #AP2041, ECM Biosciences; rabbit anti-Phospho-Akt, #4058, Cell Signaling; rabbit anti-FOXO3A, ab47285, abcam). After 2 h incubation at room temperature with agitation, the membrane was washed with TBS-T and incubated with anti-mouse or anti-rabbit IgG peroxidase secondary antibody (Sigma-Aldrich) diluted 1:1000 in 5% (*w*/*v*) nonfat dry milk in TBS-T. Immunoreactive bands were detected with enhanced chemiluminescence reagents (ECL, Amersham Pharmacia Biotech) according to the manufacturer's procedure and images were recorded using X-ray films (Amersham Hyperfilm ECL, GE Healthcare). The films were scanned in Molecular Imager Gel Doc XR + System (Bio-Rad) and analyzed with Image Lab software (v4.1, Bio-Rad). Protein loading was controlled by Ponceau S staining once the content of cytoskeletal proteins were found to be modulated by the conditions in study.

2.7. Analysis of proteolytic activity through gelatine zymography

Zymography assays were performed according to Vitorino et al. [21] with minor alterations. Briefly, the zymography was performed using a 10% SDS-PAGE separation gel with 0.1% of gelatin. Twenty μg of sample from each experimental group was incubated on charging buffer (100 mM Tris pH 6.8, 5% SDS, 20% glycerol, 0.1% bromophenol blue) for 10 min on ice, in a proportion of 1:1 (*v*/*v*). After the run, the gels were incubated in renaturation buffer (2.5% Triton X-100) for 30 min, with soft agitation. Then, the zymo gels were changed to a development buffer (50 mM Tris, 5 mM NaCl, 10 mM $CaCl_2$, 1 μm $ZnCl_2$, 0.02% (*v*/*v*) Triton X-100, pH 7.4) for more 30 min, also with soft agitation. Gels were then changed to a new development buffer, and incubated overnight at 37 °C. For specific inhibition studies zymograms were incubated in a solution containing 10 mM EDTA. The zymography gels were stained with 0.12% (*w*/*v*) Coomassie Blue G250 in 20% methanol. Gels were then destained with 25% methanol and scanned with Molecular Imager Gel Doc XR + System (Bio-Rad) and analyzed with Image Lab software (v4.1, Bio-Rad).

2.8. Data analysis

Values are given as mean ± standard deviation for all variables. Kolmogorov-Smirnov test was performed to check the normality of the data. Since all variables were normal distributed, significant differences between the groups were evaluated using a one-way analysis of variance followed by the Tukey multiple comparisons post hoc test. Results were considered significantly different when $p < 0.05$. Statistical analysis was performed with Graph Pad Prism software (version 5.0).

3. Results

3.1. Characterization of rat's response to MCT administration and/or exercise training

Significant loss of body weight was observed in SED + MCT group 4 weeks after MCT administration ($p < 0.001$ vs. SED + Cont group; Table 1). This body weight decrease was accompanied by a significant decrease in *gastrocnemius* muscle mass ($p < 0.001$ vs. SED + Cont group) suggestive of muscle wasting. Cardiac hypertrophy was also present in SED + MCT group, as evidenced by the significant increase in heart mass (12%, $p < 0.01$ vs. SED + Cont group), right ventricle mass (38%, $p < 0.001$ vs. SED + Cont group), heart-to-body weight ratio ($p < 0.001$ vs. SED + Cont group), right ventricle-to-body weight ratio ($p < 0.001$ vs. SED + Cont group) and Fulton index ($p < 0.001$ vs. SED + Cont group). Both SED + MCT and Ex + MCT groups presented increased lungs mass ($p < 0.001$ vs. SED + Cont and Ex + Cont groups, respectively).

Exercise preconditioning prevented the decrease in body weight ($p < 0.001$ vs. SED + MCT group) and *gastrocnemius* muscle mass ($p < 0.001$ vs. SED + MCT group). While heart and RV mass were significantly increased in Ex + MCT ($p < 0.001$ vs. SED + Cont and Ex + Cont groups), these differences were attenuated when normalized to body weight ($p < 0.01$ vs. SED + MCT group), suggesting that exercise preconditioning attenuated cardiac hypertrophy. Moreover, the Fulton index was significantly lower in Ex + MCT ($p < 0.05$ vs. SED + MCT group). No significant differences were observed between Ex + Cont and SED + Cont groups in all the evaluated parameters (Table 1).

3.2. Effects of MCT administration and/or exercise training on cardiac hemodynamics

Right ventricular peak systolic pressure was increased in both MCT-treated groups, but exercise preconditioning induced a non-significant attenuation (Table 2). Heart rate was reduced in MCT-treated animals ($p < 0.001$ vs. SED + Cont). No significant differences were observed among groups regarding to dP/dtmax. Contrarily to what was observed in SED + MCT group, exercise preconditioning prevented diastolic dysfunction as both end-diastolic pressure and tau were normalized. Peak rate of pressure fall was increased in both MCT-treated groups but significance was attained only in Ex + MCT (Table 2).

3.3. Right ventricle and lung morphological analysis

MCT-induced PAH resulted in cardiomyocyte hypertrophy in both MCT-treated groups ($p < 0.001$ vs. respective control group), with lesser degree in Ex + MCT ($p < 0.001$ vs. SED + MCT) (Fig. 1A and B). At the level of extracellular matrix, significant amounts of fibrosis were detected in SED + MCT ($p < 0.001$ vs. SED + Cont), while this was prevented by exercise preconditioning (Fig. 1C and D). Significant medial hypertrophy of pulmonary arteries was observed in SED + MCT ($p < 0.001$ vs. SED + Cont) but not in Ex + MCT, where a preventive effect of exercise was noted ($p < 0.001$ vs. SED + MCT) (Fig. 1E and F).

Table 1
Effect of exercise preconditioning and MCT-induced heart failure on rat body, heart, right ventricle, lungs, *gastrocnemius*, heart/body and right ventricle/body weights, and Fulton index.

Experimental group	Body weight (kg)	Heart mass (g)	Right ventricle mass (g)	Lung mass (g)	*Gastrocnemius* mass (g)	Heart/body weight ($g \cdot Kg^{-1}$)	Right ventricle/body weight ($g \cdot Kg^{-1}$)	Fulton index ($g \cdot g^{-1}$)
SED + Cont	0.34 ± 0.01	0.87 ± 0.05	0.18 ± 0.02	1.48 ± 0.30	2.13 ± 0.16	2.54 ± 0.12	0.52 ± 0.05	0.29 ± 0.04
SED + MCT	0.28 ± 0.03***	0.99 ± 0.09**	0.29 ± 0.05***	2.22 ± 0.15***	1.80 ± 0.13***	3.63 ± 0.57***	1.08 ± 0.27***	0.53 ± 0.09***
Ex + Cont	0.35 ± 0.03†††	0.95 ± 0.11	0.19 ± 0.03†††	1.51 ± 0.17†††	2.14 ± 0.29††	2.68 ± 0.17†††	0.53 ± 0.07†††	0.28 ± 0.04†††
Ex + MCT	0.34 ± 0.03†††	1.02 ± 0.08**	0.29 ± 0.02***###	2.21 ± 0.21***###	2.21 ± 0.16†††	3.00 ± 0.21*†††	0.85 ± 0.09***††###	0.45 ± 0.04***†###

Values are expressed as mean ± standard deviation (* $p < 0.05$ vs. SED + Cont, † $p < 0.05$ vs. SED + MCT, ** $p < 0.01$ vs. SED + Cont, †† $p < 0.01$ vs. SED + MCT, *** $p < 0.001$ vs. SED + Cont, ††† $p < 0.001$ vs. SED + MCT, ### $p < 0.001$ vs. Ex + Cont).

Table 2
Effect of exercise preconditioning and MCT-induced heart failure on right ventricle hemodynamics.

Experimental group	HR (bpm)	Pmax (mm Hg)	EDP (mm Hg)	dP/dtmax (mm Hg/s)	dP/dtmin (mm Hg/s)	τ (ms)
SED + Cont	413.2 ± 20.1	24.3 ± 1.8	3.6 ± 1.1	1852.1 ± 182.3	−1397.0 ± 175.6	10.7 ± 1.9
SED + MCT	337.8 ± 55.8***	42.9 ± 9.6***	5.9 ± 1.7***	2091.2 ± 583.1	−1853.8 ± 575.4	16.7 ± 3.3***
Ex + Cont	372.4 ± 24.7	27.9 ± 3.4†††	2.9 ± 0.7†††	2100.2 ± 358.1	−1587.6 ± 318.9	10.0 ± 3.4†††
Ex + MCT	370.3 ± 33.6*	37.1 ± 7.0$^{***,\#\#}$	3.2 ± 0.5†††	2062.1 ± 410.9	−2236.3 ± 564.1$^{***,\#\#}$	9.9 ± 2.3†††

Values are expressed as mean ± standard deviation ($^{*}p < 0.05$ vs. SED + Cont, ## $p < 0.01$ vs. Ex + Cont, *** $p < 0.001$ vs. SED + Cont, ††† $p < 0.001$ vs. SED + MCT).

3.4. MHC isoform profiling of right ventricle

Fig. 2 shows myosin heavy chain (MHC) isoforms' profile of RV muscle from the studied groups. Two isoforms were observed in the gel, with predominance of alpha-MHC. A significant increase in total MHC isoforms (alpha + beta isoforms) and in beta/alpha MHC ratio was observed in SED + MCT group ($p < 0.05$ and $p < 0.01$ vs. SED + Cont group, respectively). These alterations were prevented by exercise preconditioning in Ex + MCT (Fig. 2A to C).

3.5. Analysis of the protein synthesis vs. proteolysis balance in right ventricle

To determine the molecular mechanisms underlying the effect of MCT administration and/or exercise preconditioning in cardiac muscle remodeling, we evaluated the contribution of the signaling pathways activated by wasting and pro-inflammatory cytokines. Myostatin is a member of the transforming growth factor-β superfamily found predominantly in skeletal, but also in heart muscle, that has been suggested to act as negative regulator of muscle growth [22]. In our study, no differences were observed in myostatin expression levels in the RV, as well as on myostatin downstream effectors, *p*-Smad3 and p38 MAPK, involved in the canonical and non-canonical pathways, respectively (Fig. 3). So, our results suggest that myostatin pathway is not involved in RV remodeling in MCT-induced PAH.

Inflammatory cytokines from TNF superfamily have been implicated in processes of cardiac hypertrophy and fibrosis [23]. We found significantly higher levels of the pro-inflammatory cytokine TNF-α in SED + MCT group compared to SED + Cont ($p < 0.01$). Trained groups showed decreased levels of TWEAK expression, more expressive in MCT-treated animals ($p < 0.05$ Ex + MCT vs. SED + MCT group) (Fig. 4B). Once TNF signaling involves NF-κB activation, we explored the RV expression of NF-κB subunits. MCT-induced PAH promoted an increase in the expression of p100/p52 and Rel-B subunits ($p < 0.001$ and $p < 0.01$ vs. SED + Cont, respectively; Fig. 4F and G), which are known mediators of the non-canonical NF-κB pathway. Exercise preconditioning attenuated the overexpression of these mediators of the NF-κB signaling, though not significantly, and promoted a significant increase of the p105/p50 and p65 mediators from the canonical NF-κB pathway (Fig. 4C and D). The overexpression of these NF-κB mediators

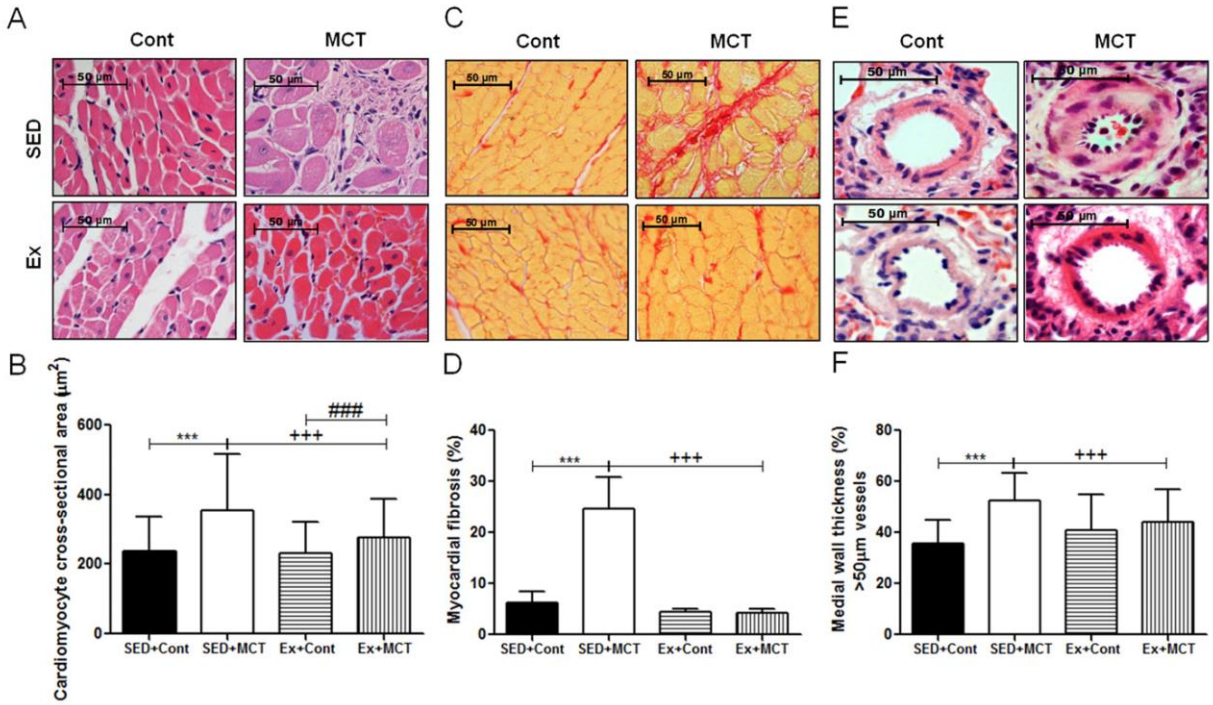

Fig. 1. Effect of exercise preconditioning and MCT-induced heart failure on cardiomyocyte cross-sectional area, myocardial fibrosis and medial wall thickness of pulmonary arteries. Histological appearance of cardiomyocytes stained with hematoxylin and eosin (A); right ventricular cardiomyocyte cross-sectional area (μm²) (B); histological appearance of cardiomyocytes stained with Picrosirius red (C); percentage of myocardial fibrosis (D); histological appearance of small pulmonary arteries stained with hematoxylin and eosin (E); pulmonary artery (>50 μm) medial layer thickness expressed as percentage of wall thickness (F). Values are expressed as mean ± standard deviation ($^{***}p < 0.001$ vs. SED + Cont, $^{+++}p < 0.001$ vs. SED + MCT, $^{###}p < 0.001$ vs. Ex + Cont).

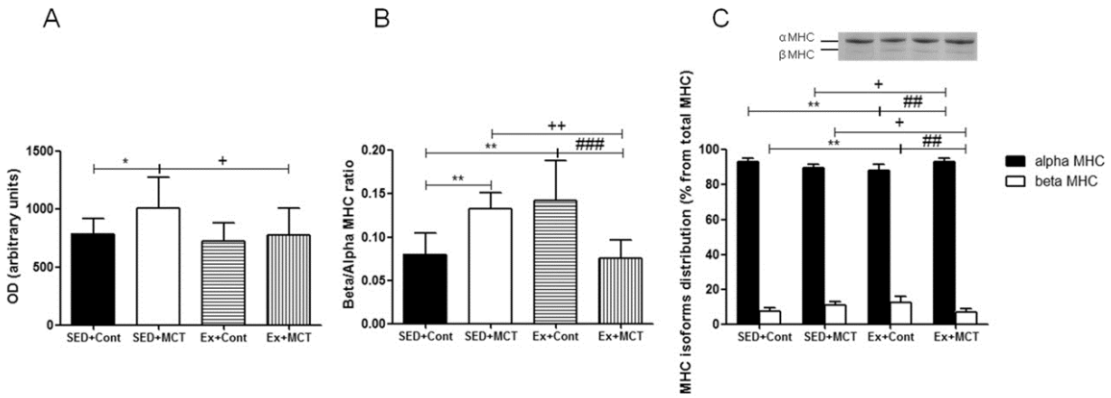

Fig. 2. Effect of exercise preconditioning and MCT-induced heart failure on total MHC (A), beta/alpha MHC ratio (B) and MHC isoform distribution (C) in the right ventricle. Values are expressed as mean ± standard deviation ($^{*}p < 0.05$ vs. SED + Cont, $^{+}p < 0.05$ vs. SED + MCT, $^{**}p < 0.01$ vs. SED + Cont, $^{++}p < 0.01$ vs. SED + MCT, $^{\#\#}p < 0.01$ vs. Ex + Cont, $^{\#\#\#}p < 0.001$ vs. Ex + Cont).

was more notorious in Ex + MCT group ($p < 0.05$ and $p < 0.01$ vs. SED + MCT). ERK1/2 is known to be a central kinase of cardiac hypertrophy signaling; however, no expression differences were noted among experimental groups (Fig. 4E), similarly to the previously reported effect of TNF-α [24].

The contribution of the ubiquitin/proteasome system to RV failure secondary to MCT-induced PAH was evaluated by western blotting analysis of TRAF6, MuRF1 and atrogin-1. TRAF6 expression was significantly increased in both MCT-treated groups ($p < 0.05$ vs. SED + Cont group), with no differences observed between SED + MCT and Ex + MCT groups (Fig. 5A). No alterations were seen among groups for MuRF1 expression (Fig. 5B). Data showed a statistically significant increase of the E3 ligase atrogin-1 in the RV of SED + MCT group ($p < 0.01$ vs. SED + Cont group). Exercise preconditioning prevented the MCT-related increase of atrogin-1 expression ($p < 0.05$ vs. SED + MCT group) (Fig. 5C). Once FoxO3/Akt axis contributes to the anti-hypertrophic signaling in the heart [25], the expression of Akt and FoxO3A was evaluated by western blotting. No expression differences were observed among groups (Fig. 5D and E).

The effect of MCT treatment and exercise preconditioning on RV proteolytic profile was evaluated by zymography with gelatine as substrate (Fig. 6). The densitometric analysis of the zymography profile displayed four common bands with the same profile in the RV of all groups (Fig. 6B and C). Zymo gels were incubated with the metalloproteinase inhibitor

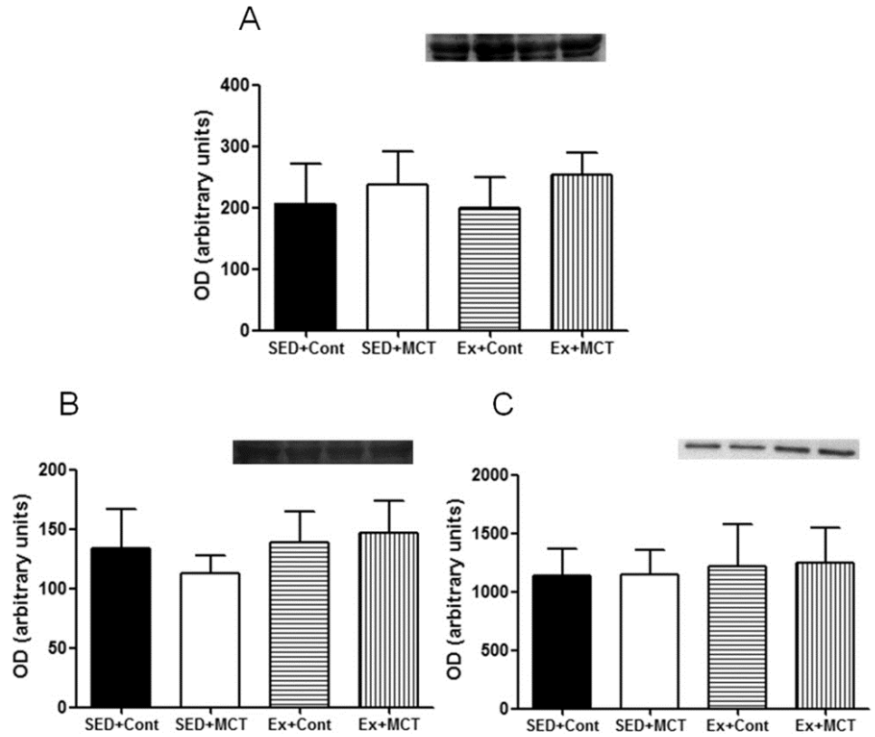

Fig. 3. Effect of exercise preconditioning and MCT treatment on myostatin (A), *p*-Smad3 (B) and p38 MAPK (C) expression in the right ventricle muscle. Representative western blots are shown above the correspondent graph. Values are expressed as mean ± standard deviation.

EDTA, at its maximum effective concentration, and the suppression of bands' activity suggests the involvement of metalloproteinase proteases (data not shown). Although no differences in the profile of zymo bands were detected among experimental groups, we observed an increased proteolytic activity of band 1 in SED + MCT group ($p < 0.05$ vs. SED + Cont group) and of band 4 in Ex + MCT group (Fig. 6A). Considering the molecular weight of the bands with gelatinolytic activity (according to Uniprot (http://www.uniprot.org/), the presence of MMP-2 (72 kDa) in gel band 4 and MMP-9 (92 kDa) in gel band 1 can be supposed.

4. Discussion

The present study demonstrates that exercise preconditioning provides protection against RV dysfunction and remodeling in MCT-induced PAH. Exercise preconditioning prevented muscle wasting, pulmonary artery remodeling, and cardiac dysfunction, hypertrophy and fibrosis. The improved cardiac phenotype promoted by exercise preconditioning was related with reduced beta/alpha-MHC ratio, and modulation of downstream mediators of pro-inflammatory cytokines signaling, more specifically TNF-α and TWEAK.

In order to study the cardioprotective phenotype induced by exercise preconditioning, we submitted exercised animals to experimental MCT-induced PAH. This model resembles several features of human PAH and is widely used to study RV dysfunction [26–30]. Exercise preconditioning was able to prevent RV diastolic dysfunction, which was the main alteration observed in the cardiac function of SED + MCT animals. HR was impaired in SED + MCT rats, being previously related with reduced responsiveness to sympathetic stimulation [31]. Ex + MCT animals also showed decreased HR but this was probably a training effect since no differences were noted in comparison to its corresponding control group. Part of this cardioprotective effect can be attributed to the prevention of RV overload, which is supported by the fact that Ex + MCT animals showed a reduction of RV Pmax and a significant reduction in the pulmonary artery remodeling. Exercise preconditioning partially prevented cardiac hypertrophy (at organ and cardiomyocyte level), as well as the fibrosis and beta-MHC isoform overexpression noticed in SED + MCT rats. Accumulation of fibrosis has a negative impact on cardiac function, affecting cardiac stiffness, promoting arrhythmias and impairing the diffusion of oxygen to cardiomyocytes [32]. The shift to the slower beta-MHC isoform observed in SED + MCT animals is associated with reduced myosin ATPase enzyme velocity, ultimately slowing the myocyte contraction rate [33,34]. Thus, reduced beta/alpha-MHC ratio and fibrosis promoted by exercise preconditioning might have also contributed to the improved cardiac function in MCT-treated animals.

Given the growing recognition of inflammation as a central player in RV dysfunction [5–8], we studied the contribution of TNF superfamily signaling, specifically TNF-α and TWEAK to RV remodeling. In animal models, TNF-α was shown to increase pulmonary vascular reactivity

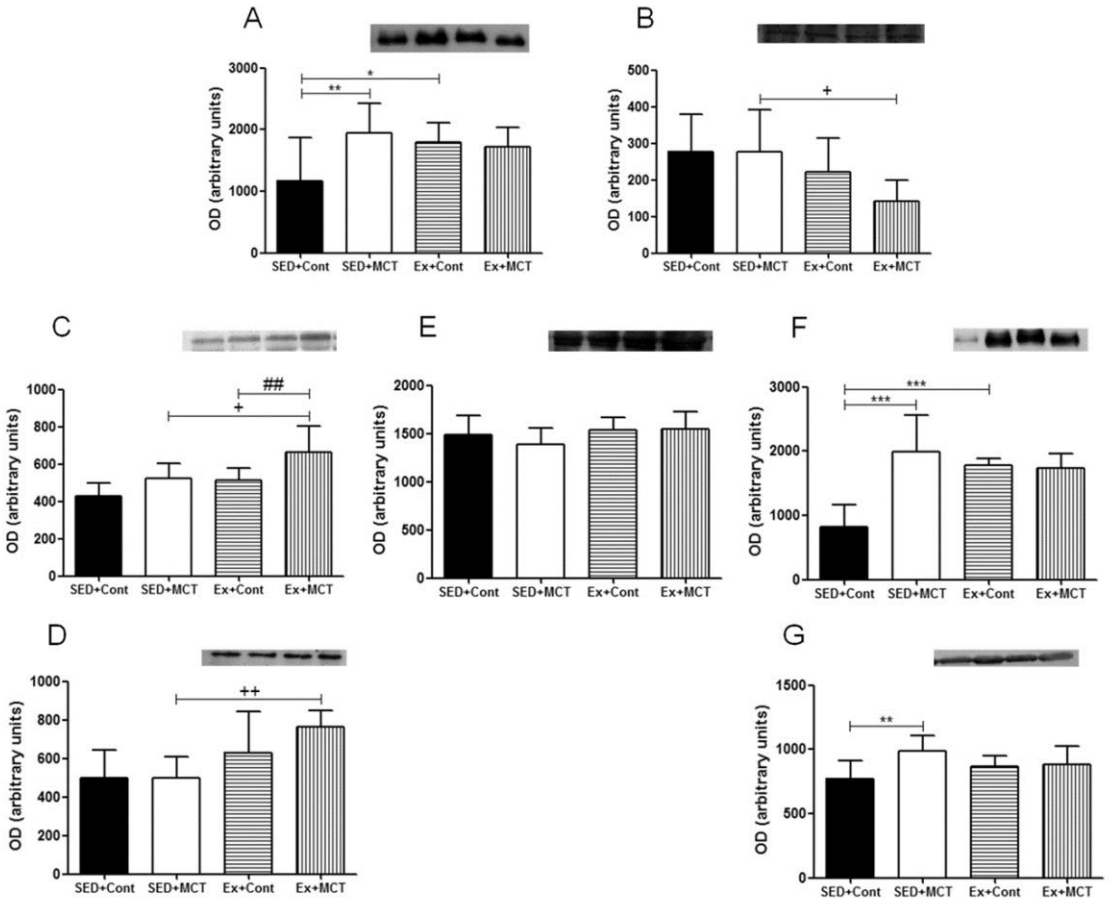

Fig. 4. Effect of exercise preconditioning and MCT treatment on TNF-α (A), TWEAK (B), NF-κB p105/p50 (C), NF-κB p65 (D), phospho-p44/p42 MAPK (Erk1/2) (E), NF-κB p100/p52 (F) and Rel-B (G) expression in the right ventricle muscle. Representative western blots are shown above the correspondent graph. Values are expressed as mean ± standard deviation ($^{*}p < 0.05$ vs. SED + Cont, $^{+}p < 0.05$ vs. SED + MCT, $^{**}p < 0.01$ vs. SED + Cont, $^{++}p < 0.01$ vs. SED + MCT, $^{\#\#}p < 0.01$ vs. Ex + Cont, $^{***}p < 0.001$ vs. SED + Cont).

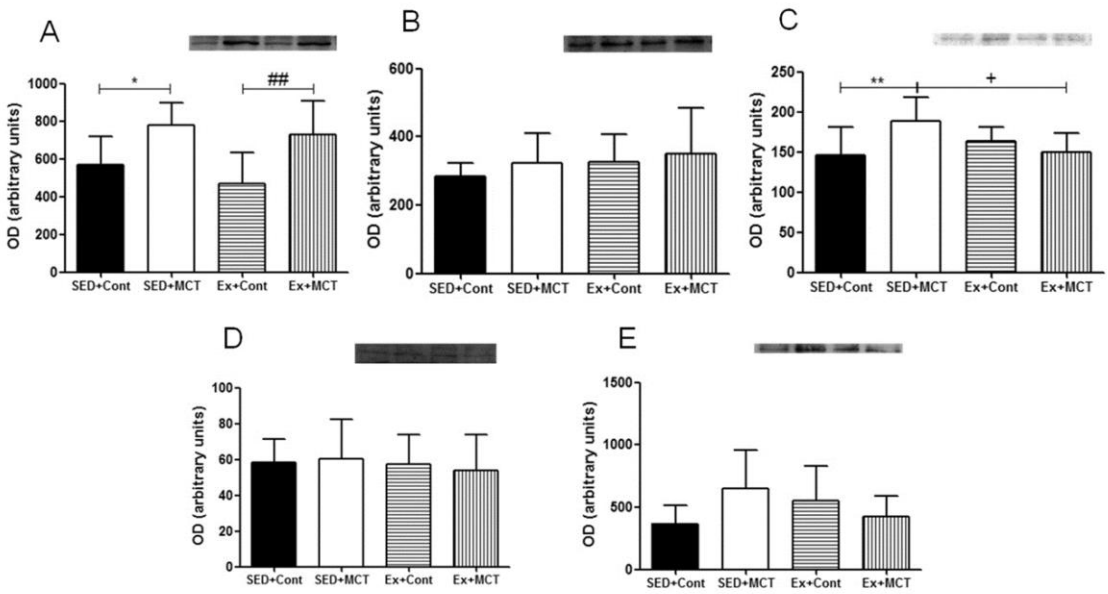

Fig. 5. Effect of exercise preconditioning and MCT treatment on TRAF6 (A), MuRF1 (B), atrogin-1 (C), *p*-Akt (D) and *p*-FoxO3A (E) expression in the right ventricle muscle. Representative western blots are shown above the correspondent graph. Values are expressed as mean ± standard deviation ($^{*}p < 0.05$ vs. SED + Cont, $^{+}p < 0.05$ vs. SED + MCT, $^{**}p < 0.01$ vs. SED + Cont, $^{\#\#}p < 0.01$ vs. Ex + Cont).

and to potentiate platelet-activating factor-induced pulmonary vasoconstriction [17]. TWEAK modulates multiple biological responses related with tissue damage and repair, such as proliferation, differentiation, inflammation, apoptosis and angiogenesis. The prognostic value of this cytokine in chronic heart failure and myocardial infarction was recently demonstrated [35], as well as its involvement in PAH pathogenesis [36]. Our data suggest that these pro-inflammatory cytokines differently contribute to the RV dysfunction secondary to MCT-induced PAH. An overexpression of TNF-α was observed in the RV of sedentary MCT-treated rats (Fig. 4A), corroborating previous reports [37]. TNF-α appears to operate via NF-κB non-canonical pathway, once the expression of the mediators NF-κB p100/p52 and Rel-B was significantly increased in the RV of SED + MCT rats (Fig. 4F and G). This is in accordance with previous observations that NF-κB signaling regulates cardiac hypertrophy, fibrosis and heart failure [38,39]. Despite no effect on the levels of TNF-α, exercise preconditioning promoted a significant decrease of TWEAK expression in MCT-treated rats (Fig. 4B). The down-regulation of TWEAK in Ex + MCT group was associated with the activation of the canonical NF-κB pathway, given by the overexpression of p105/p50 and p65 subunits. This shift from the non-canonical to the canonical NF-κB signaling seems to have cardioprotective effects. Indeed, activation of p65 subunit was previously related to myocyte survival and

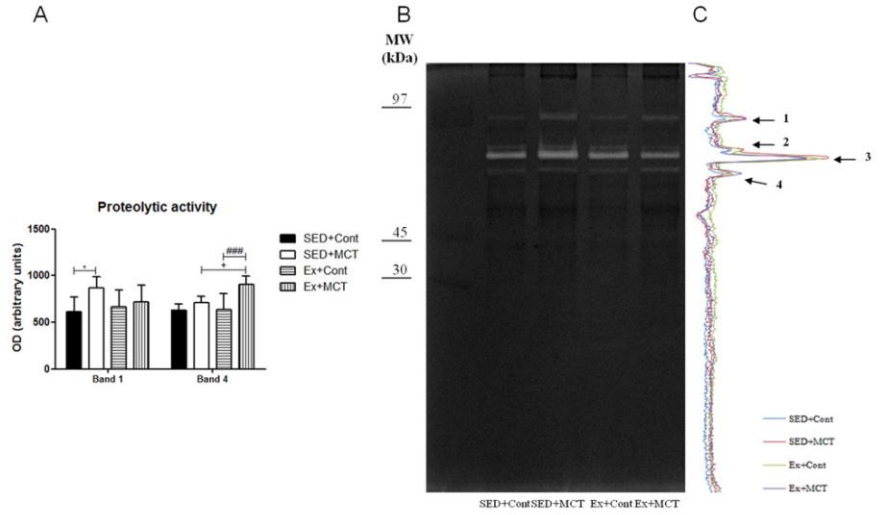

Fig. 6. Effect of exercise preconditioning and MCT treatment on right ventricle proteolytic activity. Representative image of the zymo gel evidencing four bands with proteolytic activity (B). An overlap of densitometric variation for SED + Cont, SED + MCT, Ex + Cont and Ex + MCT lanes is presented in the right side of zymo gel (C). Quantitative analysis of bands 1 and 4′ proteolytic activities for each group (A). Values are expressed as mean ± standard deviation ($^{*}p < 0.05$ vs. SED + Cont, $^{+}p < 0.05$ vs. SED + MCT, $^{\#\#\#}p < 0.001$ vs. Ex + Cont).

cardiac homeostasis while the p50 subunit seems to antagonize the development of cardiac hypertrophy and fibrosis [38]. Thus, exercise preconditioning seems to provide a cardioprotective effect related to a shift of the NF-κB signaling, through the down-regulation of TWEAK.

Alterations in the ubiquitin/proteasome system were reported to be fundamental for cardiac adaptation to pathologic stresses [40]. Indeed, the up-regulation of MuRF1, atrogin-1 and TRAF6 E3 ligases were shown to promote cardiac dysfunction [41,42]. In the present study, RV dysfunction secondary to MCT-induced PAH was paralleled by increased levels of the atrogin-1 and TRAF6 E3 ligases (Fig. 5). Exercise preconditioning prevented the MCT-related overexpression of atrogin-1 though with no effect on TRAF6 overexpression. Atrogin-1 inhibition was previously reported to prevent pressure overload-induced cardiac hypertrophy [40]. The transcription of atrogin-1 might be directly induced by FoxO3 via IGF-1/PI3K/Akt signaling axis [25]. Our data suggest that atrogin-1 expression was independent of this signaling pathway, once no differences in the expression levels of *p*-Akt and *p*-FoxO3 were noticed (Fig. 5).

TNF-induced cardiac remodeling and dysfunction was previously reported to depend on MMP activation [43], and TNF members might regulate MMP activity [23]. Moreover, Okada et al. [44] reported an increase of MMP-2 and MMP-9 expression and activity in the RV of rats treated with MCT, showing RV cardiomyocyte hypertrophy and fibrosis. In our study, MCT administration resulted in the activation of MMP-9, as previously reported in patients with PAH [45]. This gelatinase has been considered a marker of extracellular matrix breakdown, and most recently MMP-9 was suggested to play an important role in the inflammatory response and control of angiogenesis [45]. Exercise preconditioning prevented the MCT-related increase of MMP-9 activity but promoted an increase of MMP-2 activity (Fig. 6). Different expression patterns of MMP-2 and MMP-9 to angiogenic-related mechanical stimuli induced by exercise training was already reported, and seem to be explained by their involvement in dissimilar cellular processes [46]. In our work, the shift of MMP activity induced by exercise preconditioning might have contributed to the decreased accumulation of fibrosis noticed in RV from Ex + MCT (Fig. 1).

In summary, our findings suggest that MCT-induced PAH results in RV injury mediated by TNF-α pathway (via NF-κB non-canonical pathway) and the ubiquitin ligase atrogin-1. Exercise preconditioning seems to prevent PAH-related cardiac impairment through the modulation of TWEAK signaling, atrogin-1 expression and MMP activity in the RV. Of note, these improvements were observed 4 weeks after the cessation of exercise training, highlighting that the protective phenotype promoted by exercise training is maintained for several days. Exercise preconditioning could be of clinical importance in PAH, particularly as a preventive strategy in the management of the familial form of PAH, which is associated with a worsening of disease in subsequent generations that is manifested by greater severity or earlier onset.

Conflict of interest

The authors report no relationships that could be construed as a conflict of interest.

Acknowledgments

This work was supported by Fundação para a Ciência e a Tecnologia (FCT, Portugal), European Union, QREN, FEDER and COMPETE by funding the Organic Chemistry Research Unit (QOPNA) (project PEst-C/QUI/UI0062/2013), the Cardiovascular R&D Unit (project PEst-C/SAU/UI0051/2014), the Research Centre on Physical Activity Health and Leisure (CIAFEL) (UID/DTP/00617/2013) and the post-graduation students (grant numbers SFRH/BD/91067/2012 to R.N.F and SFRH/BPD/90010/2012 to D.M.G.).

References

[1] H.J. Bogaard, K. Abe, A. Vonk Noordegraaf, N.F. Voelkel, The right ventricle under pressure: cellular and molecular mechanisms of right-heart failure in pulmonary hypertension, Chest 135 (2009) 794–804.
[2] J.I. Drake, H.J. Bogaard, S. Mizuno, B. Clifton, B. Xie, Y. Gao, et al., Molecular signature of a right heart failure program in chronic severe pulmonary hypertension, Am J Respir Cell Mol Biol 45 (2011) 1239–1247.
[3] J. Gomez-Arroyo, S. Mizuno, K. Szczepanek, B. Van Tassell, R. Natarajan, C.G. dos Remedios, et al., Metabolic gene remodeling and mitochondrial dysfunction in failing right ventricular hypertrophy secondary to pulmonary arterial hypertension, Circ Heart Fail 6 (2013) 136–144.
[4] A. Vonk-Noordegraaf, F. Haddad, K.M. Chin, P.R. Forfia, S.M. Kawut, J. Lumens, et al., Right heart adaptation to pulmonary arterial hypertension: physiology and pathobiology, J Am Coll Cardiol 62 (2013) D22–D33.
[5] J.A. Watts, M.A. Gellar, M. Obraztsova, J.A. Kline, J. Zagorski, Role of inflammation in right ventricular damage and repair following experimental pulmonary embolism in rats, Int J Exp Pathol 89 (2008) 389–399.
[6] A. Belhaj, L. Dewachter, F. Kerbaul, S. Brimioulle, C. Dewachter, R. Naeije, et al., Heme oxygenase-1 and inflammation in experimental right ventricular failure on prolonged overcirculation-induced pulmonary hypertension, PLoS One 8 (2013) e69470.
[7] B. Rondelet, C. Dewachter, F. Kerbaul, X. Kang, P. Fesler, S. Brimioulle, et al., Prolonged overcirculation-induced pulmonary arterial hypertension as a cause of right ventricular failure, Eur Heart J 33 (2012) 1017–1026.
[8] J.A. Watts, J. Zagorski, M.A. Gellar, B.G. Stevinson, J.A. Kline, Cardiac inflammation contributes to right ventricular dysfunction following experimental pulmonary embolism in rats, J Mol Cell Cardiol 41 (2006) 296–307.
[9] M.E. Campian, M. Hardziyenka, K. de Bruin, B.L. van Eck-Smit, J.M. de Bakker, H.J. Verberne, et al., Early inflammatory response during the development of right ventricular heart failure in a rat model, Eur J Heart Fail 12 (2010) 653–658.
[10] J. Meloche, S. Renard, S. Provencher, S. Bonnet, Anti-inflammatory and immunosuppressive agents in PAH, Handb Exp Pharmacol 218 (2013) 437–476.
[11] M.C. Chaumais, B. Ranchoux, D. Montani, P. Dorfmuller, L. Tu, F. Lecerf, et al., N-acetylcysteine improves established monocrotaline-induced pulmonary hypertension in rats, Respir Res 15 (2014) 65.
[12] M. Rabinovitch, C. Guignabert, M. Humbert, M.R. Nicolls, Inflammation and immunity in the pathogenesis of pulmonary arterial hypertension, Circ Res 115 (2014) 165–175.
[13] A.S. Babu, R. Padmakumar, A.G. Maiya, A review of ongoing trials in exercise based rehabilitation for pulmonary arterial hypertension, Indian J Med Res 137 (2013) 900–906.
[14] D. Moreira-Goncalves, T. Henriques-Coelho, H. Fonseca, R.M. Ferreira, F. Amado, A. Leite-Moreira, et al., Moderate exercise training provides left ventricular tolerance to acute pressure overload, Am J Physiol Heart Circ Physiol 300 (2011) H1044–H1052.
[15] R. Ferreira, D. Moreira-Goncalves, A.L. Azevedo, J.A. Duarte, F. Amado, R. Vitorino, Unraveling the exercise-related proteome signature in heart, Basic Res Cardiol 110 (2015) 454.
[16] S.K. Powers, A.J. Smuder, A.N. Kavazis, J.C. Quindry, Mechanisms of exercise-induced cardioprotection, Physiology (Bethesda) 29 (2014) 27–38.
[17] Q. Wang, X.R. Zuo, Y.Y. Wang, W.P. Xie, H. Wang, M. Zhang, Monocrotaline-induced pulmonary arterial hypertension is attenuated by TNF-alpha antagonists via the suppression of TNF-alpha expression and NF-kappaB pathway in rats, Vascul Pharmacol 58 (2013) 71–77.
[18] I. Falcao-Pires, G. Palladini, N. Goncalves, J. van der Velden, D. Moreira-Goncalves, D. Miranda-Silva, et al., Distinct mechanisms for diastolic dysfunction in diabetes mellitus and chronic pressure-overload, Basic Res Cardiol 106 (2011) 801–814.
[19] R.J. Talmadge, R.R. Roy, Electrophoretic separation of rat skeletal muscle myosin heavy-chain isoforms, J Appl Physiol (1985) 75 (1993) 2337–2340.
[20] U.K. Laemmli, Cleavage of structural proteins during the assembly of the head of bacteriophage T4, Nature 227 (1970) 680–685.
[21] R. Vitorino, A. Barros, A. Caseiro, P. Domingues, J. Duarte, F. Amado, Towards defining the whole salivary peptidome, Proteomics Clin Appl 3 (2009) 528–540.
[22] P. Bonaldo, M. Sandri, Cellular and molecular mechanisms of muscle atrophy, Dis Model Mech 6 (2013) 25–39.
[23] T. Novoyatleva, A. Sajjad, F.B. Engel, TWEAK-Fn14 cytokine-receptor axis: a new player of myocardial remodeling and cardiac failure, Front Immunol 5 (2014) 50.
[24] C. Freund, R. Schmidt-Ullrich, A. Baurand, S. Dunger, W. Schneider, P. Loser, et al., Requirement of nuclear factor-kappaB in angiotensin II- and isoproterenol-induced cardiac hypertrophy in vivo, Circulation 111 (2005) 2319–2325.
[25] T.G. Schips, A. Wietelmann, K. Hohn, S. Schimanski, P. Walther, T. Braun, et al., FoxO3 induces reversible cardiac atrophy and autophagy in a transgenic mouse model, Cardiovasc Res 91 (2011) 587–597.
[26] T. Henriques-Coelho, J. Correia-Pinto, R. Roncon-Albuquerque Jr., M.J. Baptista, A.P. Lourenco, S.M. Oliveira, et al., Endogenous production of ghrelin and beneficial effects of its exogenous administration in monocrotaline-induced pulmonary hypertension, Am J Physiol Heart Circ Physiol 287 (2004) H2885–H2890.
[27] T. Henriques-Coelho, R. Roncon-Albuquerque Junior, A.P. Lourenco, M.J. Baptista, S.M. Oliveira, A. Brandao-Nogueira, et al., Ghrelin reverses molecular, structural and hemodynamic alterations of the right ventricle in pulmonary hypertension, Rev Port Cardiol 25 (2006) 55–63.
[28] I. Falcao-Pires, N. Goncalves, T. Henriques-Coelho, D. Moreira-Goncalves, R. Roncon-Albuquerque Jr., A.F. Leite-Moreira, Apelin decreases myocardial injury and improves right ventricular function in monocrotaline-induced pulmonary hypertension, Am J Physiol Heart Circ Physiol 296 (2009) H2007–H2014.
[29] J. Correia-Pinto, T. Henriques-Coelho, R. Roncon-Albuquerque Jr., A.P. Lourenco, G. Melo-Rocha, F. Vasques-Novoa, et al., Time course and mechanisms of left ventricular systolic and diastolic dysfunction in monocrotaline-induced pulmonary hypertension, Basic Res Cardiol 104 (2009) 535–545.

[30] T. Henriques-Coelho, S.M. Oliveira, R.S. Moura, R. Roncon-Albuquerque Jr., A.L. Neves, M. Santos, et al., Thymulin inhibits monocrotaline-induced pulmonary hypertension modulating interleukin-6 expression and suppressing p38 pathway, Endocrinology 149 (2008) 4367–4373.
[31] A.P. Lourenco, R. Roncon-Albuquerque Jr., C. Bras-Silva, B. Faria, J. Wieland, T. Henriques-Coelho, et al., Myocardial dysfunction and neurohumoral activation without remodeling in left ventricle of monocrotaline-induced pulmonary hypertensive rats, Am J Physiol Heart Circ Physiol 291 (2006) H1587–H1594.
[32] P.A. Harvey, L.A. Leinwand, The cell biology of disease: cellular mechanisms of cardiomyopathy, J Cell Biol 194 (2011) 355–365.
[33] S.P. Barry, S.M. Davidson, P.A. Townsend, Molecular regulation of cardiac hypertrophy, Int J Biochem Cell Biol 40 (2008) 2023–2039.
[34] P. Balakumar, G. Jagadeesh, Multifarious molecular signaling cascades of cardiac hypertrophy: can the muddy waters be cleared? Pharmacol Res 62 (2010) 365–383.
[35] M. Jasiewicz, K. Kowal, O. Kowal-Bielecka, M. Knapp, R. Skiepko, A. Bodzenta-Lukaszyk, et al., Serum levels of CD163 and TWEAK in patients with pulmonary arterial hypertension, Cytokine 66 (2014) 40–45.
[36] A. Filusch, T. Zelniker, C. Baumgartner, S. Eschricht, N. Frey, H.A. Katus, et al., Soluble TWEAK predicts hemodynamic impairment and functional capacity in patients with pulmonary arterial hypertension, Clin Res Cardiol 100 (2011) 879–885.
[37] A. Rohini, N. Agrawal, C.N. Koyani, R. Singh, Molecular targets and regulators of cardiac hypertrophy, Pharmacol Res 61 (2010) 269–280.
[38] S. Gaspar-Pereira, N. Fullard, P.A. Townsend, P.S. Banks, E.L. Ellis, C. Fox, et al., The NF-kappaB subunit c-Rel stimulates cardiac hypertrophy and fibrosis, Am J Pathol 180 (2012) 929–939.
[39] K. Van der Heiden, S. Cuhlmann, A. Luong le, M. Zakkar, P.C. Evans, Role of nuclear factor kappaB in cardiovascular health and disease, Clin Sci (Lond) 118 (2010) 593–605.
[40] T. Zaglia, G. Milan, A. Ruhs, M. Franzoso, E. Bertaggia, N. Pianca, et al., Atrogin-1 deficiency promotes cardiomyopathy and premature death via impaired autophagy, J Clin Invest 124 (2014) 2410–2424.
[41] D. Zhang, X. Liu, X. Chen, J. Gu, F. Li, W. Zhang, et al., Role of the MAPKs/TGF-beta1/TRAF6 signaling pathway in atrial fibrosis of patients with chronic atrial fibrillation and rheumatic mitral valve disease, Cardiology 129 (2014) 216–223.
[42] V. Adams, A. Linke, U. Wisloff, C. Doring, S. Erbs, N. Krankel, et al., Myocardial expression of Murf-1 and MAFbx after induction of chronic heart failure: effect on myocardial contractility, Cardiovasc Res 73 (2007) 120–129.
[43] Y.Y. Li, T. Kadokami, P. Wang, C.F. McTiernan, A.M. Feldman, MMP inhibition modulates TNF-alpha transgenic mouse phenotype early in the development of heart failure, Am J Physiol Heart Circ Physiol 282 (2002) H983–H989.
[44] M. Okada, R. Kikuzuki, T. Harada, Y. Hori, H. Yamawaki, Y. Hara, Captopril attenuates matrix metalloproteinase-2 and -9 in monocrotaline-induced right ventricular hypertrophy in rats, J Pharmacol Sci 108 (2008) 487–494.
[45] Z. Safdar, E. Tamez, W. Chan, B. Arya, Y. Ge, A. Deswal, et al., Circulating collagen biomarkers as indicators of disease severity in pulmonary arterial hypertension, JACC Heart Fail 2 (2014) 412–421.
[46] M. Bellafiore, G. Battaglia, A. Bianco, F. Farina, A. Palma, A. Paoli, The involvement of MMP-2 and MMP-9 in heart exercise-related angiogenesis, J Transl Med 11 (2013) 283.

STUDY III – HMGB1 DOWN-REGULATION MEDIATES TERAMEPROCOL VASCULAR ANTI-PROLIFERATIVE EFFECT IN EXPERIMENTAL PULMONARY HYPERTENSION

HMGB1 down-regulation mediates terameprocol vascular anti-proliferative effect in experimental pulmonary hypertension

Rita Nogueira-Ferreira[1,2†], Manuel J. Ferreira-Pinto[2†], Ana Filipa Silva[2], Rui Vitorino[2,3], Joana Justino[1], Raquel Costa[4], Daniel Moreira-Gonçalves[2,5], Jean-François Quignard[6], Thomas Ducret[6], Jean-Pierre Savineau[6], Adelino F. Leite-Moreira[2], Rita Ferreira[1], Tiago Henriques-Coelho[2*]

†Both authors contributed equally to this work

[1]QOPNA, Departamento de Química, Universidade de Aveiro, Campus Universitário de Santiago, 3810-193 Aveiro, Portugal

[2]Departamento de Cirurgia e Fisiologia, Faculdade de Medicina, Universidade do Porto, Alameda Professor Hernâni Monteiro, 4200-319 Porto, Portugal

[3]iBiMED, Departamento de Ciências Médicas, Universidade de Aveiro, Campus Universitário de Santiago, 3810-193 Aveiro, Portugal

[4]Departamento de Bioquímica, Faculdade de Medicina, Universidade do Porto, Alameda Professor Hernâni Monteiro, 4200-319 Porto, Portugal

[5]CIAFEL, Faculdade de Desporto, Universidade do Porto, R. Dr. Plácido da Costa 91, 4200-450 Porto, Portugal

[6]Université Bordeaux Segalen, Bordeaux, France; Inserm, U1045, Centre de Recherche Cardio-Thoracique, Bordeaux, France

***Corresponding author (✉):**

Tiago Henriques-Coelho

Departamento de Cirurgia e Fisiologia

Faculdade de Medicina, Universidade do Porto

Alameda Professor Hernâni Monteiro

4200-319 Porto

Portugal

e-mail: henriques.coelho@gmail.com

Running head: Terameprocol improves experimental PH

Abstract

Pulmonary arterial hypertension (PAH) is a progressive disease with a poor prognosis. Pulmonary artery smooth muscle cells (PASMCs) play a crucial role in PAH pathophysiology, displaying a hyperproliferative and apoptotic-resistant phenotype. In the present study, we evaluated the potential therapeutic role of terameprocol (TMP), an inhibitor of cellular proliferation and promoter of apoptosis, in a well-established pre-clinical model of PAH induced by monocrotaline (MCT) and studied the biological pathways modulated by TMP in PASMCs. Wistar rats injected with MCT or saline (SHAM group) were treated with TMP or vehicle. On day 21 after injection, we assessed bi-ventricular hemodynamics and cardiac and pulmonary morphometry. The effects of TMP on PASMCs were studied in a primary culture isolated from SHAM and MCT-treated rats, using an iTRAQ-based proteomic approach to investigate the molecular pathways modulated by this drug. *In vivo*, TMP significantly reduced pulmonary and cardiac remodeling and improved cardiac function in PAH. *In vitro*, TMP inhibited proliferation and induced apoptosis of PASMCs. A total of 65 proteins were differentially expressed in PASMCs from MCT rats treated with TMP, some of which involved in the modulation of transforming growth factor beta pathway and DNA transcription. Anti-proliferative effect of TMP seems to be explained, at least in part, by the down-regulation of the transcription factor HMGB1. Our findings support the beneficial role of TMP in PAH and suggest that it may be an effective therapeutic option to be considered in the clinical management of PAH.

Keywords: monocrotaline, pulmonary arterial hypertension, terameprocol, vascular remodeling

Introduction

Vascular remodeling is a central process in the pulmonary arterial hypertension (PAH) pathobiology. This process is associated with structural and functional alterations in the pulmonary artery wall, leading to muscularization of previously nonmuscular arteries, neointima formation, plexiform lesions development, which result in pulmonary artery obliteration. Hypertrophy, proliferation, migration and resistance to apoptosis are features of medial smooth muscle cells associated to the development of these changes [1-3]. Despite the increasing knowledge of PAH pathophysiology, this disease is characterized by a late diagnosis and a high mortality rate [4], justifying the urgent need for new and effective therapeutic strategies. Currently approved drugs do not revert nor halt the progression of the disease, have variable efficiency and frequent systemic side effects. Despite some of them exert slight anti-proliferative effects, their main mechanism of action is through the re-establishment of the balance between vasoconstrictors and vasodilators [5, 6]. Since proliferative vascular remodeling is a main feature in PAH, there is a growing interest in targeting proliferative and apoptotic pathways [6-8]. These features are shared by cancer cells [9, 10], therefore supporting the potential utility of anticancer agents with anti-proliferative and/or pro-apoptotic proprieties in the management of PAH [8].

Terameprocol (meso-tetra-O-methyl nordihydroguaiaretic acid, TMP) is reported to block cell cycle progression and promote apoptosis by inhibiting the transcription of genes that are dependent on the transcription factor Sp1, such as Cdc2 and survivin [11]. Previous studies demonstrated that TMP exhibits *in vitro* and *in vivo* anti-tumoral activity without relevant systemic toxicity [12-16]. Clinical trials are currently being conducted to assess the potential of TMP in several cancer types [17-19]. Given its described properties, we hypothesized that TMP might also be of value in the management of PAH. So, the present work explores the effects of TMP in an experimental model of PAH. We studied the *in vivo* effects of TMP in the monocrotaline (MCT) model and characterized the biological processes modulated by this drug in primary cultures of pulmonary artery smooth muscle cells (PASMCs).

Materials and Methods

Experimental Design

Housing and experimental treatment were in accordance with the *Guide for the Care and Use of Laboratory Animals* from the Institute for Laboratory Animal Research (ILAR, NIH Pub. No. 85-23, Revised 2011) and with the European Parliament Directive 2010/63/EU. Adult male Wistar rats (Charles River Laboratories; Barcelona, Spain) weighting 180–200 g were housed in a controlled environment under a 12:12 h light-dark cycle at room temperature of 22 ºC, with a free supply of food and water. Rats randomly received a subcutaneous injection of MCT (60 mg/kg body weight, Sigma-Aldrich) (MCT groups) or an equal volume of saline solution (2 mL/kg body weight) (SHAM groups). In the first protocol, we treated MCT and SHAM animals with TMP (166 mg/kg body weight, ip, Cayman Chemical) or an equal volume of vehicle (DMSO, Sigma-Aldrich) on days 7, 12 and 17 after MCT/saline injection, thus creating four groups: SHAM+Vehicle, SHAM+TMP, MCT+Vehicle, MCT+TMP (n=9-14 rats *per* group). At day 21 after MCT/saline injection, invasive hemodynamic evaluation was performed. In a second protocol, rats injected with MCT or saline solution (n=5 rats *per* group) were sacrificed on day 21 in order to isolate and establish a primary culture of PASMCs for *in vitro* evaluation of TMP effects.

Hemodynamic evaluation

Animals were anesthetized by inhalation of a mixture of sevoflurane (8 % for induction and 2.5-3 % for maintenance) and oxygen, endotracheally intubated for mechanical ventilation (150 min^{-1}, 100 % O_2, 14–16 cm H_2O inspiratory pressure, with tidal volume adjusted to animal weight, and 5 cm H_2O end-expiratory pressure; TOPO Small Animal Ventilator - Kent Scientific, Dual Mode) and placed over a heating pad. Under binocular surgical microscopy (Leica, Wild 384000), the right jugular vein was cannulated for fluid administration (prewarmed 0.9 % NaCl solution, 32 mL/kg/h) to compensate for perioperative losses. The heart was exposed through a median sternotomy. Conductance catheters were placed in the right ventricle (RV) and left ventricle (LV) (PVR-1045 and PVR-1035, respectively, Millar Instruments). After complete instrumentation, the animal preparation was allowed to stabilize for 15 min. Hemodynamic recordings were made with respiration suspended at end-expiration under basal conditions. Data was continuously

acquired (MPVS 300, Millar Instruments), digitally recorded at 1000 Hz (ML880 PowerLab 16/30, Millar TM Instruments), and analyzed (LabChart, ADInstruments, RRID:SCR_001620).

Morphometric and histological analysis

After complete hemodynamic assessment, animals were euthanized by exsanguination under anesthesia. The heart, lungs and *gastrocnemius* muscle were excised and weighted. The right tibia was also excised and its length was measured with a millimetric ruler. The RV free wall was dissected from the LV + septum (S), under binocular magnification (3.5x) and weighted separately. Heart, lungs, RV, and LV + S weights were normalized to body weight (BW) and *gastrocnemius* weight was normalized to tibial length. RV weight was also normalized to that of LV+S. For histological analysis, RV and lung samples were immersion fixed in 4 % paraformaldehyde and embedded in paraffin. Sections 4 μm thick were cut and stained with hematoxylin and eosin. RV free wall specimens were obtained from each heart at midway between the apex and base. Studied samples were observed at microscope, photographed with a digital camera and measured with a digital image analyzer (cell^B life science basic imaging software, Olympus). All the measurements were made directly at 400x magnification and only round to ovoid nucleated myocytes were considered for analysis. RV samples were divided into five sections and the area of fifty cardiomyocytes *per* sample was measured and averaged. On the pulmonary specimens, external diameter and medial wall thickness in small muscular arteries (diameter < 50 μm, 12-18 arteries/lung) were analyzed at 400x magnification. Orthogonal intercepts were used to generate eight random measurements of external diameter (distance between the external lamina) and sixteen random measurements of medial thickness (distance between the internal and external lamina). For each artery, medial hypertrophy was expressed as follows: %wall thickness = [(medial thickness x 2)/(external diameter)] x 100.

Isolation and primary culture of PASMCs

A primary culture of PASMCs was established using an enzymatic dissociation process adapted from a previously described protocol [20]. Animals were euthanized with an intraperitoneal injection of pentobarbital (120 mg/kg body weight). The left upper lung

lobe was removed and placed in a calcium enriched Hank's Buffered Salt Solution (HBSS, Invitrogen) (5.4 mM KCl, 137 mM NaCl, 0.44 mM KH_2PO_4, 4.2 mM $NaHCO_3$, 0.25 mM NaH_2PO_4, 1 mM D-glucose, 0.2 mM phenol red, 2 mM $CaCl_2$ and 1 mM $MgCl_2$). First order intrapulmonary artery was dissected free of connective tissue under a stereomicroscope (Leica EZ4). After extraction from the lung, the adventitia was removed, the vessel was opened longitudinally and endothelium was removed by gently rubbing the inner surface with forceps tips. In order to release smooth muscle cells, the artery, mainly consisting of medial layer, was submitted to an enzymatic dissociation process with papain (Sigma-Aldrich) and collagenase type 1 (Worthington Biochemical Corp.), in a calcium-poor HBSS solution (25 μM $CaCl_2$ and 1 mg/mL BSA). Next, a mechanical dissociation process was performed with a fire polished, silicone coated glass pipette, in order to release the cells. The cell-free tissue was removed and the solution was centrifuged (250 g, 5 min, room temperature) in order to pellet the cells. Finally, cells were seeded in DMEM culture medium (PAN Biotech), supplemented with 1 % penicillin-streptomycin-amphotericin B (Invitrogen), 1 % sodium pyruvate (Sigma-Aldrich) and 1 % nonessential aminoacids (Sigma-Aldrich) containing 10 % FBS (fetal bovine serum, Sigma-Aldrich), in a 24-well culture plate (500 μL/well) and placed in an incubator (37 ºC, 5 % CO_2). The medium was changed after 24 h and then every 48 h. Cell passage was performed when approximately 80 % confluence was achieved and they were then detached with trypsin (PAN Biotech), passaged and cultured continuously. Cells between passages 2 and 4 were used for all experiments. Smooth muscle origin was confirmed by typical morphology (fusiform shape with hills and valleys) and detection of smooth muscle α-actin expression by immunocytochemistry (data not shown).

Cell proliferation assay

The effect of TMP in cell proliferation was evaluated using the 5'-bromodeoxyuridine (BrdU) immunoassay (Roche Diagnostics). BrdU is a thymidine analogue and its incorporation in the DNA is a measure of cell proliferation. For BrdU assay, cells were seeded in 24-well plates at a density of $1.5x10^4$ cells⁄mL. After 72 h, medium was removed and cells were incubated with different concentrations of TMP prepared in DMSO (0 μM, 0.1 μM, 1 μM, 10 μM and 20 μM) for 24 h in medium without FBS. The BrdU assay was conducted following the 24 h incubation with TMP/vehicle. All protocol was followed

according to manufacturer's instructions. Each condition (concentration) was tested in triplicate and in cells from three animals *per* group.

Apoptosis assay

For apoptosis evaluation, we performed the TUNEL (TdT-mediated dUTP Nick End Labelling) assay using the In Situ Cell Death Detection kit (Roche Diagnostics), according to the manufacturer's instructions. For TUNEL assay, cells were seeded in 24-well plates, with glass coverslips, at a density of $1.5x10^4$ cells/mL. After 72 h, medium was removed and cells were incubated with different concentrations of TMP prepared in DMSO (0 μM, 0.1 μM, 1 μM, 10 μM and 20 μM) for 24 h in medium without FBS. After 24 h incubation with TMP/vehicle, cells were stained with TUNEL and DAPI (4',6-diamidino-2-phenylindole, Roche Diagnostics). The percentage of apoptotic cells was calculated by dividing the number of cells stained with TUNEL (apoptotic cells) by the total number of nuclei stained with DAPI, in at least 10 different fields at 200x magnification. Each condition (concentration) was tested in triplicate and in cells from three animals *per* group.

Preparation of protein extracts and peptide labelling with iTRAQ

For iTRAQ (Isobaric tags for relative and absolute quantification) analysis, cells were seeded in 6-well plates at a concentration of $1.5x10^4$ cells/mL. Medium was changed after 24 h and after 48 h cells were incubated for 24 h in medium without FBS, containing TMP 10 μM or DMSO (CONT). This TMP concentration was chosen based on data from proliferative and apoptotic assays. Indeed, at this concentration, the proliferation of PASMCs was significantly inhibited whereas signs of apoptosis were not evident. So, a sufficient number of cells was obtained for proteomics at an effective anti-proliferative concentration of TMP. The medium was removed from the culture plates and after a wash in ice cold 1x PBS, cells were lysed in 1x RIPA buffer (50 mM Tris-HCl, pH 7.4, 150 mM NaCl, 0.25 % sodium deoxycholate, 1 % NP-40, 1 mM EDTA) supplemented with Phosphatase Inhibitor Cocktail (Sigma-Aldrich) and protease inhibitor (200 mM PMSF) and detached from the plates using cell scrapers. Samples were vortexed (5 min), sonicated and then centrifuged (12000 g, 5 min, 4 ºC). The supernatant was collected and the protein content of the cell homogenate was assayed with the RC-DC method (Bio-Rad), following the instructions of the manufacturer, using bovine serum albumin (BSA) as standard.

Two independent assays were performed, one for SHAM cells and other for MCT cells, using three animals *per* group. An in-solution digestion was performed for iTRAQ labelling, as previously described [21]. Briefly, 100 µg of protein was precipitated with 9 volumes of cold acetone at -20 ºC for 3 h. After samples centrifugation (20000 g, 30 min, 4 ºC) and acetone removal, pellets were resuspended with 0.1 M TEAB (triethylammonium bicarbonate buffer, Sigma-Aldrich), pH 8.5 and 2 % SDS to achieve a final concentration of 0.05 %. Samples were then reduced with 50 mM TCEP (tris(2-carboxyethyl)phosphine, Sigma-Aldrich) for 1 h at 60 ºC with agitation. Then, samples were alkylated with 10 mM MMTS (S-methyl methanethiosulfonate, Sigma-Aldrich) for 10 min at room temperature with agitation. Trypsin was added to each sample and the digestion was performed for 18 h at 37 ºC. Digested sample peptides were subsequently labelled with the iTRAQ® reagent 8-plex (ABSciex) following the protocol provided by the manufacturer. Briefly, labels were reconstituted in 60 % isopropanol, added to each sample peptides and incubated for 2 h at room temperature with agitation. Labelled samples were then combined and dried in a SpeedVac. Then, labelled peptides were separated by a multidimensional LC approach, as described by Carvalhais *et al.* [21]. Sample loading was performed at 200 µL/min with buffers (A) 2 % ammonium hydroxide and 0.014 % formic acid in water, pH 10 and (B) 2 % ammonium hydroxide and 90 % ACN (acetonitrile) in water, pH 10. After 5 min of sample loading and washing, peptide fractionation was performed with linear gradient to 70 % B over 85 min. Sixty fractions were collected, dried in a SpeedVac and resuspended in 5 % ACN and 0.1 % TFA (trifluoroacetic acid). Collected fractions were then separated by LC. Briefly, peptides loaded onto a C18 pre-column (5-mm particle size, 5 mm; Dionex) connected to an RP column PepMap100 C18 (150 mm x 75-mm i.d., 3-mm particle size). The flow rate was set at 300 nL/min. The mobile phases A and B were 2 % ACN and 0.05 % TFA in water, and 90 % ACN with 0.045 % TFA in water, respectively. The gradient started at 10 min and ramped to 60 % B till 50 min and 100 % B at 55 min and retained at 100 % B till 65 min. The separation was monitored at 214 nm using a UV detector (Dionex/LC Packings). Using the micro-collector Probot (Dionex/LC Packings) and, after a lag time of 5 min, peptides eluting from the capillary column were mixed with a continuous flow of α-CHCA matrix solution (in internal standard Glu-Fib) and were directly deposited onto the LC-MALDI plates. The spectra were generated and processed with 4800 MALDI-TOF/TOF. Protein identification based on MS/MS data were

performed with ProteinPilot™ software (v.4.04, ABSciex) using Paragon search method. SwissProt from *Rattus norvegicus* (release date October 21, 2014) was used as protein database. Default search parameters used were as follows: trypsin as the digestion enzyme with 2 missed cleavages, 40-ppm tolerance, carbamidomethyl modification on cysteine residue, iTRAQ 8-plex modification of N-terminal and lysine peptide residues as fixed modification. Additionally, biological modifications with emphasis on methionine oxidation, deamidation and iTRAQ 8-plex modification of tyrosine residue and deamidation were considered variable modifications. Bias correction was applied, and proteins were identified with an unused ProtScore>1.3 with at least one peptide at a confidence level of 95 %. Proteins identified with one peptide were manually validated when MS/MS spectra presented at least 5 successive amino acids covered by *b* or *y* fragmentations. Only proteins identified with a minimum of 2 peptides at a confidence level of 95 % were included in the quantification. The quantification results were reviewed manually for all proteins found to be differentially expressed ($p<0.05$).

Immunohistochemical analysis

Cubic pieces from lung tissue were fixed [4 % (v/v) buffered paraformaldehyde] by diffusion during 24 h and subsequently dehydrated with graded ethanol and included in paraffin blocks. Serial sections (5 μm of thickness) of paraffin blocks were cut by a microtome and mounted on silane-coated slides. The slides were dewaxed in xylene and hydrated through graded alcohols finishing in PBS solution. Deparaffinized sections of lung tissue were stained for immunohistochemical staining of rabbit anti-HMGB1 (1:400 dilution; Abcam, Cat# ab79823, RRID:AB_1603373), using the secondary antibody goat biotinylated anti-rabbit (1:200 dilution; Vector Laboratories, Cat# BA-1000, RRID:AB_2313606) and counterstained with hematoxylin-eosin, as previously described [22].

Western blotting analysis

Equivalent amounts of PASMC protein from each experimental group were electrophoresed on a 15 % SDS-PAGE as described by Laemmli [23]. Gels were blotted onto nitrocellulose membranes (Whatman®, Protan®) in transfer buffer (25 mM Tris, 192 mM glycine, pH 8.3 and 20 % methanol) for 2 h (200 mA). Then, nonspecific binding was

blocked with 5 % (w/v) nonfat dry milk in TBS-T (100 mM Tris, 1.5 mM NaCl, pH 8.0 and 0.5 % Tween 20). Membranes were incubated with primary antibody solution diluted 1:10000 in 5 % (w/v) nonfat dry milk in TBS-T (rabbit anti-HMGB1, ab79823, Abcam). After 2 h incubation at room temperature with agitation, membranes were washed with TBS-T and incubated, with agitation, with anti-rabbit IgG peroxidase secondary antibody (Amersham, GE Healthcare) diluted 1:1000 in 5 % (w/v) nonfat dry milk in TBS-T. Immunoreactive bands were detected with enhanced chemiluminescence reagents (ECL, Amersham Pharmacia Biotech) according to the manufacturer's procedure and images were recorded using X-ray films (Amersham Hyperfilm ECL, GE Healthcare). The films were scanned in Molecular Imager Gel Doc XR+System (Bio-Rad) and analyzed with Image Lab software (v4.1, Bio-Rad). Protein loading was confirmed by staining the membranes with Ponceau S and immunoblotting with a mouse anti-alpha tubulin antibody (ab7291, Abcam, Cat# ab7291, RRID:AB_2241126).

Statistical analysis

Statistical analysis was performed using Prism GraphPad v6 software (RRID:SCR_002798). Group data are presented as means ± SE (standard error) and were compared using an unpaired t-test (data sets with 2 variables) or a two-way ANOVA (data sets with 4 variables). When the normality test failed, the two-way ANOVA was preceded by a logarithmic transform to obtain a normal distribution. When treatments were significantly different, the Holm-Sidak test was selected to perform pairwise multiple comparisons. Statistical significance was set at $p<0.05$.

Results

Effects of terameprocol on cardiac hemodynamics

The effects of TMP treatment in hemodynamics are summarized in table 1. Compared to the SHAM group, animals from the MCT+Vehicle group presented increased RV peak systolic pressure, dP/dt_{max} and absolute value of dP/dt_{min}, as well as a significant reduction in RV stroke volume, ejection fraction and cardiac output.

Table 1 – Hemodynamic effects of terameprocol.

	SHAM+Vehicle	SHAM+TMP	MCT+Vehicle	MCT+TMP
RV function				
HR (bpm)	381 ± 12	377 ± 12	365 ± 8	393 ± 10
Stroke volume (μL)	154 ± 9	151 ± 7	71 ± 18 *	134 ± 15 ‡
Output (mL/min)	59 ± 4	57 ± 4	26 ± 6 *	52 ± 5 ‡
EF (%)	65 ± 6	70 ± 4	29 ± 7 *	71 ± 5 ‡
PSP (mmHg)	26.1 ± 0.7	26.4 ± 0.7	58.2 ± 8.9 *	35.2 ± 1.9 ‡
dP/dt_{max} (mmHg/s)	1419 ± 56	1567 ± 81	2979 ± 365 *	2107 ± 83 ‡
EDP (mmHg)	4.5 ± 0.8	4.7 ± 0.7	5.1 ± 0.9	4.2 ± 0.7
dP/dt_{min} (mmHg/s)	-1316 ± 152	-1217 ± 71	-2747 ± 212 *	-2000 ± 97 ‡, †
LV function				
HR (bpm)	378 ± 15	383 ± 17	367 ± 8	392 ± 10
Stroke volume (μL)	243 ± 25	212 ± 18	131 ± 16 *	177 ± 23
Output (mL/min)	92 ± 8	81 ± 6	48 ± 6 *	69 ± 8
EF (%)	74 ± 4	73 ± 4	71 ± 3	69 ± 4
PSP (mmHg)	88.4 ± 6.0	98.1 ± 1.5	94.9 ± 4.9	94.4 ± 4.0
dP/dt_{max} (mmHg/s)	5582 ± 461	6871 ± 293	5724 ± 218	6047 ± 428
EDP (mmHg)	5.4 ± 1.5	4.4 ± 1.3	4.5 ± 0.7	6.6 ± 1.9
dP/dt_{min} (mmHg/s)	-6040 ± 828	-7691 ± 501	-5242 ± 458	-6831 ± 392

SHAM+Vehicle, saline-injected, vehicle-treated group; SHAM+TMP, saline-injected, terameprocol-treated group; MCT+Vehicle, monocrotaline-injected, vehicle-treated group; MCT+TMP, monocrotaline-injected, terameprocol-treated group; RV, right ventricle; LV, left ventricle; HR, heart rate; EF, ejection fraction; PSP, peak systolic pressure; dP/dt_{max}, peak rate of pressure rise; EDP, end-diastolic pressure; dP/dt_{min}, peak rate of pressure fall. Data are presented as mean ± SE. *$p < 0.05$ vs SHAM+Vehicle; †$p < 0.05$ vs SHAM+TMP; ‡$p < 0.05$ vs MCT+Vehicle.

TMP treatment improved cardiac function in MCT-induced PAH, normalizing RV peak systolic pressure, dP/dt_{max}, RV ejection fraction, stroke volume and cardiac output and attenuating the increase in the absolute value of dP/dt_{min}. Regarding LV, we found significant reduction in stroke volume and cardiac output in MCT+Vehicle, while these changes were prevented in MCT+TMP group.

Effects of terameprocol on morphometric and histological characteristics

MCT-induced RV hypertrophy was normalized by TMP treatment, as shown by RV/(LV+S) and RV cardiomyocyte cross-sectional area (Table 2 and Figure 1).

Table 2 – Morphometric effects of terameprocol.

	SHAM+Vehicle	SHAM+TMP	MCT+Vehicle	MCT+TMP
BW (g)	295 ± 8	265 ± 8 *	254 ± 7 *	247 ± 6
HW/BW (g/Kg)	2.89 ± 0.05	2.68 ± 0.08	3.59 ± 0.24 *	2.92 ± 0.11 ‡
RV/(LV+S) (g/g)	0.30 ± 0.01	0.31 ± 0.02	0.49 ± 0.03 *	0.35 ± 0.02 ‡
RV/BW (g/Kg)	0.57 ± 0.02	0.59 ± 0.04	0.94 ± 0.09 *	0.68 ± 0.04 ‡
(LV+S)/BW (g/Kg)	1.33 ± 0.05	1.20 ± 0.05	1.41 ± 0.08	1.31 ± 0.05
LuW/BW (g/Kg)	4.59 ± 0.30	4.34 ± 0.08	9.56 ± 1.01 *	5.88 ± 0.35 ‡
GW/tib (g/cm)	0.52 ± 0.01	0.49 ± 0.01	0.50 ± 0.01	0.47 ± 0.01

SHAM+Vehicle, saline-injected, vehicle-treated group; SHAM+TMP, saline-injected, terameprocol-treated group; MCT+Vehicle, monocrotaline-injected, vehicle-treated group; MCT+TMP, monocrotaline-injected, terameprocol-treated group; BW, body weight; HW, heart weight; RV, right ventricle weight; LV + S, left ventricle plus septum weight; LuW, lung weight; GW, *gastrocnemius* weight; tib, tibial length. Data are presented as mean ± SE. *$p < 0.05$ vs SHAM+Vehicle; ‡$p < 0.05$ vs MCT+Vehicle.

In the MCT group, small pulmonary arteries presented significant medial hypertrophy, which was significantly reduced by TMP. TMP treatment also normalized the lung/body weight ratio. No evidence of hepatic or renal histological damage was found in TMP treated animals (data not shown).

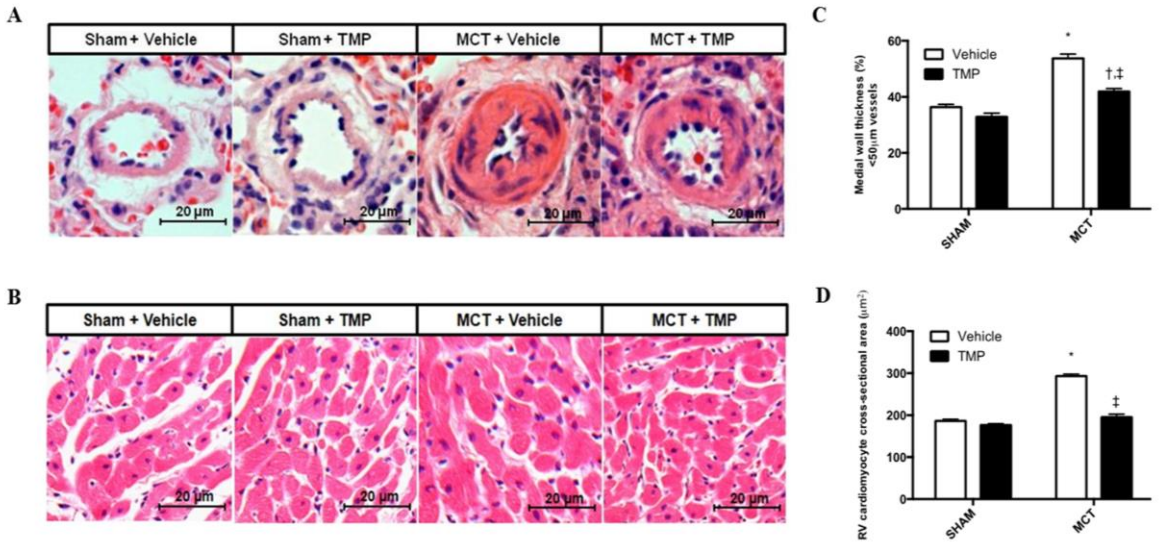

Figure 1 – Effect of terameprocol on cardiomyocyte cross-sectional area and medial wall thickness of pulmonary arteries. A) Histological appearance of small pulmonary arteries (diameter <50 µm), stained with hematoxylin and eosin. B) Histological appearance of right ventricular cardiomyocytes, stained with hematoxylin and eosin. C) Pulmonary artery medial layer thickness expressed as percentage of wall thickness. D) Right ventricular cardiomyocyte cross-sectional area (μm^2). RV, right ventricle; SHAM, saline-

injected groups; MCT, monocrotaline-injected groups; TMP, terameprocol-treated groups; Vehicle, vehicle-treated groups. Data are presented as mean ± SE. *$p < 0.05$ vs SHAM+Vehicle; †$p < 0.05$ vs SHAM+TMP; ‡$p < 0.05$ vs MCT+Vehicle.

Effects of terameprocol on pulmonary artery smooth muscle cell proliferation and apoptosis

TMP treatment (10 and 20 μM) significantly inhibited the proliferation of PASMCs from SHAM and MCT-injected rats, in a dose dependent manner (Figure 2A). At a 20 μM concentration, the inhibitory effects of TMP in the proliferation of cells from the MCT group were less marked. TMP treatment (20 μM) induced apoptosis of PASMCs from both SHAM and MCT-treated rats (Figure 2B).

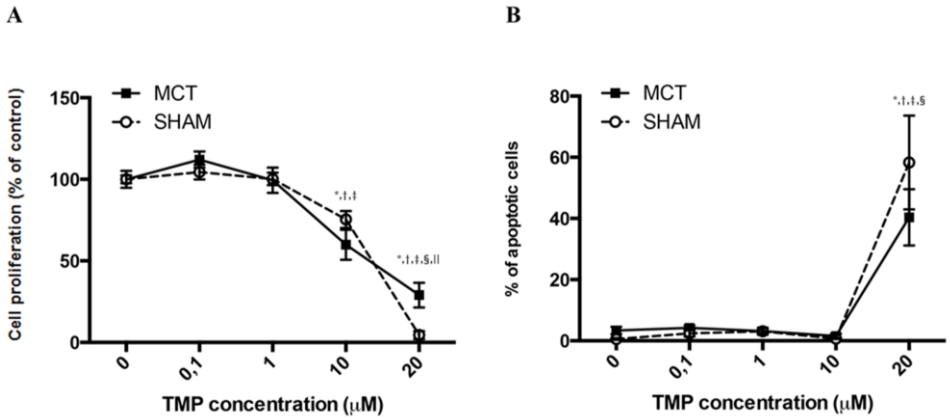

Figure 2 – Effect of terameprocol in pulmonary artery smooth muscle cell proliferation and apoptosis. A) Cell proliferation is expressed as percentage of the absorbance of control (TMP 0 μM) from the same group. B) Apoptosis is expressed as percentage of apoptotic cells. TMP, terameprocol; SHAM, saline-injected group; MCT, monocrotaline-injected group. Data are presented as mean ± SE. *$p < 0.05$ vs. control of the same group; †$p < 0.05$ vs. 0.1 μM of the same group; ‡$p < 0.05$ vs. 1 μM of the same group; §$p < 0.05$ vs. 10 μM of the same group; ||$p < 0.05$ vs. SHAM of the same TMP concentration.

Analysis of terameprocol impact on the proteomic profile of pulmonary artery smooth muscle cells

NanoLC-MS/MS analysis of PASMCs isolated from SHAM and MCT animals allowed the identification of a total of 560 distinct proteins (Supplementary Table S1). In order to detect variations in protein abundance induced by TMP treatment, iTRAQ-based quantification was performed. With this methodology, 18 and 65 proteins were found to be differentially expressed ($p<0.05$) between PASMCs treated with TMP (compared with

control), in cells from SHAM and MCT rats, respectively (Supplementary Tables S2 and S3 and Figures 3A and 3B). Nine proteins were found to be common to SHAM and MCT groups, namely brain acid soluble protein 1, moesin, non-muscle caldesmon, nucleoside diphosphate kinase B, protein disulfide-isomerase A1, protein S100-A6, tropomyosin alpha-1 chain, tropomyosin alpha-4 chain and tropomyosin beta chain. The majority of these proteins exert a role at the level of the cell's structure.

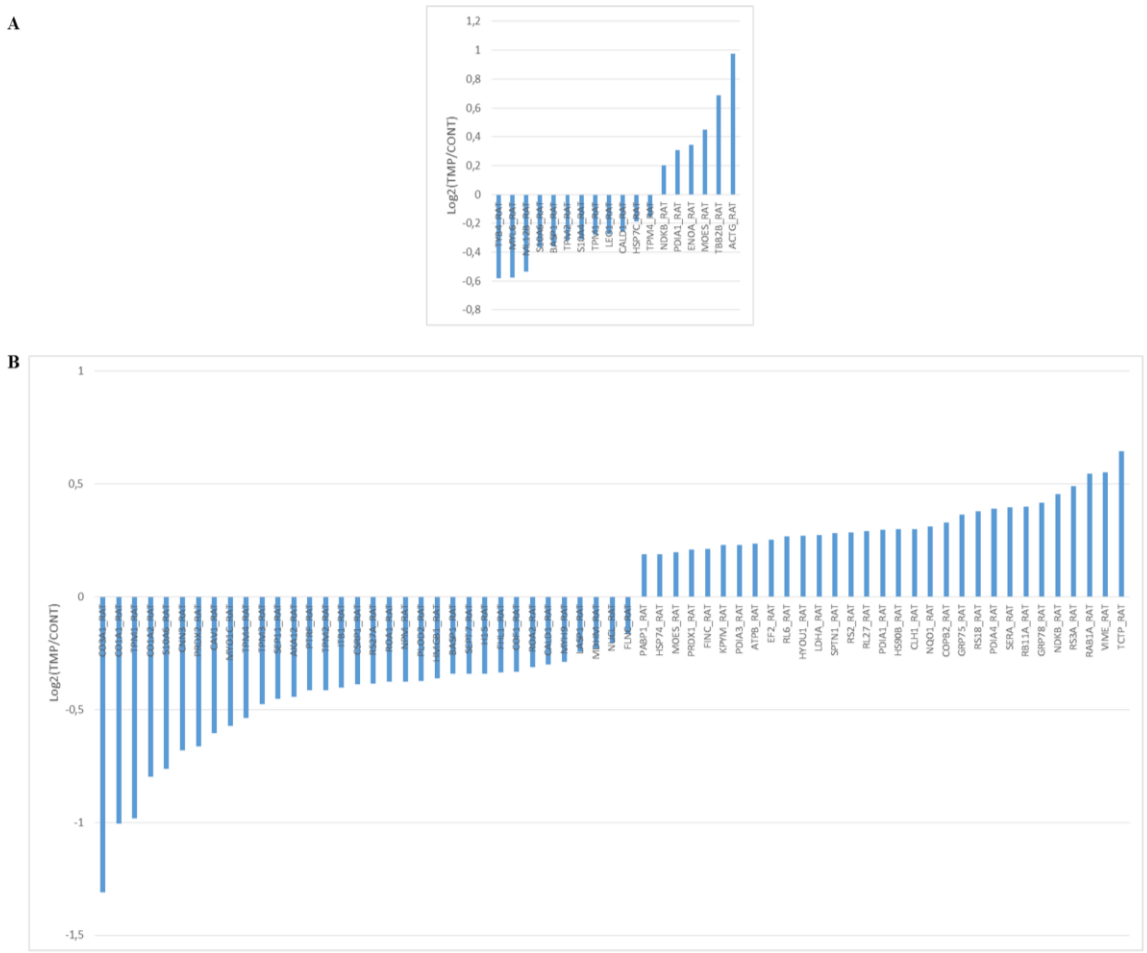

Figure 3 – Comparison of the log ratio of the relative intensity of the significantly regulated PASMC proteins among groups: (A) SHAM (TMP/CONT) and (B) MCT (TMP/CONT). Proteins are presented with the respective Gene ID showed in supplementary tables S2 and S3.

Amongst the 18 proteins that we found to be differentially expressed in cells from SHAM animals, 6 were up-regulated and 12 were down-regulated. According to PANTHER (RRID:SCR_004869) [24], 42.9 % of the proteins are involved in structural integrity of the cell. Cellular (21.1 %) and developmental (17.5 %) processes are the biological processes

associated with the majority of the proteins. Furthermore, 47.4 % of the proteins belong to the cytoskeleton (Supplementary Figure S1). Between the 65 proteins differentially expressed in cells from MCT rats, 31 proteins were found to be up-regulated and 34 were down-regulated. According to PANTHER analysis [24], structural activity (32.9 %), catalytic activity (24.7 %) and binding (23.5 %) were the main molecular functions associated with the differentially expressed proteins. Metabolic (20.8 %) and cellular (18.5 %) processes were the most prevalent biological processes. Regarding the protein class, the majority of the proteins differentially expressed were cytoskeletal proteins (21.4 %), followed by nucleic acid binding proteins (13.1 %) (Supplementary Figure S2). Although not being a major class, the protein class of transcription factors (3.6 %) was also highlighted from PANTHER analysis of PASMCs from the MCT group (but not in cells from SHAM animals). This cluster included the protein HMGB1, whose levels decreased with TMP treatment. Western blotting analysis confirmed the decreased expression of this protein in PASMCs from MCT rats treated with TMP (Figure 4A). Additionally, immunohistochemical analysis of HMGB1 in lung tissue from MCT+Vehicle and MCT+TMP groups evidenced the staining of this protein in PASMC nuclei in both groups (Figure 4B).

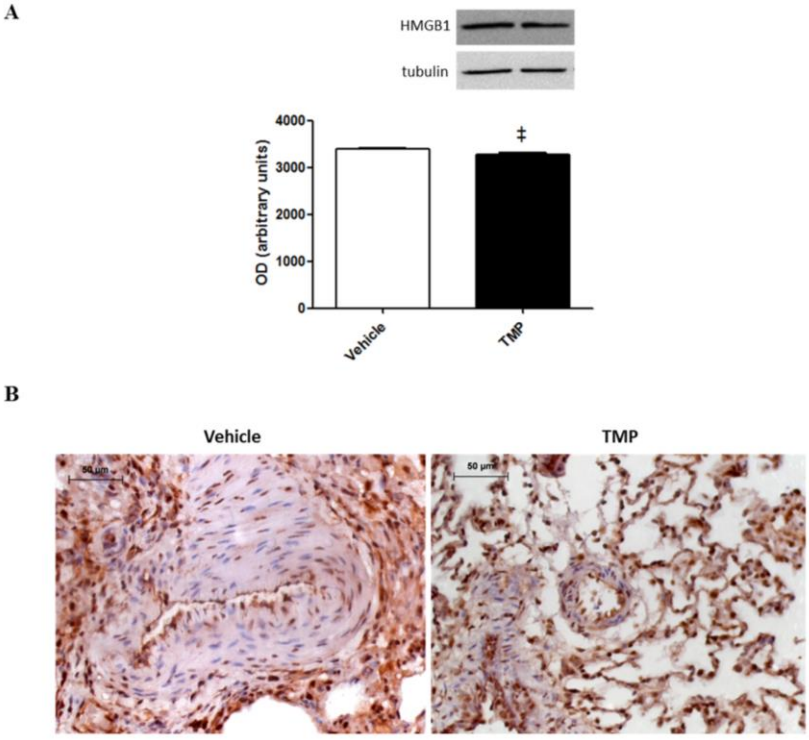

Figure 4 – Effect of terameprocol on HMGB1 expression and staining profile in pulmonary arteries from MCT rats. A) HMGB1 expression evaluated by western blotting in PASMCs from MCT rats, treated with

vehicle or TMP. Representative immunoblot is shown above the correspondent graph. B) Staining prolife of HMGB1 evaluated by immunohistochemistry in lung tissue from MCT+Vehicle and MCT+TMP rats. TMP, terameprocol-treated group; Vehicle, vehicle-treated group. Data are expressed as mean ± SE. ‡$p < 0.05$ vs Vehicle.

An integrated analysis of proteins that were found to be differentially expressed in cells from MCT rats treated with TMP was performed with Cytoscape (v3.1.1.) (RRID:SCR_003032) [25], plugins ClueGO+CluePedia [26, 27]. This analysis retrieved "positive regulation of protein binding", "regulation of cell size", "cellular response to IL-4", "cellular response to IL-1", "response to endoplasmic reticulum (ER) stress" and "removal of superoxide radicals" as the biological processes up-regulated in PASMCs treated with TMP. The biological processes "response to transforming growth factor beta (TGF-beta)", "regulation of ATPase activity", "negative regulation of anoikis", "negative regulation of mRNA metabolic process" and "DNA-templated transcription" were shown to be down-regulated by TMP (Figure 5).

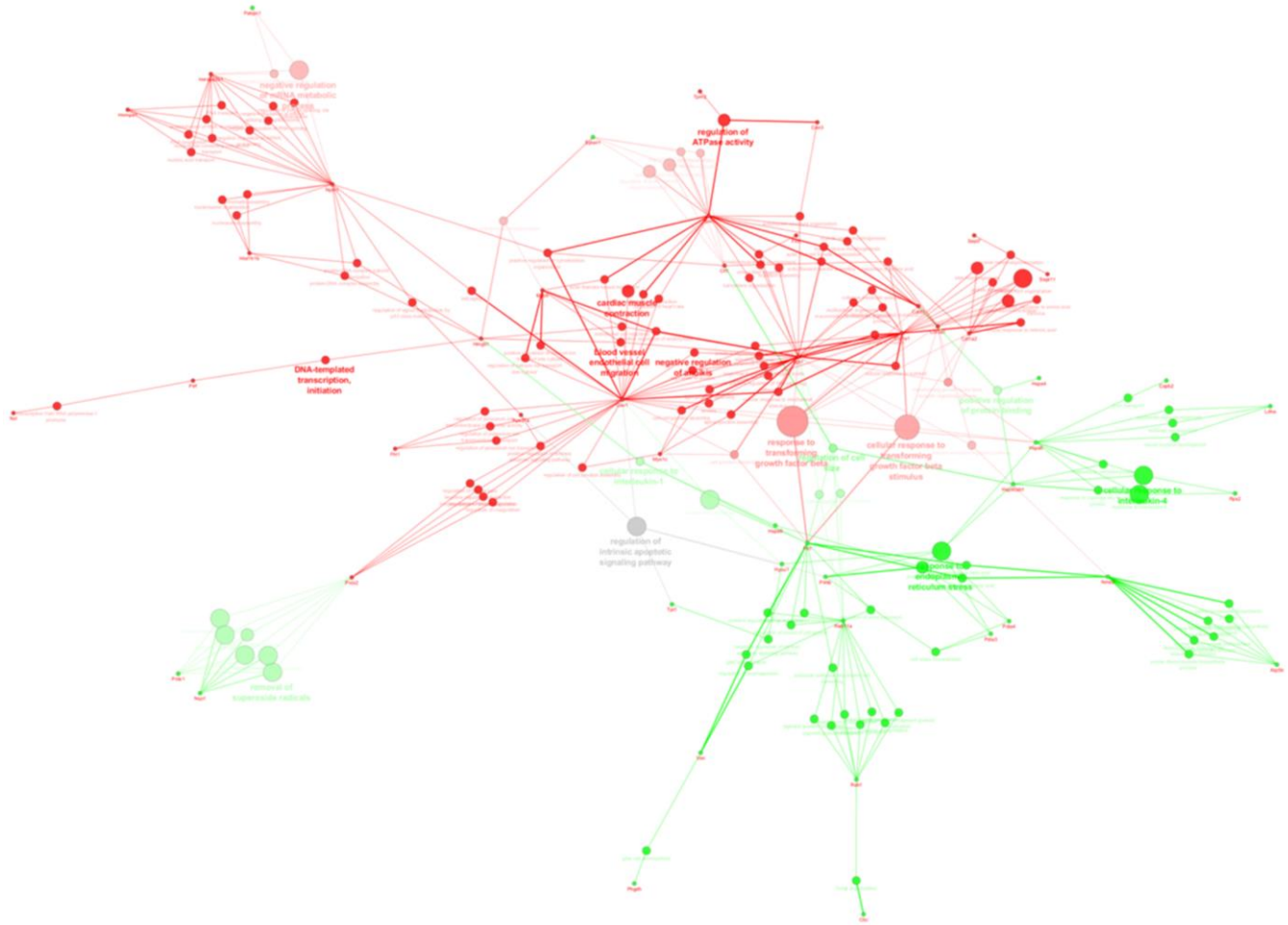

Figure 5 – ClueGo+CluePedia analysis [26, 27] of protein-protein interactions considering the proteins identified as up- and down-regulated in PASMCs from MCT rats treated with TMP. Green nodes represent the over-represented biological processes, while red nodes refer to the ones under-represented. Release date: May 15, 2015.

Finally, comparison of proteins identified experimentally with those predicted by SwissTargetPrediction tool as TMP targets (Supplementary Figures S3 and S4), evidenced common processes, such as regulation of cytoskeleton organization, cell mobility, migration and growth. So, our data suggest that the regulation of processes retrieved from proteomic analysis, such as DNA-templated transcription and response to TGF-beta, might be the specific of PASMCs treated with TMP in experimental PAH.

Discussion

The hyperproliferative and apoptotic-resistant phenotype of PASMCs constitutes an attractive target in the treatment of PAH. In order to study the potential beneficial effects of TMP in PAH, we evaluated its *in vivo* effects in MCT model of PAH and searched for the molecular mechanisms regulated by this drug in primary cultures of PASMCs using a quantitative proteomic approach. The MCT rat model has been extensively used to study the pathogenesis of PAH, as well as the effects of drug interventions. Although there are some differences between this experimental model and human PAH, MCT induces pulmonary artery medial layer remodeling [28-30], which was the focus of this study.

TMP is being studied as an anticancer drug, reported to cause growth arrest in several cancer types, both *in vitro* and *in vivo*, showing no relevant toxicity [11, 15, 18]. TMP administration improved the hemodynamic features of MCT-induced PAH, such as RV peak systolic pressure and RV ejection fraction, stroke volume and cardiac output. Importantly, TMP did not change hemodynamic parameters in the SHAM animals, suggesting it has no adverse effects on cardiac function. Additionally, cardiac hypertrophy and pulmonary vascular remodeling decreased with TMP administration in MCT-induced PAH. TMP exerted anti-proliferative and pro-apoptotic effects in PASMCs, supported by the down-regulation of proteins involved in mRNA metabolism and DNA-templated transcription. It was reported that TMP reduces the transcription of genes controlled by Sp1 [31]. Our data highlighted the modulation of the transcription factors HMGB1, Fhl-1 and Ptrf by TMP in PASMCs from PAH rats. The role of HMGB1 in PAH was already reported and implicated with pulmonary vascular remodeling by enhancing PASMC proliferation and migration [32-34]. The inhibition of HMGB1 by Glycyrrhizin was previously shown to attenuate the progression of MCT-induced PAH [35]. Therefore, our results suggest that the anti-proliferative effects of TMP on PAH can be mediated, at least

in part, by the down-regulation of HMGB1 in PASMCs. In cells from SHAM animals, TMP had no significant impact on HMGB1 levels or even on overall PASMC proteome, which presented only subtle expression differences, mainly for structural proteins, in opposition to the observed in cells from MCT rats treated with this drug.

In addition to nucleic acid binding proteins, PANTHER analysis highlighted other major cluster of proteins modulated by TMP in PAH. Within this group we found collagen alpha-1 (I) chain, collagen alpha-2 (I) chain and collagen alpha-1 (III) chain. Collagen deposition in pulmonary vessels is one of the main features of vascular remodeling seen in PAH and circulating markers of collagen metabolism have been associated with worse stages of PAH [36]. According to our data, TMP decreased the levels of these proteins, which could be mediated by TGF-beta signaling. Dysfunctional signaling of the TGF-beta pathway is associated with PAH pathogenesis, contributing to abnormal SMC proliferation [37, 38]. In addition, TGF-beta signaling inhibition was reported to prevent MCT-induced PAH development and progression, through the inhibition of PASMC proliferation [39-41]. Thus, TMP-related down-regulation of the response to TGF-beta might have contributed to the anti-proliferative effects of this drug on PASMCs from MCT rats.

Interestingly, TMP also up-regulated the biological process “response to ER stress”. This is associated with the increased levels of HSP70 and HSP90 family of chaperones (heat shock protein HSP90-beta, 78 kDa glucose-regulated protein, hypoxia upregulated protein 1 and stress-70 protein, mitochondrial) involved in the correct folding and degradation of misfolded proteins. ER stress was recently suggested as a new therapeutic target for the management of PAH. The use of some chemical chaperones in experimental PAH was shown to prevent and even reverse the disease, suppressing proliferation and inducing apoptosis of PASMCs [42].

Taken together, our results suggest that TMP may be seen as an attractive therapeutic strategy for the management of PAH since it ameliorated the hemodynamic features and both cardiac and vascular remodeling. The regulation of DNA transcription and TGF-beta pathway seems to underlie these functional and morphological adaptations.

Conflict of interest

The authors declare no conflicts of interests, financial or otherwise.

Funding

This work was supported by Portuguese Foundation for Science and Technology (FCT), European Union, QREN, FEDER and COMPETE for funding the QOPNA research unit (UID/QUI/00062/2013), CIAFEL (UID/DTP/00617/2013), Unidade de Investigação Cardiovascular (UID/IC/00051/2013) and the post-graduation students (grant numbers SFRH/BD/91067/2012 to R.N.F and SFRH/BPD/90010/2012 to D.M.G.).

Acknowledgements

The authors are thankful to Nádia Gonçalves, Maria José Mendes, Marta Oliveira, Joana Brandão and Fábio Carneiro for their technical assistance in animal studies and sample processing. We gratefully acknowledge Dr. Delfim Duarte and Professors Raquel Soares, Rita Negrão and Laura Ribeiro from the Department of Biochemistry, Faculty of Medicine of Porto, for their invaluable technical contribution to the cell culture experiments. We also thank Celeste Resende from Faculty of Sport, University of Porto for skilled assistance in immunohistochemistry experiments.

References

1. Crosswhite, P. and Z. Sun, *Molecular mechanisms of pulmonary arterial remodeling.* Mol Med, 2014. **20**: p. 191-201.
2. Nogueira-Ferreira, R., R. Ferreira, and T. Henriques-Coelho, *Cellular interplay in pulmonary arterial hypertension: implications for new therapies.* Biochim Biophys Acta, 2014. **1843**(5): p. 885-93.
3. Tajsic, T. and N.W. Morrell, *Smooth muscle cell hypertrophy, proliferation, migration and apoptosis in pulmonary hypertension.* Compr Physiol, 2011. **1**(1): p. 295-317.
4. Mcgoon, M.D., R.L. Benza, P. Escribano-Subias, X. Jiang, D.P. Miller, A.J. Peacock, J. Pepke-Zaba, T. Pulido, S. Rich, S. Rosenkranz, S. Suissa, and M. Humbert, *Pulmonary arterial hypertension: epidemiology and registries.* J Am Coll Cardiol, 2013. **62**(25 Suppl): p. D51-9.
5. Provencher, S. and J.T. Granton, *Current treatment approaches to pulmonary arterial hypertension.* Can J Cardiol, 2015. **31**(4): p. 460-77.

6. Gurtu, V. and E.D. Michelakis, *Emerging therapies and future directions in pulmonary arterial hypertension.* Can J Cardiol, 2015. **31**(4): p. 489-501.
7. Huang, J.B., Y.L. Liu, P.W. Sun, X.D. Lv, K. Bo, and X.M. Fan, *Novel strategy for treatment of pulmonary arterial hypertension: enhancement of apoptosis.* Lung, 2010. **188**(3): p. 179-89.
8. Guignabert, C., L. Tu, M. Le Hiress, N. Ricard, C. Sattler, A. Seferian, A. Huertas, M. Humbert, and D. Montani, *Pathogenesis of pulmonary arterial hypertension: lessons from cancer.* Eur Respir Rev, 2013. **22**(130): p. 543-51.
9. Rai, P.R., C.D. Cool, J.A. King, T. Stevens, N. Burns, R.A. Winn, M. Kasper, and N.F. Voelkel, *The cancer paradigm of severe pulmonary arterial hypertension.* Am J Respir Crit Care Med, 2008. **178**(6): p. 558-64.
10. Voelkel, N.F., C. Cool, S.D. Lee, L. Wright, M.W. Geraci, and R.M. Tuder, *Primary pulmonary hypertension between inflammation and cancer.* Chest, 1998. **114**(3 Suppl): p. 225S-230S.
11. Chang, C.C., J.D. Heller, J. Kuo, and R.C. Huang, *Tetra-O-methyl nordihydroguaiaretic acid induces growth arrest and cellular apoptosis by inhibiting Cdc2 and survivin expression.* Proc Natl Acad Sci U S A, 2004. **101**(36): p. 13239-44.
12. Fulciniti, M., S. Amin, P. Nanjappa, S. Rodig, R. Prabhala, C. Li, S. Minvielle, Y.T. Tai, P. Tassone, H. Avet-Loiseau, T. Hideshima, K.C. Anderson, and N.C. Munshi, *Significant biological role of sp1 transactivation in multiple myeloma.* Clin Cancer Res, 2011. **17**(20): p. 6500-9.
13. Heller, J.D., J. Kuo, T.C. Wu, W.M. Kast, and R.C. Huang, *Tetra-O-methyl nordihydroguaiaretic acid induces G2 arrest in mammalian cells and exhibits tumoricidal activity in vivo.* Cancer Res, 2001. **61**(14): p. 5499-504.
14. Lambert, J.D., R.O. Meyers, B.N. Timmermann, and R.T. Dorr, *tetra-O-methylnordihydroguaiaretic acid inhibits melanoma in vivo.* Cancer Lett, 2001. **171**(1): p. 47-56.
15. Lopez, R.A., A.B. Goodman, M. Rhodes, J.A. Blomberg, and J. Heller, *The anticancer activity of the transcription inhibitor terameprocol (meso-tetra-O-methyl nordihydroguaiaretic acid) formulated for systemic administration.* Anticancer Drugs, 2007. **18**(8): p. 933-9.

16. Park, R., C.C. Chang, Y.C. Liang, Y. Chung, R.A. Henry, E. Lin, D.E. Mold, and R.C. Huang, *Systemic treatment with tetra-O-methyl nordihydroguaiaretic acid suppresses the growth of human xenograft tumors.* Clin Cancer Res, 2005. **11**(12): p. 4601-9.
17. Church, D.N. and D.C. Talbot, *Survivin in solid tumors: rationale for development of inhibitors.* Curr Oncol Rep, 2012. **14**(2): p. 120-8.
18. Lu, J.M., J. Nurko, S.M. Weakley, J. Jiang, P. Kougias, P.H. Lin, Q. Yao, and C. Chen, *Molecular mechanisms and clinical applications of nordihydroguaiaretic acid (NDGA) and its derivatives: an update.* Med Sci Monit, 2010. **16**(5): p. RA93-100.
19. Ryan, B.M., N. O'donovan, and M.J. Duffy, *Survivin: a new target for anti-cancer therapy.* Cancer Treat Rev, 2009. **35**(7): p. 553-62.
20. Ducret, T., J. El Arrouchi, A. Courtois, J.F. Quignard, R. Marthan, and J.P. Savineau, *Stretch-activated channels in pulmonary arterial smooth muscle cells from normoxic and chronically hypoxic rats.* Cell Calcium, 2010. **48**(5): p. 251-9.
21. Carvalhais, V., N. Cerca, M. Vilanova, and R. Vitorino, *Proteomic profile of dormancy within Staphylococcus epidermidis biofilms using iTRAQ and label-free strategies.* Appl Microbiol Biotechnol, 2015. **99**(6): p. 2751-2762.
22. Moreira-Goncalves, D., T. Henriques-Coelho, H. Fonseca, R.M. Ferreira, F. Amado, A. Leite-Moreira, and J.A. Duarte, *Moderate exercise training provides left ventricular tolerance to acute pressure overload.* Am J Physiol Heart Circ Physiol, 2011. **300**(3): p. H1044-52.
23. Laemmli, U.K., *Cleavage of structural proteins during the assembly of the head of bacteriophage T4.* Nature, 1970. **227**(5259): p. 680-5.
24. Mi, H., A. Muruganujan, and P.D. Thomas, *PANTHER in 2013: modeling the evolution of gene function, and other gene attributes, in the context of phylogenetic trees.* Nucleic Acids Res, 2013. **41**(Database issue): p. D377-86.
25. Shannon, P., A. Markiel, O. Ozier, N.S. Baliga, J.T. Wang, D. Ramage, N. Amin, B. Schwikowski, and T. Ideker, *Cytoscape: a software environment for integrated models of biomolecular interaction networks.* Genome Res, 2003. **13**(11): p. 2498-504.

26. Bindea, G., J. Galon, and B. Mlecnik, *CluePedia Cytoscape plugin: pathway insights using integrated experimental and in silico data.* Bioinformatics, 2013. **29**(5): p. 661-3.
27. Bindea, G., B. Mlecnik, H. Hackl, P. Charoentong, M. Tosolini, A. Kirilovsky, W.H. Fridman, F. Pages, Z. Trajanoski, and J. Galon, *ClueGO: a Cytoscape plug-in to decipher functionally grouped gene ontology and pathway annotation networks.* Bioinformatics, 2009. **25**(8): p. 1091-3.
28. Maarman, G., S. Lecour, G. Butrous, F. Thienemann, and K. Sliwa, *A comprehensive review: the evolution of animal models in pulmonary hypertension research; are we there yet?* Pulm Circ, 2013. **3**(4): p. 739-56.
29. Ryan, J.J., G. Marsboom, and S.L. Archer, *Rodent models of group 1 pulmonary hypertension.* Handb Exp Pharmacol, 2013. **218**: p. 105-49.
30. Stenmark, K.R., B. Meyrick, N. Galie, W.J. Mooi, and I.F. Mcmurtry, *Animal models of pulmonary arterial hypertension: the hope for etiological discovery and pharmacological cure.* Am J Physiol Lung Cell Mol Physiol, 2009. **297**(6): p. L1013-32.
31. Huang, R.C., C.C. Chang, and D. Mold, *Survivin-dependent and -independent pathways and the induction of cancer cell death by tetra-O-methyl nordihydroguaiaretic acid.* Semin Oncol, 2006. **33**(4): p. 479-85.
32. Bauer, E.M., R. Shapiro, H. Zheng, F. Ahmad, D. Ishizawar, S.A. Comhair, S.C. Erzurum, T.R. Billiar, and P.M. Bauer, *High mobility group box 1 contributes to the pathogenesis of experimental pulmonary hypertension via activation of Toll-like receptor 4.* Mol Med, 2012. **18**: p. 1509-18.
33. Sadamura-Takenaka, Y., T. Ito, S. Noma, Y. Oyama, S. Yamada, K. Kawahara, H. Inoue, and I. Maruyama, *HMGB1 promotes the development of pulmonary arterial hypertension in rats.* PLoS One, 2014. **9**(7): p. e102482.
34. Wang, H.L., L.P. Peng, W.J. Chen, S.H. Tang, B.Z. Sun, C.L. Wang, R. Huang, Z.J. Xu, and W.F. Lei, *HMGB1 enhances smooth muscle cell proliferation and migration in pulmonary artery remodeling.* Int J Clin Exp Pathol, 2014. **7**(7): p. 3836-44.
35. Yang, P.S., D.H. Kim, Y.J. Lee, S.E. Lee, W.J. Kang, H.J. Chang, and J.S. Shin, *Glycyrrhizin, inhibitor of high mobility group box-1, attenuates monocrotaline-*

induced pulmonary hypertension and vascular remodeling in rats. Respir Res, 2014. **15**: p. 148.

36. Safdar, Z., E. Tamez, W. Chan, B. Arya, Y. Ge, A. Deswal, B. Bozkurt, A. Frost, and M. Entman, *Circulating collagen biomarkers as indicators of disease severity in pulmonary arterial hypertension.* JACC Heart Fail, 2014. **2**(4): p. 412-21.
37. Davies, R.J., A.M. Holmes, J. Deighton, L. Long, X. Yang, L. Barker, C. Walker, D.C. Budd, P.D. Upton, and N.W. Morrell, *BMP type II receptor deficiency confers resistance to growth inhibition by TGF-beta in pulmonary artery smooth muscle cells: role of proinflammatory cytokines.* Am J Physiol Lung Cell Mol Physiol, 2012. **302**(6): p. L604-15.
38. Morrell, N.W., X. Yang, P.D. Upton, K.B. Jourdan, N. Morgan, K.K. Sheares, and R.C. Trembath, *Altered growth responses of pulmonary artery smooth muscle cells from patients with primary pulmonary hypertension to transforming growth factor-beta(1) and bone morphogenetic proteins.* Circulation, 2001. **104**(7): p. 790-5.
39. Long, L., A. Crosby, X. Yang, M. Southwood, P.D. Upton, D.K. Kim, and N.W. Morrell, *Altered bone morphogenetic protein and transforming growth factor-beta signaling in rat models of pulmonary hypertension: potential for activin receptor-like kinase-5 inhibition in prevention and progression of disease.* Circulation, 2009. **119**(4): p. 566-76.
40. Thomas, M., C. Docx, A.M. Holmes, S. Beach, N. Duggan, K. England, C. Leblanc, C. Lebret, F. Schindler, F. Raza, C. Walker, A. Crosby, R.J. Davies, N.W. Morrell, and D.C. Budd, *Activin-like kinase 5 (ALK5) mediates abnormal proliferation of vascular smooth muscle cells from patients with familial pulmonary arterial hypertension and is involved in the progression of experimental pulmonary arterial hypertension induced by monocrotaline.* Am J Pathol, 2009. **174**(2): p. 380-9.
41. Zaiman, A.L., M. Podowski, S. Medicherla, K. Gordy, F. Xu, L. Zhen, L.A. Shimoda, E. Neptune, L. Higgins, A. Murphy, S. Chakravarty, A. Protter, P.B. Sehgal, H.C. Champion, and R.M. Tuder, *Role of the TGF-beta/Alk5 signaling pathway in monocrotaline-induced pulmonary hypertension.* Am J Respir Crit Care Med, 2008. **177**(8): p. 896-905.

42. Dromparis, P., R. Paulin, T.H. Stenson, A. Haromy, G. Sutendra, and E.D. Michelakis, *Attenuating endoplasmic reticulum stress as a novel therapeutic strategy in pulmonary hypertension.* Circulation, 2013. **127**(1): p. 115-25.

43. Gfeller, D., A. Grosdidier, M. Wirth, A. Daina, O. Michielin, and V. Zoete, *SwissTargetPrediction: a web server for target prediction of bioactive small molecules.* Nucleic Acids Res, 2014. **42**(Web Server issue): p. W32-8.

CHAPTER IV
GENERAL DISCUSSION

General Discussion

Pulmonary arterial hypertension is a disease characterized by pulmonary vascular remodeling, vasoconstriction, inflammation and thrombosis. These vascular changes lead to a progressive increase in PVR, imposing a pressure overload to the RV. Initially, the RV adapts by developing hypertrophy but heart failure and premature death will eventually occur (Montani, Gunther et al. 2013; Baldi, Fuso et al. 2014; McLaughlin, Shah et al. 2015). The symptoms of PAH are non-specific and mainly related to progressive RV dysfunction. Initial symptoms are typically induced by exertion while symptoms at rest occur only in advanced cases. They include shortness of breath, fatigue, syncope and dizziness, which negatively impact the functional capacity and quality of life (Matura, McDonough et al. 2012; Delcroix and Howard 2015; Galie, Humbert et al. 2016). Despite the advances in recent years in disease-targeted therapies, PAH remains an incurable disease with a high mortality rate (Humbert, Lau et al. 2014; McLaughlin, Shah et al. 2015), justifying the need of novel preventive and therapeutic strategies. In this sense, we studied the potential application of a non-pharmacological (exercise training) and a pharmacological (TMP) strategy in the clinical management of this disease (Studies II and III from Chapter III).

Despite the well-established health benefits of exercise training (Powers, Lennon et al. 2002; La Gerche and Claessen 2015), the molecular mechanisms underlying its cardioprotective role need to be better clarified. The majority of the studies have focused on the LV, but RV function is a critical determinant of survival in pathological conditions such as PAH (La Gerche and Claessen 2015). Some reports suggest that exercise training induces distinct structural and functional adaptations in both ventricles (Benito, Gay-Jordi et al. 2011; Gay-Jordi, Guash et al. 2013; La Gerche, Roberts et al. 2014). However, the molecular pathways underlying these adaptations have not been explored. Aiming to add new insights on this issue, we analyzed LV and RV functional, structural and molecular adaptations promoted by one year of endurance exercise training in an animal model (Study I). Rats were submitted to endurance training for 54 weeks, one of the longest exercise training programs performed in animal models, and corresponds to approximately 35 years of exercise in humans (Sengupta 2013). Our data showed that long-term, moderate exercise training improved bi-ventricular diastolic function, as shown by the

lower end-diastolic pressure (EDP). In RV, we observed a decrease in fibrosis in exercised animals, which can in part, explain the lower RV mass that we found in trained animals. Our data do not support the contribution of the formation of new cardiomyocytes from progenitor/stem cells, given by c-kit expression, to the cardiac growth induced by exercise training previously reported (Waring, Vicinanza et al. 2014; Xiao, Xu et al. 2014; Tao, Bei et al. 2015). C-kit positive cardiac stem cells are reported to be necessary and sufficient for the regeneration and repair of myocardial damage (Ellison, Vicinanza et al. 2013). The aging process can, at least in part, justify these contradictory results, once it was reported that the percentage of cardiomyocytes emerging from the c-kit positive lineage decreases with aging (van Berlo, Kanisicak et al. 2014). Also, the low-to-moderate intensity of our exercise training protocol could be a contributing factor as it was shown that c-kit positive cardiac stem cells activation is exercise-intensity dependent (Waring, Vicinanza et al. 2014).

The main molecular adaptations of the heart to 54 weeks of exercise training were seen at the metabolic level, mainly in the RV. A metabolic adaptation of RV towards an oxidative phenotype was observed, that can be related with the increase of nitrated proteins, due to augmented nitric oxide (NO) levels. Exercise training seems to generate greater levels of NO that reacted with superoxide anion with the formation of peroxynitrite, which may react with proteins' tyrosine residues (van der Loo, Labugger et al. 2000). This exercise training-related oxidative phenotype was not directly related to increased mitochondrial biogenesis, as previously reported (Vettor, Valerio et al. 2014). Indeed, the content of mitochondria, roughly assessed by citrate synthase activity (Figueiredo, Ferreira et al. 2008), did not increase in RV or LV from trained rats, as well as of peroxisome proliferator-activated receptor gamma coactivator-1 alpha (PGC-1α), a key regulator of genes involved in myocardial fuel metabolism and mitochondrial biogenesis (Li, Muhlfeld et al. 2011). Nevertheless, the impact of exercise training on mitochondrial biogenesis in the heart is not clear. For instance, 6 weeks of swimming was shown to promote an up-regulation of mitochondrial biogenesis in heart (Vettor, Valerio et al. 2014), whereas 3 months of running did not impact mitochondrial density in LV (Li, Muhlfeld et al. 2011). The effect of lifelong exercise training was mainly noticed in the up-regulation of sirtuin 3 (SIRT3) and manganese-dependent superoxide dismutase (MnSOD) in RV. Activation of the deacetylase SIRT3 is important in the regulation of PGC-1α expression (Li, Muhlfeld

et al. 2011; Mann and Rosenzweig 2012). Additionally, it has been suggested that the deacetylation of MnSOD by SIRT3 increases the activity of MnSOD, contributing to protect the heart against oxidative stress (Amado, Barros et al. 2014; Powers, Smuder et al. 2014; Bindu, Pillai et al. 2016). Indeed, a cardioprotective role has been attributed to SIRT3, once this deacetylase is related with the activation of many targets that, *via* modifying their respective signaling molecules, block cardiac hypertrophy, fibrosis and apoptosis and promote cardiomyocyte survival (Bindu, Pillai et al. 2016).

Following these advantageous effects of long-term moderate exercise training on RV, we aimed to evaluate the potential preventive role of exercise training on RV dysfunction and remodeling underlying PAH (Study II). Recent studies support the benefit and safety of supervised exercise training programs in patients with stable PAH (Buys, Avila et al. 2015; Pandey, Garg et al. 2015; Yuan, Yuan et al. 2015; Ehlken, Lichtblau et al. 2016). However, it remains to be evaluated if exercise training has a preventive role in PAH, which is of great relevance if we consider that the majority of PAH patients are diagnosed at advanced stages of the disease, when RV impairment is already present. The comprehension of this crosstalk is even more important in the clinical set of familial form of PAH once exercise preconditioning might be seen as a measure to prevent the severity or early onset of the disease. To accomplish our aim we used an animal model of PAH induced by MCT administration. MCT is a pyrrolizidine alkaloid found in the plant *Crotalaria spectabilis*. After being bioactivated in the liver, its bioactive metabolite (MCT pyrrole) is transported by the circulatory system to the lungs, where it induces pulmonary artery molecular and structural changes, increasing PVR and PAP, leading to RV hypertrophy. In the dosage of 60 mg/kg, RV hypertrophy is observed by the third week and progresses to failure and death around the fourth week (Schultze and Roth 1998; Henriques-Coelho, Correia-Pinto et al. 2004; Henriques-Coelho, Oliveira et al. 2008; Correia-Pinto, Henriques-Coelho et al. 2009; Handoko, de Man et al. 2009). Thus, the preventive effect of exercise training was studied using a protocol consisting in 4 weeks of treadmill running before (preconditioning) disease development by MCT injection, followed by 4 weeks of sedentary behavior.

In this study we focused on inflammatory pathways in the RV, given the recognized role of inflammation in RV dysfunction (Watts, Zagorski et al. 2006; Watts, Gellar et al. 2008; Rondelet, Dewachter et al. 2012; Belhaj, Dewachter et al. 2013; Vonk-Noordegraaf,

Haddad et al. 2013). We studied the contribution of tumor necrosis factor (TNF) superfamily signaling, specifically TNF-α and TNF-related weak inducer of apoptosis (TWEAK) to RV remodeling. These pro-inflammatory cytokines seem to contribute differently to the RV dysfunction secondary to MCT-induced PAH. An increased expression of TNF-α and members from the nuclear factor kappa B (NF-κB) non-canonical pathway (NF-κB p100/p52 and Rel-B) was observed in the RV of sedentary MCT-treated rats. Exercise preconditioning did not affect the levels of TNF-α, but decreased TWEAK expression and modulated the expression of NF-κB p105/p50 and NF-κB p65 proteins (members of the canonical NF-κB pathway) in MCT-treated rats. This is in accordance with previous findings that TWEAK and NF-κB signaling regulate cardiac hypertrophy, fibrosis and heart failure (Van der Heiden, Cuhlmann et al. 2010; Novoyatleva, Sajjad et al. 2014). This shift from the non-canonical to the canonical NF-κB signaling seems to have cardioprotective effects. Indeed, activation of p65 subunit was previously related to myocyte survival and cardiac homeostasis while the p50 subunit seems to antagonize the development of cardiac hypertrophy and fibrosis (Gaspar-Pereira, Fullard et al. 2012).

Concomitantly, exercise preconditioning prevented the MCT-related overexpression of the ubiquitin ligase atrogin-1 and increase of matrix metalloproteinase (MMP)-9 activity. Atrogin-1 inhibition was previously reported to prevent pressure overload-induced cardiac hypertrophy (Zaglia, Milan et al. 2014) whereas inactivation of metalloproteinases in the RV is expected to prevent cardiomyocyte hypertrophy and fibrosis (Okada, Kikuzuki et al. 2008). Indeed, RV fibrosis was prevented in trained MCT rats as well as beta-myosin heavy chain (MHC) isoform overexpression, highlighting the role of exercise preconditioning in the prevention of contractile cardiac dysfunction, once both fibrosis and the shift to the beta-MHC isoform are related with an impaired contractile function (Barry, Davidson et al. 2008; Harvey and Leinwand 2011). However, the exercise preconditioning-related decrease of MMP-9 activity in MCT-treated rats was paralleled by an increase of MMP-2 activity. This shift of MMP activity might have contributed to the decreased accumulation of fibrosis observed in the RV of trained MCT-treated rats. Different expression patterns of MMP-2 and MMP-9 to angiogenic-related mechanical stimuli induced by exercise training was already reported, and seem to be explained by their involvement in dissimilar cellular processes (Bellafiore, Battaglia et al. 2013). These molecular events were probably underlying the preventive effect of exercise training

against RV diastolic dysfunction, which is supported by the reduction of EDP. Exercise preconditioning also prevented pulmonary artery remodeling and led to a decrease in cardiac hypertrophy observed in MCT-treated rats. Of note, our data also support the notion that cardioprotection promoted by exercise training can be sustained for several weeks after the cessation of the exercise training protocol.

Despite the experimental evidences of the therapeutic benefits of exercise training for the clinical management of PAH, most of the patients do not tolerate exercise at the time of diagnosis (Fowler, Gain et al. 2012; Babu, Arena et al. 2016). Given that the current guidelines support the use of exercise training only in clinically stable patients and considering that PAH is lacking from effective drugs (Gurtu and Michelakis 2015; Galie, Humbert et al. 2016), it was also our aim to test a pharmacological approach. Because of the role of proliferative and apoptotic pathways on the remodeling of the pulmonary vasculature, we searched for a drug with the potential to target these processes and decided to test TMP. TMP is a methylated derivate of nordihydroguaiaretic acid, found in the plant *Larrea tridentate*, which is being studied as an anticancer drug and reported to cause growth arrest in several cancer types, both *in vitro* and *in vivo*, without relevant toxicity. TMP was reported to block cell cycle progression and promote apoptosis by competing with Sp1-DNA binding, decreasing the transcription of genes dependent from this transcription factor, such as Cdc2 and survivin (Chang, Heller et al. 2004; Ryan, O'Donovan et al. 2009; Lu, Nurko et al. 2010; Church and Talbot 2012). In order to evaluate the potential therapeutic effect of TMP in PAH, we searched for the molecular mechanisms regulated by this drug in primary cultures of PASMCs using a quantitative proteomic approach (Study III). To achieve this, we used the MCT experimental model. MCT administration induces changes in the medial layer characterized by hypertrophy and hyperplasia of smooth muscle, resistance of PASMCs to apoptosis and extension of smooth muscle to normally nonmuscular pulmonary arteries (Schultze and Roth 1998; Maarman, Lecour et al. 2013).

In our study, TMP treatment was able to improve cardiac function of MCT-treated rats, and this was accompanied by a significant reduction of pulmonary and cardiac remodeling. TMP exerted anti-proliferative and pro-apoptotic effects in SMCs isolated from the pulmonary artery from MCT-treated rats. Aiming to explore the molecular mechanisms associated with these effects, a mass spectrometry-based approach was used for

quantitative comparison of proteome profiles of PASMCs isolated from MCT and saline treated rats, treated or not with TMP. To the best of our knowledge, this is the first study that characterized proteome alterations in PASMCs isolated from rats treated with MCT.

TMP had no impact on overall PASMC proteome of saline-treated rats, presenting only subtle expression differences, mainly for structural proteins as tropomyosin beta chain, myosin light polypeptide 6 and moesin. However, in PASMCs from MCT-treated rats, TMP modulated the biological processes "regulation of cell size", "response to endoplasmic reticulum (ER) stress", "response to transforming growth factor beta (TGF-beta)" and "DNA-templated transcription". The biological process "DNA-templated transcription" was found down-regulated in these TMP-treated cells, which was related to the decrease of the transcription factor high mobility group box 1 (HMGB1). This chromatin-binding protein participates in maintaining nucleosome structure and regulating gene transcription. Several reports showed that HMGB1 plays a role in the pulmonary vascular remodeling underlying PAH by enhancing PASMC proliferation and migration (Bauer, Shapiro et al. 2012; Sadamura-Takenaka, Ito et al. 2014; Wang, Peng et al. 2014; Zabini, Crnkovic et al. 2015). Furthermore, the inhibition of HMGB1 was previously shown to attenuate the progression of MCT-induced PAH (Yang, Kim et al. 2014).

TMP also modulated collagen alpha-1 (I) chain, collagen alpha-2 (I) chain and collagen alpha-1 (III) chain levels. Collagen deposition in pulmonary vessels is one of the main features of vascular remodeling observed in PAH and circulating markers of collagen metabolism have been associated with worse stages of PAH (Safdar, Tamez et al. 2014). According to our data, TMP decreased the levels of these proteins, which could be mediated by TGF-beta signaling. Dysfunctional signaling of the TGF-beta pathway is associated with PAH pathogenesis, contributing to abnormal SMC proliferation. In addition, TGF-beta signaling inhibition prevented MCT-induced PAH development and progression, involving PASMC proliferation decrease (Zaiman, Podowski et al. 2008; Long, Crosby et al. 2009; Thomas, Docx et al. 2009). Thus, TMP-related down-regulation of the response to TGF-beta can also contribute to the anti-proliferative effects on PASMCs from MCT-treated rats. Interestingly, TMP also up-regulated the biological process "response to ER stress". This is associated with the increased levels of heat shock protein (HSP)70 and HSP90 family of chaperones (heat shock protein HSP90-beta, 78 kDa glucose-regulated protein, hypoxia up-regulated protein 1 and stress-70 protein,

mitochondrial) involved in the correct folding and degradation of misfolded proteins. ER stress has been described in the pulmonary arteries of PAH patients and it was recently suggested as a new therapeutic target. The use of some chemical chaperones in experimental PAH was shown to prevent and even reverse the disease, suppressing proliferation and inducing apoptosis of PASMCs (Dromparis, Paulin et al. 2013). So, the observed molecular alterations induced by TMP treatment may underlie our *in vivo* findings of significant attenuation of the increased pulmonary artery medial wall thickness, which may have contributed to decrease the RV dysfunction and hypertrophy associated to MCT-induced PAH.

In overall, our data highlighted that both exercise training, as a non-pharmacological approach and TMP, as a pharmacological strategy, can positively interfere with the RV dysfunction and pulmonary vascular remodeling underlying PAH, supporting their clinical relevance in the management of this disease. The observed benefits are associated with the modulation of inflammation-related signaling pathways in both preventive and therapeutic strategies.

CHAPTER V
CONCLUSIONS

Conclusions

Pulmonary arterial hypertension is a devastating disease associated with right heart failure and premature death. Although current therapies have allowed an increase on patient survival, this disease remains without a cure and PAH-related mortality is still enormously high. Aiming to find novel preventive and therapeutic strategies, three experimental studies were developed to assess the potential application of exercise training and the anticancer drug TMP in the management of PAH. Data obtained allowed to conclude that:

i) One year of moderate exercise training improves the cardiac function by increasing RV antioxidant capacity and mitochondrial ability to produce ATP, though with no significant impact on mitochondrial biogenesis.

ii) Prior exercise training prevents pulmonary artery remodeling and cardiac dysfunction, hypertrophy and fibrosis associated to MCT-induced PAH, supporting its beneficial role for the prevention of this disease. These functional and morphological alterations were related with reduced beta/alpha-MHC ratio, modulation of TWEAK/NF-κB signaling and atrogin-1 levels and induction of a shift of MMPs activity from MMP-9 to MMP-2 activity in the RV.

iii) TMP might be seen as a novel therapeutic strategy for the clinical management of PAH once promotes the reduction of the maladaptive vascular remodeling and attenuates RV dysfunction and hypertrophy associated to the disease. These effects were related to the modulation of the biological processes “regulation of cell size”, “response to endoplasmic reticulum stress”, “response to transforming growth factor beta” and “DNA-templated transcription” in PASMCs collected from MCT-treated rats. The transcription factor HMGB1 seems to be a key target of TMP, whose down-regulation may justify, at least in part, its anti-proliferative effects in PASMCs.

Taken together, data suggest that preconditioning exercise training and TMP treatment can be of clinical relevance in the management of PAH. Further studies describing the molecular mechanisms underlying exercise training effects on PAH, focusing not only in

the heart, but also in the pulmonary artery and skeletal muscle will assist in the recommendation of exercise training for the clinical management of PAH. Additionally, future work focused on the evaluation of TMP effects in other pulmonary artery cell types, such as endothelial cells, and also in the heart will contribute to propose this anticancer drug as a novel therapeutic alternative in PAH treatment.

REFERENCES

References

Amado, F. M., A. Barros, et al. (2014). "An integrated perspective and functional impact of the mitochondrial acetylome." Expert Rev Proteomics **11**(3): 383-394.

Babu, A. S., R. Arena, et al. (2016). "Exercise intolerance in pulmonary hypertension: mechanism, evaluation and clinical implications." Expert Rev Respir Med **10**(9): 979-990.

Baldi, F., L. Fuso, et al. (2014). "Optimal management of pulmonary arterial hypertension: prognostic indicators to determine treatment course." Ther Clin Risk Manag **10**: 825-839.

Baptista, R., J. Meireles, et al. (2013). "Pulmonary hypertension in Portugal: first data from a nationwide registry." Biomed Res Int **2013**: 489574.

Barry, S. P., S. M. Davidson, et al. (2008). "Molecular regulation of cardiac hypertrophy." Int J Biochem Cell Biol **40**(10): 2023-2039.

Bauer, E. M., R. Shapiro, et al. (2012). "High mobility group box 1 contributes to the pathogenesis of experimental pulmonary hypertension via activation of Toll-like receptor 4." Mol Med **18**: 1509-1518.

Belhaj, A., L. Dewachter, et al. (2013). "Heme oxygenase-1 and inflammation in experimental right ventricular failure on prolonged overcirculation-induced pulmonary hypertension." PLoS One **8**(7): e69470.

Bellafiore, M., G. Battaglia, et al. (2013). "The involvement of MMP-2 and MMP-9 in heart exercise-related angiogenesis." J Transl Med **11**: 283.

Benito, B., G. Gay-Jordi, et al. (2011). "Cardiac arrhythmogenic remodeling in a rat model of long-term intensive exercise training." Circulation **123**(1): 13-22.

Bindu, S., V. B. Pillai, et al. (2016). "Role of sirtuins in regulating pathophysiology of the heart." Trends Endocrinol Metab **27**(8): 563-573.

Buys, R., A. Avila, et al. (2015). "Exercise training improves physical fitness in patients with pulmonary arterial hypertension: a systematic review and meta-analysis of controlled trials." BMC Pulm Med **15**: 40.

Campian, M. E., M. Hardziyenka, et al. (2010). "Early inflammatory response during the development of right ventricular heart failure in a rat model." Eur J Heart Fail **12**(7): 653-658.

Chang, C. C., J. D. Heller, et al. (2004). "Tetra-O-methyl nordihydroguaiaretic acid induces growth arrest and cellular apoptosis by inhibiting Cdc2 and survivin expression." Proc Natl Acad Sci U S A **101**(36): 13239-13244.

Church, D. N. and D. C. Talbot (2012). "Survivin in solid tumors: rationale for development of inhibitors." Curr Oncol Rep **14**(2): 120-128.

Correia-Pinto, J., T. Henriques-Coelho, et al. (2009). "Time course and mechanisms of left ventricular systolic and diastolic dysfunction in monocrotaline-induced pulmonary hypertension." Basic Res Cardiol **104**(5): 535-545.

D'Alonzo, G. E., R. J. Barst, et al. (1991). "Survival in patients with primary pulmonary hypertension: results from a national prospective registry." Ann Intern Med **115**(5): 343-349.

de Man, F. S., M. L. Handoko, et al. (2009). "Effects of exercise training in patients with idiopathic pulmonary arterial hypertension." Eur Respir J **34**(3): 669-675.

Delcroix, M. and L. Howard (2015). "Pulmonary arterial hypertension: the burden of disease and impact on quality of life." Eur Respir Rev **24**(138): 621-629.

Dromparis, P., R. Paulin, et al. (2013). "Attenuating endoplasmic reticulum stress as a novel therapeutic strategy in pulmonary hypertension." Circulation **127**(1): 115-125.

Ehlken, N., M. Lichtblau, et al. (2016). "Exercise training improves peak oxygen consumption and haemodynamics in patients with severe pulmonary arterial hypertension and inoperable chronic thrombo-embolic pulmonary hypertension: a prospective, randomized, controlled trial." Eur Heart J **37**(1): 35-44.

Ellison, Georgina M., C. Vicinanza, et al. (2013). "Adult c-kit(pos) cardiac stem cells are necessary and sufficient for functional cardiac regeneration and repair." Cell **154**(4): 827-842.

Ferreira, R., D. Moreira-Goncalves, et al. (2015). "Unraveling the exercise-related proteome signature in heart." Basic Res Cardiol **110**(1): 454.

Figueiredo, P. A., R. M. Ferreira, et al. (2008). "Age-induced morphological, biochemical, and functional alterations in isolated mitochondria from murine skeletal muscle." J Gerontol A Biol Sci Med Sci **63**(4): 350-359.

Fowler, R. M., K. R. Gain, et al. (2012). "Exercise intolerance in pulmonary arterial hypertension." Pulm Med **2012**: 359204.

Galie, N., M. Humbert, et al. (2016). "2015 ESC/ERS Guidelines for the diagnosis and treatment of pulmonary hypertension: The Joint Task Force for the Diagnosis and Treatment of Pulmonary Hypertension of the European Society of Cardiology (ESC) and the European Respiratory Society (ERS): Endorsed by: Association for European Paediatric and Congenital Cardiology (AEPC), International Society for Heart and Lung Transplantation (ISHLT)." Eur Heart J **37**(1): 67-119.

Gaspar-Pereira, S., N. Fullard, et al. (2012). "The NF-kappaB subunit c-Rel stimulates cardiac hypertrophy and fibrosis." Am J Pathol **180**(3): 929-939.

Gay-Jordi, G., E. Guash, et al. (2013). "Losartan prevents heart fibrosis induced by long-term intensive exercise in an animal model." PLoS One **8**(2): e55427.

Gielen, S., V. Adams, et al. (2003). "Anti-inflammatory effects of exercise training in the skeletal muscle of patients with chronic heart failure." J Am Coll Cardiol **42**(5): 861-868.

Grunig, E., N. Ehlken, et al. (2011). "Effect of exercise and respiratory training on clinical progression and survival in patients with severe chronic pulmonary hypertension." Respiration **81**(5): 394-401.

Grunig, E., M. Lichtblau, et al. (2012). "Safety and efficacy of exercise training in various forms of pulmonary hypertension." Eur Respir J **40**(1): 84-92.

Guignabert, C., L. Tu, et al. (2015). "New molecular targets of pulmonary vascular remodeling in pulmonary arterial hypertension: importance of endothelial communication." Chest **147**(2): 529-537.

Gurtu, V. and E. D. Michelakis (2015). "Emerging therapies and future directions in pulmonary arterial hypertension." Can J Cardiol **31**(4): 489-501.

Handoko, M. L., F. S. de Man, et al. (2009). "Opposite effects of training in rats with stable and progressive pulmonary hypertension." Circulation **120**(1): 42-49.

Harvey, P. A. and L. A. Leinwand (2011). "The cell biology of disease: cellular mechanisms of cardiomyopathy." J Cell Biol **194**(3): 355-365.

Henriques-Coelho, T., J. Correia-Pinto, et al. (2004). "Endogenous production of ghrelin and beneficial effects of its exogenous administration in monocrotaline-induced pulmonary hypertension." Am J Physiol Heart Circ Physiol **287**(6): H2885-2890.

Henriques-Coelho, T., S. M. Oliveira, et al. (2008). "Thymulin inhibits monocrotaline-induced pulmonary hypertension modulating interleukin-6 expression and suppressing p38 pathway." Endocrinology **149**(9): 4367-4373.

Hoeper, M. M., H. J. Bogaard, et al. (2013). "Definitions and diagnosis of pulmonary hypertension." J Am Coll Cardiol **62**(25 Suppl): D42-50.

Huang, J. B., Y. L. Liu, et al. (2010). "Novel strategy for treatment of pulmonary arterial hypertension: enhancement of apoptosis." Lung **188**(3): 179-189.

Humbert, M., E. M. Lau, et al. (2014). "Advances in therapeutic interventions for patients with pulmonary arterial hypertension." Circulation **130**(24): 2189-2208.

La Gerche, A. and G. Claessen (2015). "Is exercise good for the right ventricle? Concepts for health and disease." Can J Cardiol **31**(4): 502-508.

La Gerche, A., T. Roberts, et al. (2014). "The response of the pulmonary circulation and right ventricle to exercise: exercise-induced right ventricular dysfunction and structural remodeling in endurance athletes (2013 Grover Conference series)." Pulm Circ **4**(3): 407-416.

Li, L., C. Muhlfeld, et al. (2011). "Mitochondrial biogenesis and PGC-1alpha deacetylation by chronic treadmill exercise: differential response in cardiac and skeletal muscle." Basic Res Cardiol **106**(6): 1221-1234.

Long, L., A. Crosby, et al. (2009). "Altered bone morphogenetic protein and transforming growth factor-beta signaling in rat models of pulmonary hypertension: potential for activin receptor-like kinase-5 inhibition in prevention and progression of disease." Circulation **119**(4): 566-576.

Lourenco, A. P., D. Fontoura, et al. (2012). "Current pathophysiological concepts and management of pulmonary hypertension." Int J Cardiol **155**(3): 350-361.

Lu, J. M., J. Nurko, et al. (2010). "Molecular mechanisms and clinical applications of nordihydroguaiaretic acid (NDGA) and its derivatives: an update." Med Sci Monit **16**(5): RA93-100.

Maarman, G., S. Lecour, et al. (2013). "A comprehensive review: the evolution of animal models in pulmonary hypertension research; are we there yet?" Pulm Circ **3**(4): 739-756.

Malenfant, S., A. S. Neyron, et al. (2013). "Signal transduction in the development of pulmonary arterial hypertension." Pulm Circ **3**(2): 278-293.

Mandegar, M., Y. C. Fung, et al. (2004). "Cellular and molecular mechanisms of pulmonary vascular remodeling: role in the development of pulmonary hypertension." Microvasc Res **68**(2): 75-103.

Mann, N. and A. Rosenzweig (2012). "Can exercise teach us how to treat heart disease?" Circulation **126**(22): 2625-2635.

Matura, L. A., A. McDonough, et al. (2012). "Cluster analysis of symptoms in pulmonary arterial hypertension: a pilot study." Eur J Cardiovasc Nurs **11**(1): 51-61.

McGoon, M. D., R. L. Benza, et al. (2013). "Pulmonary arterial hypertension: epidemiology and registries." J Am Coll Cardiol **62**(25 Suppl): D51-59.

McLaughlin, V. V., S. J. Shah, et al. (2015). "Management of pulmonary arterial hypertension." J Am Coll Cardiol **65**(18): 1976-1997.

Mereles, D., N. Ehlken, et al. (2006). "Exercise and respiratory training improve exercise capacity and quality of life in patients with severe chronic pulmonary hypertension." Circulation **114**(14): 1482-1489.

Montani, D., S. Gunther, et al. (2013). "Pulmonary arterial hypertension." Orphanet J Rare Dis **8**: 97.

Moreira-Goncalves, D., R. Ferreira, et al. (2015). "Cardioprotective effects of early and late aerobic exercise training in experimental pulmonary arterial hypertension." Basic Res Cardiol **110**(6): 57.

Novoyatleva, T., A. Sajjad, et al. (2014). "TWEAK-Fn14 cytokine-receptor axis: a new player of myocardial remodeling and cardiac failure." Front Immunol **5**: 50.

Okada, M., R. Kikuzuki, et al. (2008). "Captopril attenuates matrix metalloproteinase-2 and -9 in monocrotaline-induced right ventricular hypertrophy in rats." J Pharmacol Sci **108**(4): 487-494.

Pandey, A., S. Garg, et al. (2015). "Efficacy and safety of exercise training in chronic pulmonary hypertension: systematic review and meta-analysis." Circ Heart Fail **8**(6): 1032-1043.

Peacock, A. J., N. F. Murphy, et al. (2007). "An epidemiological study of pulmonary arterial hypertension." Eur Respir J **30**(1): 104-109.

Powers, S. K., S. L. Lennon, et al. (2002). "Exercise and cardioprotection." Curr Opin Cardiol **17**(5): 495-502.

Powers, S. K., A. J. Smuder, et al. (2014). "Mechanisms of exercise-induced cardioprotection." Physiology (Bethesda) **29**(1): 27-38.

Provencher, S. and J. T. Granton (2015). "Current treatment approaches to pulmonary arterial hypertension." Can J Cardiol **31**(4): 460-477.

Rondelet, B., C. Dewachter, et al. (2012). "Prolonged overcirculation-induced pulmonary arterial hypertension as a cause of right ventricular failure." Eur Heart J **33**(8): 1017-1026.

Ryan, B. M., N. O'Donovan, et al. (2009). "Survivin: a new target for anti-cancer therapy." Cancer Treat Rev **35**(7): 553-562.

Ryan, J. J., G. Marsboom, et al. (2013). "Rodent models of group 1 pulmonary hypertension." Handb Exp Pharmacol **218**: 105-149.

Sadamura-Takenaka, Y., T. Ito, et al. (2014). "HMGB1 promotes the development of pulmonary arterial hypertension in rats." PLoS One **9**(7): e102482.

Safdar, Z., E. Tamez, et al. (2014). "Circulating collagen biomarkers as indicators of disease severity in pulmonary arterial hypertension." JACC Heart Fail **2**(4): 412-421.

Sakao, S., K. Tatsumi, et al. (2010). "Reversible or irreversible remodeling in pulmonary arterial hypertension." Am J Respir Cell Mol Biol **43**(6): 629-634.

Schultze, A. E. and R. A. Roth (1998). "Chronic pulmonary hypertension--the monocrotaline model and involvement of the hemostatic system." J Toxicol Environ Health B Crit Rev **1**(4): 271-346.

Sengupta, P. (2013). "The laboratory rat: relating its age with human's." Int J Prev Med **4**(6): 624-630.

Shimoda, L. A. and S. S. Laurie (2013). "Vascular remodeling in pulmonary hypertension." J Mol Med (Berl) **91**(3): 297-309.

Simonneau, G., M. A. Gatzoulis, et al. (2013). "Updated clinical classification of pulmonary hypertension." J Am Coll Cardiol **62**(25 Suppl): D34-41.

Tao, L., Y. Bei, et al. (2015). "Exercise for the heart: signaling pathways." Oncotarget **6**(25): 20773-20784.

Thomas, M., C. Docx, et al. (2009). "Activin-like kinase 5 (ALK5) mediates abnormal proliferation of vascular smooth muscle cells from patients with familial pulmonary

arterial hypertension and is involved in the progression of experimental pulmonary arterial hypertension induced by monocrotaline." Am J Pathol **174**(2): 380-389.

Umar, S., P. Steendijk, et al. (2010). "Novel approaches to treat experimental pulmonary arterial hypertension: a review." J Biomed Biotechnol **2010**: 702836.

van Berlo, J. H., O. Kanisicak, et al. (2014). "c-kit+ cells minimally contribute cardiomyocytes to the heart." Nature **509**(7500): 337-341.

Van der Heiden, K., S. Cuhlmann, et al. (2010). "Role of nuclear factor kappaB in cardiovascular health and disease." Clin Sci (Lond) **118**(10): 593-605.

van der Loo, B., R. Labugger, et al. (2000). "Enhanced peroxynitrite formation is associated with vascular aging." J Exp Med **192**(12): 1731-1744.

Vettor, R., A. Valerio, et al. (2014). "Exercise training boosts eNOS-dependent mitochondrial biogenesis in mouse heart: role in adaptation of glucose metabolism." Am J Physiol Endocrinol Metab **306**(5): E519-528.

Voelkel, N. F., J. Gomez-Arroyo, et al. (2012). "Pathobiology of pulmonary arterial hypertension and right ventricular failure." Eur Respir J **40**(6): 1555-1565.

Vonk-Noordegraaf, A., F. Haddad, et al. (2013). "Right heart adaptation to pulmonary arterial hypertension: physiology and pathobiology." J Am Coll Cardiol **62**(25 Suppl): D22-33.

Wang, H. L., L. P. Peng, et al. (2014). "HMGB1 enhances smooth muscle cell proliferation and migration in pulmonary artery remodeling." Int J Clin Exp Pathol **7**(7): 3836-3844.

Waring, C. D., C. Vicinanza, et al. (2014). "The adult heart responds to increased workload with physiologic hypertrophy, cardiac stem cell activation, and new myocyte formation." Eur Heart J **35**(39): 2722-2731.

Watts, J. A., M. A. Gellar, et al. (2008). "Role of inflammation in right ventricular damage and repair following experimental pulmonary embolism in rats." Int J Exp Pathol **89**(5): 389-399.

Watts, J. A., J. Zagorski, et al. (2006). "Cardiac inflammation contributes to right ventricular dysfunction following experimental pulmonary embolism in rats." J Mol Cell Cardiol **41**(2): 296-307.

Xiao, J., T. Xu, et al. (2014). "Exercise-induced physiological hypertrophy initiates activation of cardiac progenitor cells." Int J Clin Exp Pathol **7**(2): 663-669.

Yang, P. S., D. H. Kim, et al. (2014). "Glycyrrhizin, inhibitor of high mobility group box-1, attenuates monocrotaline-induced pulmonary hypertension and vascular remodeling in rats." Respir Res **15**: 148.

Yuan, P., X. T. Yuan, et al. (2015). "Exercise training for pulmonary hypertension: a systematic review and meta-analysis." Int J Cardiol **178**: 142-146.

Zabini, D., S. Crnkovic, et al. (2015). "High-mobility group box-1 induces vascular remodelling processes via c-Jun activation." J Cell Mol Med **19**(5): 1151-1161.

Zaglia, T., G. Milan, et al. (2014). "Atrogin-1 deficiency promotes cardiomyopathy and premature death via impaired autophagy." J Clin Invest **124**(6): 2410-2424.

Zaiman, A. L., M. Podowski, et al. (2008). "Role of the TGF-beta/Alk5 signaling pathway in monocrotaline-induced pulmonary hypertension." Am J Respir Crit Care Med **177**(8): 896-905.

APPENDIX – SUPPLEMENTARY DATA

REVIEW II – MECHANISMS UNDERLYING THE IMPACT OF EXERCISE TRAINING IN PULMONARY ARTERIAL HYPERTENSION

Supplementary Table S1 – Summary of clinical studies assessing exercise training effects in pulmonary arterial hypertension.

Patient characteristics	Exercise training program	Major findings	References
Control group • N=15 • Age=53 ± 14 • 67% female • PAH (n=11) and CTEPH (n=4) • WHO – FC II-IV (80% III) Training Group • N=15 • 47 ± 12 • 67% female • PAH (n=13) and CTEPH (n=2) • WHO – FC II-IV (67% III)	*In hospital (3 weeks)* • 7 days/week of interval bicycle ergometer training at lower workload for 1⁄2 min and a higher workload for 1 min, for 10 to 25 min/day, (60% to 80% of peak HR). • 60 min of walking, 5 days/week (flat-ground and uphill walking). • Mental training, 5 days/week. • 30 min of dumbbell training of single muscle groups with low weights (500 to 1000 g) and 30 min of respiratory training, 5 days/week. *Home-based intervention (12 weeks)* • Bicycle exercise training, once daily, 15-30 min, 5 days/week. • Respiratory exercise and dumbbell training every other day, 15-30 min. • Walking training twice a week.	↑6MWD ↑QOL ↓WHO – FC ↑VO_2 (peak + AT) ↑Workload (maximal + AT) = SPAP Adverse events: dizziness, 2 patients	[1]
Training Group • N=2 • 50 and 57 years • 50% female • Idiopathic PAH (1) and Associated PAH (CTD) (1) • NYHA – FC II (100% II)	*Institution based (6 weeks)* • Cycle ergometry at workloads progressing from 50% to 80% of peak workload, 3 days/week. Each session consisted of 5 min of warm-up, 35 min of loaded cycling, and 5 min of cool down.	↑6MWD ↑QOL ↓NYHA – FC ↑VO_2 (AT) ↑Workload (AT) No adverse events	[2]
Training Group • N=19 • 42 ± 13 • 79% female • Idiopathic PAH (19) • NYHA – FC II-III (84% III)	*Institution based (12 weeks)* • Bicycle training. • Quadriceps strength and endurance training.	= 6MWD = Peak exercise capacity ↑Endurance capacity ↑Quadriceps strength and endurance ↑Capillaries *per* muscle fiber (muscle biopsies) = CSA and fiber type distribution ↑Oxidative enzyme activity	[3]

		= BNP levels Adverse events: dizziness, 2 patients	
Control Group • N=4 • 33 ± 6 • 25% female • Associated PAH (CHD) (4) • NYHA – FC II-III (50% III) Training Group • N=4 • 23 ± 7 • 50% female • Associated PAH (CHD) (4) • NYHA – FC II-III (75% III)	*Institution based (3 months)* *2 days/week:* • 10 min warming up, with stretching of long muscles. • Resisted exercises (1–2 kg). • Aerobic interval training in a bicycle ergometer during 24 min with bases at 10–25W and 30-second peaks of 20–50W (80% of HR reached in the 6MWT). • Education. *From 3rd to 12th month:* • Flat-ground walking daily. • Similar rehabilitation exercises as done in the rehabilitation sessions.	↑6MWD ↓NYHA – FC ↑O_2 saturation = Hand and leg strength = QOL = BNP levels No adverse events	[4]
Training Group • N=5 • 40 ± 15 • 80% female • Idiopathic PAH (5) • WHO – FC II-III (60% II)	*Institution based (12 weeks)* *3 days/week:* • 10 to 15 min of cycling exercise with workload initially set to 60% of the maximal workload achieved during incremental exercise test. • 2 sets of 10 to 12 repetitions for 6 to 8 different exercises involving single muscle groups (arms and quadriceps). • 15 min of brisk walking on a treadmill (85% of the mean speed of 6MWT).	↑6MWD ↓Minute ventilation ↓Type IIx muscle fiber proportion No adverse events	[5]
Control Group • N=11 • 46 ± 5 • 45% female • Idiopathic PAH (7) and Associated PAH (CTD) (4) • NYHA – FC II-III (82% II) Training Group • N=11 • 57 ± 4 • 91% female • Idiopathic PAH (3), Associated PAH (CTD, CHD) (6) and CTEPH (2) • NYHA – FC II-III (64% III)	*Institution based (12 weeks)* *2 days/week* 1-hour sessions of exercise training, two 6-week blocks (60-80% of CPET HRmax): • *first block:* interval training with treadmill walking, cycling, and step climbing *second block:* longer periods of continuous aerobic exercise, with resistance training by step climbing, unsupported arm/leg exercises with and without dumbbells (500-1000 g), and supporting body weight over a chair • daily home-based exercise with stair-climbing and brisk walking	↑6MWD ↑Peak VO_2 ↑Peak work rate = BNP levels = SPAP = CO No adverse events	[6]

Training Group • N=58 • 51 ± 12 • 72% female • Idiopathic PAH (37), Heritable PAH (3), Associated PAH (CTD, CHD, Portal Hypertension, HIV) (7), LD-PH (3), CTEPH (6) and Others (2) • WHO – FC II-IV (76% III)	*In hospital (3 weeks) + Home-based intervention (12 weeks)* Same as [1]. 24 ± 12 months follow-up	↑6MWD ↑QOL ↓WHO – FC ↓Rest heart rate ↑VO_2 (peak + AT) ↑Workload (maximal + AT) Survival: 1year, 100%; 2 years, 95% Adverse events: dizziness, 2 patients; respiratory infections, 7 patients	[7]
Training Group • N=183 • 53 ± 15 • 69% female • Idiopathic PAH (83), Heritable PAH (4), Drug- and toxin-induced PAH (3), Associated PAH (CTD, CHD, Portal Hypertension, HIV) (43), LHD-PH (8), LD-PH (11) and CTEPH (31) • WHO – FC I-IV (75% III)	*In hospital (3 weeks) + Home-based intervention (12 weeks)* Same as [1].	↑6MWD (in all PH forms and FC, including IV) ↑QOL ↓WHO – FC ↑VO_2 (peak + AT) ↓Rest heart rate ↓SPAP ↑Maximal workload Adverse events: respiratory infections, 14 patients; syncope, 2 patients; presyncope, 6 patients	[8]
Training Group • N=21 • 52 ± 18 • 95% female • Associated PAH (CTD) (21) • WHO – FC II-IV (43% II)	*In hospital (3 weeks) + Home-based intervention (12 weeks)* Same as [1]. 2.9 ± 1.9 years follow-up	↑6MWD ↑QOL ↑VO_2 (peak + AT) ↓Rest heart rate ↑O_2 saturation ↑Maximal workload ↓SPAP = BNP levels Survival: 1 year, 100%; 2 years, 100%; 3 years,73% Adverse events: gastrointestinal infection with	[9]

		diarrhea, 1 patient; respiratory infections, 2 patients	
Control Group • N=10 • 54 ± 14 • 60% female • Idiopathic PAH (4), Heritable PAH (1), Associated PAH (CTD, Portal Hypertension) (2) and CTEPH (3) • WHO – FC II-III (90% III) Training Group • N=10 • 47 ± 8 • 80% female • Idiopathic PAH (7), Associated PAH (CTD, Portal Hypertension) (2) and CTEPH (1) • WHO – FC II-III (70% III)	*In hospital (3 weeks)* Same as [1].	↑6MWD ↑MRI flow peak velocity ↑MRI perfusion (pulmonary blood volume) No adverse events	[10]
Training Group • N=20 • 48 ± 11 • 80% female • Associated PAH (CHD) (20) • WHO – FC II-III (70% III)	*In hospital (3 weeks) + Home-based intervention (12 weeks)* Same as [1]. 21 ± 14 months follow-up	↑6MWD ↑QOL ↑Peak VO_2 = SPAP ↑Maximal workload ↑BNP levels Survival: 1 year, 100%; 2 years, 100%; 3 years, 95% Adverse events: respiratory infections, 4 patients	[11]
Control Group • N=13 • 56 ± 9 • 100% female • Idiopathic PAH (3), Drug-induced PAH (1) and Associated PAH (CTD) (9) • WHO/NYHA – FC II-III (62% II)	*Institution based (10 weeks)* • 24-30 sessions of treadmill walking for 30-45 min *per* session at 70-80% of heart rate reserve and education.	↑6MWD ↑QOL ↑time to exercise intolerance ↑Peak work rate No adverse events	[12]

Training Group • N= 10 • 53 ± 13 • 100% female • Idiopathic PAH (2) and Associated PAH (CTD) (8) • WHO/NYHA – FC I-IV (40% II=III)			
Control Group • N=13 • 55 ± 9 • 100% female • Idiopathic PAH (4) and Associated PAH (CTD) (9) • WHO/NYHA – FC II-III (62% II) Training Group • N=11 • 53 ± 12 • 100% female • Idiopathic PAH (2) and Associated PAH (CTD) (9) • WHO/NYHA – FC I-IV (45% III)	*Institution based (10 weeks)* • 24-30 sessions of treadmill walking for 30-45 min *per* session at 70-80% of heart rate reserve, 3 days/week and education.	↑ physical activity ↓fatigue ↑6MWD ↑peak power output ↑symptom limited treadmill exercise test duration No adverse events	[13]
Training Group • N=7 • 60 ± 11 • 57% female • Idiopathic PAH (5) and Associated PAH (CTD) (2) • WHO – FC III-IV (86% III)	*In hospital (3 weeks) + Home-based intervention (12 weeks)* Same as [1].	↑6MWD ↑respiratory muscle strength No adverse events	[14]
Control Group • N=46 • 53 ± 10 • 65% female • Idiopathic PAH (18), Associated PAH (CTD, CHD, Portal Hypertension, HIV) (12), LD-PH (5), CTEPH (8) and Others (3) • WHO – FC II-IV (70% III) Training Group • N=58 • 51 ± 12	*In hospital (3 weeks) + Home-based intervention (12 weeks)* Same as [1]. 24 ± 12 months follow-up	↑time to clinical worsening ↑QOL ↓healthcare costs Survival: 1year, 100%; 2 years, 95% No adverse events	[15]

• 72% female • Idiopathic PAH (37), Heritable PAH (3), Associated PAH (CTD, CHD, Portal Hypertension, HIV) (7), LD-PH (3), CTEPH (6) and Others (2) • WHO – FC II-IV (76% III)			
Training Group • N=17 • 62 ± 13 • 65% female • PAH (14) and CTEPH (3) • WHO – FC II-III (65% III)	*Institution based (10 months)* • 90 min once a month at low workloads (10 to 60 W): 30 min breathing exercises, 30 min moderate strengthening exercises and very moderate endurance training of orthostatic leg muscles with general coordination movements and 30 min education. • Repetition of respiratory and exercise training at home once daily for a total of 15-30 min, 5 days/week.	= 6MWD ↑QOL No adverse events	[16]
Control Group • N=41 • 57 ± 15 • 51% female • PAH (26) and CTEPH (15) • WHO – FC II-IV (75% III) Training Group • N=46 • 55 ± 15 • 57% female • PAH (35) and CTEPH (11) • WHO – FC II-III (82% III)	*In hospital (3 weeks) + Home-based intervention (12 weeks)* Same as [1].	↑6MWD ↑QOL ↑Peak VO_2 ↑CI (rest and during exercise) ↑CO (rest and during exercise) ↓mPAP ↓PVR ↑Exercise capacity = BNP levels No adverse events	[17]

Legend: ↑, increase; ↓, decrease; =, no change; 6MWD, 6-minute walk distance; 6MWT, 6-minute walk test; AT, anaerobic threshold; BNP, brain natriuretic peptide; CHD, congenital heart disease; CI, cardiac index; CO, cardiac output; CPET, cardiopulmonary exercise testing; CSA, cross-sectional area; CTD, connective tissue disease; CTEPH, chronic thromboembolic pulmonary hypertension; HIV, human immunodeficiency virus; HR, heart rate; LD-PH, PH due to lung diseases; LHD-PH, PH due to left heart diseases; mPAP, mean pulmonary artery pressure; MRI, magnetic resonance imaging; NYHA – FC, New York Heart Association functional class; PAH, pulmonary arterial hypertension; PVR, pulmonary vascular resistance; QOL, quality of life; SPAP, systolic pulmonary artery pressure; VO_2, oxygen uptake; WHO – FC, World Health Organization functional class.

1. Mereles, D., N. Ehlken, S. Kreuscher, S. Ghofrani, M.M. Hoeper, M. Halank, F.J. Meyer, G. Karger, J. Buss, J. Juenger, N. Holzapfel, C. Opitz, J. Winkler, F.F. Herth, H. Wilkens, H.A. Katus, H. Olschewski, and E. Grunig, *Exercise and respiratory training improve exercise capacity and quality of life in patients with severe chronic pulmonary hypertension.* Circulation, 2006. **114**(14): p. 1482-9.
2. Shoemaker, M.J., J.L. Wilt, R. Dasgupta, and R.J. Oudiz, *Exercise training in patients with pulmonary arterial hypertension: a case report.* Cardiopulm Phys Ther J, 2009. **20**(4): p. 12-8.
3. De Man, F.S., M.L. Handoko, H. Groepenhoff, A.J. Van 'T Hul, J. Abbink, R.J. Koppers, H.P. Grotjohan, J.W. Twisk, H.J. Bogaard, A. Boonstra, P.E. Postmus, N. Westerhof, W.J. Van Der Laarse, and A. Vonk-Noordegraaf, *Effects of exercise training in patients with idiopathic pulmonary arterial hypertension.* Eur Respir J, 2009. **34**(3): p. 669-75.
4. Martinez-Quintana, E., G. Miranda-Calderin, A. Ugarte-Lopetegui, and F. Rodriguez-Gonzalez, *Rehabilitation program in adult congenital heart disease patients with pulmonary hypertension.* Congenit Heart Dis, 2010. **5**(1): p. 44-50.
5. Mainguy, V., F. Maltais, D. Saey, P. Gagnon, S. Martel, M. Simon, and S. Provencher, *Effects of a rehabilitation program on skeletal muscle function in idiopathic pulmonary arterial hypertension.* J Cardiopulm Rehabil Prev, 2010. **30**(5): p. 319-23.
6. Fox, B.D., M. Kassirer, I. Weiss, Y. Raviv, N. Peled, D. Shitrit, and M.R. Kramer, *Ambulatory rehabilitation improves exercise capacity in patients with pulmonary hypertension.* J Card Fail, 2011. **17**(3): p. 196-200.
7. Grunig, E., N. Ehlken, A. Ghofrani, G. Staehler, F.J. Meyer, J. Juenger, C.F. Opitz, H. Klose, H. Wilkens, S. Rosenkranz, H. Olschewski, and M. Halank, *Effect of exercise and respiratory training on clinical progression and survival in patients with severe chronic pulmonary hypertension.* Respiration, 2011. **81**(5): p. 394-401.
8. Grunig, E., M. Lichtblau, N. Ehlken, H.A. Ghofrani, F. Reichenberger, G. Staehler, M. Halank, C. Fischer, H.J. Seyfarth, H. Klose, A. Meyer, S. Sorichter, H. Wilkens, S. Rosenkranz, C. Opitz, H. Leuchte, G. Karger, R. Speich, and C. Nagel, *Safety and efficacy of exercise training in various forms of pulmonary hypertension.* Eur Respir J, 2012. **40**(1): p. 84-92.

9. Grunig, E., F. Maier, N. Ehlken, C. Fischer, M. Lichtblau, N. Blank, C. Fiehn, F. Stockl, F. Prange, G. Staehler, F. Reichenberger, H. Tiede, M. Halank, H.J. Seyfarth, S. Wagner, and C. Nagel, *Exercise training in pulmonary arterial hypertension associated with connective tissue diseases.* Arthritis Res Ther, 2012. **14**(3): p. R148.
10. Ley, S., C. Fink, F. Risse, N. Ehlken, C. Fischer, J. Ley-Zaporozhan, H.U. Kauczor, H. Klose, and E. Gruenig, *Magnetic resonance imaging to assess the effect of exercise training on pulmonary perfusion and blood flow in patients with pulmonary hypertension.* Eur Radiol, 2013. **23**(2): p. 324-31.
11. Becker-Grunig, T., H. Klose, N. Ehlken, M. Lichtblau, C. Nagel, C. Fischer, M. Gorenflo, H. Tiede, D. Schranz, A. Hager, H. Kaemmerer, O. Miera, S. Ulrich, R. Speich, S. Uiker, and E. Grunig, *Efficacy of exercise training in pulmonary arterial hypertension associated with congenital heart disease.* Int J Cardiol, 2013. **168**(1): p. 375-81.
12. Chan, L., L.M. Chin, M. Kennedy, J.G. Woolstenhulme, S.D. Nathan, A.A. Weinstein, G. Connors, N.A. Weir, B. Drinkard, J. Lamberti, and R.E. Keyser, *Benefits of intensive treadmill exercise training on cardiorespiratory function and quality of life in patients with pulmonary hypertension.* Chest, 2013. **143**(2): p. 333-43.
13. Weinstein, A.A., L.M. Chin, R.E. Keyser, M. Kennedy, S.D. Nathan, J.G. Woolstenhulme, G. Connors, and L. Chan, *Effect of aerobic exercise training on fatigue and physical activity in patients with pulmonary arterial hypertension.* Respir Med, 2013. **107**(5): p. 778-84.
14. Kabitz, H.J., H.C. Bremer, A. Schwoerer, F. Sonntag, S. Walterspacher, D.J. Walker, N. Ehlken, G. Staehler, W. Windisch, and E. Grunig, *The combination of exercise and respiratory training improves respiratory muscle function in pulmonary hypertension.* Lung, 2014. **192**(2): p. 321-8.
15. Ehlken, N., C. Verduyn, H. Tiede, G. Staehler, G. Karger, R. Nechwatal, C.F. Opitz, H. Klose, H. Wilkens, S. Rosenkranz, M. Halank, and E. Grunig, *Economic evaluation of exercise training in patients with pulmonary hypertension.* Lung, 2014. **192**(3): p. 359-66.

16. Ihle, F., S. Weise, A. Waelde, T. Meis, N. Kneidinger, C. Schild, G. Zimmermann, J. Behr, and C. Neurohr, *An integrated outpatient training program for patients with pulmonary hypertension-the Munich Pilot Project.* Int J Phys Med Rehabil, 2014. **2014**.

17. Ehlken, N., M. Lichtblau, H. Klose, J. Weidenhammer, C. Fischer, R. Nechwatal, S. Uiker, M. Halank, K. Olsson, W. Seeger, H. Gall, S. Rosenkranz, H. Wilkens, D. Mertens, H.J. Seyfarth, C. Opitz, S. Ulrich, B. Egenlauf, and E. Grunig, *Exercise training improves peak oxygen consumption and haemodynamics in patients with severe pulmonary arterial hypertension and inoperable chronic thrombo-embolic pulmonary hypertension: a prospective, randomized, controlled trial.* Eur Heart J, 2016. **37**(1): p. 35-44.

STUDY I – DIFFERENT SUSCEPTIBILITY TO METABOLIC ADAPTATIONS IN THE RIGHT AND LEFT VENTRICLE OF RATS FOLLOWING ONE YEAR OF MODERATE EXERCISE TRAINING

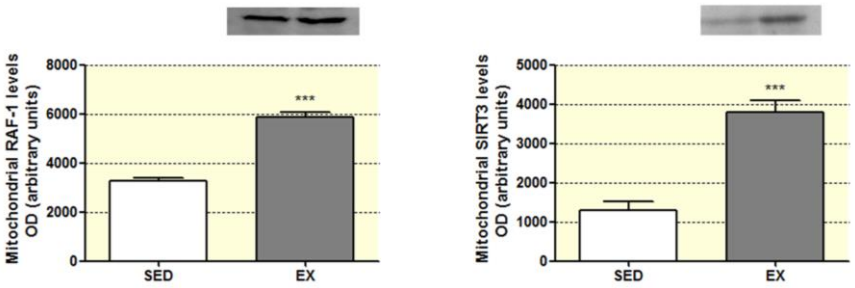

Supplementary Figure S1 – Effect of exercise training on RAF-1 and SIRT3 content in isolated mitochondria. *** P<0.001 vs. SED group.

STUDY III – HMGB1 DOWN-REGULATION MEDIATES TERAMEPROCOL VASCULAR ANTI-PROLIFERATIVE EFFECT IN EXPERIMENTAL PULMONARY HYPERTENSION

Supplementary Table S1 – List of all PASMC proteins identified using LC-MS/MS.

N	Unused	Total	% Cov	Accession #	Name	Species	Peptides (95%)	TMP10:CONT	*p* value
42	104,59	104,59	43,7	sp|Q62812|MYH9_RAT	Myosin-9 OS=Rattus norvegicus GN=Myh9 PE=1 SV=3	RAT	53	0,8182	0,0001
211	82,54	82,75	34,7	sp|D3ZHA0|FLNC_RAT	Filamin-C OS=Rattus norvegicus GN=Flnc PE=1 SV=1	RAT	40	0,9849	0,6548
53	69,8	69,8	81,1	sp|P31000|VIME_RAT	Vimentin OS=Rattus norvegicus GN=Vim PE=1 SV=2	RAT	45	1,4669	0,0003
307	68,43	68,43	64,4	sp|P06761|GRP78_RAT	78 kDa glucose-regulated protein OS=Rattus norvegicus GN=Hspa5 PE=1 SV=1	RAT	35	1,3363	0
108	57,06	57,06	56,2	sp|P48679|LMNA_RAT	Prelamin-A/C OS=Rattus norvegicus GN=Lmna PE=1 SV=1	RAT	25	1,1141	0,1314
441	55,6	56,57	32,4	sp|P16086|SPTN1_RAT	Spectrin alpha chain, non-erythrocytic 1 OS=Rattus norvegicus GN=Sptan1 PE=1 SV=2	RAT	25	1,2167	0
37	51,35	51,42	81,9	sp|P09495|TPM4_RAT	Tropomyosin alpha-4 chain OS=Rattus norvegicus GN=Tpm4 PE=1 SV=3	RAT	28	0,9349	0,3553
487	50,11	54,4	58,2	sp|P63018|HSP7C_RAT	Heat shock cognate 71 kDa protein OS=Rattus norvegicus GN=Hspa8 PE=1 SV=1	RAT	30	1,184	0,1908
241	49,43	49,82	72,8	sp|P60711|ACTB_RAT	Actin, cytoplasmic 1 OS=Rattus norvegicus GN=Actb PE=1 SV=1	RAT	71	0,8454	
278	49,17	49,17	43,1	sp|Q9QXQ0|ACTN4_RAT	Alpha-actinin-4 OS=Rattus norvegicus GN=Actn4 PE=1 SV=2	RAT	24	1,0369	0,7046
368	48,71	50,65	20,7	sp|P30427|PLEC_RAT	Plectin OS=Rattus norvegicus GN=Plec PE=1 SV=2	RAT	22	1,0905	0,1302
282	42,68	43,77	37,9	sp|Q66HD0|ENPL_RAT	Endoplasmin OS=Rattus norvegicus GN=Hsp90b1 PE=1 SV=2	RAT	19	1,0813	0,3144
222	39,46	39,53	61,2	sp|P11980|KPYM_RAT	Pyruvate kinase PKM OS=Rattus norvegicus GN=Pkm PE=1 SV=3	RAT	18	1,1723	0,0076
76	38,55	42,79	43	sp|P34058|HS90B_RAT	Heat shock protein HSP 90-beta OS=Rattus norvegicus GN=Hsp90ab1 PE=1 SV=4	RAT	20	1,2315	0,0195
312	36,86	36,86	35,7	sp|P02454|CO1A1_RAT	Collagen alpha-1(I) chain OS=Rattus norvegicus GN=Col1a1 PE=1 SV=5	RAT	27	0,498	0,0003
393	32,63	32,83	30,9	sp|P05197|EF2_RAT	Elongation factor 2 OS=Rattus norvegicus GN=Eef2 PE=1 SV=4	RAT	16	1,1923	0,0168
401	31,77	31,77	64,8	sp|Q62736|CALD1_RAT	Non-muscle caldesmon OS=Rattus norvegicus GN=Cald1 PE=1 SV=1	RAT	18	0,9377	0,0509
399	31,38	31,38	56,5	sp|P04797|G3P_RAT	Glyceraldehyde-3-phosphate dehydrogenase OS=Rattus norvegicus GN=Gapdh PE=1 SV=3	RAT	17	1,1577	0,141
491	30,96	30,96	60,7	sp|P07150|ANXA1_RAT	Annexin A1 OS=Rattus norvegicus GN=Anxa1 PE=1 SV=2	RAT	17	0,9533	0,4697
239	30,01	30,08	51,8	sp|P69897|TBB5_RAT	Tubulin beta-5 chain OS=Rattus norvegicus GN=Tubb5 PE=1 SV=1	RAT	20	0,8058	0,1798
162	29,4	48,89	47,2	sp|Q9Z1P2|ACTN1_RAT	Alpha-actinin-1 OS=Rattus norvegicus GN=Actn1 PE=1 SV=1	RAT	22	1,2287	0,0779

210	26,47	26,83	38,2	sp|P15999|ATPA_RAT	ATP synthase subunit alpha, mitochondrial OS=Rattus norvegicus GN=Atp5a1 PE=1 SV=2	RAT	14	1,0003	0,9956
83	26,4	26,45	39,4	sp|P48037|ANXA6_RAT	Annexin A6 OS=Rattus norvegicus GN=Anxa6 PE=1 SV=2	RAT	11	1,0234	0,7643
432	26,31	26,31	88,2	sp|Q05175|BASP1_RAT	Brain acid soluble protein 1 OS=Rattus norvegicus GN=Basp1 PE=1 SV=2	RAT	15	1,0105	0,7913
529	25,99	25,99	75,6	sp|P31232|TAGL_RAT	Transgelin OS=Rattus norvegicus GN=Tagln PE=1 SV=2	RAT	16	1,0565	0,1876
412	25,61	25,68	37	sp|P18418|CALR_RAT	Calreticulin OS=Rattus norvegicus GN=Calr PE=1 SV=1	RAT	14	1,144	0,3526
387	24,69	41,65	70,1	sp|P04692|TPM1_RAT	Tropomyosin alpha-1 chain OS=Rattus norvegicus GN=Tpm1 PE=1 SV=3	RAT	30	0,8235	0,01
244	24,68	24,87	64,9	sp|P63102|1433Z_RAT	14-3-3 protein zeta/delta OS=Rattus norvegicus GN=Ywhaz PE=1 SV=1	RAT	12	0,9172	0,8815
103	23,38	23,68	39,4	sp|P63039|CH60_RAT	60 kDa heat shock protein, mitochondrial OS=Rattus norvegicus GN=Hspd1 PE=1 SV=1	RAT	11	1,1562	0,1075
66	23,25	23,43	39,8	sp|P16617|PGK1_RAT	Phosphoglycerate kinase 1 OS=Rattus norvegicus GN=Pgk1 PE=1 SV=2	RAT	11	0,9794	0,7629
374	22,98	23,12	54,8	sp|Q63716|PRDX1_RAT	Peroxiredoxin-1 OS=Rattus norvegicus GN=Prdx1 PE=1 SV=1	RAT	14	1,1572	0,0138
186	22,98	23,05	20,1	sp|Q5QD51|AKA12_RAT	A-kinase anchor protein 12 OS=Rattus norvegicus GN=Akap12 PE=1 SV=1	RAT	11	0,7352	0,0047
98	22,67	22,98	39	sp|P68370|TBA1A_RAT	Tubulin alpha-1A chain OS=Rattus norvegicus GN=Tuba1a PE=1 SV=1	RAT	14	2,2037	
366	22,49	22,54	58,1	sp|P52944|PDLI1_RAT	PDZ and LIM domain protein 1 OS=Rattus norvegicus GN=Pdlim1 PE=2 SV=4	RAT	11	1,0195	0,7973
240	22,31	22,55	30,7	sp|P46462|TERA_RAT	Transitional endoplasmic reticulum ATPase OS=Rattus norvegicus GN=Vcp PE=1 SV=3	RAT	12	1,081	0,5236
259	22,15	22,35	34,4	sp|Q63598|PLST_RAT	Plastin-3 OS=Rattus norvegicus GN=Pls3 PE=2 SV=2	RAT	12	0,9222	0,1955
62	22,12	22,12	40,8	sp|P63259|ACTG_RAT	Actin, cytoplasmic 2 OS=Rattus norvegicus GN=Actg1 PE=1 SV=1	RAT	15	1,9656	0
354	21,97	23,38	14,8	sp|P11442|CLH1_RAT	Clathrin heavy chain 1 OS=Rattus norvegicus GN=Cltc PE=1 SV=3	RAT	11	1,2324	0,0009
143	21,81	21,91	44,2	sp|P05982|NQO1_RAT	NAD(P)H dehydrogenase [quinone] 1 OS=Rattus norvegicus GN=Nqo1 PE=1 SV=4	RAT	11	1,2422	0,0119
377	21,3	21,51	46,4	sp|Q63081|PDIA6_RAT	Protein disulfide-isomerase A6 OS=Rattus norvegicus GN=Pdia6 PE=1 SV=2	RAT	10	1,15	0,2451
39	20,93	20,93	27,8	sp|P02466|CO1A2_RAT	Collagen alpha-2(I) chain OS=Rattus norvegicus GN=Col1a2 PE=1 SV=3	RAT	13	0,5759	0,0011
154	20,61	20,69	40,1	sp|P10719|ATPB_RAT	ATP synthase subunit beta, mitochondrial OS=Rattus norvegicus GN=Atp5b PE=1 SV=2	RAT	11	1,258	0,0958
448	20,46	20,46	67,8	sp|Q5XFX0|TAGL2_RAT	Transgelin-2 OS=Rattus norvegicus GN=Tagln2 PE=1 SV=1	RAT	17	1,0336	0,5085
217	20,4	20,41	25,7	sp|Q5RKI0|WDR1_RAT	WD repeat-containing protein 1 OS=Rattus norvegicus GN=Wdr1 PE=1 SV=3	RAT	11	0,9936	0,9412
233	19,96	20,16	34,1	sp|Q68FR6|EF1G_RAT	Elongation factor 1-gamma OS=Rattus norvegicus GN=Eef1g PE=1 SV=3	RAT	8	1,0872	0,0982
306	19,8	20,01	79	sp|P15865|H14_RAT	Histone H1.4 OS=Rattus norvegicus GN=Hist1h1e PE=1 SV=3	RAT	9	1,0364	0,7589
177	19,67	19,76	30,7	sp|Q62952|DPYL3_RAT	Dihydropyrimidinase-related protein 3 OS=Rattus norvegicus GN=Dpysl3 PE=1 SV=2	RAT	10	0,9539	0,6931
88	19,46	19,74	45,3	sp|P04636|MDHM_RAT	Malate dehydrogenase, mitochondrial OS=Rattus norvegicus GN=Mdh2 PE=1 SV=2	RAT	10	1,079	0,2762

353	19,44	19,54	61,3	sp|Q5XFX0|TAGL2_RAT	Transgelin-2 OS=Rattus norvegicus GN=Tagln2 PE=2 SV=1	RAT	11	0,9383	0,659
230	17,52	17,52	48,6	sp|P04764|ENOA_RAT	Alpha-enolase OS=Rattus norvegicus GN=Eno1 PE=1 SV=4	RAT	10	1,2706	0,0006
140	17,52	17,52	44,5	sp|P25113|PGAM1_RAT	Phosphoglycerate mutase 1 OS=Rattus norvegicus GN=Pgam1 PE=1 SV=4	RAT	9	1,0181	0,8781
256	17,34	17,52	31,7	sp|P10860|DHE3_RAT	Glutamate dehydrogenase 1, mitochondrial OS=Rattus norvegicus GN=Glud1 PE=1 SV=2	RAT	10	1,0576	0,311
85	17,28	17,28	47	sp|P49242|RS3A_RAT	40S ribosomal protein S3a OS=Rattus norvegicus GN=Rps3a PE=1 SV=2	RAT	9	1,4054	0,0265
477	17,19	17,25	54,7	sp|P21533|RL6_RAT	60S ribosomal protein L6 OS=Rattus norvegicus GN=Rpl6 PE=1 SV=5	RAT	9	1,2032	0,0241
109	17,18	17,51	27,3	sp|P07153|RPN1_RAT	Dolichyl-diphosphooligosaccharide--protein glycosyltransferase subunit 1 OS=Rattus norvegicus GN=Rpn1 PE=2 SV=1	RAT	8	1,2021	0,1348
433	17,15	17,15	83,5	sp|P10111|PPIA_RAT	Peptidyl-prolyl cis-trans isomerase A OS=Rattus norvegicus GN=Ppia PE=1 SV=2	RAT	8	1,0645	0,5375
254	17,06	17,06	41,9	sp|P04642|LDHA_RAT	L-lactate dehydrogenase A chain OS=Rattus norvegicus GN=Ldha PE=1 SV=1	RAT	8	1,2101	0,0316
253	17,01	17,35	24,6	sp|P13941|CO3A1_RAT	Collagen alpha-1(III) chain OS=Rattus norvegicus GN=Col3a1 PE=2 SV=3	RAT	12	0,4031	0
100	16,93	17,19	45,5	sp|P14668|ANXA5_RAT	Annexin A5 OS=Rattus norvegicus GN=Anxa5 PE=1 SV=3	RAT	12	1,218	0,1316
119	16,78	16,93	18,3	sp|Q9ESN0|NIBAN_RAT	Protein Niban OS=Rattus norvegicus GN=Fam129a PE=2 SV=2	RAT	9	0,9938	0,9383
449	16,58	16,62	14,3	sp|P04937|FINC_RAT	Fibronectin OS=Rattus norvegicus GN=Fn1 PE=1 SV=2	RAT	8	1,159	0,048
310	16,5	16,58	24,4	sp|Q6P502|TCPG_RAT	T-complex protein 1 subunit gamma OS=Rattus norvegicus GN=Cct3 PE=1 SV=1	RAT	9	1,1931	0,2574
514	16,46	16,46	28,3	sp|P11884|ALDH2_RAT	Aldehyde dehydrogenase, mitochondrial OS=Rattus norvegicus GN=Aldh2 PE=1 SV=1	RAT	9	0,9646	0,727
336	16,27	16,36	97,7	sp|P62329|TYB4_RAT	Thymosin beta-4 OS=Rattus norvegicus GN=Tmsb4x PE=2 SV=2	RAT	10	0,9313	0,693
381	15,95	16,08	59,2	sp|P19804|NDKB_RAT	Nucleoside diphosphate kinase B OS=Rattus norvegicus GN=Nme2 PE=1 SV=1	RAT	7	1,3715	0,0228
470	15,81	15,87	47,5	sp|P18420|PSA1_RAT	Proteasome subunit alpha type-1 OS=Rattus norvegicus GN=Psma1 PE=1 SV=2	RAT	9	0,9562	0,5502
172	15,72	15,91	53,2	sp|P62982|RS27A_RAT	Ubiquitin-40S ribosomal protein S27a OS=Rattus norvegicus GN=Rps27a PE=1 SV=2	RAT	8	1,2402	0,0533
207	15,63	15,71	24,1	sp|Q08163|CAP1_RAT	Adenylyl cyclase-associated protein 1 OS=Rattus norvegicus GN=Cap1 PE=1 SV=3	RAT	8	1,0962	0,1371
67	15,29	34,63	47,9	sp|P82995|HS90A_RAT	Heat shock protein HSP 90-alpha OS=Rattus norvegicus GN=Hsp90aa1 PE=1 SV=3	RAT	15	1,0702	0,3891
268	15,06	15,06	77,3	sp|P62329|TYB4_RAT	Thymosin beta-4 OS=Rattus norvegicus GN=Tmsb4x PE=1 SV=2	RAT	11	1,0409	0,623
128	14,66	15,37	28,5	sp|P07943|ALDR_RAT	Aldose reductase OS=Rattus norvegicus GN=Akr1b1 PE=1 SV=3	RAT	7	1,1227	0,0966
170	14,61	14,67	42,7	sp|P41123|RL13_RAT	60S ribosomal protein L13 OS=Rattus norvegicus GN=Rpl13 PE=1 SV=2	RAT	7	0,9786	0,7893
521	14,58	14,85	50,6	sp|P14669|ANXA3_RAT	Annexin A3 OS=Rattus norvegicus GN=Anxa3 PE=1 SV=4	RAT	7	1,0555	0,6127
384	14,17	14,17	50,4	sp|P11762|LEG1_RAT	Galectin-1 OS=Rattus norvegicus GN=Lgals1 PE=1 SV=2	RAT	10	1,1709	0,0549
5	14,05	14,05	44,2	sp|P04785|PDIA1_RAT	Protein disulfide-isomerase OS=Rattus norvegicus GN=P4hb PE=1 SV=2	RAT	10	1,2391	0,0013

536	13,66	13,85	26,2	sp|P50137|TKT_RAT	Transketolase OS=Rattus norvegicus GN=Tkt PE=1 SV=1	RAT	8	0,9799	0,8694
169	13,51	13,51	78,3	sp|P23928|CRYAB_RAT	Alpha-crystallin B chain OS=Rattus norvegicus GN=Cryab PE=1 SV=1	RAT	11	1,2382	0,0524
95	13,49	13,77	27,2	sp|P54001|P4HA1_RAT	Prolyl 4-hydroxylase subunit alpha-1 OS=Rattus norvegicus GN=P4ha1 PE=2 SV=2	RAT	7	0,8847	0,0573
102	13,41	13,43	55,4	sp|P45592|COF1_RAT	Cofilin-1 OS=Rattus norvegicus GN=Cfl1 PE=1 SV=3	RAT	9	1,0957	0,1724
12	13,3	13,87	21	sp|O88600|HSP74_RAT	Heat shock 70 kDa protein 4 OS=Rattus norvegicus GN=Hspa4 PE=1 SV=1	RAT	7	1,1406	0,0304
8	13,27	13,72	23,9	sp|Q9ER34|ACON_RAT	Aconitate hydratase, mitochondrial OS=Rattus norvegicus GN=Aco2 PE=1 SV=2	RAT	6	1,0811	0,3053
247	12,76	47,27	69,7	sp|P58775|TPM2_RAT	Tropomyosin beta chain OS=Rattus norvegicus GN=Tpm2 PE=3 SV=1	RAT	28	0,7512	0,0133
273	12,74	12,9	38,8	sp|P37397|CNN3_RAT	Calponin-3 OS=Rattus norvegicus GN=Cnn3 PE=1 SV=1	RAT	7	0,8396	0,0805
494	12,64	13,02	54,2	sp|P62755|RS6_RAT	40S ribosomal protein S6 OS=Rattus norvegicus GN=Rps6 PE=1 SV=1	RAT	7	1,2106	0,0808
438	12,59	12,82	21,2	sp|Q63355|MYO1C_RAT	Unconventional myosin-Ic OS=Rattus norvegicus GN=Myo1c PE=1 SV=2	RAT	8	0,9274	0,2627
185	12,2	12,48	22	sp|Q5M7W5|MAP4_RAT	Microtubule-associated protein 4 OS=Rattus norvegicus GN=Map4 PE=1 SV=1	RAT	6	1,023	0,8081
152	12,1	38,31	63,4	sp|P62738|ACTA_RAT	Actin, aortic smooth muscle OS=Rattus norvegicus GN=Acta2 PE=2 SV=1	RAT	48	0,8496	0,2494
248	12,05	12,17	48,6	sp|P62909|RS3_RAT	40S ribosomal protein S3 OS=Rattus norvegicus GN=Rps3 PE=1 SV=1	RAT	6	1,1073	0,3016
279	12,01	12,01	47,8	sp|P41350|CAV1_RAT	Caveolin-1 OS=Rattus norvegicus GN=Cav1 PE=1 SV=3	RAT	6	0,8329	0,0857
83	12	12,09	52,1	sp|P62963|PROF1_RAT	Profilin-1 OS=Rattus norvegicus GN=Pfn1 PE=1 SV=2	RAT	9	1,1157	0,4877
475	11,91	12,24	42,3	sp|P61980|HNRPK_RAT	Heterogeneous nuclear ribonucleoprotein K OS=Rattus norvegicus GN=Hnrnpk PE=1 SV=1	RAT	5	0,9453	0,6069
262	11,74	12,11	59	sp|P62752|RL23A_RAT	60S ribosomal protein L23a OS=Rattus norvegicus GN=Rpl23a PE=2 SV=1	RAT	6	1,0687	0,6925
468	11,74	18,58	51,4	sp|P61983|1433G_RAT	14-3-3 protein gamma OS=Rattus norvegicus GN=Ywhag PE=1 SV=2	RAT	9	1,0195	0,7653
422	11,64	11,8	21,4	sp|P28480|TCPA_RAT	T-complex protein 1 subunit alpha OS=Rattus norvegicus GN=Tcp1 PE=1 SV=1	RAT	7	1,1388	0,3719
471	11,62	11,77	18,5	sp|Q811A3|PLOD2_RAT	Procollagen-lysine,2-oxoglutarate 5-dioxygenase 2 OS=Rattus norvegicus GN=Plod2 PE=2 SV=1	RAT	7	0,9269	0,511
43	11,52	11,53	41,9	sp|P04906|GSTP1_RAT	Glutathione S-transferase P OS=Rattus norvegicus GN=Gstp1 PE=1 SV=2	RAT	6	1,1574	0,2535
392	11,45	12,85	46,1	sp|Q08290|CNN1_RAT	Calponin-1 OS=Rattus norvegicus GN=Cnn1 PE=2 SV=1	RAT	7	0,927	0,4292
188	11,41	17,7	36,7	sp|P47942|DPYL2_RAT	Dihydropyrimidinase-related protein 2 OS=Rattus norvegicus GN=Dpysl2 PE=1 SV=1	RAT	10	0,9728	0,7505
158	11,28	11,62	36,7	sp|Q9JI85|NUCB2_RAT	Nucleobindin-2 OS=Rattus norvegicus GN=Nucb2 PE=2 SV=1	RAT	4	1,1212	0,2546
77	11,06	11,2	26,7	sp|Q66X93|SND1_RAT	Staphylococcal nuclease domain-containing protein 1 OS=Rattus norvegicus GN=Snd1 PE=2 SV=1	RAT	5	1,0319	0,7029
87	11,04	11,8	22,4	sp|P51583|PUR6_RAT	Multifunctional protein ADE2 OS=Rattus norvegicus GN=Paics PE=2 SV=3	RAT	6	1,1171	0,1508
275	10,91	11,17	26,3	sp|P21531|RL3_RAT	60S ribosomal protein L3 OS=Rattus norvegicus GN=Rpl3 PE=1 SV=3	RAT	6	1,0898	0,2136

28	10,84	12,88	31,8	sp|P35704|PRDX2_RAT	Peroxiredoxin-2 OS=Rattus norvegicus GN=Prdx2 PE=1 SV=3	RAT	6	1,1022	0,2097
14	10,79	10,79	25,2	sp|Q6AYC4|CAPG_RAT	Macrophage-capping protein OS=Rattus norvegicus GN=Capg PE=1 SV=1	RAT	6	0,9626	0,5721
447	10,65	10,65	39,5	sp|Q6NYB7|RAB1A_RAT	Ras-related protein Rab-1A OS=Rattus norvegicus GN=Rab1A PE=1 SV=3	RAT	4	1,4589	0,0046
234	10,62	32,2	76,2	sp|Q63610|TPM3_RAT	Tropomyosin alpha-3 chain OS=Rattus norvegicus GN=Tpm3 PE=1 SV=2	RAT	24	0,9162	0,1066
92	10,59	10,59	34,3	sp|P10888|COX41_RAT	Cytochrome c oxidase subunit 4 isoform 1, mitochondrial OS=Rattus norvegicus GN=Cox4i1 PE=1 SV=1	RAT	5	1,0886	0,6403
11	10,41	10,41	20,2	sp|P05370|G6PD_RAT	Glucose-6-phosphate 1-dehydrogenase OS=Rattus norvegicus GN=G6pdx PE=1 SV=3	RAT	5	1,0003	0,9975
531	10,4	10,53	26,8	sp|Q6AXS5|PAIRB_RAT	Plasminogen activator inhibitor 1 RNA-binding protein OS=Rattus norvegicus GN=Serbp1 PE=1 SV=2	RAT	5	1,0874	0,3491
411	10,36	10,6	33,8	sp|P62425|RL7A_RAT	60S ribosomal protein L7a OS=Rattus norvegicus GN=Rpl7a PE=1 SV=2	RAT	3	1,0781	0,386
139	10,33	10,36	51,6	sp|P62961|YBOX1_RAT	Nuclease-sensitive element-binding protein 1 OS=Rattus norvegicus GN=Ybx1 PE=1 SV=3	RAT	5	1,0714	0,9363
450	10,33	10,33	26,1	sp|Q9WUH4|FHL1_RAT	Four and a half LIM domains protein 1 OS=Rattus norvegicus GN=Fhl1 PE=2 SV=1	RAT	5	0,7936	0,0109
43	10,28	10,68	26,4	sp|Q9WVC0|SEPT7_RAT	Septin-7 OS=Rattus norvegicus GN=Sept7 PE=1 SV=1	RAT	5	0,9379	0,4371
274	10,07	10,11	32,4	sp|Q3MIE4|VAT1_RAT	Synaptic vesicle membrane protein VAT-1 homolog OS=Rattus norvegicus GN=Vat1 PE=1 SV=1	RAT	5	0,9667	0,8154
24	10,01	10,01	17,7	sp|Q9Z1Z9|PDLI7_RAT	PDZ and LIM domain protein 7 OS=Rattus norvegicus GN=Pdlim7 PE=1 SV=1	RAT	5	0,9482	0,5718
73	9,95	10,08	27,5	sp|Q5RKI1|IF4A2_RAT	Eukaryotic initiation factor 4A-II OS=Rattus norvegicus GN=Eif4a2 PE=1 SV=1	RAT	5	0,9833	0,9066
89	9,88	9,98	16	sp|Q68FP1|GELS_RAT	Gelsolin OS=Rattus norvegicus GN=Gsn PE=1 SV=1	RAT	5	1,1362	0,4397
161	9,87	9,96	49,5	sp|P62898|CYC_RAT	Cytochrome c, somatic OS=Rattus norvegicus GN=Cycs PE=1 SV=2	RAT	5	0,9278	0,4643
72	9,85	10,12	23,5	sp|P38659|PDIA4_RAT	Protein disulfide-isomerase A4 OS=Rattus norvegicus GN=Pdia4 PE=1 SV=2	RAT	4	1,31	0,0037
33	9,81	9,91	54,9	sp|P07483|FABPH_RAT	Fatty acid-binding protein, heart OS=Rattus norvegicus GN=Fabp3 PE=1 SV=2	RAT	6	1,1531	0,1693
258	9,67	10,34	16,4	sp|P21396|AOFA_RAT	Amine oxidase [flavin-containing] A OS=Rattus norvegicus GN=Maoa PE=1 SV=1	RAT	5	1,1026	0,386
349	9,61	9,76	42	sp|P12001|RL18_RAT	60S ribosomal protein L18 OS=Rattus norvegicus GN=Rpl18 PE=2 SV=2	RAT	5	1,4028	0,0891
483	9,51	9,74	22,8	sp|Q5RJR8|LRC59_RAT	Leucine-rich repeat-containing protein 59 OS=Rattus norvegicus GN=Lrrc59 PE=1 SV=1	RAT	4	1,308	0,1765
530	9,49	9,7	15,3	sp|P49134|ITB1_RAT	Integrin beta-1 OS=Rattus norvegicus GN=Itgb1 PE=2 SV=1	RAT	4	0,8252	0,152
405	9,46	41,91	76,1	sp|P58775|TPM2_RAT	Tropomyosin beta chain OS=Rattus norvegicus GN=Tpm2 PE=2 SV=1	RAT	30	0,8019	0,0088
243	9,4	9,51	19,2	sp|Q9JLJ3|AL9A1_RAT	4-trimethylaminobutyraldehyde dehydrogenase OS=Rattus norvegicus GN=Aldh9a1 PE=1 SV=1	RAT	4	1,1508	0,1132
324	9,36	9,44	19,4	sp|Q5XIM9|TCPB_RAT	T-complex protein 1 subunit beta OS=Rattus norvegicus GN=Cct2 PE=1 SV=3	RAT	5	1,1102	0,5186
388	9,31	9,75	14,2	sp|Q9JK11|RTN4_RAT	Reticulon-4 OS=Rattus norvegicus GN=Rtn4 PE=1 SV=1	RAT	5	0,9947	0,9819
32	9,27	9,27	25,9	sp|Q9EPH8|PABP1_RAT	Polyadenylate-binding protein 1 OS=Rattus norvegicus GN=Pabpc1 PE=1	RAT	5	1,1391	0,0463

					SV=1				
53	9,21	9,36	15,7	sp|P06685|AT1A1_RAT	Sodium/potassium-transporting ATPase subunit alpha-1 OS=Rattus norvegicus GN=Atp1a1 PE=1 SV=1	RAT	4	0,9446	0,442
301	9,17	11,21	11,2	sp|P38650|DYHC1_RAT	Cytoplasmic dynein 1 heavy chain 1 OS=Rattus norvegicus GN=Dync1h1 PE=1 SV=1	RAT	4	1,1142	0,141
473	8,99	10,97	67,1	sp|P24368|PPIB_RAT	Peptidyl-prolyl cis-trans isomerase B OS=Rattus norvegicus GN=Ppib PE=1 SV=3	RAT	5	1,1527	0,1074
507	8,95	9,6	50,6	sp|P11030|ACBP_RAT	Acyl-CoA-binding protein OS=Rattus norvegicus GN=Dbi PE=1 SV=3	RAT	5	1,25	0,0675
395	8,82	9,04	25,2	sp|P19945|RLA0_RAT	60S acidic ribosomal protein P0 OS=Rattus norvegicus GN=Rplp0 PE=1 SV=2	RAT	4	1,0425	0,7447
389	8,79	8,79	72,5	sp|P62161|CALM_RAT	Calmodulin OS=Rattus norvegicus GN=Calm1 PE=1 SV=2	RAT	8		
97	8,78	10,75	61,8	sp|Q7M0E3|DEST_RAT	Destrin OS=Rattus norvegicus GN=Dstn PE=1 SV=3	RAT	7	0,9026	0,2954
303	8,69	8,74	39,2	sp|Q8VHK7|HDGF_RAT	Hepatoma-derived growth factor OS=Rattus norvegicus GN=Hdgf PE=1 SV=2	RAT	4	0,8914	0,0929
485	8,58	8,58	25,3	sp|P48500|TPIS_RAT	Triosephosphate isomerase OS=Rattus norvegicus GN=Tpi1 PE=1 SV=2	RAT	4	0,9727	0,6686
297	8,5	8,5	37,5	sp|P51635|AK1A1_RAT	Alcohol dehydrogenase [NADP(+)] OS=Rattus norvegicus GN=Akr1a1 PE=1 SV=2	RAT	4	1,1046	0,1905
165	8,48	8,58	43,6	sp|Q5XI73|GDIR1_RAT	Rho GDP-dissociation inhibitor 1 OS=Rattus norvegicus GN=Arhgdia PE=1 SV=1	RAT	5	1,1072	0,668
3	8,41	8,54	15,9	sp|Q63617|HYOU1_RAT	Hypoxia up-regulated protein 1 OS=Rattus norvegicus GN=Hyou1 PE=1 SV=1	RAT	4	1,2071	0,0451
26	8,4	8,52	19,4	sp|P55260|ANXA4_RAT	Annexin A4 OS=Rattus norvegicus GN=Anxa4 PE=1 SV=3	RAT	4	1,1144	0,2153
99	8,34	8,47	45,5	sp|P17074|RS19_RAT	40S ribosomal protein S19 OS=Rattus norvegicus GN=Rps19 PE=2 SV=3	RAT	4	1,2417	0,1005
197	8,24	8,34	28,9	sp|O35987|NSF1C_RAT	NSFL1 cofactor p47 OS=Rattus norvegicus GN=Nsfl1c PE=1 SV=1	RAT	4	0,9983	0,9792
420	8,13	8,13	20,2	sp|Q99NA5|IDH3A_RAT	Isocitrate dehydrogenase [NAD] subunit alpha, mitochondrial OS=Rattus norvegicus GN=Idh3a PE=1 SV=1	RAT	4	1,0955	0,4157
406	8,11	8,22	15,4	sp|O35567|PUR9_RAT	Bifunctional purine biosynthesis protein PURH OS=Rattus norvegicus GN=Atic PE=1 SV=2	RAT	4	1,2789	0,2662
114	8,1	8,24	19	sp|Q68FQ0|TCPE_RAT	T-complex protein 1 subunit epsilon OS=Rattus norvegicus GN=Cct5 PE=1 SV=1	RAT	4	0,9954	0,9386
97	8,04	8,11	14,6	sp|P16036|MPCP_RAT	Phosphate carrier protein, mitochondrial OS=Rattus norvegicus GN=Slc25a3 PE=1 SV=1	RAT	4	1,0951	0,4432
36	8,03	8,1	42,9	sp|Q3T1J1|IF5A1_RAT	Eukaryotic translation initiation factor 5A-1 OS=Rattus norvegicus GN=Eif5a PE=1 SV=3	RAT	4	1,1998	0,5932
214	8	8,27	20,8	sp|P17764|THIL_RAT	Acetyl-CoA acetyltransferase, mitochondrial OS=Rattus norvegicus GN=Acat1 PE=1 SV=1	RAT	4	0,905	0,3589
352	7,94	8,02	27,6	sp|P62919|RL8_RAT	60S ribosomal protein L8 OS=Rattus norvegicus GN=Rpl8 PE=2 SV=2	RAT	3	1,0701	0,3094
318	7,9	7,98	28,4	sp|P08082|CLCB_RAT	Clathrin light chain B OS=Rattus norvegicus GN=Cltb PE=1 SV=1	RAT	4	0,9787	0,8795
291	7,79	8,17	32,3	sp|P50878|RL4_RAT	60S ribosomal protein L4 OS=Rattus norvegicus GN=Rpl4 PE=1 SV=3	RAT	4	1,0238	0,849
415	7,72	7,81	48,9	sp|P67779|PHB_RAT	Prohibitin OS=Rattus norvegicus GN=Phb PE=1 SV=1	RAT	4	0,9962	0,9372

213	7,69	7,76	23,8	sp|Q91Y81|SEPT2_RAT	Septin-2 OS=Rattus norvegicus GN=Sept2 PE=1 SV=1	RAT	4	0,9689	0,6653
104	7,68	7,83	10,8	sp|Q62940|NEDD4_RAT	E3 ubiquitin-protein ligase NEDD4 OS=Rattus norvegicus GN=Nedd4 PE=1 SV=1	RAT	4	1,1661	0,3919
294	7,66	7,8	16,9	sp|Q99PF5|FUBP2_RAT	Far upstream element-binding protein 2 OS=Rattus norvegicus GN=Khsrp PE=1 SV=1	RAT	4	0,9741	0,7924
218	7,63	7,73	53,9	sp|P23358|RL12_RAT	60S ribosomal protein L12 OS=Rattus norvegicus GN=Rpl12 PE=2 SV=1	RAT	3	0,9371	0,6015
461	7,57	7,74	49,6	sp|Q00715|H2B1_RAT	Histone H2B type 1 OS=Rattus norvegicus PE=1 SV=2	RAT	4	0,8608	0,1788
376	7,4	7,44	23,8	sp|P63029|TCTP_RAT	Translationally-controlled tumor protein OS=Rattus norvegicus GN=Tpt1 PE=1 SV=1	RAT	4	2,0437	0,0756
219	7,39	7,48	39,2	sp|Q68FU3|ETFB_RAT	Electron transfer flavoprotein subunit beta OS=Rattus norvegicus GN=Etfb PE=2 SV=3	RAT	4	1,1999	0,1073
404	7,29	7,45	21,6	sp|P50399|GDIB_RAT	Rab GDP dissociation inhibitor beta OS=Rattus norvegicus GN=Gdi2 PE=1 SV=2	RAT	4	1,0769	0,385
48	7,18	7,18	36,1	sp|P18666|ML12B_RAT	Myosin regulatory light chain 12B OS=Rattus norvegicus GN=Myl12b PE=1 SV=3	RAT	5	0,7447	0,0549
293	7,12	9,7	22,3	sp|P70615|LMNB1_RAT	Lamin-B1 OS=Rattus norvegicus GN=Lmnb1 PE=1 SV=3	RAT	5	1,1913	0,0969
171	7,08	7,16	23,9	sp|Q4V7C7|ARP3_RAT	Actin-related protein 3 OS=Rattus norvegicus GN=Actr3 PE=1 SV=1	RAT	4	1,242	0,1816
369	7,05	7,07	29,4	sp|P24050|RS5_RAT	40S ribosomal protein S5 OS=Rattus norvegicus GN=Rps5 PE=1 SV=3	RAT	3	1,2387	0,0621
212	6,98	7,17	21,5	sp|Q794E4|HNRPF_RAT	Heterogeneous nuclear ribonucleoprotein F OS=Rattus norvegicus GN=Hnrnpf PE=1 SV=3	RAT	4	1,0388	0,7978
277	6,91	6,91	20,5	sp|Q3KRE8|TBB2B_RAT	Tubulin beta-2B chain OS=Rattus norvegicus GN=Tubb2b PE=1 SV=1	RAT	5	1,6101	0,0067
17	6,86	6,98	7,4	sp|P50475|SYAC_RAT	Alanine--tRNA ligase, cytoplasmic OS=Rattus norvegicus GN=Aars PE=1 SV=3	RAT	3	1,2731	0,1138
20	6,8	6,94	31,7	sp|O88989|MDHC_RAT	Malate dehydrogenase, cytoplasmic OS=Rattus norvegicus GN=Mdh1 PE=1 SV=3	RAT	3	1,09	0,1526
71	6,79	6,94	31,5	sp|Q62920|PDLI5_RAT	PDZ and LIM domain protein 5 OS=Rattus norvegicus GN=Pdlim5 PE=1 SV=2	RAT	3	0,9061	0,092
52	6,77	6,87	19,6	sp|Q62826|HNRPM_RAT	Heterogeneous nuclear ribonucleoprotein M OS=Rattus norvegicus GN=Hnrnpm PE=1 SV=4	RAT	4	0,9746	0,7746
80	6,67	6,69	30,3	sp|P04904|GSTA3_RAT	Glutathione S-transferase alpha-3 OS=Rattus norvegicus GN=Gsta3 PE=1 SV=3	RAT	4	1,343	0,2004
499	6,64	6,64	15,6	sp|P16975|SPRC_RAT	SPARC OS=Rattus norvegicus GN=Sparc PE=1 SV=4	RAT	4	1,0003	0,9981
481	6,64	6,77	28,4	sp|Q63945|SET_RAT	Protein SET OS=Rattus norvegicus GN=Set PE=2 SV=2	RAT	3	0,9522	0,8056
535	6,53	6,6	15,9	sp|P25235|RPN2_RAT	Dolichyl-diphosphooligosaccharide--protein glycosyltransferase subunit 2 OS=Rattus norvegicus GN=Rpn2 PE=2 SV=2	RAT	3	0,9659	0,829
495	6,47	6,61	13,4	sp|Q6P6V0|G6PI_RAT	Glucose-6-phosphate isomerase OS=Rattus norvegicus GN=Gpi PE=1 SV=1	RAT	3	1,0954	0,5136
403	6,42	6,56	14	sp|P35565|CALX_RAT	Calnexin OS=Rattus norvegicus GN=Canx PE=1 SV=1	RAT	3	1,2065	0,4642
304	6,39	6,39	43,8	sp|P11232|THIO_RAT	Thioredoxin OS=Rattus norvegicus GN=Txn PE=1 SV=2	RAT	4	1,029	0,7545
322	6,36	16,7	28,5	sp|P31977|EZRI_RAT	Ezrin OS=Rattus norvegicus GN=Ezr PE=1 SV=3	RAT	8	1,0347	0,6468

84	6,31	6,57	17,8	sp|Q9Z1A6|VIGLN_RAT	Vigilin OS=Rattus norvegicus GN=Hdlbp PE=2 SV=1	RAT	3	1,0187	0,7631
236	6,2	28,28	50,8	sp|Q6P9T8|TBB4B_RAT	Tubulin beta-4B chain OS=Rattus norvegicus GN=Tubb4b PE=1 SV=1	RAT	19	0,8982	0,7004
335	6,14	6,19	24,2	sp|P52555|ERP29_RAT	Endoplasmic reticulum resident protein 29 OS=Rattus norvegicus GN=Erp29 PE=1 SV=2	RAT	3	1,4325	0,147
311	6,13	6,22	31,9	sp|P41562|IDHC_RAT	Isocitrate dehydrogenase [NADP] cytoplasmic OS=Rattus norvegicus GN=Idh1 PE=1 SV=1	RAT	2	1,173	0,1857
124	6,12	6,12	15,7	sp|P70490|MFGM_RAT	Lactadherin OS=Rattus norvegicus GN=Mfge8 PE=2 SV=1	RAT	3	0,8873	0,4977
86	6,11	6,41	24,5	sp|P04897|GNAI2_RAT	Guanine nucleotide-binding protein G(i) subunit alpha-2 OS=Rattus norvegicus GN=Gnai2 PE=1 SV=3	RAT	3	1,0763	0,4804
334	6,04	6,12	26,9	sp|P62494|RB11A_RAT	Ras-related protein Rab-11A OS=Rattus norvegicus GN=Rab11a PE=1 SV=3	RAT	3	1,3189	0,0382
398	6,04	6,25	27,6	sp|P09895|RL5_RAT	60S ribosomal protein L5 OS=Rattus norvegicus GN=Rpl5 PE=1 SV=3	RAT	3	1,2515	0,2452
136	6	6	18,1	sp|P30009|MARCS_RAT	Myristoylated alanine-rich C-kinase substrate OS=Rattus norvegicus GN=Marcks PE=1 SV=2	RAT	5	0,9826	0,854
371	6	10,78	79,6	sp|P63312|TYB10_RAT	Thymosin beta-10 OS=Rattus norvegicus GN=Tmsb10 PE=2 SV=2	RAT	7	0,9093	
149	6	6	27,2	sp|Q64119|MYL6_RAT	Myosin light polypeptide 6 OS=Rattus norvegicus GN=Myl6 PE=1 SV=3	RAT	4	0,8682	0,2797
305	5,96	6,09	19,9	sp|Q7TPB1|TCPD_RAT	T-complex protein 1 subunit delta OS=Rattus norvegicus GN=Cct4 PE=1 SV=3	RAT	4	1,1828	0,586
260	5,94	6,11	28	sp|P27952|RS2_RAT	40S ribosomal protein S2 OS=Rattus norvegicus GN=Rps2 PE=1 SV=1	RAT	3	1,2187	0,0441
326	5,9	14,5	52,9	sp|P35213|1433B_RAT	14-3-3 protein beta/alpha OS=Rattus norvegicus GN=Ywhab PE=1 SV=3	RAT	7	0,8101	0,3045
226	5,88	6,1	11,1	sp|O35142|COPB2_RAT	Coatomer subunit beta' OS=Rattus norvegicus GN=Copb2 PE=1 SV=3	RAT	3	1,2577	0,0473
309	5,86	5,86	32,5	sp|P07632|SODC_RAT	Superoxide dismutase [Cu-Zn] OS=Rattus norvegicus GN=Sod1 PE=1 SV=2	RAT	7	1,1152	0,2254
155	5,78	5,9	12,3	sp|P24268|CATD_RAT	Cathepsin D OS=Rattus norvegicus GN=Ctsd PE=1 SV=1	RAT	3	0,9738	0,7585
245	5,7	5,86	29,8	sp|O35783|CALU_RAT	Calumenin OS=Rattus norvegicus GN=Calu PE=1 SV=1	RAT	3	1,1106	0,6721
338	5,68	5,68	30,5	sp|Q9R063|PRDX5_RAT	Peroxiredoxin-5, mitochondrial OS=Rattus norvegicus GN=Prdx5 PE=1 SV=1	RAT	3	1,2283	0,156
348	5,65	5,74	64,4	sp|P02401|RLA2_RAT	60S acidic ribosomal protein P2 OS=Rattus norvegicus GN=Rplp2 PE=1 SV=2	RAT	3	1,2513	0,1356
115	5,61	5,71	26,7	sp|Q8CFN2|CDC42_RAT	Cell division control protein 42 homolog OS=Rattus norvegicus GN=Cdc42 PE=1 SV=2	RAT	3	0,9784	0,7851
58	5,6	5,73	22,9	sp|Q9Z0W7|CLIC4_RAT	Chloride intracellular channel protein 4 OS=Rattus norvegicus GN=Clic4 PE=1 SV=3	RAT	3	1,265	0,0525
497	5,6	5,6	32,9	sp|P13084|NPM_RAT	Nucleophosmin OS=Rattus norvegicus GN=Npm1 PE=1 SV=1	RAT	5	1,0373	0,7789
375	5,58	5,6	23,8	sp|A7VJC2|ROA2_RAT	Heterogeneous nuclear ribonucleoproteins A2/B1 OS=Rattus norvegicus GN=Hnrnpa2b1 PE=1 SV=1	RAT	4	0,9834	0,8396
516	5,57	5,97	15,8	sp|Q2PQA9|KINH_RAT	Kinesin-1 heavy chain OS=Rattus norvegicus GN=Kif5b PE=1 SV=1	RAT	3	1,0956	0,275
68	5,52	7,88	29,5	sp|B3GNI6|SEP11_RAT	Septin-11 OS=Rattus norvegicus GN=Sept11 PE=1 SV=1	RAT	4	0,8896	0,1133
195	5,44	5,46	19,8	sp|P21775|THIKA_RAT	3-ketoacyl-CoA thiolase A, peroxisomal OS=Rattus norvegicus GN=Acaa1a PE=1 SV=2	RAT	3	1,1221	0,6456

339	5,42	8,04	25,4	sp|O35814|STIP1_RAT	Stress-induced-phosphoprotein 1 OS=Rattus norvegicus GN=Stip1 PE=1 SV=1	RAT	4	1,0941	0,3388
423	5,37	5,37	24,2	sp|Q4KM74|SC22B_RAT	Vesicle-trafficking protein SEC22b OS=Rattus norvegicus GN=Sec22b PE=1 SV=3	RAT	3	1,1387	0,5741
478	5,32	5,32	11	sp|Q00438|PTBP1_RAT	Polypyrimidine tract-binding protein 1 OS=Rattus norvegicus GN=Ptbp1 PE=1 SV=1	RAT	3	0,8943	0,1318
175	5,29	5,31	10,7	sp|O08651|SERA_RAT	D-3-phosphoglycerate dehydrogenase OS=Rattus norvegicus GN=Phgdh PE=1 SV=3	RAT	3	1,3174	0,0156
451	5,27	5,27	21,1	sp|O35763|MOES_RAT	Moesin OS=Rattus norvegicus GN=Msn PE=1 SV=3	RAT	3	1,3645	0,0041
508	5,22	5,24	10,3	sp|Q5BJK8|GOLI4_RAT	Golgi integral membrane protein 4 OS=Rattus norvegicus GN=Golim4 PE=1 SV=2	RAT	3	1,1966	0,1999
464	5,18	5,3	9,9	sp|P52296|IMB1_RAT	Importin subunit beta-1 OS=Rattus norvegicus GN=Kpnb1 PE=1 SV=1	RAT	3	1,2654	0,2065
235	5,14	5,31	20,7	sp|P97584|PTGR1_RAT	Prostaglandin reductase 1 OS=Rattus norvegicus GN=Ptgr1 PE=2 SV=3	RAT	2	1,3517	0,1651
181	5,09	5,09	55,9	sp|P26772|CH10_RAT	10 kDa heat shock protein, mitochondrial OS=Rattus norvegicus GN=Hspe1 PE=1 SV=3	RAT	4	1,1707	0,0727
63	5,05	5,05	29,4	sp|P61314|RL15_RAT	60S ribosomal protein L15 OS=Rattus norvegicus GN=Rpl15 PE=1 SV=2	RAT	2	0,9625	0,7784
88	4,94	5	27,5	sp|O88767|PARK7_RAT	Protein DJ-1 OS=Rattus norvegicus GN=Park7 PE=1 SV=1	RAT	2	0,9033	0,2657
56	4,92	7,17	18,5	sp|Q8VHV7|HNRH1_RAT	Heterogeneous nuclear ribonucleoprotein H OS=Rattus norvegicus GN=Hnrnph1 PE=1 SV=2	RAT	3	0,9885	0,8706
22	4,91	5,09	48,9	sp|P62907|RL10A_RAT	60S ribosomal protein L10a OS=Rattus norvegicus GN=Rpl10a PE=1 SV=2	RAT	2	0,8884	0,1157
276	4,9	5,03	21	sp|P85515|ACTZ_RAT	Alpha-centractin OS=Rattus norvegicus GN=Actr1a PE=1 SV=1	RAT	3	1,2653	0,2653
300	4,88	4,88	24,7	sp|P63255|CRIP1_RAT	Cysteine-rich protein 1 OS=Rattus norvegicus GN=Crip1 PE=1 SV=2	RAT	3	1,1025	0,664
202	4,88	4,93	16,2	sp|P13803|ETFA_RAT	Electron transfer flavoprotein subunit alpha, mitochondrial OS=Rattus norvegicus GN=Etfa PE=1 SV=4	RAT	2	1,0715	0,8251
17	4,87	4,9	41,6	sp|P05964|S10A6_RAT	Protein S100-A6 OS=Rattus norvegicus GN=S100a6 PE=1 SV=3	RAT	3	1,2379	0,4442
458	4,73	4,73	63,8	sp|P62271|RS18_RAT	40S ribosomal protein S18 OS=Rattus norvegicus GN=Rps18 PE=1 SV=3	RAT	3	1,2997	0,0339
134	4,69	4,83	43,3	sp|P62243|RS8_RAT	40S ribosomal protein S8 OS=Rattus norvegicus GN=Rps8 PE=1 SV=2	RAT	2	1,0033	0,9891
91	4,68	4,78	15,7	sp|Q63347|PRS7_RAT	26S protease regulatory subunit 7 OS=Rattus norvegicus GN=Psmc2 PE=1 SV=3	RAT	2	1,1168	0,4532
426	4,63	4,63	73,9	sp|P62859|RS28_RAT	40S ribosomal protein S28 OS=Rattus norvegicus GN=Rps28 PE=1 SV=1	RAT	2	1,2194	0,2264
357	4,63	4,69	50,8	sp|P31044|PEBP1_RAT	Phosphatidylethanolamine-binding protein 1 OS=Rattus norvegicus GN=Pebp1 PE=1 SV=3	RAT	2	1,0829	0,4898
538	4,63	4,63	20,5	sp|P00507|AATM_RAT	Aspartate aminotransferase, mitochondrial OS=Rattus norvegicus GN=Got2 PE=1 SV=2	RAT	2	1,0656	0,6353
288	4,6	4,61	9	sp|Q6P6R2|DLDH_RAT	Dihydrolipoyl dehydrogenase, mitochondrial OS=Rattus norvegicus GN=Dld PE=1 SV=1	RAT	2	1,1203	0,4694
356	4,57	4,78	15,6	sp|Q9QZA2|PDC6I_RAT	Programmed cell death 6-interacting protein OS=Rattus norvegicus GN=Pdcd6ip PE=1 SV=2	RAT	2	1,0471	0,6965
101	4,53	4,53	37,2	sp|P36972|APT_RAT	Adenine phosphoribosyltransferase OS=Rattus norvegicus GN=Aprt PE=1 SV=1	RAT	2	1,3582	0,0865

168	4,53	4,75	12,7	sp|Q5M7U6|ARP2_RAT	Actin-related protein 2 OS=Rattus norvegicus GN=Actr2 PE=1 SV=1	RAT	2	0,9875	0,9114
198	4,52	4,72	22,1	sp|Q6P799|SYSC_RAT	Serine--tRNA ligase, cytoplasmic OS=Rattus norvegicus GN=Sars PE=1 SV=3	RAT	3	1,28	0,324
296	4,5	8,06	41,8	sp|P10536|RAB1B_RAT	Ras-related protein Rab-1B OS=Rattus norvegicus GN=Rab1b PE=1 SV=1	RAT	3	1,0803	0,3746
292	4,47	4,47	9,8	sp|P00762|TRY1_RAT	Anionic trypsin-1 OS=Rattus norvegicus GN=Prss1 PE=1 SV=1	RAT	4	0,9618	
176	4,46	4,61	22,8	sp|Q3KR86|MIC60_RAT	MICOS complex subunit Mic60 (Fragment) OS=Rattus norvegicus GN=Immt PE=1 SV=1	RAT	3	0,9492	0,6208
337	4,45	4,46	14,3	sp|Q5XIU9|PGRC2_RAT	Membrane-associated progesterone receptor component 2 OS=Rattus norvegicus GN=Pgrmc2 PE=2 SV=1	RAT	2	1,3831	0,0575
269	4,44	4,57	38,2	sp|P61354|RL27_RAT	60S ribosomal protein L27 OS=Rattus norvegicus GN=Rpl27 PE=2 SV=2	RAT	2	1,2236	0,0379
138	4,44	4,44	29,7	sp|P12749|RL26_RAT	60S ribosomal protein L26 OS=Rattus norvegicus GN=Rpl26 PE=1 SV=1	RAT	2	1,0859	0,5654
413	4,43	4,54	10	sp|Q5U300|UBA1_RAT	Ubiquitin-like modifier-activating enzyme 1 OS=Rattus norvegicus GN=Uba1 PE=1 SV=1	RAT	2	1,2332	0,3446
74	4,38	4,45	32,3	sp|Q925G0|RBM3_RAT	Putative RNA-binding protein 3 OS=Rattus norvegicus GN=Rbm3 PE=1 SV=2	RAT	2	0,9793	0,7902
3	4,38	4,65	37,8	sp|P84100|RL19_RAT	60S ribosomal protein L19 OS=Rattus norvegicus GN=Rpl19 PE=1 SV=1	RAT	3	0,9724	0,782
130	4,36	4,36	29,5	sp|P06302|PTMA_RAT	Prothymosin alpha OS=Rattus norvegicus GN=Ptma PE=1 SV=2	RAT	3	1,158	
79	4,36	4,44	40,2	sp|P29314|RS9_RAT	40S ribosomal protein S9 OS=Rattus norvegicus GN=Rps9 PE=1 SV=4	RAT	2	1,0951	0,486
15	4,36	4,6	9,8	sp|P18484|AP2A2_RAT	AP-2 complex subunit alpha-2 OS=Rattus norvegicus GN=Ap2a2 PE=1 SV=3	RAT	2	0,8246	0,4719
135	4,35	5,38	14,6	sp|Q68FS4|AMPL_RAT	Cytosol aminopeptidase OS=Rattus norvegicus GN=Lap3 PE=1 SV=1	RAT	2	1,1528	0,7075
397	4,35	4,56	12,5	sp|Q63377|AT1B3_RAT	Sodium/potassium-transporting ATPase subunit beta-3 OS=Rattus norvegicus GN=Atp1b3 PE=2 SV=1	RAT	3	0,8593	0,2329
126	4,33	4,43	18,5	sp|Q05962|ADT1_RAT	ADP/ATP translocase 1 OS=Rattus norvegicus GN=Slc25a4 PE=1 SV=3	RAT	4	1,8074	0,282
196	4,32	4,32	39,8	sp|Q62658|FKB1A_RAT	Peptidyl-prolyl cis-trans isomerase FKBP1A OS=Rattus norvegicus GN=Fkbp1a PE=1 SV=3	RAT	2	1,1842	0,2001
65	4,29	4,29	9,6	sp|Q4KMA2|RD23B_RAT	UV excision repair protein RAD23 homolog B OS=Rattus norvegicus GN=Rad23b PE=1 SV=1	RAT	2	1,1483	0,3601
460	4,26	4,26	42,6	sp|P05942|S10A4_RAT	Protein S100-A4 OS=Rattus norvegicus GN=S100a4 PE=2 SV=1	RAT	2	1,1133	0,2824
360	4,24	4,3	36,4	sp|Q9Z2L0|VDAC1_RAT	Voltage-dependent anion-selective channel protein 1 OS=Rattus norvegicus GN=Vdac1 PE=1 SV=4	RAT	2	1,1362	0,1884
192	4,22	4,35	42,3	sp|P05426|RL7_RAT	60S ribosomal protein L7 OS=Rattus norvegicus GN=Rpl7 PE=1 SV=2	RAT	2	1,3891	0,1504
112	4,2	4,23	13,8	sp|P85845|FSCN1_RAT	Fascin OS=Rattus norvegicus GN=Fscn1 PE=1 SV=2	RAT	2	0,9954	0,9914
502	4,19	4,19	20,2	sp|P11598|PDIA3_RAT	Protein disulfide-isomerase A3 OS=Rattus norvegicus GN=Pdia3 PE=1 SV=2	RAT	4	1,2231	0,2911
23	4,19	6,68	66,7	sp|D3ZBN0|H15_RAT	Histone H1.5 OS=Rattus norvegicus GN=Hist1h1b PE=3 SV=1	RAT	3	0,8455	0,1066
281	4,16	4,16	15,6	sp|P16391|HA12_RAT	RT1 class I histocompatibility antigen, AA alpha chain OS=Rattus norvegicus PE=1 SV=2	RAT	2	1,0346	0,7251
512	4,12	18,3	17,8	sp|Q9JLT0|MYH10_RAT	Myosin-10 OS=Rattus norvegicus GN=Myh10 PE=2 SV=1	RAT	7	1,1158	0,7127

227	4,11	4,11	30,9	sp|P29457|SERPH_RAT	Serpin H1 OS=Rattus norvegicus GN=Serpinh1 PE=1 SV=1	RAT	3	1,4447	0,122
378	4,11	4,11	14,6	sp|P16290|PGAM2_RAT	Phosphoglycerate mutase 2 OS=Rattus norvegicus GN=Pgam2 PE=2 SV=2	RAT	3	1,1888	0,5921
323	4,11	5,2	14,8	sp|O88656|ARC1B_RAT	Actin-related protein 2/3 complex subunit 1B OS=Rattus norvegicus GN=Arpc1b PE=2 SV=3	RAT	3	1,1072	0,6165
520	4,09	4,09	29,1	sp|P42930|HSPB1_RAT	Heat shock protein beta-1 OS=Rattus norvegicus GN=Hspb1 PE=1 SV=1	RAT	3	1,3457	0,2085
205	4,09	4,15	18,7	sp|P00763|TRY2_RAT	Anionic trypsin-2 OS=Rattus norvegicus GN=Prss2 PE=1 SV=2	RAT	4	0,9676	
492	4,02	6,93	26,9	sp|Q5RJP0|ALD1_RAT	Aldose reductase-related protein 1 OS=Rattus norvegicus GN=Akr1b7 PE=1 SV=1	RAT	3	1,1955	0,3246
308	4,02	4,06	10,5	sp|Q4AEF8|COPG1_RAT	Coatomer subunit gamma-1 OS=Rattus norvegicus GN=Copg1 PE=2 SV=1	RAT	2	1,1228	0,5888
94	4,02	4,29	19,3	sp|P85834|EFTU_RAT	Elongation factor Tu, mitochondrial OS=Rattus norvegicus GN=Tufm PE=1 SV=1	RAT	2	0,8274	0,5065
11	4,01	4,17	16,1	sp|F1LMZ8|PSD11_RAT	26S proteasome non-ATPase regulatory subunit 11 OS=Rattus norvegicus GN=Psmd11 PE=3 SV=2	RAT	2	1,0964	0,6415
48	4	4	4,7	sp|P11980|KPYM_RAT	Pyruvate kinase isozymes M1/M2 OS=Rattus norvegicus GN=Pkm PE=1 SV=3	RAT	2	1,337	0,2125
85	4	4	25,5	sp|Q7M767|UB2V2_RAT	Ubiquitin-conjugating enzyme E2 variant 2 OS=Rattus norvegicus GN=Ube2v2 PE=1 SV=3	RAT	2	1,2958	0,3498
19	4	4,09	9,7	sp|P10760|SAHH_RAT	Adenosylhomocysteinase OS=Rattus norvegicus GN=Ahcy PE=1 SV=3	RAT	2	1,0771	0,6152
501	4	4	14,3	sp|P13383|NUCL_RAT	Nucleolin OS=Rattus norvegicus GN=Ncl PE=1 SV=3	RAT	2	1,0133	0,922
316	4	4	14,9	sp|P62260|1433E_RAT	14-3-3 protein epsilon OS=Rattus norvegicus GN=Ywhae PE=1 SV=1	RAT	3	0,9994	
431	3,97	4,07	13,2	sp|Q5I0G4|SYG_RAT	Glycine--tRNA ligase (Fragment) OS=Rattus norvegicus GN=Gars PE=1 SV=1	RAT	4	1,3534	0,0574
156	3,96	3,98	27,6	sp|Q62785|HAP28_RAT	28 kDa heat- and acid-stable phosphoprotein OS=Rattus norvegicus GN=Pdap1 PE=1 SV=1	RAT	2	1,0594	0,6721
90	3,95	4,46	10,3	sp|Q62902|LMAN1_RAT	Protein ERGIC-53 OS=Rattus norvegicus GN=Lman1 PE=1 SV=1	RAT	2	0,9237	0,6677
96	3,92	3,92	19,8	sp|P09527|RAB7A_RAT	Ras-related protein Rab-7a OS=Rattus norvegicus GN=Rab7a PE=1 SV=2	RAT	2	1,2015	0,5741
345	3,9	3,93	46,9	sp|Q64598|H2A1F_RAT	Histone H2A type 1-F OS=Rattus norvegicus PE=3 SV=3	RAT	2	1,0461	0,9553
187	3,9	3,96	18,3	sp|Q920J4|TXNL1_RAT	Thioredoxin-like protein 1 OS=Rattus norvegicus GN=Txnl1 PE=1 SV=3	RAT	2	1,0282	0,733
232	3,89	3,89	9,4	sp|P48721|GRP75_RAT	Stress-70 protein, mitochondrial OS=Rattus norvegicus GN=Hspa9 PE=1 SV=3	RAT	2	1,2941	0,2603
107	3,88	3,96	9,7	sp|Q641X8|EIF3E_RAT	Eukaryotic translation initiation factor 3 subunit E OS=Rattus norvegicus GN=Eif3e PE=2 SV=1	RAT	2	1,2775	0,0946
191	3,85	3,86	25,8	sp|P18421|PSB1_RAT	Proteasome subunit beta type-1 OS=Rattus norvegicus GN=Psmb1 PE=1 SV=3	RAT	2	1,2445	0,2667
40	3,84	3,86	12,5	sp|P04762|CATA_RAT	Catalase OS=Rattus norvegicus GN=Cat PE=1 SV=3	RAT	2	1,2924	0,1867
383	3,83	3,97	33,5	sp|Q5XI32|CAPZB_RAT	F-actin-capping protein subunit beta OS=Rattus norvegicus GN=Capzb PE=1 SV=1	RAT	3	1,2225	0,3164
68	3,8	4,33	22,6	sp|P08081|CLCA_RAT	Clathrin light chain A OS=Rattus norvegicus GN=Clta PE=1 SV=1	RAT	2	1,0795	
343	3,79	3,83	6,8	sp|P26051|CD44_RAT	CD44 antigen OS=Rattus norvegicus GN=Cd44 PE=1 SV=2	RAT	2	1,1068	0,3993

82	3,73	3,89	13,8	sp|P21670|PSA4_RAT	Proteasome subunit alpha type-4 OS=Rattus norvegicus GN=Psma4 PE=1 SV=1	RAT	2	0,8307	0,5121
57	3,72	3,83	17,8	sp|B2GUZ5|CAZA1_RAT	F-actin-capping protein subunit alpha-1 OS=Rattus norvegicus GN=Capza1 PE=1 SV=1	RAT	2	0,8969	0,5568
270	3,71	3,71	20,8	sp|Q6RUV5|RAC1_RAT	Ras-related C3 botulinum toxin substrate 1 OS=Rattus norvegicus GN=Rac1 PE=1 SV=1	RAT	2	0,8871	0,3523
287	3,71	4,07	10	sp|Q641Y8|DDX1_RAT	ATP-dependent RNA helicase DDX1 OS=Rattus norvegicus GN=Ddx1 PE=2 SV=1	RAT	2	0,8845	0,5635
178	3,7	3,7	39,8	sp|Q6B345|S10AB_RAT	Protein S100-A11 OS=Rattus norvegicus GN=S100a11 PE=2 SV=1	RAT	3	1,275	0,2542
367	3,69	3,69	28,1	sp|Q63190|EMD_RAT	Emerin OS=Rattus norvegicus GN=Emd PE=2 SV=1	RAT	2	1,4905	
331	3,69	3,77	15,5	sp|Q6AYT3|RTCB_RAT	tRNA-splicing ligase RtcB homolog OS=Rattus norvegicus GN=Rtcb PE=2 SV=1	RAT	2	1,0847	0,5637
436	3,68	3,68	20,8	sp|P35434|ATPD_RAT	ATP synthase subunit delta, mitochondrial OS=Rattus norvegicus GN=Atp5d PE=1 SV=2	RAT	2	1,0382	0,8024
325	3,67	3,68	43,9	sp|Q03344|ATIF1_RAT	ATPase inhibitor, mitochondrial OS=Rattus norvegicus GN=Atpif1 PE=3 SV=2	RAT	2	1,2339	0,4014
410	3,67	16,77	27,9	sp|Q5XIF6|TBA4A_RAT	Tubulin alpha-4A chain OS=Rattus norvegicus GN=Tuba4a PE=2 SV=1	RAT	11	1,1526	0,5334
350	3,65	3,72	13,3	sp|Q62871|DC1I2_RAT	Cytoplasmic dynein 1 intermediate chain 2 OS=Rattus norvegicus GN=Dync1i2 PE=1 SV=1	RAT	2	1,0069	0,9579
160	3,65	3,95	8,2	sp|P97536|CAND1_RAT	Cullin-associated NEDD8-dissociated protein 1 OS=Rattus norvegicus GN=Cand1 PE=1 SV=1	RAT	2	0,9793	0,8884
228	3,64	3,73	25,3	sp|P62914|RL11_RAT	60S ribosomal protein L11 OS=Rattus norvegicus GN=Rpl11 PE=1 SV=2	RAT	2	0,9529	0,8086
359	3,63	14,44	43,1	sp|P68511|1433F_RAT	14-3-3 protein eta OS=Rattus norvegicus GN=Ywhah PE=1 SV=2	RAT	7	0,9694	0,7156
519	3,62	3,64	13,3	sp|P63245|GBLP_RAT	Guanine nucleotide-binding protein subunit beta-2-like 1 OS=Rattus norvegicus GN=Gnb2l1 PE=1 SV=3	RAT	2	1,0064	0,9298
142	3,59	3,59	27,5	sp|Q9QX67|DAP1_RAT	Death-associated protein 1 OS=Rattus norvegicus GN=Dap PE=3 SV=3	RAT	2	0,99	0,9365
164	3,58	3,65	33,6	sp|P62902|RL31_RAT	60S ribosomal protein L31 OS=Rattus norvegicus GN=Rpl31 PE=2 SV=1	RAT	2	1,177	0,6177
203	3,57	3,57	13,5	sp|P32551|QCR2_RAT	Cytochrome b-c1 complex subunit 2, mitochondrial OS=Rattus norvegicus GN=Uqcrc2 PE=1 SV=2	RAT	2	1,1699	0,2163
98	3,55	3,73	39,4	sp|P63324|RS12_RAT	40S ribosomal protein S12 OS=Rattus norvegicus GN=Rps12 PE=1 SV=2	RAT	3	1,453	0,5181
220	3,55	3,65	16,9	sp|P20070|NB5R3_RAT	NADH-cytochrome b5 reductase 3 OS=Rattus norvegicus GN=Cyb5r3 PE=1 SV=2	RAT	2	1,1557	0,4671
204	3,53	4,48	14,3	sp|Q62667|MVP_RAT	Major vault protein OS=Rattus norvegicus GN=Mvp PE=1 SV=4	RAT	3	1,7867	0,2131
361	3,45	3,45	10,6	sp|P01946|HBA_RAT	Hemoglobin subunit alpha-1/2 OS=Rattus norvegicus GN=Hba1 PE=1 SV=3	RAT	2	1,5238	0,1792
184	3,44	3,44	24,6	sp|O35244|PRDX6_RAT	Peroxiredoxin-6 OS=Rattus norvegicus GN=Prdx6 PE=1 SV=3	RAT	2	1,0856	0,4352
504	3,43	3,43	16,5	sp|Q498E0|TXD12_RAT	Thioredoxin domain-containing protein 12 OS=Rattus norvegicus GN=Txndc12 PE=2 SV=2	RAT	2	1,1262	0,5814
362	3,42	3,59	10,6	sp|Q6IRK9|CBPQ_RAT	Carboxypeptidase Q OS=Rattus norvegicus GN=Cpq PE=1 SV=1	RAT	2	1,1764	0,2689
523	3,42	3,44	34	sp|P63025|VAMP3_RAT	Vesicle-associated membrane protein 3 OS=Rattus norvegicus GN=Vamp3 PE=1 SV=1	RAT	2	1,098	0,6314

141	3,37	3,5	24,1	sp|Q5XIH7|PHB2_RAT	Prohibitin-2 OS=Rattus norvegicus GN=Phb2 PE=1 SV=1	RAT	2	1,0518	0,655
67	3,35	3,38	13,8	sp|B4F7E8|NIBL1_RAT	Niban-like protein 1 OS=Rattus norvegicus GN=Fam129b PE=2 SV=1	RAT	2	0,8786	0,2109
435	3,31	3,32	39,8	sp|P01041|CYTB_RAT	Cystatin-B OS=Rattus norvegicus GN=Cstb PE=1 SV=1	RAT	2	1,1925	0,2065
70	3,3	3,34	35,2	sp|P62828|RAN_RAT	GTP-binding nuclear protein Ran OS=Rattus norvegicus GN=Ran PE=1 SV=3	RAT	2	1,11	0,7512
382	3,3	3,3	17,7	sp|Q5U318|PEA15_RAT	Astrocytic phosphoprotein PEA-15 OS=Rattus norvegicus GN=Pea15 PE=1 SV=1	RAT	2	0,8651	0,4043
418	3,28	3,36	16	sp|P50503|F10A1_RAT	Hsc70-interacting protein OS=Rattus norvegicus GN=St13 PE=1 SV=1	RAT	2	1,2131	0,3175
121	3,24	3,28	10,5	sp|Q6Q0N1|CNDP2_RAT	Cytosolic non-specific dipeptidase OS=Rattus norvegicus GN=Cndp2 PE=1 SV=1	RAT	2	1,2849	0,219
474	3,19	3,25	16,8	sp|Q5FVQ4|MLEC_RAT	Malectin OS=Rattus norvegicus GN=Mlec PE=2 SV=1	RAT	2	1,1019	0,826
314	3,17	3,17	20	sp|P38983|RSSA_RAT	40S ribosomal protein SA OS=Rattus norvegicus GN=Rpsa PE=1 SV=3	RAT	3	1,2684	0,2652
189	3,14	3,41	10,5	sp|Q5PQX1|TOIP1_RAT	Torsin-1A-interacting protein 1 OS=Rattus norvegicus GN=Tor1aip1 PE=1 SV=1	RAT	2	0,9141	0,6366
59	3,14	3,32	19,7	sp|Q66H98|SDPR_RAT	Serum deprivation-response protein OS=Rattus norvegicus GN=Sdpr PE=1 SV=3	RAT	2	0,7825	0,0972
327	3,11	3,11	16,9	sp|P62630|EF1A1_RAT	Elongation factor 1-alpha 1 OS=Rattus norvegicus GN=Eef1a1 PE=1 SV=1	RAT	3	1,2295	0,1545
480	3,1	3,1	28,4	sp|P05943|S10AA_RAT	Protein S100-A10 OS=Rattus norvegicus GN=S100a10 PE=1 SV=2	RAT	2	1,5162	0,3655
445	3,1	3,1	29,1	sp|P62804|H4_RAT	Histone H4 OS=Rattus norvegicus GN=Hist1h4b PE=1 SV=2	RAT	2	1,0042	0,9974
252	3,09	3,09	11,6	sp|Q6AY84|SCRN1_RAT	Secernin-1 OS=Rattus norvegicus GN=Scrn1 PE=1 SV=1	RAT	2	1,1886	0,3412
251	3,08	3,23	22,8	sp|Q63584|TMEDA_RAT	Transmembrane emp24 domain-containing protein 10 OS=Rattus norvegicus GN=Tmed10 PE=1 SV=2	RAT	2	1,1247	0,5954
101	3,06	3,06	35,7	sp|P12075|COX5B_RAT	Cytochrome c oxidase subunit 5B, mitochondrial OS=Rattus norvegicus GN=Cox5b PE=1 SV=2	RAT	2	1,4063	
358	3,04	3,04	42,3	sp|P36201|CRIP2_RAT	Cysteine-rich protein 2 OS=Rattus norvegicus GN=Crip2 PE=2 SV=1	RAT	1	0,8666	0,647
465	3,02	3,02	26,5	sp|P11250|RL34_RAT	60S ribosomal protein L34 OS=Rattus norvegicus GN=Rpl34 PE=1 SV=3	RAT	2	1,0426	0,7692
506	2,98	3,03	14,5	sp|P05369|FPPS_RAT	Farnesyl pyrophosphate synthase OS=Rattus norvegicus GN=Fdps PE=2 SV=2	RAT	2	1,0137	0,9472
41	2,96	2,97	6,8	sp|P08461|ODP2_RAT	Dihydrolipoyllysine-residue acetyltransferase component of pyruvate dehydrogenase complex, mitochondrial OS=Rattus norvegicus GN=Dlat PE=1 SV=3	RAT	2	1,0749	0,6159
402	2,92	2,92	49,1	sp|P24368|PPIB_RAT	Peptidyl-prolyl cis-trans isomerase B OS=Rattus norvegicus GN=Ppib PE=2 SV=3	RAT	5	1,0334	0,7294
118	2,87	2,96	15,9	sp|Q6AYH5|DCTN2_RAT	Dynactin subunit 2 OS=Rattus norvegicus GN=Dctn2 PE=1 SV=1	RAT	2	1,2569	0,2637
36	2,81	2,93	9,7	sp|P11507|AT2A2_RAT	Sarcoplasmic/endoplasmic reticulum calcium ATPase 2 OS=Rattus norvegicus GN=Atp2a2 PE=1 SV=1	RAT	1	1,199	0,3847
32	2,81	3,02	21,2	sp|B2RZ37|REEP5_RAT	Receptor expression-enhancing protein 5 OS=Rattus norvegicus GN=Reep5 PE=1 SV=1	RAT	1	1,1736	0,1196
272	2,76	2,86	16,5	sp|P48004|PSA7_RAT	Proteasome subunit alpha type-7 OS=Rattus norvegicus GN=Psma7 PE=1 SV=1	RAT	2	1,2877	0,2486

1	2,74	3,05	7,4	sp|P52873|PYC_RAT	Pyruvate carboxylase, mitochondrial OS=Rattus norvegicus GN=Pc PE=1 SV=2	RAT	1	1,3528	0,1328
490	2,74	2,77	11,6	sp|Q9JJ54|HNRPD_RAT	Heterogeneous nuclear ribonucleoprotein D0 OS=Rattus norvegicus GN=Hnrnpd PE=1 SV=1	RAT	1	0,9677	0,8068
37	2,74	3,16	32,9	sp|P52925|HMGB2_RAT	High mobility group protein B2 OS=Rattus norvegicus GN=Hmgb2 PE=2 SV=2	RAT	2	0,7864	0,1145
513	2,73	2,73	7,4	sp|Q8VIF7|SBP1_RAT	Selenium-binding protein 1 OS=Rattus norvegicus GN=Selenbp1 PE=1 SV=1	RAT	1	1,1746	0,4674
532	2,7	2,74	13,2	sp|Q01205|ODO2_RAT	Dihydrolipoyllysine-residue succinyltransferase component of 2-oxoglutarate dehydrogenase complex, mitochondrial OS=Rattus norvegicus GN=Dlst PE=1 SV=2	RAT	2	1,1722	0,3577
49	2,69	2,81	8,1	sp|P62944|AP2B1_RAT	AP-2 complex subunit beta OS=Rattus norvegicus GN=Ap2b1 PE=1 SV=1	RAT	1	0,9691	0,69
484	2,68	2,77	21,2	sp|P34064|PSA5_RAT	Proteasome subunit alpha type-5 OS=Rattus norvegicus GN=Psma5 PE=2 SV=1	RAT	1	1,4924	0,1583
313	2,68	2,79	18,8	sp|P27605|HPRT_RAT	Hypoxanthine-guanine phosphoribosyltransferase OS=Rattus norvegicus GN=Hprt1 PE=1 SV=1	RAT	1	1,0364	0,7953
427	2,67	2,76	26,7	sp|P47727|CBR1_RAT	Carbonyl reductase [NADPH] 1 OS=Rattus norvegicus GN=Cbr1 PE=1 SV=2	RAT	1	1,0695	0,509
87	2,65	2,81	38,3	sp|Q63507|RL14_RAT	60S ribosomal protein L14 OS=Rattus norvegicus GN=Rpl14 PE=1 SV=3	RAT	1	1,1468	0,3873
459	2,63	3,25	16,7	sp|Q794F9|4F2_RAT	4F2 cell-surface antigen heavy chain OS=Rattus norvegicus GN=Slc3a2 PE=1 SV=1	RAT	1	1,2679	0,2698
429	2,63	2,64	14,9	sp|Q63965|SFXN1_RAT	Sideroflexin-1 OS=Rattus norvegicus GN=Sfxn1 PE=2 SV=4	RAT	1	1,1683	0,2996
321	2,58	2,65	15,3	sp|Q5EAJ6|IKIP_RAT	Inhibitor of nuclear factor kappa-B kinase-interacting protein OS=Rattus norvegicus GN=Ikbip PE=2 SV=1	RAT	1	1,2202	0,1536
2	2,58	2,86	22	sp|A0JPM9|EIF3J_RAT	Eukaryotic translation initiation factor 3 subunit J OS=Rattus norvegicus GN=Eif3j PE=2 SV=1	RAT	2	1,1615	0,3731
390	2,58	2,68	21,3	sp|Q66HR2|MARE1_RAT	Microtubule-associated protein RP/EB family member 1 OS=Rattus norvegicus GN=Mapre1 PE=1 SV=3	RAT	1	1,1305	0,4655
456	2,58	2,79	11,8	sp|Q1JU68|EIF3A_RAT	Eukaryotic translation initiation factor 3 subunit A OS=Rattus norvegicus GN=Eif3a PE=2 SV=2	RAT	2	1,0227	0,7739
163	2,57	2,66	18,4	sp|Q9JLZ1|GLRX3_RAT	Glutaredoxin-3 OS=Rattus norvegicus GN=Glrx3 PE=1 SV=2	RAT	1	1,2487	0,296
482	2,57	2,57	37,3	sp|P04550|PTMS_RAT	Parathymosin OS=Rattus norvegicus GN=Ptms PE=1 SV=2	RAT	2	1,0176	0,8919
94	2,53	2,55	8,1	sp|Q64361|LXN_RAT	Latexin OS=Rattus norvegicus GN=Lxn PE=1 SV=1	RAT	1	1,2318	0,2985
129	2,53	2,59	6,4	sp|Q62733|LAP2_RAT	Lamina-associated polypeptide 2, isoform beta OS=Rattus norvegicus GN=Tmpo PE=1 SV=3	RAT	2	1,019	0,9246
496	2,52	2,52	13,7	sp|Q68A21|PURB_RAT	Transcriptional activator protein Pur-beta OS=Rattus norvegicus GN=Purb PE=1 SV=3	RAT	1	0,9662	0,8492
116	2,47	2,59	27,8	sp|P05712|RAB2A_RAT	Ras-related protein Rab-2A OS=Rattus norvegicus GN=Rab2a PE=1 SV=1	RAT	1	1,3138	0,2286
51	2,45	2,45	18,3	sp|O35264|PA1B2_RAT	Platelet-activating factor acetylhydrolase IB subunit beta OS=Rattus norvegicus GN=Pafah1b2 PE=1 SV=1	RAT	1	1,2961	
39	2,44	2,46	17	sp|P62083|RS7_RAT	40S ribosomal protein S7 OS=Rattus norvegicus GN=Rps7 PE=1 SV=1	RAT	1	1,2344	0,3168
79	2,43	2,43	14,7	sp|Q6LED0|H31_RAT	Histone H3.1 OS=Rattus norvegicus PE=1 SV=3	RAT	2	0,8591	0,3769

66	2,4	2,4	11,3	sp|B0BNA5|COTL1_RAT	Coactosin-like protein OS=Rattus norvegicus GN=Cotl1 PE=1 SV=1	RAT	1	1,3199	0,3781
45	2,4	2,45	7,6	sp|Q4FZT9|PSMD2_RAT	26S proteasome non-ATPase regulatory subunit 2 OS=Rattus norvegicus GN=Psmd2 PE=2 SV=1	RAT	2	1,1792	0,7915
524	2,38	2,4	14,6	sp|Q08013|SSRG_RAT	Translocon-associated protein subunit gamma OS=Rattus norvegicus GN=Ssr3 PE=2 SV=2	RAT	2	0,9558	0,9207
190	2,37	2,44	6,6	sp|Q64678|CP1B1_RAT	Cytochrome P450 1B1 OS=Rattus norvegicus GN=Cyp1b1 PE=1 SV=1	RAT	1	1,2306	0,6404
133	2,36	2,72	14	sp|Q10728|MYPT1_RAT	Protein phosphatase 1 regulatory subunit 12A OS=Rattus norvegicus GN=Ppp1r12a PE=1 SV=2	RAT	1	0,9787	0,9061
69	2,35	3,87	8,8	sp|P81155|VDAC2_RAT	Voltage-dependent anion-selective channel protein 2 OS=Rattus norvegicus GN=Vdac2 PE=1 SV=2	RAT	2	0,9538	0,7224
150	2,34	2,45	13,7	sp|P62703|RS4X_RAT	40S ribosomal protein S4, X isoform OS=Rattus norvegicus GN=Rps4x PE=2 SV=2	RAT	1	1,2358	0,2877
64	2,29	2,32	14	sp|O55096|DPP3_RAT	Dipeptidyl peptidase 3 OS=Rattus norvegicus GN=Dpp3 PE=1 SV=2	RAT	2	1,2709	
263	2,26	3,3	20,8	sp|Q6MG61|CLIC1_RAT	Chloride intracellular channel protein 1 OS=Rattus norvegicus GN=Clic1 PE=1 SV=1	RAT	2	0,9425	
42	2,25	2,32	7,1	sp|P21588|5NTD_RAT	5'-nucleotidase OS=Rattus norvegicus GN=Nt5e PE=1 SV=1	RAT	1	2,0382	0,1062
120	2,22	2,22	17,2	sp|P29411|KAD3_RAT	GTP:AMP phosphotransferase AK3, mitochondrial OS=Rattus norvegicus GN=Ak3 PE=2 SV=2	RAT	1	1,0676	0,6291
216	2,21	2,25	9,7	sp|P70566|TMOD2_RAT	Tropomodulin-2 OS=Rattus norvegicus GN=Tmod2 PE=1 SV=1	RAT	2	2,439	
59	2,21	2,22	9,7	sp|Q64428|ECHA_RAT	Trifunctional enzyme subunit alpha, mitochondrial OS=Rattus norvegicus GN=Hadha PE=1 SV=2	RAT	1	0,9896	0,9328
525	2,2	2,96	56,1	sp|P17078|RL35_RAT	60S ribosomal protein L35 OS=Rattus norvegicus GN=Rpl35 PE=1 SV=3	RAT	1	1,0676	0,7544
167	2,2	2,24	6,6	sp|P14562|LAMP1_RAT	Lysosome-associated membrane glycoprotein 1 OS=Rattus norvegicus GN=Lamp1 PE=1 SV=1	RAT	2	1,0389	
242	2,19	2,19	14,1	sp|Q99MZ8|LASP1_RAT	LIM and SH3 domain protein 1 OS=Rattus norvegicus GN=Lasp1 PE=1 SV=1	RAT	3	1,2794	0,2433
40	2,19	2,31	18,6	sp|P85968|6PGD_RAT	6-phosphogluconate dehydrogenase, decarboxylating OS=Rattus norvegicus GN=Pgd PE=1 SV=1	RAT	1	1,0227	0,8278
64	2,19	2,31	12	sp|P05708|HXK1_RAT	Hexokinase-1 OS=Rattus norvegicus GN=Hk1 PE=1 SV=4	RAT	1	0,9462	0,6592
47	2,18	2,34	12,8	sp|O70199|UGDH_RAT	UDP-glucose 6-dehydrogenase OS=Rattus norvegicus GN=Ugdh PE=2 SV=1	RAT	1	1,067	0,7735
127	2,18	2,38	7,8	sp|Q04462|SYVC_RAT	Valine--tRNA ligase OS=Rattus norvegicus GN=Vars PE=2 SV=2	RAT	1	0,9148	0,8729
47	2,15	2,2	31,2	sp|P62853|RS25_RAT	40S ribosomal protein S25 OS=Rattus norvegicus GN=Rps25 PE=2 SV=1	RAT	1	1,1775	0,321
365	2,13	2,13	29,6	sp|P21571|ATP5J_RAT	ATP synthase-coupling factor 6, mitochondrial OS=Rattus norvegicus GN=Atp5j PE=1 SV=1	RAT	1	1,2827	0,2459
416	2,13	2,13	22,3	sp|P19511|AT5F1_RAT	ATP synthase F(0) complex subunit B1, mitochondrial OS=Rattus norvegicus GN=Atp5f1 PE=1 SV=1	RAT	1	1,1849	0,096
15	2,12	2,12	17,2	sp|P13471|RS14_RAT	40S ribosomal protein S14 OS=Rattus norvegicus GN=Rps14 PE=2 SV=3	RAT	1	1,4469	0,1682
147	2,12	2,19	12,8	sp|Q5FVM4|NONO_RAT	Non-POU domain-containing octamer-binding protein OS=Rattus norvegicus GN=Nono PE=1 SV=3	RAT	1	1,049	0,775
92	2,12	2,15	7,2	sp|Q5U301|AKAP2_RAT	A-kinase anchor protein 2 OS=Rattus norvegicus GN=Akap2 PE=1 SV=1	RAT	1	1,048	0,785

225	2,12	2,16	9,1	sp|Q9R1J8|P3H1_RAT	Prolyl 3-hydroxylase 1 OS=Rattus norvegicus GN=Lepre1 PE=1 SV=1	RAT	1	1,0118	0,9261
540	2,11	2,35	9,2	sp|P02770|ALBU_RAT	Serum albumin OS=Rattus norvegicus GN=Alb PE=1 SV=2	RAT	1	1,038	0,7716
421	2,11	2,29	19,3	sp|Q06647|ATPO_RAT	ATP synthase subunit O, mitochondrial OS=Rattus norvegicus GN=Atp5o PE=1 SV=1	RAT	1	1,0085	0,9673
8	2,1	2,1	32,9	sp|P62250|RS16_RAT	40S ribosomal protein S16 OS=Rattus norvegicus GN=Rps16 PE=1 SV=2	RAT	1	1,3315	0,227
479	2,1	2,26	11,3	sp|Q63228|GMFB_RAT	Glia maturation factor beta OS=Rattus norvegicus GN=Gmfb PE=1 SV=2	RAT	1	1,3232	
111	2,1	2,64	13,3	sp|P34067|PSB4_RAT	Proteasome subunit beta type-4 OS=Rattus norvegicus GN=Psmb4 PE=1 SV=2	RAT	1	1,1122	0,4869
424	2,1	2,14	47,4	sp|P11951|CX6C2_RAT	Cytochrome c oxidase subunit 6C-2 OS=Rattus norvegicus GN=Cox6c2 PE=1 SV=3	RAT	1	0,8517	0,4079
105	2,09	2,09	10,8	sp|P62246|RS15A_RAT	40S ribosomal protein S15a OS=Rattus norvegicus GN=Rps15a PE=1 SV=2	RAT	1	1,1691	0,4795
246	2,09	2,15	10,3	sp|P29315|RINI_RAT	Ribonuclease inhibitor OS=Rattus norvegicus GN=Rnh1 PE=1 SV=2	RAT	1	0,8555	0,2035
173	2,08	2,1	5,2	sp|P07335|KCRB_RAT	Creatine kinase B-type OS=Rattus norvegicus GN=Ckb PE=1 SV=2	RAT	1	1,1998	0,4392
320	2,08	2,16	12,7	sp|P84025|SMAD3_RAT	Mothers against decapentaplegic homolog 3 OS=Rattus norvegicus GN=Smad3 PE=1 SV=1	RAT	1	0,9665	
391	2,07	2,13	16,3	sp|Q8VHF5|CISY_RAT	Citrate synthase, mitochondrial OS=Rattus norvegicus GN=Cs PE=1 SV=1	RAT	2	1,1936	0,1057
93	2,06	2,12	17,3	sp|P49432|ODPB_RAT	Pyruvate dehydrogenase E1 component subunit beta, mitochondrial OS=Rattus norvegicus GN=Pdhb PE=1 SV=2	RAT	1	1,4925	0,1702
518	2,06	2,24	19,1	sp|Q5RJR2|TWF1_RAT	Twinfilin-1 OS=Rattus norvegicus GN=Twf1 PE=2 SV=1	RAT	1	1,0832	0,5689
539	2,06	3,32	13,6	sp|P40329|SYRC_RAT	Arginine--tRNA ligase, cytoplasmic OS=Rattus norvegicus GN=Rars PE=1 SV=2	RAT	2	1,009	0,9527
229	2,06	2,33	17,8	sp|P27321|ICAL_RAT	Calpastatin OS=Rattus norvegicus GN=Cast PE=1 SV=3	RAT	1	0,9333	0,5639
81	2,05	2,1	23,5	sp|P02793|FRIL1_RAT	Ferritin light chain 1 OS=Rattus norvegicus GN=Ftl1 PE=1 SV=3	RAT	1	1,7245	0,1279
295	2,05	2,05	10,5	sp|Q9Z0V6|PRDX3_RAT	Thioredoxin-dependent peroxide reductase, mitochondrial OS=Rattus norvegicus GN=Prdx3 PE=1 SV=2	RAT	1	1,3433	0,5617
351	2,05	2,12	21,1	sp|P62850|RS24_RAT	40S ribosomal protein S24 OS=Rattus norvegicus GN=Rps24 PE=2 SV=1	RAT	1	1,283	0,3191
511	2,05	2,27	8,1	sp|Q9HB97|PARVA_RAT	Alpha-parvin OS=Rattus norvegicus GN=Parva PE=1 SV=2	RAT	1	0,9155	
342	2,05	2,37	13,2	sp|Q63692|CDC37_RAT	Hsp90 co-chaperone Cdc37 OS=Rattus norvegicus GN=Cdc37 PE=1 SV=2	RAT	1	0,9109	0,5389
290	2,04	2,11	5,8	sp|Q05030|PGFRB_RAT	Platelet-derived growth factor receptor beta OS=Rattus norvegicus GN=Pdgfrb PE=2 SV=2	RAT	1	1,4277	0,1885
396	2,04	2,04	24,2	sp|P63159|HMGB1_RAT	High mobility group protein B1 OS=Rattus norvegicus GN=Hmgb1 PE=1 SV=2	RAT	1	1,1613	0,3725
527	2,04	2,04	5,4	sp|P17046|LAMP2_RAT	Lysosome-associated membrane glycoprotein 2 OS=Rattus norvegicus GN=Lamp2 PE=1 SV=2	RAT	1	0,9781	0,8658
45	2,04	2,22	4,6	sp|Q9WU82|CTNB1_RAT	Catenin beta-1 OS=Rattus norvegicus GN=Ctnnb1 PE=1 SV=1	RAT	1	0,9666	0,803
137	2,04	2,1	6,5	sp|Q9QZK5|HTRA1_RAT	Serine protease HTRA1 OS=Rattus norvegicus GN=Htra1 PE=2 SV=1	RAT	1		
51	2,03	2,32	14,1	sp|Q07009|CAN2_RAT	Calpain-2 catalytic subunit OS=Rattus norvegicus GN=Capn2 PE=1 SV=3	RAT	1	1,4086	0,3179

16	2,03	2,56	12,6	sp|B2RYG6|OTUB1_RAT	Ubiquitin thioesterase OTUB1 OS=Rattus norvegicus GN=Otub1 PE=1 SV=1	RAT	1	1,0782	
231	2,03	2,04	17,5	sp|B0BN18|PFD2_RAT	Prefoldin subunit 2 OS=Rattus norvegicus GN=Pfdn2 PE=2 SV=1	RAT	1	1,0275	
283	2,03	2,03	11,1	sp|P84083|ARF5_RAT	ADP-ribosylation factor 5 OS=Rattus norvegicus GN=Arf5 PE=1 SV=2	RAT	1	0,9607	
453	2,02	2,02	5,6	sp|P97546|NPTN_RAT	Neuroplastin OS=Rattus norvegicus GN=Nptn PE=1 SV=2	RAT	1	3,3469	
73	2,02	2,1	5,4	sp|P13697|MAOX_RAT	NADP-dependent malic enzyme OS=Rattus norvegicus GN=Me1 PE=1 SV=2	RAT	1	1,7751	
372	2,02	2,12	6,5	sp|D3ZBP4|MICA1_RAT	Protein-methionine sulfoxide oxidase MICAL1 OS=Rattus norvegicus GN=Mical1 PE=3 SV=1	RAT	1	1,3364	
330	2,02	2,02	7,1	sp|O54975|XPP1_RAT	Xaa-Pro aminopeptidase 1 OS=Rattus norvegicus GN=Xpnpep1 PE=1 SV=1	RAT	1	1,1917	0,3283
57	2,02	2,22	7,3	sp|Q5U367|PLOD3_RAT	Procollagen-lysine,2-oxoglutarate 5-dioxygenase 3 OS=Rattus norvegicus GN=Plod3 PE=2 SV=1	RAT	1	1,1068	0,5139
266	2,02	2,1	9,5	sp|P68101|IF2A_RAT	Eukaryotic translation initiation factor 2 subunit 1 OS=Rattus norvegicus GN=Eif2s1 PE=1 SV=2	RAT	1	0,9607	0,7554
237	2,02	2,39	31,5	sp|P63170|DYL1_RAT	Dynein light chain 1, cytoplasmic OS=Rattus norvegicus GN=Dynll1 PE=1 SV=1	RAT	1	0,9476	0,8625
75	2,01	2,75	26,5	sp|P11517|HBB2_RAT	Hemoglobin subunit beta-2 OS=Rattus norvegicus PE=1 SV=2	RAT	2	4,1219	
193	2,01	2,04	14,5	sp|Q4FZX7|SRPRB_RAT	Signal recognition particle receptor subunit beta OS=Rattus norvegicus GN=Srprb PE=2 SV=1	RAT	1	2,5725	
534	2,01	2,15	39,5	sp|P83732|RL24_RAT	60S ribosomal protein L24 OS=Rattus norvegicus GN=Rpl24 PE=2 SV=1	RAT	1	1,6162	0,0195
425	2,01	2,04	7,8	sp|Q9Z2X5|HOME3_RAT	Homer protein homolog 3 OS=Rattus norvegicus GN=Homer3 PE=2 SV=2	RAT	1	1,3407	
44	2,01	2,01	35,1	sp|Q4KLF8|ARPC5_RAT	Actin-related protein 2/3 complex subunit 5 OS=Rattus norvegicus GN=Arpc5 PE=1 SV=3	RAT	1	1,3001	
472	2,01	2,05	2,6	sp|A1L1J9|LMF2_RAT	Lipase maturation factor 2 OS=Rattus norvegicus GN=Lmf2 PE=2 SV=1	RAT	1	1,0827	
257	2,01	21,14	43,6	sp|P85108|TBB2A_RAT	Tubulin beta-2A chain OS=Rattus norvegicus GN=Tubb2a PE=1 SV=1	RAT	14	1,0575	
344	2,01	2,01	27,4	sp|P61959|SUMO2_RAT	Small ubiquitin-related modifier 2 OS=Rattus norvegicus GN=Sumo2 PE=1 SV=1	RAT	1	0,9712	
408	2,01	2,06	6,7	sp|Q9Z327|SYNPO_RAT	Synaptopodin OS=Rattus norvegicus GN=Synpo PE=2 SV=2	RAT	1	0,7934	
54	2,01	2,28	45,8	sp|P05765|RS21_RAT	40S ribosomal protein S21 OS=Rattus norvegicus GN=Rps21 PE=1 SV=1	RAT	1		
18	2	2,04	3,6	sp|P10960|SAP_RAT	Sulfated glycoprotein 1 OS=Rattus norvegicus GN=Psap PE=1 SV=1	RAT	1	2,1259	
182	2	2,17	19,3	sp|P19944|RLA1_RAT	60S acidic ribosomal protein P1 OS=Rattus norvegicus GN=Rplp1 PE=3 SV=1	RAT	1	1,916	
298	2	2,03	23,2	sp|Q6GQP4|RAB31_RAT	Ras-related protein Rab-31 OS=Rattus norvegicus GN=Rab31 PE=1 SV=2	RAT	1	1,9015	
208	2	2,03	8,7	sp|Q62636|RAP1B_RAT	Ras-related protein Rap-1b OS=Rattus norvegicus GN=Rap1b PE=2 SV=2	RAT	1	1,8404	
123	2	2	11,8	sp|Q07936|ANXA2_RAT	Annexin A2 OS=Rattus norvegicus GN=Anxa2 PE=1 SV=2	RAT	1	1,8369	
250	2	8,07	15,5	sp|Q62764|YBOX3_RAT	Y-box-binding protein 3 OS=Rattus norvegicus GN=Ybx3 PE=2 SV=1	RAT	4	1,8171	
364	2	2	6,8	sp|P85972|VINC_RAT	Vinculin OS=Rattus norvegicus GN=Vcl PE=1 SV=1	RAT	1	1,7995	

466	2	2,67	8,2	sp|P43244|MATR3_RAT	Matrin-3 OS=Rattus norvegicus GN=Matr3 PE=1 SV=2	RAT	1	1,7774	
443	2	2,07	7,4	sp|B5DEH2|ERLN2_RAT	Erlin-2 OS=Rattus norvegicus GN=Erlin2 PE=1 SV=1	RAT	1	1,7388	
285	2	2	6,3	sp|P05065|ALDOA_RAT	Fructose-bisphosphate aldolase A OS=Rattus norvegicus GN=Aldoa PE=1 SV=2	RAT	1	1,7318	
444	2	2	4,3	sp|Q7TP48|APMAP_RAT	Adipocyte plasma membrane-associated protein OS=Rattus norvegicus GN=Apmap PE=2 SV=2	RAT	1	1,5779	
467	2	2	21,9	sp|P62628|DLRB1_RAT	Dynein light chain roadblock-type 1 OS=Rattus norvegicus GN=Dynlrb1 PE=1 SV=3	RAT	1	1,4635	
340	2	3,93	15,5	sp|P35280|RAB8A_RAT	Ras-related protein Rab-8A OS=Rattus norvegicus GN=Rab8a PE=1 SV=2	RAT	2	1,4633	
146	2	2	22,9	sp|P62832|RL23_RAT	60S ribosomal protein L23 OS=Rattus norvegicus GN=Rpl23 PE=2 SV=1	RAT	1	1,4473	
159	2	2	6,9	sp|Q6VV72|IF1A_RAT	Eukaryotic translation initiation factor 1A OS=Rattus norvegicus GN=Eif1a PE=2 SV=3	RAT	1	1,4395	
400	2	2,02	23,6	sp|P83883|RL36A_RAT	60S ribosomal protein L36a OS=Rattus norvegicus GN=Rpl36a PE=1 SV=2	RAT	1	1,4183	
505	2	2,4	15,1	sp|Q9EQX9|UBE2N_RAT	Ubiquitin-conjugating enzyme E2 N OS=Rattus norvegicus GN=Ube2n PE=1 SV=1	RAT	1	1,3887	
271	2	2,07	5,7	sp|P11915|NLTP_RAT	Non-specific lipid-transfer protein OS=Rattus norvegicus GN=Scp2 PE=1 SV=3	RAT	1	1,3808	
341	2	2	11,4	sp|P13668|STMN1_RAT	Stathmin OS=Rattus norvegicus GN=Stmn1 PE=1 SV=2	RAT	1	1,3785	
332	2	2,14	6	sp|P15684|AMPN_RAT	Aminopeptidase N OS=Rattus norvegicus GN=Anpep PE=1 SV=2	RAT	2	1,3446	
347	2	2	6,1	sp|Q68FR9|EF1D_RAT	Elongation factor 1-delta OS=Rattus norvegicus GN=Eef1d PE=1 SV=2	RAT	1	1,2869	
221	2	22,97	37,2	sp|Q6AYZ1|TBA1C_RAT	Tubulin alpha-1C chain OS=Rattus norvegicus GN=Tuba1c PE=1 SV=1	RAT	14	1,2612	
174	2	2	9,8	sp|Q07984|SSRD_RAT	Translocon-associated protein subunit delta OS=Rattus norvegicus GN=Ssr4 PE=2 SV=1	RAT	1	1,2417	
131	2	2,05	10,7	sp|P62634|CNBP_RAT	Cellular nucleic acid-binding protein OS=Rattus norvegicus GN=Cnbp PE=2 SV=1	RAT	1	1,2212	
515	2	2,03	8,9	sp|P61751|ARF4_RAT	ADP-ribosylation factor 4 OS=Rattus norvegicus GN=Arf4 PE=2 SV=2	RAT	1	1,2076	
417	2	2,02	8,7	sp|Q6P7B0|SYWC_RAT	Tryptophan--tRNA ligase, cytoplasmic OS=Rattus norvegicus GN=Wars PE=1 SV=2	RAT	1	1,1975	
93	2	2,16	13,9	sp|P62890|RL30_RAT	60S ribosomal protein L30 OS=Rattus norvegicus GN=Rpl30 PE=3 SV=2	RAT	1	1,189	
249	2	2	15,4	sp|O35796|C1QBP_RAT	Complement component 1 Q subcomponent-binding protein, mitochondrial OS=Rattus norvegicus GN=C1qbp PE=1 SV=2	RAT	1	1,1838	
46	2	2,02	8,8	sp|P37996|ARL3_RAT	ADP-ribosylation factor-like protein 3 OS=Rattus norvegicus GN=Arl3 PE=1 SV=2	RAT	1	1,1676	
394	2	2,13	8,2	sp|Q9Z269|VAPB_RAT	Vesicle-associated membrane protein-associated protein B OS=Rattus norvegicus GN=Vapb PE=1 SV=3	RAT	1	1,1671	
329	2	2	22,7	sp|P47198|RL22_RAT	60S ribosomal protein L22 OS=Rattus norvegicus GN=Rpl22 PE=2 SV=2	RAT	1	1,1659	
355	2	2	20,2	sp|P60868|RS20_RAT	40S ribosomal protein S20 OS=Rattus norvegicus GN=Rps20 PE=3 SV=1	RAT	1	1,1606	
455	2	2	22,4	sp|P63326|RS10_RAT	40S ribosomal protein S10 OS=Rattus norvegicus GN=Rps10 PE=2 SV=1	RAT	1	1,1302	0,6757

437	2	2	17,3	sp|Q63945|SET_RAT	Protein SET OS=Rattus norvegicus GN=Set PE=1 SV=2	RAT	1	1,1246	
71	2	2	5,5	sp|P13852|PRIO_RAT	Major prion protein OS=Rattus norvegicus GN=Prnp PE=1 SV=2	RAT	1	1,1016	
148	2	2,08	14,3	sp|Q9JHY2|SFXN3_RAT	Sideroflexin-3 OS=Rattus norvegicus GN=Sfxn3 PE=2 SV=1	RAT	1	1,0871	
261	2	2	18,3	sp|P62959|HINT1_RAT	Histidine triad nucleotide-binding protein 1 OS=Rattus norvegicus GN=Hint1 PE=1 SV=5	RAT	1	1,076	
194	2	2	13	sp|P47875|CSRP1_RAT	Cysteine and glycine-rich protein 1 OS=Rattus norvegicus GN=Csrp1 PE=2 SV=2	RAT	1	1,0654	
9	2	2,24	9,4	sp|Q63028|ADDA_RAT	Alpha-adducin OS=Rattus norvegicus GN=Add1 PE=2 SV=2	RAT	1	1,0329	
117	2	9,84	30,6	sp|P68255|1433T_RAT	14-3-3 protein theta OS=Rattus norvegicus GN=Ywhaq PE=1 SV=1	RAT	5	1,0305	
89	2	2	20,6	sp|P11240|COX5A_RAT	Cytochrome c oxidase subunit 5A, mitochondrial OS=Rattus norvegicus GN=Cox5a PE=1 SV=1	RAT	1	1,0224	
55	2	2	49,3	sp|P29419|ATP5I_RAT	ATP synthase subunit e, mitochondrial OS=Rattus norvegicus GN=Atp5i PE=1 SV=3	RAT	1	1,0185	
223	2	2	22,2	sp|Q71UE8|NEDD8_RAT	NEDD8 OS=Rattus norvegicus GN=Nedd8 PE=1 SV=1	RAT	1	1,0178	
463	2	3,96	18,4	sp|Q5U316|RAB35_RAT	Ras-related protein Rab-35 OS=Rattus norvegicus GN=Rab35 PE=1 SV=1	RAT	2	1,0036	
38	2	2	7,2	sp|P04256|ROA1_RAT	Heterogeneous nuclear ribonucleoprotein A1 OS=Rattus norvegicus GN=Hnrnpa1 PE=1 SV=3	RAT	1	0,9945	
509	2	2,07	24,1	sp|P83941|ELOC_RAT	Transcription elongation factor B polypeptide 1 OS=Rattus norvegicus GN=Tceb1 PE=1 SV=1	RAT	1	0,9578	
132	2	2,13	5,2	sp|Q4V8C3|EMAL1_RAT	Echinoderm microtubule-associated protein-like 1 OS=Rattus norvegicus GN=Eml1 PE=2 SV=2	RAT	1	0,929	
434	2	2,09	31,2	sp|Q9Z1H9|PRDBP_RAT	Protein kinase C delta-binding protein OS=Rattus norvegicus GN=Prkcdbp PE=1 SV=1	RAT	1	0,9079	
110	2	2,05	8,2	sp|P13596|NCAM1_RAT	Neural cell adhesion molecule 1 OS=Rattus norvegicus GN=Ncam1 PE=1 SV=1	RAT	1	0,8177	
145	2	2,03	21,1	sp|P84817|FIS1_RAT	Mitochondrial fission 1 protein OS=Rattus norvegicus GN=Fis1 PE=1 SV=1	RAT	1	0,8096	
209	2	2,03	7,4	sp|Q99372|ELN_RAT	Elastin OS=Rattus norvegicus GN=Eln PE=1 SV=2	RAT	1	0,7733	
166	2	2	6,5	sp|Q9EPH2|MRP_RAT	MARCKS-related protein OS=Rattus norvegicus GN=Marcksl1 PE=2 SV=3	RAT	1	0,7699	
76	2	2	6,6	sp|O08628|PCOC1_RAT	Procollagen C-endopeptidase enhancer 1 OS=Rattus norvegicus GN=Pcolce PE=1 SV=1	RAT	1	0,3894	
510	2	2,05	7,1	sp|P13264|GLSK_RAT	Glutaminase kidney isoform, mitochondrial OS=Rattus norvegicus GN=Gls PE=1 SV=2	RAT	1		
317	2	2,01	7,6	sp|P85973|PNPH_RAT	Purine nucleoside phosphorylase OS=Rattus norvegicus GN=Pnp PE=1 SV=1	RAT	1		
34	1,96	2	6,3	sp|P61972|NTF2_RAT	Nuclear transport factor 2 OS=Rattus norvegicus GN=Nutf2 PE=1 SV=1	RAT	1	0,8697	
537	1,96	2	11,8	sp|Q9WUC4|ATOX1_RAT	Copper transport protein ATOX1 OS=Rattus norvegicus GN=Atox1 PE=1 SV=1	RAT	1	0,8315	
489	1,95	2,02	5,5	sp|P84092|AP2M1_RAT	AP-2 complex subunit mu OS=Rattus norvegicus GN=Ap2m1 PE=1 SV=1	RAT	1	1,1429	0,6347
414	1,95	2,01	19,4	sp|P19234|NDUV2_RAT	NADH dehydrogenase [ubiquinone] flavoprotein 2, mitochondrial OS=Rattus norvegicus GN=Ndufv2 PE=1 SV=2	RAT	1	0,8978	0,4758

286	1,94	2,54	6,5	sp|P16638|ACLY_RAT	ATP-citrate synthase OS=Rattus norvegicus GN=Acly PE=1 SV=1	RAT	1	1,2843	0,269
35	1,92	1,93	4	sp|P01048|KNT1_RAT	T-kininogen 1 OS=Rattus norvegicus GN=Map1 PE=1 SV=2	RAT	1		
12	1,9	2,61	6,3	sp|P10688|PLCD1_RAT	1-phosphatidylinositol 4,5-bisphosphate phosphodiesterase delta-1 OS=Rattus norvegicus GN=Plcd1 PE=1 SV=1	RAT	1	1,157	
78	1,9	2,12	35,8	sp|P61589|RHOA_RAT	Transforming protein RhoA OS=Rattus norvegicus GN=Rhoa PE=1 SV=1	RAT	2	1,0274	0,9168
486	1,89	1,95	21,2	sp|P62775|MTPN_RAT	Myotrophin OS=Rattus norvegicus GN=Mtpn PE=1 SV=2	RAT	1	0,9607	
328	1,89	1,95	5,3	sp|Q9Z0J5|TRXR2_RAT	Thioredoxin reductase 2, mitochondrial OS=Rattus norvegicus GN=Txnrd2 PE=1 SV=3	RAT	1	0,9025	
503	1,86	2,03	26,7	sp|P04644|RS17_RAT	40S ribosomal protein S17 OS=Rattus norvegicus GN=Rps17 PE=1 SV=3	RAT	1	1,1972	
457	1,85	2	23,5	sp|Q5BJP3|UFM1_RAT	Ubiquitin-fold modifier 1 OS=Rattus norvegicus GN=Ufm1 PE=3 SV=1	RAT	1	1,6911	
528	1,85	1,93	8,3	sp|P85970|ARPC2_RAT	Actin-related protein 2/3 complex subunit 2 OS=Rattus norvegicus GN=Arpc2 PE=1 SV=1	RAT	1	1,0878	
363	1,85	4,26	18,1	sp|P08753|GNAI3_RAT	Guanine nucleotide-binding protein G(k) subunit alpha OS=Rattus norvegicus GN=Gnai3 PE=1 SV=3	RAT	2	0,8842	
488	1,83	1,83	9,8	sp|Q63083|NUCB1_RAT	Nucleobindin-1 OS=Rattus norvegicus GN=Nucb1 PE=1 SV=1	RAT	1	1,1456	0,4336
4	1,83	1,93	17,6	sp|Q75UQ2|CFDP1_RAT	Craniofacial development protein 1 OS=Rattus norvegicus GN=Cfdp1 PE=2 SV=1	RAT	1	1,111	
10	1,82	1,82	2,5	sp|Q5M7A4|UBA5_RAT	Ubiquitin-like modifier-activating enzyme 5 OS=Rattus norvegicus GN=Uba5 PE=2 SV=1	RAT	1	1,2171	
60	1,82	1,82	8,9	sp|P85125|PTRF_RAT	Polymerase I and transcript release factor OS=Rattus norvegicus GN=Ptrf PE=1 SV=1	RAT	1	1,1362	
46	1,82	1,86	4,6	sp|P31430|DPEP1_RAT	Dipeptidase 1 OS=Rattus norvegicus GN=Dpep1 PE=2 SV=2	RAT	1	1,0726	
91	1,81	1,82	4,2	sp|Q60587|ECHB_RAT	Trifunctional enzyme subunit beta, mitochondrial OS=Rattus norvegicus GN=Hadhb PE=1 SV=1	RAT	1	1,5739	
180	1,81	1,85	13,8	sp|Q68FS2|CSN4_RAT	COP9 signalosome complex subunit 4 OS=Rattus norvegicus GN=Cops4 PE=1 SV=1	RAT	1	0,9338	0,711
476	1,79	1,79	15,2	sp|P06762|HMOX1_RAT	Heme oxygenase 1 OS=Rattus norvegicus GN=Hmox1 PE=1 SV=1	RAT	1	2,6228	0,1107
370	1,77	1,82	7,8	sp|P46413|GSHB_RAT	Glutathione synthetase OS=Rattus norvegicus GN=Gss PE=1 SV=1	RAT	1	1,2461	
333	1,76	1,83	15,1	sp|Q9EQS0|TALDO_RAT	Transaldolase OS=Rattus norvegicus GN=Taldo1 PE=1 SV=2	RAT	1	0,8833	0,5244
522	1,74	1,79	3,5	sp|Q63016|LAT1_RAT	Large neutral amino acids transporter small subunit 1 OS=Rattus norvegicus GN=Slc7a5 PE=1 SV=2	RAT	1	1,7202	
380	1,74	1,74	4,7	sp|Q5PQP1|RBMS1_RAT	RNA-binding motif, single-stranded-interacting protein 1 OS=Rattus norvegicus GN=Rbms1 PE=2 SV=1	RAT	1	1,0329	
500	1,72	1,92	18,5	sp|Q3KRD5|TOM34_RAT	Mitochondrial import receptor subunit TOM34 OS=Rattus norvegicus GN=Tomm34 PE=1 SV=1	RAT	1	1,0575	0,8229
157	1,72	1,72	27,2	sp|Q6PDU1|SRSF2_RAT	Serine/arginine-rich splicing factor 2 OS=Rattus norvegicus GN=Srsf2 PE=1 SV=3	RAT	1	0,996	
299	1,72	1,78	21,6	sp|P35435|ATPG_RAT	ATP synthase subunit gamma, mitochondrial OS=Rattus norvegicus GN=Atp5c1 PE=1 SV=2	RAT	1	0,9178	

379	1,69	1,69	13,5	sp|P07895|SODM_RAT	Superoxide dismutase [Mn], mitochondrial OS=Rattus norvegicus GN=Sod2 PE=1 SV=2	RAT	1	1,3245	0,2546
6	1,69	1,73	10,9	sp|Q4V8H8|EHD2_RAT	EH domain-containing protein 2 OS=Rattus norvegicus GN=Ehd2 PE=1 SV=1	RAT	1	1,2851	0,1404
22	1,68	1,91	14,1	sp|Q2LAP6|TES_RAT	Testin OS=Rattus norvegicus GN=Tes PE=1 SV=1	RAT	1	1,2107	0,4195
10	1,68	1,68	5,3	sp|P60901|PSA6_RAT	Proteasome subunit alpha type-6 OS=Rattus norvegicus GN=Psma6 PE=1 SV=1	RAT	1	0,793	
24	1,67	2,04	6,7	sp|P09811|PYGL_RAT	Glycogen phosphorylase, liver form OS=Rattus norvegicus GN=Pygl PE=1 SV=5	RAT	1	1,1972	
96	1,67	1,81	15,8	sp|O08557|DDAH1_RAT	N(G),N(G)-dimethylarginine dimethylaminohydrolase 1 OS=Rattus norvegicus GN=Ddah1 PE=1 SV=3	RAT	2	0,859	
469	1,64	1,69	9,4	sp|Q9QZR6|SEPT9_RAT	Septin-9 OS=Rattus norvegicus GN=Sept9 PE=1 SV=1	RAT	1	1,0914	
44	1,64	1,73	16,3	sp|P62912|RL32_RAT	60S ribosomal protein L32 OS=Rattus norvegicus GN=Rpl32 PE=1 SV=2	RAT	1	0,9893	
440	1,64	1,64	3,3	sp|Q9EPJ0|NUCKS_RAT	Nuclear ubiquitous casein and cyclin-dependent kinase substrate 1 OS=Rattus norvegicus GN=Nucks1 PE=1 SV=1	RAT	1	0,903	
302	1,62	1,64	11,2	sp|Q6TUG0|DJB11_RAT	DnaJ homolog subfamily B member 11 OS=Rattus norvegicus GN=Dnajb11 PE=2 SV=1	RAT	1	1,3369	0,2104
430	1,61	1,61	11,2	sp|Q62969|PTGIS_RAT	Prostacyclin synthase OS=Rattus norvegicus GN=Ptgis PE=2 SV=1	RAT	1	1,0576	0,511
33	1,6	1,63	13,6	sp|E9PU28|IMDH2_RAT	Inosine-5'-monophosphate dehydrogenase 2 OS=Rattus norvegicus GN=Impdh2 PE=3 SV=1	RAT	1	1,1711	0,4307
533	1,59	1,62	7,3	sp|P17077|RL9_RAT	60S ribosomal protein L9 OS=Rattus norvegicus GN=Rpl9 PE=1 SV=1	RAT	1	1,3416	
201	1,59	1,66	5,3	sp|Q9WTT6|GUAD_RAT	Guanine deaminase OS=Rattus norvegicus GN=Gda PE=1 SV=1	RAT	1	1,1741	
26	1,57	1,57	14,8	sp|Q6URK4|ROA3_RAT	Heterogeneous nuclear ribonucleoprotein A3 OS=Rattus norvegicus GN=Hnrnpa3 PE=1 SV=1	RAT	2	1,1338	0,4262
541	1,55	1,73	13,6	sp|Q66HF9|LRRF1_RAT	Leucine-rich repeat flightless-interacting protein 1 OS=Rattus norvegicus GN=Lrrfip1 PE=1 SV=1	RAT	1	1,3797	0,3281
407	1,55	2,37	23,4	sp|Q5I0E7|TMED9_RAT	Transmembrane emp24 domain-containing protein 9 OS=Rattus norvegicus GN=Tmed9 PE=1 SV=1	RAT	1	1,3624	0,4548
419	1,55	1,55	7,2	sp|Q6AYD6|PDLI2_RAT	PDZ and LIM domain protein 2 OS=Rattus norvegicus GN=Pdlim2 PE=1 SV=1	RAT	1	1,274	
82	1,52	1,52	11,6	sp|Q7TP40|PCNP_RAT	PEST proteolytic signal-containing nuclear protein OS=Rattus norvegicus GN=Pcnp PE=2 SV=1	RAT	1	1,1314	
446	1,51	1,51	4,2	sp|P28073|PSB6_RAT	Proteasome subunit beta type-6 OS=Rattus norvegicus GN=Psmb6 PE=1 SV=3	RAT	1	1,4239	
280	1,49	1,57	11,1	sp|O08629|TIF1B_RAT	Transcription intermediary factor 1-beta OS=Rattus norvegicus GN=Trim28 PE=1 SV=2	RAT	1	1,1803	0,6213
493	1,49	1,49	23,4	sp|Q03344|ATIF1_RAT	ATPase inhibitor, mitochondrial OS=Rattus norvegicus GN=Atpif1 PE=2 SV=2	RAT	1	0,9757	
255	1,48	1,56	23,1	sp|P62268|RS23_RAT	40S ribosomal protein S23 OS=Rattus norvegicus GN=Rps23 PE=1 SV=3	RAT	1	1,492	0,1583
498	1,48	1,48	23,6	sp|Q6IG12|K2C7_RAT	Keratin, type II cytoskeletal 7 OS=Rattus norvegicus GN=Krt7 PE=2 SV=1	RAT	1	0,714	0,6212
386	1,47	1,47	6,8	sp|Q63690|BAX_RAT	Apoptosis regulator BAX OS=Rattus norvegicus GN=Bax PE=1 SV=2	RAT	1	1,792	
99	1,47	5,99	23,5	sp|Q5U206|CALL3_RAT	Calmodulin-like protein 3 OS=Rattus norvegicus GN=Calml3 PE=2 SV=1	RAT	4		

265	1,46	1,56	10,5	sp|Q6MG60|DDAH2_RAT	N(G),N(G)-dimethylarginine dimethylaminohydrolase 2 OS=Rattus norvegicus GN=Ddah2 PE=1 SV=1	RAT	1	0,8488	
385	1,46	1,58	5,6	sp|P02773|FETA_RAT	Alpha-fetoprotein OS=Rattus norvegicus GN=Afp PE=2 SV=1	RAT	1	0,7834	
319	1,43	21,68	41,6	sp|Q4QRB4|TBB3_RAT	Tubulin beta-3 chain OS=Rattus norvegicus GN=Tubb3 PE=1 SV=1	RAT	16	1,2267	
452	1,43	1,56	9,4	sp|Q9Z2Q1|SC31A_RAT	Protein transport protein Sec31A OS=Rattus norvegicus GN=Sec31a PE=1 SV=2	RAT	1	0,9436	0,5381
224	1,39	1,42	9,5	sp|O89046|COR1B_RAT	Coronin-1B OS=Rattus norvegicus GN=Coro1b PE=1 SV=1	RAT	1	1,1452	0,269
199	1,37	1,41	7	sp|Q9JMI1|AACS_RAT	Acetoacetyl-CoA synthetase OS=Rattus norvegicus GN=Aacs PE=1 SV=1	RAT	1	1,5969	
4	1,37	1,4	26,9	sp|P25886|RL29_RAT	60S ribosomal protein L29 OS=Rattus norvegicus GN=Rpl29 PE=1 SV=3	RAT	1	0,9932	0,9586
72	1,37	1,37	5,2	sp|O89049|TRXR1_RAT	Thioredoxin reductase 1, cytoplasmic OS=Rattus norvegicus GN=Txnrd1 PE=1 SV=5	RAT	1	0,9696	0,9282
267	1,35	1,62	11,5	sp|B5DFC8|EIF3C_RAT	Eukaryotic translation initiation factor 3 subunit C OS=Rattus norvegicus GN=Eif3c PE=2 SV=1	RAT	1	1,4354	0,0475
373	1,33	1,33	24,2	sp|Q5XI72|IF4H_RAT	Eukaryotic translation initiation factor 4H OS=Rattus norvegicus GN=Eif4h PE=1 SV=1	RAT	1	0,9989	
54	1,32	1,35	17,6	sp|Q9ES40|PRAF3_RAT	PRA1 family protein 3 OS=Rattus norvegicus GN=Arl6ip5 PE=1 SV=1	RAT	1	2,232	
428	1,32	1,36	8,1	sp|Q62786|FPRP_RAT	Prostaglandin F2 receptor negative regulator OS=Rattus norvegicus GN=Ptgfrn PE=1 SV=1	RAT	1	1,2184	
442	1,32	1,34	16,7	sp|Q6PEC1|TBCA_RAT	Tubulin-specific chaperone A OS=Rattus norvegicus GN=Tbca PE=1 SV=1	RAT	1	1,1565	0,3894

Supplementary Table S2 – Proteins differentially expressed in PASMCs treated with TMP compared with control in SHAM group.

SHAM				
Acession	**Gene ID**	**Name**	**Log2 (TMP/CONT)**	***p* value**
P62329	TYB4_RAT	Thymosin beta-4	-0.5825	0.0416
Q64119	MYL6_RAT	Myosin light polypeptide 6	-0.5756	0.0463
P18666	ML12B_RAT	Myosin regulatory light chain 12B	-0.5328	0.0150
P05964	S10A6_RAT	Protein S100-A6	-0.3655	0.0052
Q05175	BASP1_RAT	Brain acid soluble protein 1	-0.3623	0.0001
P58775	TPM2_RAT	Tropomyosin beta chain	-0.3185	0.0088
P05942	S10A4_RAT	Protein S100-A4	-0.3129	0.0057
P04692	TPM1_RAT	Tropomyosin alpha-1 chain	-0.2802	0.0100
P11762	LEG1_RAT	Galectin-1	-0.2735	0.0193
Q62736	CALD1_RAT	Non-muscle caldesmon	-0.2576	0.0002
P63018	HSP7C_RAT	Heat shock cognate 71 kDa protein	-0.1875	0.0042
P09495	TPM4_RAT	Tropomyosin alpha-4 chain	-0.1568	0.0154
P19804	NDKB_RAT	Nucleoside diphosphate kinase B	0.2016	0.0481
P04785	PDIA1_RAT	Protein disulfide-isomerase A1	0.3093	0.0013
P04764	ENOA_RAT	Alpha-enolase	0.3455	0.0006
O35763	MOES_RAT	Moesin	0.4484	0.0041
Q3KRE8	TBB2B_RAT	Tubulin beta-2B chain	0.6872	0.0067
P63259	ACTG_RAT	Actin, cytoplasmic 2	0.9750	0.0000

Supplementary Table S3 – Proteins differentially expressed in PASMCs treated with TMP compared with control in MCT group.

MCT				
Acession	**Gene ID**	**Name**	**Log2 (TMP/CONT)**	***p* value**
P13941	CO3A1_RAT	Collagen alpha-1(III) chain	-1.3108	0.0000
P02454	CO1A1_RAT	Collagen alpha-1(I) chain	-1.0058	0.0003
P04692	TPM1_RAT	Tropomyosin alpha-1 chain	-0.9811	0.0000
P02466	CO1A2_RAT	Collagen alpha-2(I) chain	-0.7961	0.0011
P05964	S10A6_RAT	Protein S100-A6	-0.7634	0.0156
P37397	CNN3_RAT	Calponin-3	-0.6808	0.0042
P35704	PRDX2_RAT	Peroxiredoxin-2	-0.6613	0.0371
P41350	CAV1_RAT	Caveolin-1	-0.6054	0.0455
Q63355	MYO1C_RAT	Unconventional myosin-Ic	-0.5720	0.0120
P09495	TPM4_RAT	Tropomyosin alpha-4 chain	-0.5355	0.0003
Q63610	TPM3_RAT	Tropomyosin alpha-3 chain	-0.4761	0.0000
B3GNI6	SEP11_RAT	Septin-11	-0.4521	0.0182
Q5QD51	AKA12_RAT	A-kinase anchor protein 12	-0.4438	0.0047
P85125	PTRF_RAT	Polymerase I and transcript release factor	-0.4152	0.0057

P58775	TPM2_RAT	Tropomyosin beta chain	-0.4127	0.0133
P49134	ITB1_RAT	Integrin beta-1	-0.4016	0.0076
P47875	CSRP1_RAT	Cysteine and glycine-rich protein 1	-0.3876	0.0002
P62982	RS27A_RAT	Ubiquitin-40S ribosomal protein S27a	-0.3857	0.0256
P04256	ROA1_RAT	Heterogeneous nuclear ribonucleoprotein A1	-0.3761	0.0312
P13084	NPM_RAT	Nucleophosmin	-0.3748	0.0211
Q811A3	PLOD2_RAT	Procollagen-lysine,2-oxoglutarate 5-dioxygenase 2	-0.3731	0.0010
P63159	HMGB1_RAT	High mobility group protein B1	-0.3609	0.0388
Q05175	BASP1_RAT	Brain acid soluble protein 1	-0.3412	0.0212
Q9WVC0	SEPT7_RAT	Septin-7	-0.3408	0.0030
D3ZBN0	H15_RAT	Histone H1.5	-0.3401	0.0468
Q9WUH4	FHL1_RAT	Four and a half LIM domains protein 1	-0.3335	0.0109
P45592	COF1_RAT	Cofilin-1	-0.3312	0.0176
A7VJC2	ROA2_RAT	Heterogeneous nuclear ribonucleoproteins A2/B1	-0.3103	0.0460
Q62736	CALD1_RAT	Non-muscle caldesmon	-0.3006	0.0052
Q62812	MYH9_RAT	Myosin-9	-0.2895	0.0001
Q99MZ8	LASP1_RAT	LIM and SH3 domain protein 1	-0.2447	0.0105
P04636	MDHM_RAT	Malate dehydrogenase, mitochondrial	-0.2316	0.0051
P13383	NUCL_RAT	Nucleolin	-0.2022	0.0058
D3ZHA0	FLNC_RAT	Filamin-C	-0.1647	0.0107
Q9EPH8	PABP1_RAT	Polyadenylate-binding protein 1	0.1879	0.0463
O88600	HSP74_RAT	Heat shock 70 kDa protein 4	0.1898	0.0304
O35763	MOES_RAT	Moesin	0.1975	0.0310
Q63716	PRDX1_RAT	Peroxiredoxin-1	0.2106	0.0138
P04937	FINC_RAT	Fibronectin	0.2129	0.0480
P11980	KPYM_RAT	Pyruvate kinase PKM	0.2293	0.0076
P11598	PDIA3_RAT	Protein disulfide-isomerase A3	0.2309	0.0276
P10719	ATPB_RAT	ATP synthase subunit beta, mitochondrial	0.2370	0.0464
P05197	EF2_RAT	Elongation factor 2	0.2537	0.0168
P21533	RL6_RAT	60S ribosomal protein L6	0.2669	0.0241
Q63617	HYOU1_RAT	Hypoxia up-regulated protein 1	0.2715	0.0451
P04642	LDHA_RAT	L-lactate dehydrogenase A chain	0.2751	0.0316
P16086	SPTN1_RAT	Spectrin alpha chain, non-erythrocytic 1	0.2830	0.0000
P27952	RS2_RAT	40S ribosomal protein S2	0.2853	0.0441
P61354	RL27_RAT	60S ribosomal protein L27	0.2911	0.0379
P04785	PDIA1_RAT	Protein disulfide-isomerase A1	0.2985	0.0011
P34058	HS90B_RAT	Heat shock protein HSP 90-beta	0.3004	0.0195
P11442	CLH1_RAT	Clathrin heavy chain 1	0.3015	0.0009
P05982	NQO1_RAT	NAD(P)H dehydrogenase [quinone] 1	0.3129	0.0119
O35142	COPB2_RAT	Coatomer subunit beta	0.3308	0.0473
P48721	GRP75_RAT	Stress-70 protein, mitochondrial	0.3657	0.0009
P62271	RS18_RAT	40S ribosomal protein S18	0.3782	0.0339

P38659	PDIA4_RAT	Protein disulfide-isomerase A4	0.3896	0.0037
O08651	SERA_RAT	D-3-phosphoglycerate dehydrogenase	0.3977	0.0156
P62494	RB11A_RAT	Ras-related protein Rab-11A	0.3993	0.0382
P06761	GRP78_RAT	78 kDa glucose-regulated protein	0.4182	0.0000
P19804	NDKB_RAT	Nucleoside diphosphate kinase B	0.4558	0.0228
P49242	RS3A_RAT	40S ribosomal protein S3a	0.4910	0.0265
Q6NYB7	RAB1A_RAT	Ras-related protein Rab-1A	0.5449	0.0046
P31000	VIME_RAT	Vimentin	0.5528	0.0003
P63029	TCTP_RAT	Translationally-controlled tumor protein	0.6450	0.0426

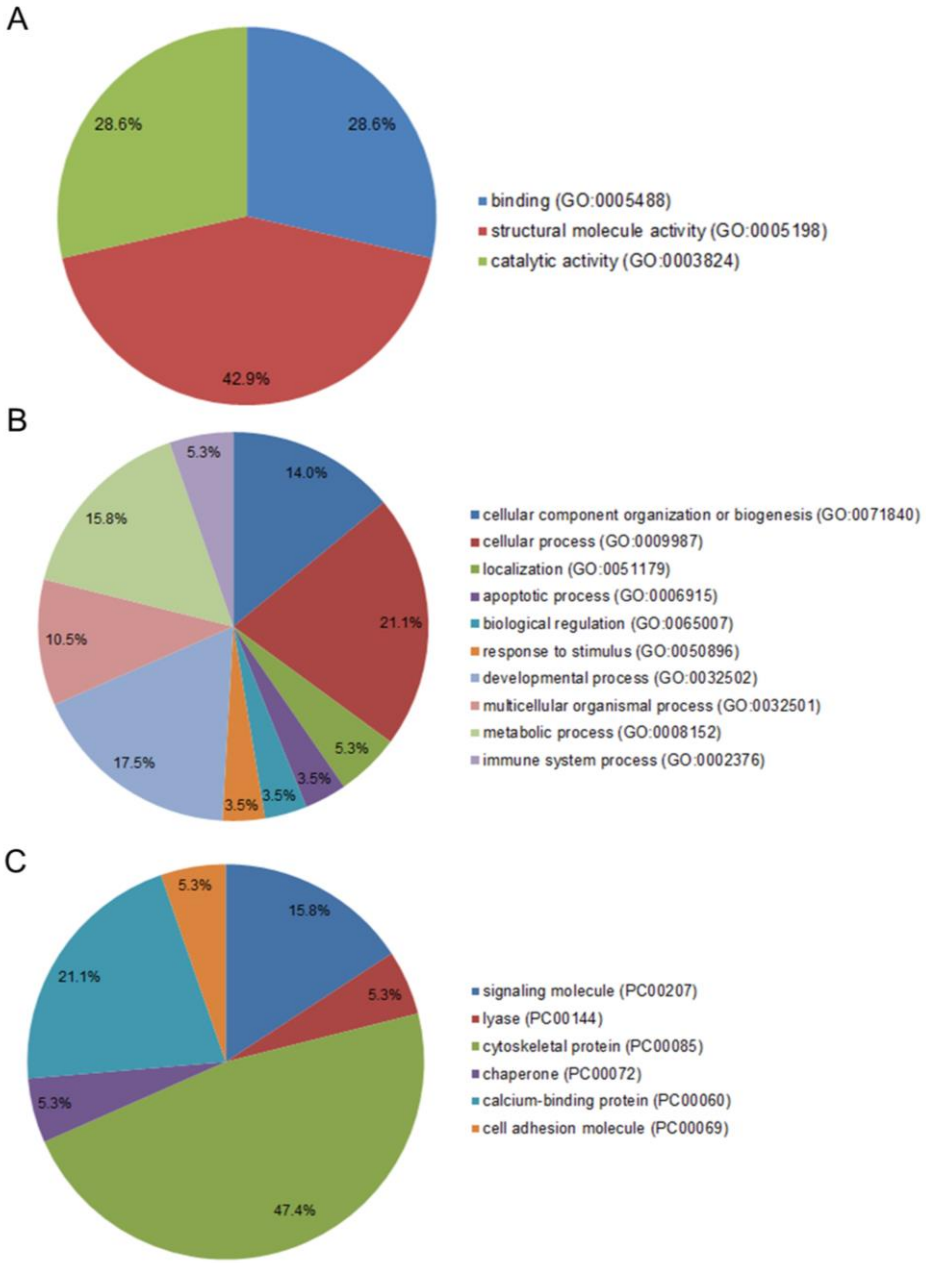

Supplementary Figure S1 – Pie charts of proteins identified in the PASMCs from SHAM rats grouped based on their molecular function (A), biological process (B) and protein class (C), by PANTHER, v8.0 [24]. PANTHER analysis showed that 42.9 % of the proteins have structural molecule activity. Cellular (21.1 %) and developmental (17.5 %) processes are the biological processes associated with the majority of the proteins. Furthermore, 47.4 % of the proteins are cytoskeletal. Release date: June 20, 2015.

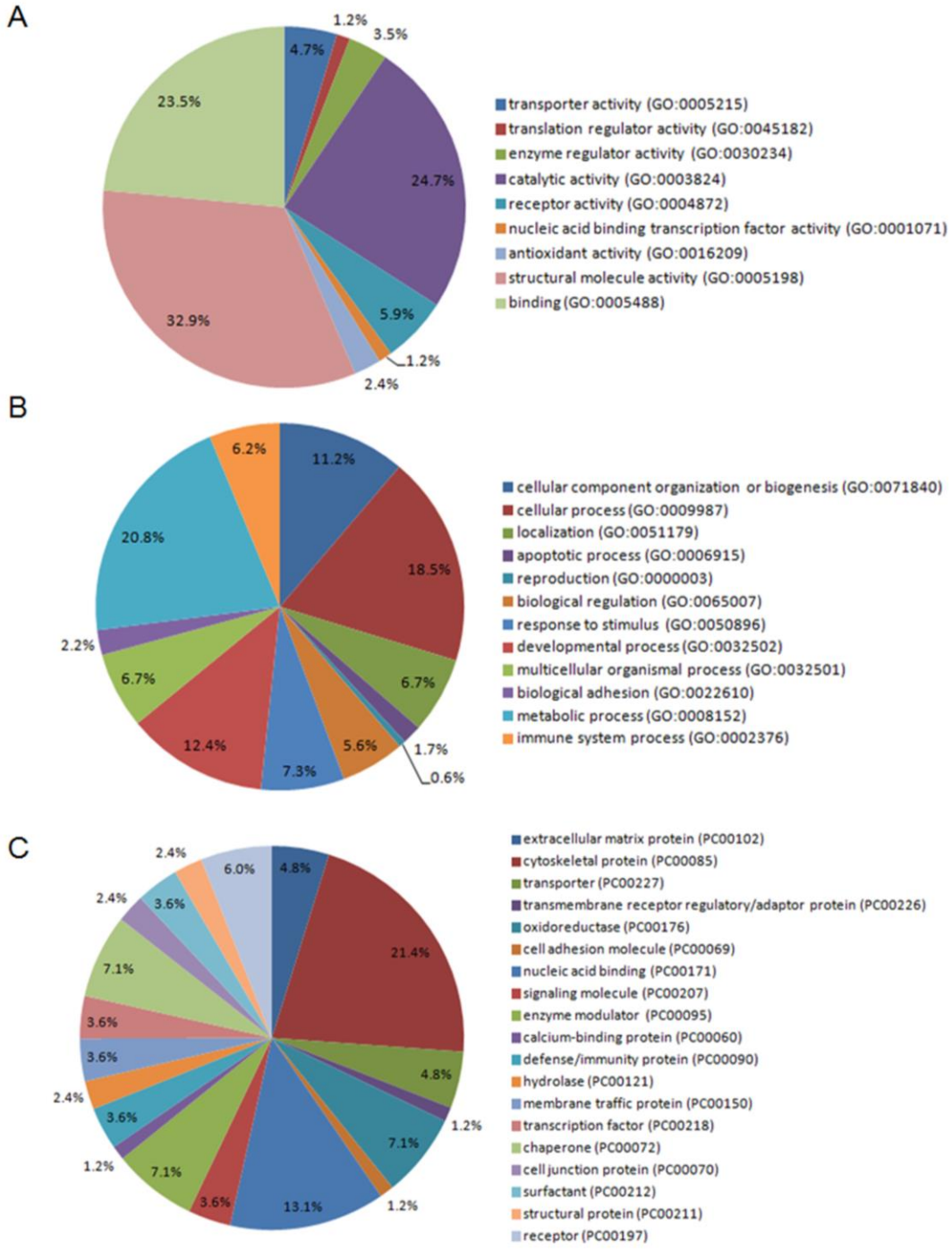

Supplementary Figure S2 – Pie charts of proteins identified in the PASMCs from MCT rats grouped based on their molecular function (A), biological process (B) and protein class (C), by PANTHER, v8.0 [24]. PANTHER analysis showed that 32.9 % of the proteins have structural molecule activity, 24.7 % have catalytic activity and 23.5 % have binding function. Metabolic (20.8 %) and cellular (18.5 %) processes are the biological processes associated with the majority of the proteins. Furthermore, 21.4 % of the proteins are cytoskeletal and 13.1 % are nucleic acid binding proteins. Release date: June 20, 2015.

SwissTargetPrediction report:

Reference:
Gfeller D., Michielin O. & Zoete V.
Shaping the interaction landscape of bioactive molecules, *Bioinformatics* (2013) 29:3073-3079.

Query Molecule

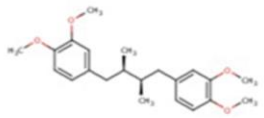

Frequency of Target Class

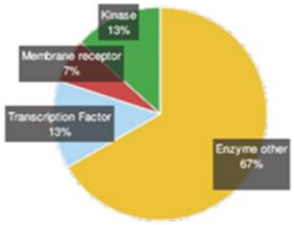

Target	Uniprot ID	Gene code	ChEMBL ID	Probability	# sim. cmpds (3D / 2D)	Target Class
Arachidonate 12-lipoxygenase, leukocyte-type *(by homology)*	Q02759	Alox12l	CHEMBL2741		1 / 21	Enzyme
Arachidonate lipoxygenase, epidermal (Predicted) *(by homology)*	D3ZQF9	Alox12e			1 / 21	Enzyme
Protein Alox12 *(by homology)*	F1LQ70	Alox12			1 / 21	Enzyme
Carbonic anhydrase 5A, mitochondrial *(by homology)*	P43165	Ca5a	CHEMBL2138		35 / 9	Enzyme
Carbonic anhydrase 5B, mitochondrial *(by homology)*	Q66HG6	Ca5b			35 / 9	Enzyme
Glucocorticoid receptor *(by homology)*	E9PT44	Nr3c1			175 / 39	Transcription Factor
Glucocorticoid receptor *(by homology)*	G3V7U9	Nr3c1			175 / 39	Transcription Factor
5-hydroxytryptamine (Serotonin) receptor 1A *(by homology)*	G3V7B9	Htr1a			9 / 80	Membrane receptor
Tyrosine-protein kinase receptor *(by homology)*	F1LN53	Insr			103 / 14	Tyr Kinase
Insulin-like growth factor 1 receptor *(by homology)*	P24062	Igf1r	CHEMBL1075098		103 / 14	Tyr Kinase
Cytochrome P450 19A1 *(by homology)*	F1LPY2	Cyp19a1			281 / 26	Enzyme
Arachidonate 5-lipoxygenase *(by homology)*	F1LMM5	Alox5			38 / 25	Enzyme
Tyrosyl-DNA phosphodiesterase 1 *(by homology)*	Q4G056	Tdp1			201 / 30	Enzyme
Protein LOC100912596 *(by homology)*	M0R7W4	LOC100912596			155 / 6	Enzyme
FAD-linked sulfhydryl oxidase ALR *(by homology)*	Q63042	Gfer			155 / 6	Enzyme

Supplementary Figure S3 – Terameprocol protein targets prediction (SwissTargetPrediction) [43]. Release date: September 8, 2014.

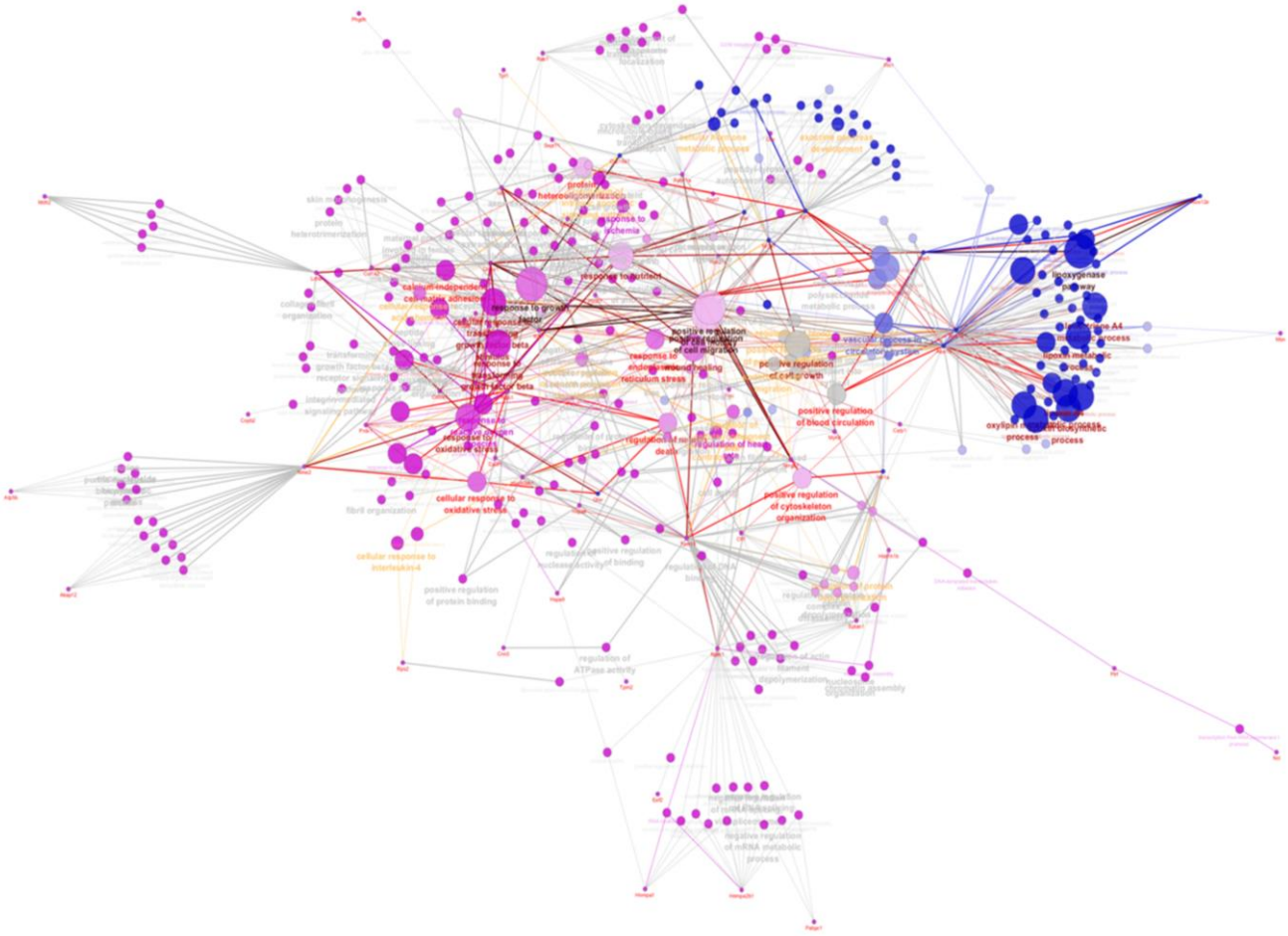

Supplementary Figure S4 – ClueGo+CluePedia analysis [26, 27] of protein-protein interactions considering the proteins identified as up- and down-regulated in PASMCs from MCT rats treated with TMP. Purple nodes represent the biological processes related with the proteins identified experimentally, while blue nodes refer to the ones predicted using SwissTargetPrediction tool [43]. Release date: May 15, 2015.